ADAPTIVE CONTROL FOR SHIP ROLL STABILIZATION USING ANTI-ROLL TANKS

By

Reza Moaleji

A Thesis Submitted for the Degree of
Doctor of Philosophy

Department of Mechanical Engineering
University College London

Torrington Place
London, WC1E 7JE

December 2006

UMI Number: U592341

All rights reserved

INFORMATION TO ALL USERS
The quality of this reproduction is dependent upon the quality of the copy submitted.

In the unlikely event that the author did not send a complete manuscript
and there are missing pages, these will be noted. Also, if material had to be removed,
a note will indicate the deletion.

UMI U592341
Published by ProQuest LLC 2013. Copyright in the Dissertation held by the Author.
Microform Edition © ProQuest LLC.
All rights reserved. This work is protected against
unauthorized copying under Title 17, United States Code.

ProQuest LLC
789 East Eisenhower Parkway
P.O. Box 1346
Ann Arbor, MI 48106-1346

I, Reza Moaleji, confirm that the work presented in this thesis is my own. Where information has been derived from other sources, I confirm that this has been indicated in the thesis.

To my parents and my wife, Mahsa, who sacrificed their big hearts and kind souls to make it possible for me to write these lines.

Abstract

Roll reduction of ships at slow or zero speeds still remains a challenge in marine engineering. This thesis revisits tank stabilization systems, and starts with a critical review of their development since 1883 to the present. It goes on to investigate the application of modern control techniques, power consumption, and different tank configuration to monohulls and trimarans. It is shown that during the development of tank stabilizing systems the weak link in most cases was the control system, the technology to implement them was not available. Only now with advanced control theory and high speed computing power can the potential of some of these systems be exploited. This thesis applies the current advanced technological and computational techniques to some older ideas that could not be practically realized before.

It is shown that the lack of an effective control system of anti-roll tanks is due to the philosophy of trying to control the system with feedback control while a much more suitable approach for this particular application is feedforward control. The thesis develops two strategies (both feedforward) to control the pumps used in active tanks:

1) Auto regression is used to predict the incident wave motion. The predicted wave motion is used as the input to the tank/pump system.
2) Control of the actuating pumps of an active U-tank with an adaptive inverse controller using a filtered-x least mean square algorithm.

Both the methods are shown to provide excellent roll stabilization in different sea conditions for monohull and trimaran vessels.

Historically tank stabilization systems have only been fitted to monohulls. The application of tank stabilization systems is extended to multihulls, the performance of U-tanks and free flooding (or n-tanks) is compared. The n-tanks can be located in the low value volume of the side hulls with minimum impact on the box structure, thus providing good ship stabilization at low speed with low ship impact.

Acknowledgments

My particular thanks and warmest regards to Dr Alistair Greig, my supervisor, for all his support, guidance, and exceptional vision and to my second supervisor Dr Trevor Sutton. I will forever be grateful to them for all their technical, emotional and social support during my enjoyable years at the Control Laboratory of the Mechanical Engineering Department at UCL.

The financial support provided by the IMarEST Stanley Gray Fellowship Award is also gratefully acknowledged.

Table of Contents

List of Figures

List of Symbols

A_r, A_d cross sectional area of the reservoirs and the duct respectively

a_{ij} generalized added mass or inertia coefficient; i^{th} force or moment due to j^{th} unit acceleration

$a_{i\tau}$ i^{th} force or moment due to unit tank angle acceleration

$a_{\tau i}$ tank moment due to i^{th} unit acceleration

$a_{\tau\tau}$ tank added mass coefficient i^{th}

b_{ij} generalized damping coefficient; i^{th} force or moment due to j^{th} unit velocity

$b_{i\tau}$ i^{th} force or moment due to unit tank angle velocity

$b_{\tau i}$ tank moment due to i^{th} unit velocity

$b_{\tau\tau}$ tank damping coefficient

c_{ij} generalized stiffness coefficient; i^{th} force or moment due to j^{th} unit displacement

$c_{4\tau}$ roll moment applied by tank due to unit roll displacement

$c_{\tau 4}$ tank moment due to unit roll displacement

$c_{\tau\tau}$ tank moment due to unit tank angle

d diameter of the pipe

d_e effective diameter of a non-circular pipe

d desired signal of the adaptive processor

e desired signal of the adaptive processor

F_i i^{th} force or moment required to sustain general oscillation

f friction factor

$\overline{GM}$ metacentric height

g acceleration due to gravity ($\approx 9.81 m/s^2$)

h distance of the tank above the rolling centre

h_w apparent wave height

$(h_w)_{1/3}$ significant wave height

I_{44} ship's longitude mass moment of inertia

k_1 tank viscous damping coefficient

k_2 tank quadratic damping coefficient

k_s constant relating the roll velocity to the stabilizing moment

k, K damping coefficient of the tank and ship respectively

L lever arm of the tank

L_w apparent wave length

m_r, m_d mass of the liquid inside the reservoirs and the duct respectively

m_s mass of the structure

m_o total mass of the structure and tank together

P instantaneous air pressure in the upper part of the reservoirs

$\mathbf{P}$ cross-correlation matrix between the input signal and the desired response

P_f pressure loss in a pipe

Q non-potential force term in the Lagrange equation

r_{mse} geometric ratio of the mean square error

$\mathbf{R}$ input-correlation matrix of the adaptive filter

S stabilizing moment

$S(w)$ wave spectrum

t time

T kinematic energy

T_c apparent wave period

T_w moment induced by the waves

T_z apparent zero crossing period of wave

u control input

U potential energy

V mass velocity of fluid

w_i individual gains of the adaptive filter

W ship displacement

$\mathbf{W}$ weight vector of the adaptive processor

x input signal to the adaptive processor

$\mathbf{X}$ input vector to the adaptive processor

y output signal of the adaptive processor

z displacement of fluid surface from tank equilibrium position

z_d horizontal displacement of fluid in the tank duct

α actual position of the pump blade

α_0 maximum wave slope

α_c required position of the pump blade (control signal)

γ specific heat ratio

ε error signal of the adaptive processor

ξ mean square error

wave elevation

ξ_a wave amplitude

$\bar{\xi}_a$ average wave amplitude

λ eigen value of the matrix **R**

μ free surface coefficient factor or viscosity of the fluid

adaptation coefficient

τ tank angle

υ kinematic viscosity of the fluid (1.2×10^{-6}m/s^{-2} for water)

ω frequency of the encountered wave

ω_t, ω_s roll Natural frequency of the tank and ship respectively

$x_1, \dot{x}_1, \ddot{x}_1$ surge, surge velocity and surge acceleration

$x_2, \dot{x}_2, \ddot{x}_2$ sway, sway velocity and sway acceleration

$x_3, \dot{x}_3, \ddot{x}_3$ heave, heave velocity and heave acceleration

$x_4, \dot{x}_4, \ddot{x}_4$ roll, roll velocity and roll acceleration

$x_5, \dot{x}_5, \ddot{x}_5$ pitch, pitch velocity and pitch acceleration

$x_6, \dot{x}_6, \ddot{x}_6$ yaw, yaw velocity and yaw acceleration

A major disadvantage of the fin-type stabilizers is that they depend upon the forward movement of the vessel in order to give the necessary lift, and this lift reduces very rapidly as the speed drops (approximately by the square of the speed). Many vessels have occasions to operate at low speed; Mine Countermeasures ships (MCM), Floating Production, Storage and Off Loading vessels (FPSO), ships during launching or recovering boats or loads, cable layers, and survey ships. Relying merely on fins leaves the ship at the mercy of the waves. Therefore ships operating at low speeds require an alternative system for stabilization; one solution is anti-roll tanks.

The simplest type of roll stabilisation tank is the free surface tank; this is simply a tank with uniform cross-section partly filled with water, usually located well above the centre of gravity. The notion of making use of a free liquid, quelling oscillations, is not new. The method of testing whether an egg is raw or cooked, by making it oscillate in the direction of its largest diameter, and observing whether the oscillations are few or many, will suggest itself as an example of a semi-liquid reducing oscillations. This is basically the first type of tank to be developed with pioneering work conducted by Sir Philip Watts [68;69] in 1885.

As the water moves from one side of the tank to the other side, the position of the centre of gravity of the water inside the tank changes, causing a moment equal to the weight of the water times the distance between the centre of gravity of the tank and the centre of gravity of the ship (close to the middle line plane). This moment opposes the moment induced by the waves and tends to stabilize the ship. The overall function of the system is independent of the ship forward speed, therefore suitable for low speed or even stationary operations.

Over time different kinds of anti-roll tanks have been developed and in some cases implemented in ships. However, in many cases the hull geometry of a ship may preclude the application of these tanks. Further more it is difficult to control the water, sloshing from one side of the tank to the other, threatening the safety of the ship in rough weather. The main disadvantage of tanks is, however, that although there is considerable roll

reduction when the encountered waves have the same frequency as the ship's roll resonance frequency, the roll is increased in other excitation frequencies due to the extra degree of freedom tanks induce, and in reality a ship is mostly excited by waves having frequencies other than the roll natural frequency. The water in the tank does not get athwart ships quickly enough as the ship rolls. This means that the system has a time delay when responding to a signal demanding a stabilizing moment. The efficiency of the tank would be improved generally if changes were made to enable the water to get athwart ships more quickly.

The roll stabilization of ships at slow or zero speeds still remains a challenge in marine engineering and is further complicated by the introduction of multi-hull ships. At the 1999 RINA Trimaran conference, slow speed roll stabilization was identified as a key issue in the design and assessment of Trimaran FSCs [57].

It will be seen that during the development of a tank stabilizing system the weak link in most systems was the control system. While the ideas of the 19th and early to mid 20th Centuries were sound the technology to implement them was not available, only now with advanced control theory and high speed computing power can the potential of some of these systems be exploited. For all above it seemed that there is a need for a thorough investigation in the domain of anti-roll tanks.

1.1 Aims and objectives

The major objective of this thesis is to apply current advanced technological and computational techniques to some older ideas that could not be developed in the past because of practical/theoretical limitations. It is therefore intended to:

- Explore the area and identify the reason for previous failings of anti-roll tanks by a thorough review of the literature available on the subject.
- Initial investigations suggest that anti-roll tanks have always been controlled using feedback controllers. This is while roll stabilization is a form of noise

Chapter 1

1 Introduction

Since the rise of steam power for ship propulsion and the consequent disappearance of sails on seagoing ships, there have been many attempts to reduce the roll motion of ships. The term 'roll stabilizer' is in fact a misnomer, since all ships operating under normal conditions are inherently stable in themselves. In fact any device fitted to a ship to reduce the roll should be called a 'roll damper'.

The importance of roll stabilization depends on the type of the ship. However, no matter what the application of the ship is, a stable platform is always desirable for many reasons including:

- Increasing the safety of ships
- Increasing the efficiency of ships
- Passenger comfort and minimising the effect of sea sickness
- Increasing the efficiency of crew and machinery
- Preventing damage to cargo
- Increasing the safety of aircraft landing
- Increasing the accuracy of missile targeting and radar

There have been many devices to reduce or damp the roll motion of the ships. Fins are perhaps the most widely used roll stabilizers, which have the capability of reducing the roll up to 80%, and only consuming little weight and volume of the ship, however they do increase drag.

cancellation and noise cancellation it is widely performed with feedforward controllers. It is therefore intended to apply some of the control strategies used in other noise cancellation applications to the challenging problem of roll stabilization and investigate the feasibility of applying feedforward control.

- The method is then further investigated more practically to determine whether the power consumption is justifiable.
- This project also aims to develop a new technique which can solve the problem of roll stabilization of multihull ships in particular at slow speeds. The method involves investigating the possibility of using free flooding roll stabilizing tanks in the side hulls which are low value volumes and can be effectively used for the purpose of roll stabilization.

In order to reach these objectives, the layout of this thesis is as follows:

Chapter 2 reviews the development of ship anti-roll tanks from the 1880's to the present day including their modelling and control strategies. Mention is also made of other ship roll stabilization systems and the application of the technology to stabilization of other structures. The potential for the use of roll stabilization tanks on modern, high speed multi-hull craft which also have a low speed operational requirement is also discussed. This chapter provides the reader with a general idea of the problems involved in roll stabilization at slow speeds and anti-roll tanks in particular. The reader therefore becomes aware of the essential work that is lacking from the domain, and the necessity of this PhD becomes clearer. This chapter formed the basis of a review paper published in "Ocean Engineering" journal [45].

Chapter 3 introduces the general theory of adaptation and explains some models used in adaptation, the common methods used for adapting these models and some applications of adaptive systems. The limited time and space precludes explanation of every aspect of adaptive theory, and that is not the goal of this thesis. The aim is to familiarise someone who already has knowledge of automatic control with the theoretical concepts that are required to understand fully the applications presented in the following chapters.

Chapter 4 introduces one of nature's forces that is responsible for rolling a ship: sea waves. It explains the physics of waves and the statistical modelling usually applied. It then investigates the predictability of waves on a short period of time and describes different models for predicting them using the concepts of adaptive control explained in Chapter 3. The results from this chapter are used in the following chapters.

In Chapter 5, U-shape anti-roll tanks are mathematically modelled by two different approaches: one method uses an Euler equation and is based on fluid mechanics principles; the other uses the Lagrange energy method and is based on dynamics of solid materials. The intention of this chapter is to compare the two approaches and investigate that given a tank of specific parameters and using same assumptions whether two methods so different in their fundamentals provide the same model or not.

Chapter 6 presents a new strategy in controlling the actuating pumps of an active U-tank (dynamics of which is explained in Chapter 5) based on predicting the waves (explained in Chapter 4) reaching the ship in the near future according to the history of the waves in the past few minutes. The pumps therefore move the water in a manner to counteract the wave moments by the time they arrive. The idea is then examined through simulation on some existing ships and has demonstrates overwhelming results. It is also examined whether using a blower, instead of a pump, could be feasible and further improve the roll stabilization effect of the anti-roll tanks.

Chapter 7 focuses more on the control side problem of the active U-tank and presents a genuine strategy in controlling the actuating pumps of an active U-tank with an adaptive inverse controller using filtered-x least mean square (LMS) algorithm. The concept on adaptive control is explained briefly based on the knowledge the reader has already acquired from Chapter 3. The idea is then investigated through simulation of some ships. This chapter is based on a paper presented at the 7th IFAC Conference on Manoeuvring and Control of Marine Craft (MCMC'2006) held in Lisbon, Portugal, September 2006 [43] (See Appendix III).

Chapter 8 considers a different tank configuration which is called "n-tank", also known as free flooding tanks. It suggests that parts of the side hulls in multi-hulls be used as a means of roll stabilization using the sea water. The port and starboard legs are open to the sea and there is no internal water connection between the two tanks but there may be an air connection at the top of the tanks. The configuration of "n-tanks" makes them particularly useful for application to multi-hull craft. A requirement is developing for high speed multihulls to have good sea keeping at low speeds. Different controls of the opening port and use of compressed air to assist emptying the tanks is then investigated on a simulation model of a trimaran. This chapter is also based on a paper presented at the World Maritime Conference (WMTC) in London, March 2006 [44] (See Appendix III).

Chapter 9 summarizes the results of the projects and suggests some further work to follow this PhD.

The area of active anti-roll tanks is an area yet to be explored. There are many new ideas that are well worth investigating, and many existing ideas that can be further developed. This project has aimed to fulfil these gaps and apply advanced control strategies to the existing anti-roll tanks together with originating new and genuine ideas to solve the problem of roll stabilization at slow speeds.

Chapter 2

2 Development of Anti-roll Tanks

2.1 Introduction

The excessive motion of a ship can seriously degrade the performance of machinery and personnel. Roll has typically the largest amplitude of the all the degrees of freedom and yet it is often the least damped. Simple damping of roll motion can be achieved by adjusting the underwater hull shape and by the addition of bilge keels but the addition of any hull appendages will inevitably increase the hull resistance. Damping can only reduce motion, never eliminate it.

In the age of sail roll was not such a problem as the roll of large sailing vessels was controlled by the action of the wind on the sails and the large keel. Additionally there was no power available to drive any stabilizing machinery. It was not until the advent of ocean going steam ships, with no sails and large coal bunkers that roll became a serious problem. Many ideas were suggested for the reduction of roll. Some very early systems had cabins, or whole sections of the ship, mounted on gimbals. In 1906 a German torpedo boat was fitted with a large gyroscope to try and reduce roll motion. A more serious solution involved moving a large mass transversely to achieve the required restoring moment. This system was not very successful or popular. It required considerable power and had a slow response time; in addition it occupied a considerable volume in a prime location within the ship. This idea has been recently revisited on a Japanese 190t displacement high speed survey vessel which had a 3.5t mass on a curved track under computer control [36]. The French aircraft carrier *Charles de Gaulle* has 500t of moveable masses mounted under its flight deck; these are used for heel compensation during tight turning manoeuvres rather than roll compensation. An adaptive control system is used which moves the masses to counteract the forces induced by rudder motion [56].

In the 1870's it was suggested that the single moving mass be replaced with a transversely mounted tank partly filled with water, this improved the response time, eliminated the powering requirement and permitted tuning of the system by varying the depth of the water in the tank. The simple free surface tank was subsequently replaced by a pair of tanks, one port the other starboard which were connected by a water duct at their base, in some configurations a second connection is made between the top of the tanks to permit control of the air flow between them. This configuration of tanks is known as U-tank system (from its shape) and it solves many of the problems of Watts' simple free surface tank. More recently U-tanks have evolved further and the connecting duct at the base of the tanks permitting transfer of fluid has been removed completely. Instead the tanks are open to the sea. There is usually a duct at the top of the tanks to permit transfer of air. This configuration is usually called free-flooding tanks but because of the possible control of the air pressure the tanks are not truly free-flooding. An alternative name which relates to their shape and is consistent with the previous type of tanks is n-tanks. As will be shown free-flooding tanks are particularly suitable for multi-hull craft. In their paper, Sellers and Martin [54] have described the selection and evaluation procedure of different roll stabilizing systems with emphasis on practical aspects. They have suggested that anti-roll tanks can be employed not only in roll stabilization but also in operations requiring reduction of roll acceleration by increasing the roll period. Application of moving masses and tanks is not restricted to ship stabilization. They have been successfully used for vibration damping of tall buildings due to wind induced vibrations (e.g. John Hancock Building Boston has tuned mass dampers and the Nagasaki airport control tower has a tuned liquid column damper) and earthquakes (many Tokyo and Kobe tower blocks) as well as offshore floating structures and even some satellite vibrations. A good review on the application of liquid dampers is provided by Yalla [74].

An alterative strategy to moving the centre of gravity of the ship transversely to create a restoring moment is to apply it directly. With the possible exception of air cushion vehicles the power required to do this directly with jets of water or air would be excessive. Another approach is to use the lift generated by a hydrofoil. The force counteracting the roll motion is generated by the passage of the foil through the water and only minimal power is required to vary the angle of attack. The rate of response is very high as the fin angle can be changed rapidly. There is a significant resistance penalty. Even a good fin system can only achieve a lift to drag ratio of little more than 4:1 and unless the fins are retractable (with the cost and complication associated with this) they are always going to provide drag even when not in use. As drag is proportional to

speed squared this is a particular issue for high speed vessels. As stabilizer fins are external to the hull they are vulnerable. Their size is usually compromised by vulnerability considerations and they are usually shorter than ideal. Short fins are less effective as a greater proportion of their span is submerged in the hull's boundary layer. Because fin stabilizers rely on forward motion to produce lift they are less effective at slow speeds and below about 5 or 6 knots virtually useless and it is recognised that alternative stabilisation systems are required such as tanks [47]. By comparison tank based systems are most effective at lower speeds, even when stopped.

No stabilizing system, tank or fin, can be effective without a good control system and the two must be considered together. It will be seen that during the development of tank stabilizing system the weak link in most systems was the control system. While the ideas of the 19th and early to mid 20th Centuries were sound the technology to implement them was not available, only now with advanced control theory and high speed computing power can the potential of some of these systems be exploited.

2.2 The development and types of tanks

2.2.1 Free Surface Tank

This was the first type of roll stabilizing tank to be developed and was based on the pioneering work conducted by Sir Philip Watts, he read a paper at a meeting of Royal Institution of Naval Architects (RINA) in 1883 with another paper two years later [68;69]. He proposed a large, uniform cross-section tank partly filled with water, placed athwartships and usually located well above the centre of gravity, see Fig. 2-1. The principle was based on the work by William Froude [26] who was the first to frame the effect of waves on the rolling motion of ships. In the papers and the discussion thereon, Watt and Froude described in detail the mechanism by which a roll damping moment is created by the wave action of a fluid in a rectangular tank placed aboard a ship. The shifting mass of the fluid as it flows backwards and forwards across the tank exerts a roll moment on the ship and, by suitable design, this can be arranged to damp the rolling motion.

Watts suggested that the way in which an anti-roll tank operates in this respect would be readily understood by regarding the water as doing the reverse to what is done by men in the process of rolling a ship in still water. In the Eighteen and Nineteenth centuries it was common practice for a team of men to run from side to side to test the stability of a ship. Watts' description is reproduced below:

"The men are timed to run from side to side in advance of the roll, and their weight tends to increase the heel; whereas the chamber, which is arranged to keep time with the ship, necessarily lags behind the roll, as the chamber must become inclined before the water has any tendency to run across by its own weight, and therefore tends to diminish the heel. Imagine the ship is at rest and the men are at the middle of the port and the starboard. Now, if the men were moved instantaneously from the middle line to the port end, the ship would start rolling by harmonic motion, and if at the instant she arrives at the extreme inclination the men were again instantaneously shifted to the starboard end the return roll would be more than the one reached at the port side, and so on; the rolling angle would increase as the men are moved to the other side successively. As, instead of moving over instantaneously, the men require a definite time in moving over, their motion must lead the rolling motion in order to be most effective in increasing the roll. The longer they can remain at the side at the end of each run, the more effect will their weight have in rolling the ship, but they must start from any side when the ship heels towards that side, as so to cross the middle line when the heel is a maximum, i.e., they must run ***uphill****. Now, if the ship were rolling from any cause, and it were sought to bring her to rest by running men from side to side, it is obvious that their motion must be the reverse of above, i.e., they must always be running* ***downhill*** *instead of* ***uphill.***

It will be obvious that the motion of the centre of gravity of the water in the water chamber of a ship rolling amongst waves, will tend to approximate to that of the men when running as described for the purpose of reducing rolling. Thus, if the shape of the water chamber and the depth of the water are such that the centre of gravity of the water moves as described, the effect of the water chamber is to increase the righting force and cause the ship to move more slowly than she otherwise would, so that she acquires less angular momentum on reaching the upright, and therefore tends to roll less deeply the other way" [69]. (Fig. 2-1)

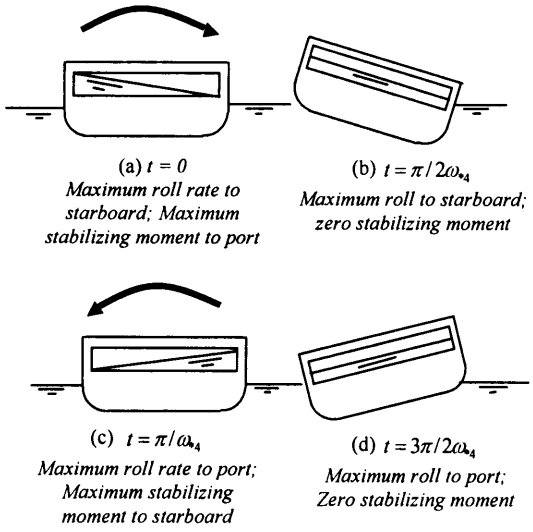

Fig. 2-1 Ideal motion of water in the tank (Based on Watts [69])

In 1882 Watts and Froude examined this theory with a full-scale trial and excited *HMS Inflexible* by moving men. They managed to roll the ship by 12°. The motion of the ship was recorded with a variety of water depths in the tank. It was observed that the roll damping was most effective when the tank was about half full, which made the natural period of the water the same as the natural period of the ship and reduced the roll by 37.5%. They realized that the water in the tank did not travel athwart ships quickly enough as the ship rolled; they suggested that the efficiency of the tank would be improved if changes were made to enable the water to get across the ship more quickly. They also noticed that beyond 4° heel the rolling resistant force of the tank reached its maximum and remained the same, the phenomenon known as 'saturation' in the modern control. Although the tank acted satisfactorily, interest died away in the years that followed and the works of Watts seems to have been nearly forgotten. It is not clear from the literature why such tanks fell into disuse, although the inefficient steam engines and boilers of the day may have been contributory factors, since large quantities of coal were required and all available space was used to carry it. Noise generated in the tank may also have been a factor. Free surface passive tanks have not been abandoned and in 1998 one was retrofitted to the *MV Searoad Tamar* in Australia. The tank was 23m×7m×5m and extended across the full beam so while it had a significant impact on the ship's upper deck it drastically reduced the roll motion. An unexpected bonus was an 8% reduction in fuel consumption due to improved course keeping and drag reduction [23].

In 1966, Vugts [67] experimentally investigated the concept of rectangular tanks using a model with certain simplifying assumptions; the motion was considered periodic and the magnitude of the motion created by the moving water mass, the influence of tank parameters on the amplitude and phase of the moment was examined [13]. They calculated the effect of four different tanks on a cargo-liner of "Straat H"-class of the Royal Interocean Lines in irregular waves. The tanks ranged between 0.5% to 1.1% of water displacement and theoretically introduced up to 80% roll reduction in periodic waves and up to 50% in irregular waves. They stated that an advantage of rectangular tanks is that they can easily be adapted to another condition of loading by changing the water depth, a feature not so readily achieved in U- tanks or n- tanks (explained later).

More recent experimental work was done by Ikeda and Yoshiyama [32], in which the coupling effect on the performance of a rectangular anti-rolling tank was investigated. The results of the bench test of an anti-rolling tank including the effect of sway motion as well as roll motion demonstrated that the sway motion reduced the reduction of the roll angle by the anti-rolling tank and lengthened the natural period of the tank. Bass [7], conducted full-scale sea trials of free-surface tanks in which three sister vessels took part: the *Newfoundland Tradition*, the *Newfoundland Explorer*, and the *Newfoundland Mariner*. Results showed up to 82% roll reduction in light wave conditions. The penalties identified were the volume occupied by the tanks and the reduction of stability due to the free-surface effect, a particular concern when a tank is to be retrofitted to an existing ship.

It was observed that the performance of free-surface tanks is maximized when the natural frequency of the tank is tuned to be close to the roll natural frequency of the ship. This is mainly done by altering the water level inside the tank. This confirmed the findings of Watts and Froude from a century earlier. Different responses of tanks can be obtained by changing their shapes, two modifications of such tanks are presented in Fig. 2-2.

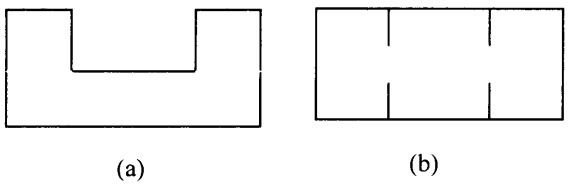

Fig. 2-2 Plan view of modified tanks a) C-shape tank b) rectangular tank with baffles

One disadvantage of rectangular tanks is that it is difficult to control the water, rushing freely from side to side in the tank, threatening the safety of the ship in rough weather. Sometimes a limited control is exerted over the motion of the fluid by installing a restriction or baffle in the centre of the tank. Lee and Vassalos [37] experimentally showed that the performance characteristics of an anti-roll tank could be 'tailor-made' by a judicious application of flow obstructions. The baffles they used in their rectangular tank together with the roll amplitude response of the ship are presented in Fig. 2-3 and Fig. 2-4. It is clear from the figures that the undesirable effect of roll increase at frequencies lower than the natural frequency has been eliminated.

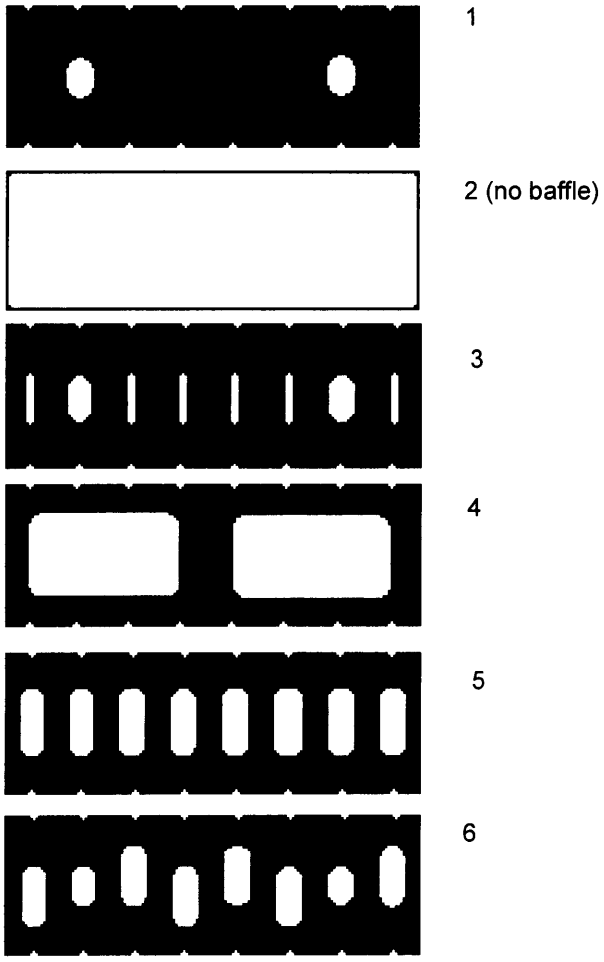

Fig. 2-3 Configurations of baffles tested (From Lee and Vassalos [37])

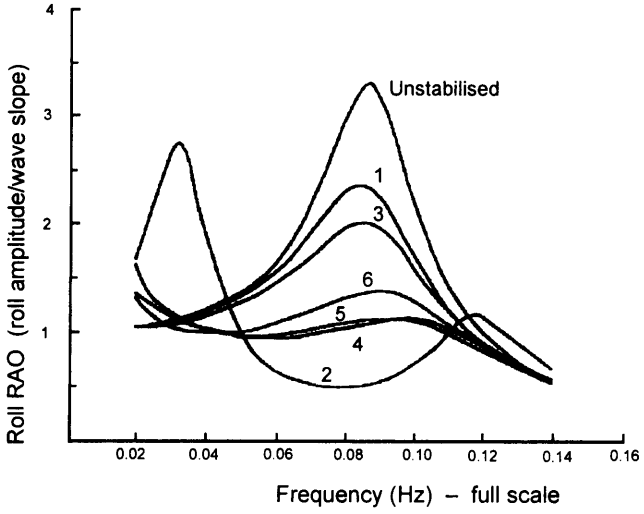

Fig. 2-4 Estimated RAO of the vessel, GM=2 m, $\gamma = 0.15$, $\alpha = 2.5$ deg (From Lee and Vassalos[37])

About the same time, Francescutto and co-workers [25] also described the effect of baffled anti-roll tanks and showed similar results to Lee and Vassalos'. They developed a mathematical model of the partially filled tank based on Reynolds Averaged Navier-Stokes equations. Numerical simulations for a baffled and unbaffled rectangular tank were validated with experimental tests and showed good agreement. The main conclusions derived were that for the unbaffled rectangular tank, the ship becomes a lightly damped two degree-of-freedom system in which two different natural frequencies appear (see curve 2, Fig. 2-4) The values of which are strictly related to the characteristics and the level of the water in the tank, the tank geometry and its own position in the ship. The roll reduction depends solely on the level of the water inside the tank. In the case of a baffled tank, the two natural resonance peaks are not as sharp as the unbaffled case and the response tends to get smoother as the water height increases compared to the baffle height. The baffles generate large amplitude travelling waves, and dissipate energy by generating vortices in the water. The baffled tank acts as a strong damper and results in almost 50% roll reduction. One of the most valuable results derived from this paper was that passive tanks can "detune" as well as increase damping.

Based on the same concept, Birmingham and co-workers [12], designed a passive-controlled tank using moving obstructions. The preliminary design of the valve mechanism was based on

an array of four inter-connected butterfly valves, to be actuated in tandem and with operating angles between 0° and 90°. They suggested, but did not implement, artificial intelligence to control the valves, so the system would be able to function to maximum effectiveness at all times, despite changing loading and operating conditions and sea states. Simulation results were confirmed using a model excited by 'regular' waves; they matched with Lee and Vassalos's results.

Recently studies have tried to perform numerical simulations of the complicated 3D motion of water in tanks together with the sloshing at the free surface, both for simple open tanks and U-tanks. A specific numerical study using a 2D finite element method for U-tube passive anti-rolling tanks was done by Zhong and co-workers [76] and Popov and co-workers [51] who reported numerical analysis of sloshing in a road container with a Marker and Cell (MAC) type method for tracing the free surface evolution. Many papers have reported on the sloshing phenomenon in a rigid rectangular tank and theoretical and experimental research has been carried out by means of the shallow water wave theory ([66], [62], [6], [46], [22], and [31]); boundary element methods [38]; finite element methods, Volume of Fluid (VOF) method [18]. Extensive comparative studies on sloshing loads has been made by Cariou and Casella [17] and Sames and co-workers [53]. Most of the methods reported were based upon finite difference, finite volume approaches or even shallow water equation solvers [60].

Another interesting solution was proposed by Souto and co-workers [58-60]. They simulated the motion of water using the smoothed particle hydrodynamics method where the fluid is represented by a set of particles which follow the fluid motion and have the fluid quantities such as mass and momentum. Associated with each particle are its position, velocity, and mass. They validated their method by performing experiments on different kinds of free-surface tanks such as rectangular tanks with and without baffles and on a C-tank, see Fig. 2-2a, and showed very good agreement between the simulation and experimental results.

2.2.2 U-Tanks

The simple free surface tank has three practical problems; two due to the sloshing of the large free surface and the third to its location. Sloshing makes it difficult to control the water and adversely affects stability while the tanks required location, above the centre of gravity and near

the centre of the ship, is prime usable space. These problems were solved simultaneously with the U-shaped tank suggested by Frahm [24]. Two reservoirs were connected at the bottom by a water duct, and at the top by an air duct. In some later designs the air duct was removed and the tanks vented to atmosphere. The water oscillation in each reservoir could be controlled by the air connections (Fig. 2-5). The air duct served first of all to stop the movement of the water by simply blocking the connection. Besides, the air passing through the upper connection could be more or less throttled in order to adjust the oscillations of the water to the condition of the sea. Frahm tested a U-tank on two passenger steamers *Ypiranga* and *Corcovado* and gained significant roll reduction by using tanks of 1.3% to 1.5% of the ship's displacement. He also commented that the best location to place the tanks is above the centre of gravity, but they are now moved away from the centre of the ship. Subsequently Biles [11], used a model to further investigate Frahm's tank and commented that the tanks perform better if the ratio of the natural period of the tank to the natural period of the ship was 0.79 than when it was approximately 1.0. The later being the optimal case for free surface tanks. He also realized that although there was considerable roll reduction at resonance frequency, the roll was increased at other frequencies. An obvious method of controlling the fluid flow is to insert valves in the fluid channel.

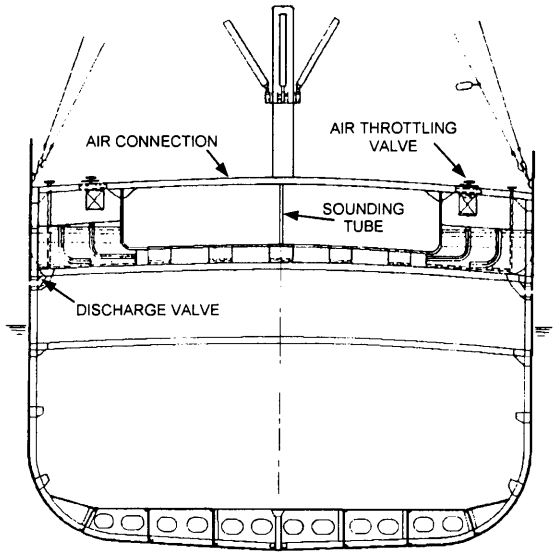

Fig. 2-5 Frahm tank on SS Ypiranga (From Vasta and co-workers [65])

Before World War II, Frahm's passive tanks were installed in over a million tons of German shipping, including the passenger liners *Europa* and *Hamburg* and met with moderate success. It was found that for ships with a small metacentric height operating in seas with a regular wave pattern, good results were obtained with a roll reduction of approximately 50%. However, in choppy seas with no regular pattern, the results were poor, frequently with no observed roll reduction at all [9].

A logical development of the Frahm system was to pump the water from one leg of the U to the other, rather than relying on the ship's rolling motion exclusively for the transfer. By doing so, a limitation of the passive tanks with their dependence on resonance could be largely overcome. Such tanks are generally known as U-shape activated tanks or simply "active tanks". A system was evolved by Bell and Walker [8], which achieved more than the damping effect of a passive–type tank and also did not involve setting into motion a long column of fluid. Fig. 2-6 shows the arrangement of this system. It is seen that the impeller which rotates continuously drives fluid from the lower to the upper of the two ducts connecting the port and starboard tanks. Fig. 2-6a shows the condition when no signal is developed in the sensing unit. The control valves in the ducts are then maintained in the halfway position and the fluid circulates into and out of both tanks, the level in each tank being the same. In Fig. 2-6b a signal has been received due to the wave on the port side of the vessel causing a rolling acceleration, and the valves are operated, the exit from the port tank being closed while its entry is fully open, and conversely the exit from the starboard is fully open and the entry closed. The fluid flows from one tank to the other to counter the roll acceleration due to the forces of the sea. In Fig. 2-6c the signal is presumed to have continued in spite of the opposing moment due to the tank on the port side being filled, and saturation of the stabilizer occurs. The impeller remains rotating at constant speed, maintaining the different fluid level between the two tanks, but transferring no more fluid.

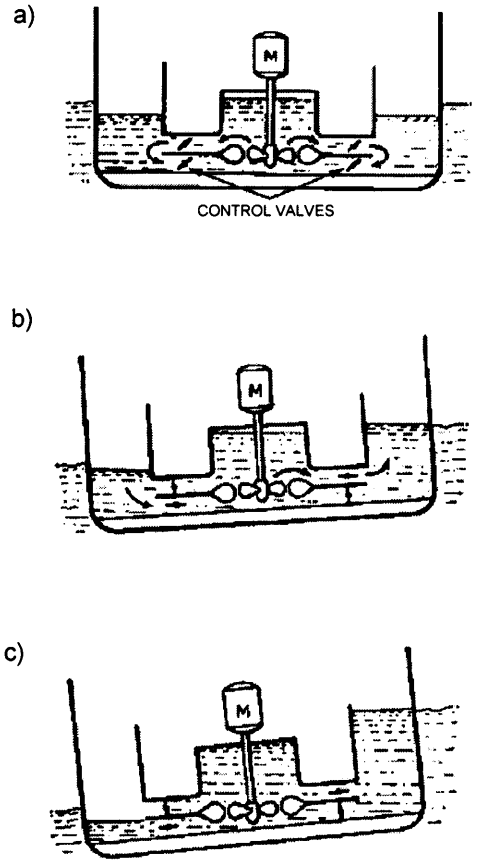

Fig. 2-6 Activated anti-roll tank (From Bell and Walker [8])

For an activated-tank stabilizer system to be successful it must not require excessive power to operate the impeller or the valves. Ample area must be provided in the ducts to keep the fluid velocity low, and the tanks designed for a minimum of head difference to give the stabilizing moment required. Depending upon the size of the vessel the head may vary from 0.3m up to about 2.5m for large vessels. The exact value is a compromise between the head of fluid, which must be as small as possible for minimum power, and the tank cross section which must also be small to limit the free-surface effect. Thus, for a given weight of fluid required for stabilization, the smaller the head the smaller the power, but the larger the cross section required with the corresponding loss of metacentric height.

Another feature of the system is that, as may be seen in the figures, a central tank may be provided from which fluid may flow on demand in the direction permitted by the valves. This tends to act as a buffer against the varying load on the impeller drive, smoothing the extremes of power but at the expense of a larger and more complex system.

Another application of the activated tank system was installed on the World War II German cruiser, *Prinz Eugen.* Here the rapid transfer of water from one tank to the other was accomplished by air pressure provided by a turbine-driven blower. The quantity of water displaced was governed by a small gyroscopic control mechanism. For moderate-sized vessels, a valve system in the fluid channel is quite a feasible piece of engineering but, as the size of the vessel increases, and also in the case of bulk carries and oil tankers where the metacentric height also increases, the valve required becomes impracticably large and would require very considerable power to operate. An alternative for control is immediately apparent, as seen in Fig. 2-7. The tank system is arranged to be effectively sealed, although a small vent can be provided, and the port and starboard tanks connected by the fluid channel below in the opposite direction. If the control is now achieved by valves in the air channel, a considerable economy can be affected and, because air is compressible, there will be no harmful hammer effects if a valve is closed rapidly. A secondary effect of control by the air channel is that, since the air is compressible, the precision of the control will be reduced, but it has been found in practice that effective controlled passive stabilization can be achieved using this method.

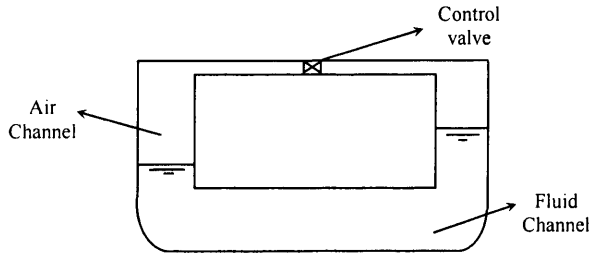

Fig. 2-7 Arrangement of air controlled passive tank (Based on Bell and Walker [8])

Since 1999 a number articles have been published suggesting methods of improving the response of anti-roll tanks ([1-4]). One of them is Flume's HEEL-AWAY List Control System, which utilises an axial flow pump driven by an internal hydraulic motor and is said to have a much faster reaction time than those which utilise centrifugal, constant speed, axial flow pumps. The system is always running and available for immediate response to any correction requirements. In the second article it is noted that using multiple passive stabilization tanks provides better results than using a single massive tank. Intering of Germany, now owned by Rolls Royce,

produce U-tanks where the water level is controlled by air pressure. An interesting innovation is to replace water with a denser fluid which is claimed to reduce the required volume by more than 30%. They have also developed a system for damping parametric roll, a particular problem of Panamax container ships and cruise liners.

2.2.3 Free-flooding tanks

Various modifications of the original 1911 Frahm anti-rolling tank system have been developed and installed. In some installations, the horizontal leg of the U-tank was entirely removed and the bottoms of the tanks were opened to the sea, Fig. 2-8. One of the few cases of installation of free-flooding tanks was in 1931 and 1932 when tanks were retrofitted to 6 USN cruisers of the *Pensacola* and *Northampton* classes. The tanks had no air cross connection, despite initial misgivings the tanks were successful reducing the roll motion by 30-40% and increasing the roll period by 20%. Unfortunately no other information is available to see whether the roll reduction claimed occurs for all wave frequencies and amplitudes or it is the maximum roll reduction reached in a particular working condition.

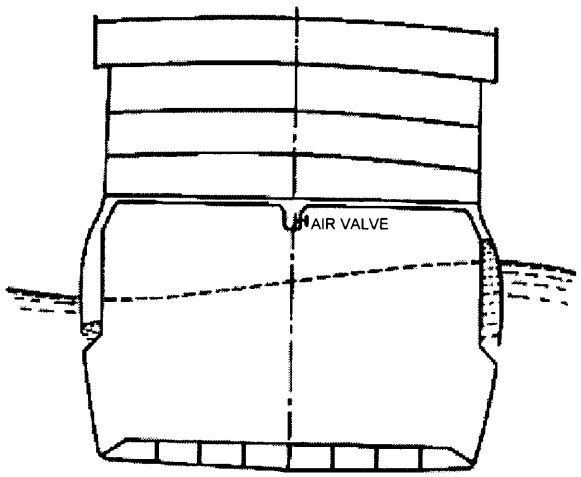

Fig. 2-8 Frahm tank with horizontal leg removed as fitted on the *Deutschland* (From Vasta and co-workers [65])

In 1958 a more advanced version of free-flooding tanks were tested on a model in the Denny Model Ship Tank at Stevens Institute of Technology (Fig. 2-9). It bears some resemblance to one of the types of Frahm tanks but the operation is entirely different. Two tanks are provided, one on either side of the vessel and each is open to the sea, but there is no cross connection to permit direct transfer of water between the two. There is a pipe connecting the tops of the tanks but this is for the supply of low pressure air. If the ship rolls and the valve in the interconnecting air channel is left open, the tank on the lower side will fill with water. At the end of the roll, the valve is closed, this traps the water in the tank and it is then lifted during the next half roll, at the end of which the valve is opened briefly. During this interval water is discharged from one tank and enters the other. The full tank is now in the lower position, and damping of the motion of the vessel occurs as each tank is in turn raised full of water. Results showed that this system could reduce roll by about 60% ([65]).

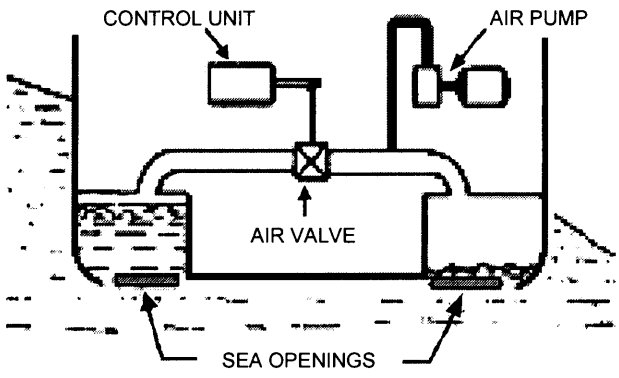

Fig. 2-9 Denny model tank (From Bell and Walker [8])

The Slo-Rol system developed by Dr G Bergman of SeaTek International Inc. uses a similar principle but it relies on compressed air for control of the water levels, there are no valves at the base of the tank. It was designed for, and has been installed on, various stationary drilling rigs and vessels used in the oil industry. The tank tops are below the water line so that by venting the tanks they flood completely effectively switching off the system. A disadvantage of this system is that the tanks must be built and regularly tested to withstand high air pressures.

In 1988 two configurations of free-flooding tanks (modified Slo-Rol tanks and tuned free-flooding) were analysed and model tested by Webster and co-workers [72], for retrofitting to the aircraft carrier, *USS Midway*. Both demonstrated that a significant reduction in roll could be achieved but both systems were compromised by having to be fitted into the existing and restricted volumes.

The effectiveness of the free-flooding tanks falls off as the ship speed increases, because at higher speeds, water cannot get into the flooding port. The main advantage of free-flooding tanks is that they do not need a water crossover duct, and therefore do not require major modifications of the ship when installation is contemplated in an existing ship. Free-flooding tanks use seawater as working fluid and this can have considerable impact on the design in terms of corrosion, fouling and maintenance. They also require a large flooding port in the side of the ship to allow the seawater to enter and leave the tanks. These flooding ports do not have a significant drag in calm water. However, as a result of water flowing into and out of the tanks when the ship is underway, a more significant momentum drag can ensue. At high speeds they can either be drained to reduce displacement or pressed full, the openings will still provide a small drag penalty. The entrance and exit flows at the flooding port are complex and difficult to model. In general free-flooding tanks are more difficult to analyse as the water's motion can no longer be approximated to a 2D case and more complex 3D solutions are required. Although free-flooding tanks have been demonstrated as successful, there has been a perceived reluctance of ship owners and shipbuilders to a system that opened the ship to sea water and alternative systems were sought for the commercial market.

2.3 Modelling the Tank-Ship system

The roll motion of the ship was first formulated by Froude [26]:

$$I_{44}\ddot{x}_4 + k_1\dot{x}_4 + k_2\dot{x}_4^2 + W\overline{GM}x_4 = W\overline{GM}\alpha_0 \sin\omega t \qquad \textbf{(2-1)}$$

where

$\overline{GM}$	Metacentric height
I_{44}	Ship longitudinal mass moment of inertia
k_1	Ship viscous damping coefficient

k_2 Ship quadratic damping coefficient

t Time

ω Frequency of the encountered waves

W Ship displacement

$x_4, \dot{x}_4, \ddot{x}_4$ Roll, roll velocity, roll acceleration

α_0 is the maximum wave slope; wave slope is obtained by differentiating the equations of wave height; and ς_0 is the maximum wave height (since $\alpha_0 = k\varsigma_0$ where k is the wave number) wave propertites are explained in greater details in Chapter 4.

Froude considered the effect of the tank by addition of a new term *S*, the stabilizing moment, into (2-1):

$$I_{44}\ddot{x}_4 + k_1\dot{x}_4 + k_2\dot{x}_4^2 + W\overline{GM}x_4 + S = W\overline{GM}\alpha_0 \sin\omega t \qquad \textbf{(2-2)}$$

He did not formulate the motion of the fluid inside the tank.

Goodrich [27], represented the combined motion of a ship with a tank stabiliser by two linear differential equations (τ is the tank angle and defined in Fig. 2-10):

Tank: $$\ddot{\tau} + k\dot{\tau} + \omega_t^2\tau = \omega_t^2 x_4 - \frac{\omega_t^2 h}{g}\ddot{x}_4 \qquad \textbf{(2-3)}$$

Ship: $$\ddot{x}_4 + K\dot{x}_4 + \omega_s{}^2 x_4 - \mu\omega_s{}^2\tau = \omega_s{}^2\alpha_0 \cos\omega t \qquad \textbf{(2-4)}$$

Where

k, K Damping coefficient of the tank and ship respectively

ω_t, ω_s Roll Natural frequency of the tank and ship respectively

h Distance of the tank above the rolling centre

μ Free surface coefficient factor

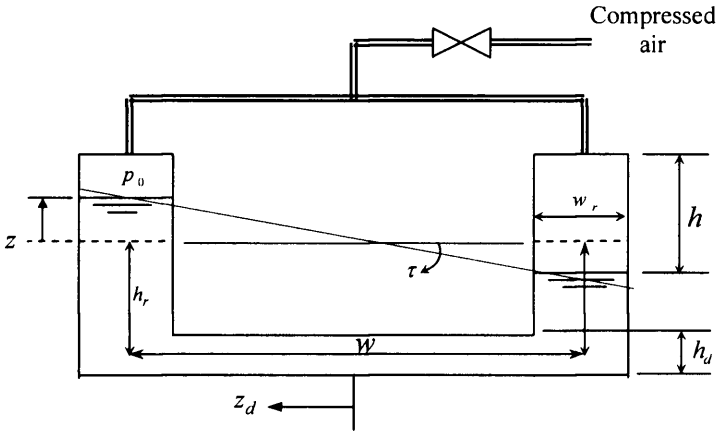

Fig. 2-10 U-tank and its geometric parameters (Based on Shyu and Kuo [55])

Comparing equation (2-4) with (2-2) it can be seen that $S = -\mu\omega_s^2 I_{44}\tau$, which means that the stabilizing moment is proportional to the tank angle. The only difference is that equation (2-4) does not contain the term $k_2\dot{x}_4^2$ which would make it non-linear. This is a justifiable simplification as $k_2 << k_1$ and it is now generally agreed that the roll motion of the ship is to a great degree of accuracy linear and no non-linear terms appear in the derivation of the equation of motion [37;40]. Solving the equations yields that amplification $A_{(\omega)}$ and phase angle $\phi_{(\omega)}$:

$$A_{(\omega)} = \frac{\omega_s^2}{\sqrt{X^2 + Y^2}} \tag{2-5}$$

$$\phi_{(\omega)} = -\tan^{-1}\frac{Y}{X}$$

Where

$$X = \left(\omega_s^2 - \omega^2\right) - \frac{\mu\omega_t^2\omega_s^2\left(1 + h\omega^2/g\right)\left(\omega_t^2 - \omega^2\right)}{\left(\omega_t^2 - \omega^2\right)^2 + k^2\omega^2}$$

$$Y = \omega\left[K + \frac{\mu k\omega_t^2\omega_s^2\left(1 + h\omega^2/g\right)}{\left(\omega_t^2 - \omega^2\right)^2 + k^2\omega^2}\right]$$

Goodrich then investigated the variation of tank damping, natural frequency, size and position on the amplitude and phase of the ship response theoretically and experimentally and realized the undesirable increase of roll angle at frequencies lower than the natural frequency, an example is shown in Fig. 2-11. This effect is even more pronounced if the natural frequency of the tank is not tuned to the natural frequency of the ship as demonstrated in Fig. 2-12. If the free surface coefficient μ is set to zero the tank is effectively removed from the ship.

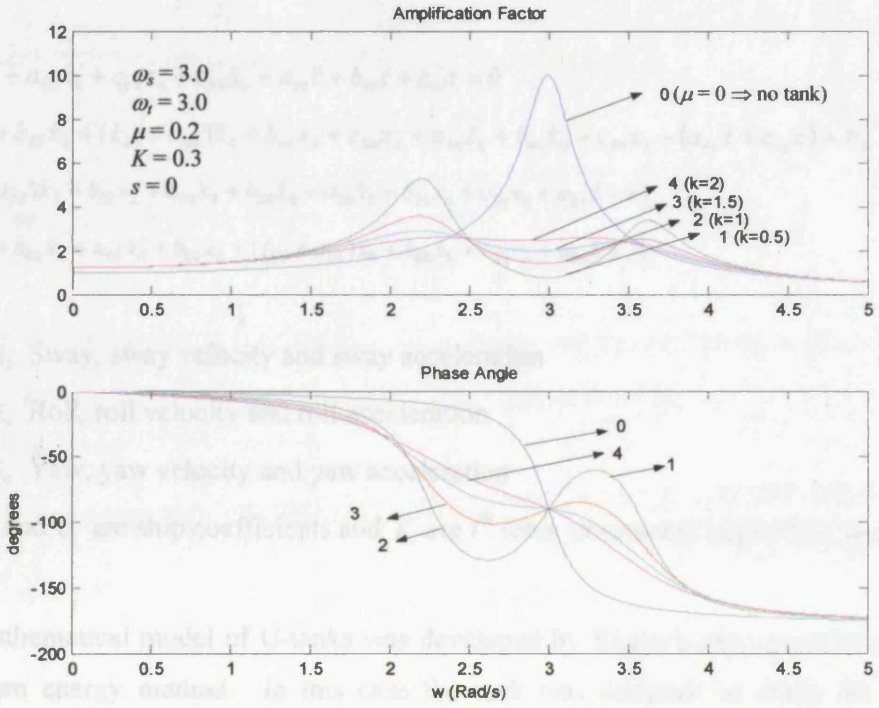

Fig. 2-11 Effect of variation of tank damping k with $\omega_t = \omega_s$ (Based on Goodrich [27])

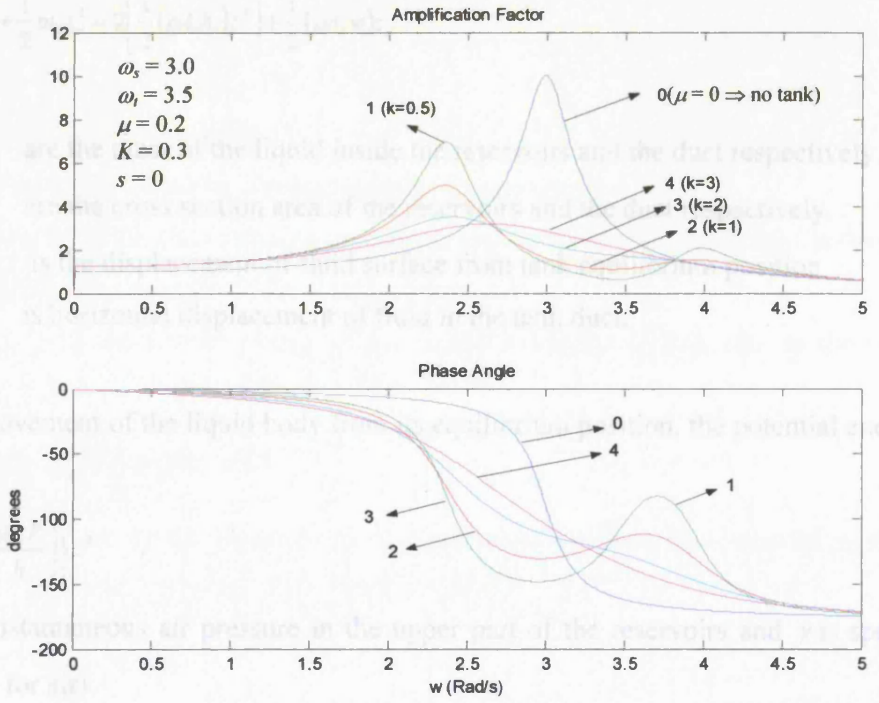

Fig. 2-12 Effect of variation of tank damping k with $\omega_t > \omega_s$ (Based on Goodrich [27])

Stigter [61], developed a theory for passive U-tanks using *Euler's* equation. A simplified version suggested by Lloyd [40], concludes that the equations of motions are:

Tank: $a_{\tau 2}\ddot{x}_2 + a_{\tau 4}\ddot{x}_4 + c_{\tau 4}x_4 + a_{\tau 6}\ddot{x}_6 + a_{\tau\tau}\ddot{\tau} + b_{\tau\tau}\dot{\tau} + c_{\tau\tau}\tau = 0$ **(2-6)**

Roll: $a_{42}\ddot{x}_2 + b_{42}\dot{x}_2 + (I_{44} + a_{44})\ddot{x}_4 + b_{44}\dot{x}_4 + c_{44}x_4 + a_{46}\ddot{x}_6 + b_{46}\dot{x}_6 + c_{46}x_6 - (a_{4\tau}\ddot{\tau} + c_{4\tau}\tau) = F_4$

Sway: $(m + a_{22})\ddot{x}_2 + b_{22}\dot{x}_2 + a_{24}\ddot{x}_4 + b_{24}\dot{x}_4 + a_{26}\ddot{x}_6 + b_{26}\dot{x}_6 + c_{26}x_6 + a_{2\tau}\ddot{\tau} = F_2$

Yaw: $a_{62}\ddot{x}_2 + b_{62}\dot{x}_2 + a_{64}\ddot{x}_4 + b_{64}\dot{x}_4 + (I_{66} + a_{66})\ddot{x}_6 + b_{66}\dot{x}_6 + c_{66}x_6 + a_{6\tau}\ddot{\tau} = F_6$

where

$x_2, \dot{x}_2, \ddot{x}_2$ Sway, sway velocity and sway acceleration

$x_4, \dot{x}_4, \ddot{x}_4$ Roll, roll velocity and roll acceleration

$x_6, \dot{x}_6, \ddot{x}_6$ Yaw, yaw velocity and yaw acceleration

a_{ij}, b_{ij} and c_{ij} are ship coefficients and F_i are i^{th} force or moment applied by the waves.

A simple mathematical model of U-tanks was developed by Kagawa and co-workers ([34] and [33]) using an energy method. In this case the tank was designed to damp the horizontal vibration of skyscrapers during earthquakes. The kinetic energy of the liquid inside the U-tank (Fig. 2-10) is as follows;

$$T = 2\left[\frac{1}{2}m_r\dot{z}^2\right] + \frac{1}{2}m_d\dot{z}_d^2 = 2\left[\frac{1}{2}(\rho A_r h_r)\dot{z}^2\right] + \frac{1}{2}(\rho A_d w)\dot{z}_d \qquad \textbf{(2-7)}$$

Where

m_r, m_d are the mass of the liquid inside the reservoirs and the duct respectively.

A_r, A_d are the cross section area of the reservoirs and the duct respectively.

z is the displacement of fluid surface from tank equilibrium position

z_d is horizontal displacement of fluid in the tank duct.

Due to the movement of the liquid body from its equilibrium position, the potential energy of the reservoirs is

$$U = \left\{\rho g A_r + \left(\frac{\gamma A_r P}{h}\right)\right\} z^2 \qquad \textbf{(2-8)}$$

where P is instantaneous air pressure in the upper part of the reservoirs and γ is specific heat ratio ($\gamma \approx 1.4$ for air).

From the continuity equation of the fluid is follows that

$$z_d = \frac{A_r}{A_d} z$$

Therefore the overall kinematic energy of the fluid inside the tank is

$$T = \frac{1}{2}\rho\left\{2A_r h_r + A_d w\left(\frac{A_r}{A_d}\right)^2\right\}\dot{z}^2 \qquad \textbf{(2-9)}$$

Based on the energy method

$$T_{max} = U_{max} \qquad \textbf{(2-10)}$$

Assuming the fluid response, z, is in the form of $z_0 \sin \omega t$ and by substituting equations (2-8) and (2-9) into equation (2-10) the natural frequency of the tank is obtained as

$$\omega^2 = \frac{2g + \frac{2\gamma}{\rho}\left(\frac{P}{h}\right)}{2h_r + \left(\frac{A_r}{A_d}\right)w} \rightarrow f = \frac{1}{2\pi}\sqrt{\frac{2g + \frac{2\gamma}{\rho}\left(\frac{P}{h}\right)}{L_e}} \qquad \textbf{(2-11)}$$

Where L_e is the effective length of tank being equal to $2h_r + \frac{A_r}{A_d}w$

Seven years later Shyu and Kuo [55] used the Lagrange method to develop Kagawa and co-workers' results to derive the dynamic equation of motion for the fluid inside U-type tanks. Again this was to damp the sway motion of structures in earthquakes, but the method could be extended to roll motion in ships. The derivation of the equations is based on the following assumptions:

1- The liquid is incompressible.
2- The air in the air chamber is assumed to be an ideal gas.
3- The velocity of the fluid remains constant along the reservoirs and along the duct.
4- No breaking waves occur in the liquid surface.

Based on Fig. 2-10 the kinetic energy of the liquid inside the U-tank can be shown to be as follows:

$$T = 2\left[\frac{1}{2}\rho A_r h_r\left(\dot{z}^2 + \dot{x}_2{}^2\right)\right] + \frac{1}{2}\rho A_d w(\dot{z}_d + \dot{x}_2)^2 \qquad \textbf{(2-12)}$$

Due to the movement of the liquid from its equilibrium position, the potential energy of the reservoirs is:

$$U = mg\Delta h = 2(\rho A_r z)g\left(\frac{z}{2}\right) = \rho g A_r z^2 \qquad \textbf{(2-13)}$$

From the continuity: $A_r\dot{z} = A_d\dot{z}_d$ **(2-14)**

Assuming that the liquid flow is fully developed and laminar and approximating the duct to a pipe of circular cross section of diameter *d*, then the pressure drop over a length *L*, is given by Poiseulle's equation , hence;

$$\Delta P = 32\frac{\mu L\bar{u}}{d^2} \quad \textbf{(2-15)}$$

where $\bar{u}$ is the mean velocity of the fluid and μ its viscosity.

According to the perfect gas law, pressure changes inside the air chamber can be expressed as

$$P_0V_0^{\gamma} = P_1(V_0 - A_r z)^{\gamma} = p_2(V_0 - A_r z)^{\gamma} \quad \textbf{(2-16)}$$

P_0 and V_0 are the corresponding pressure and volume of the air chambers when the liquid elevations in the reservoirs are in equilibrium. From equation (2-16) the pressure differential between the two air chambers is

$$P_1 - P_2 = P_0\left\{\left[1-\left(\frac{z}{h}\right)\right]^{-\gamma} - \left[1+\left(\frac{z}{h}\right)\right]^{-\gamma}\right\} \quad \textbf{(2-17)}$$

The non-potential force term in the Lagrange equation can be shown to be as follows

$$Q = \left[16\pi\mu h_r + 8\pi\mu L_e\left(\frac{A_r}{A_d}\right)\right]\dot{z} + P_0A_r\left\{\left[1-\left(\frac{z}{h}\right)\right]^{-\gamma} - \left[1+\left(\frac{z}{h}\right)\right]^{-\gamma}\right\} \quad \textbf{(2-18)}$$

L_e being the equivalent length of the pipe. From the Lagrange function, equations (2-12) and (2-13), the non-potential force equation, and using Lagrange method as

$$\frac{d}{dt}\left(\frac{\partial T}{\partial \dot{z}}\right) - \frac{\partial T}{\partial z} + \frac{\partial F}{\partial \dot{z}} + \frac{\partial U}{\partial z} = Q$$

The equation of motion of the liquid inside the U-tube tank becomes

$$\left[2\rho h_r A_r + \rho w A_d\left(\frac{A_r}{A_d}\right)^2\right]\ddot{z} + \left[16\pi\mu h_r + 8\pi\mu L_e\left(\frac{A_r}{A_d}\right)\right]\dot{z} + 2\rho g A_r z + P_0A_r\left\{\left[1-\left(\frac{z}{h}\right)\right]^{-\gamma} - \left[1+\left(\frac{z}{h}\right)\right]^{-\gamma}\right\} + \rho w A_r\ddot{x}_2 = 0 \quad \textbf{(2-19)}$$

If the liquid movement inside the tank is small compared to *h*, say $z/h < 0.25$, then

$$\left[1-\left(\frac{z}{h}\right)\right]^{-\gamma} - \left[1+\left(\frac{z}{h}\right)\right]^{-\gamma} \approx 2\frac{\gamma z}{h} \quad \textbf{(2-20)}$$

and equation (2-19) can be simplified as follows

$$\ddot{z}+\left[\frac{16\pi\upsilon\left(\frac{1}{A_r}\right)+8\pi\upsilon L_e\left(\frac{1}{A_d}\right)}{2\pi+w\left(\frac{A_r}{A_d}\right)}\right]\dot{z}+\left[\frac{2g+\frac{2\gamma P_0}{\rho h}}{2h_r+\left(\frac{A_r}{A_d}\right)}\right]z+\left[\frac{w}{2h_r+w\left(\frac{A_r}{A_d}\right)}\right]\ddot{x}_2=0 \qquad \textbf{(2-21)}$$

Therefore the sway equation of the structure becomes;

$$\ddot{x}_2+2\frac{m_s}{m_o}\omega_s\zeta_s\dot{x}_2+\frac{m_s}{m_o}\omega_s^2x_2+\frac{1}{m_o}\rho A_d\ddot{z}+\frac{1}{m_o}8\pi\mu L_e\left(\frac{A_r}{A_d}\right)\dot{z}-\frac{1}{m_o}\rho A_d\left(\frac{A_r}{A_d}\right)^2\dot{z}|\dot{z}|=\frac{1}{m_o}F_{excite} \qquad \textbf{(2-22)}$$

where ω_s is the natural frequency of the structure

ζ_s is the damping ratio of the structure.

m_s is the mass of the structure

m_o is the total mass of the structure and tank together.

The fifth term on the left hand side of (2-22) is the shearing force of the liquid acting on the tank wall and the last term is the force due to the change of the flow direction. Using simulation they derived the relation between the tank natural frequency and *P*, see Fig. 2-13. They also showed that when the mass ratio of the tank to the structure is greater than 3%, there is no significant improvement in efficiency.

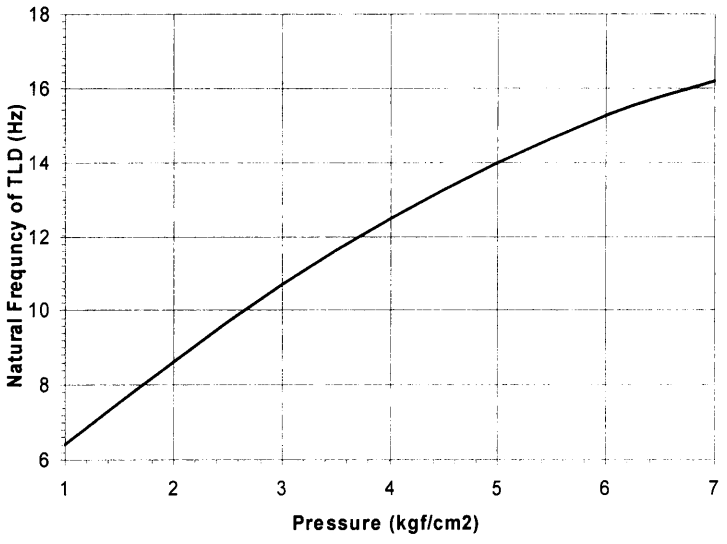

Fig. 2-13 Natural frequency of tank versus pressure (After Shyu and Kuo [55])

The simplifications made in this approach, although providing a better insight into the dynamics of the tank, may not be fully justifiable. The flow is assumed to be laminar and fully developed, for typical flow rates and dimension the flow will be neither fully developed nor laminar. A further simplification is that the duct is assumed to be straight with a length of $2h_r + w$, no account is taken of the head loss or eddies at the bends.

Gawad and co-workers [5], investigated the effect of tank mass and geometry on roll angle and tank angle and concluded that for U-tanks when the ratio of w_r / w is small (in Fig. 2-10), the natural frequency of the tank can be tuned by changing the height of water in the reservoirs. The research was further developed by [75], who investigated the performance of a S60-70 ship with a passive tank in various sea states with different encounter wave directions, using LAMP code (Large Amplitude Motion Program) to solve the 6 DOF equations of motion. The unstabilized and stabilized roll motion of the ship with forward speed and beam waves was analysed. They noticed that for high-amplitude waves, the unstabilized roll angle exhibits typical nonlinear phenomenon: a shift in the resonance frequency, multi-valued resonance, and jumps. Fig. 2-14 shows the variation of the roll angle with the non-dimensional encounter wave frequency. For small wave amplitude the response is single-valued and linear. As the wave amplitude increases, the inherent nonlinearity of the system bends the response curves to the right and shifts the frequency at maximum amplitude to values higher than the natural frequency. The curve connecting the peak amplitudes is called the 'backbone' curve. It is bent to the right, indicating that the nonlinearity is of the hardening type. They noted that passive anti-roll tanks tuned in the linear or nonlinear ranges are very effective in reducing the roll motion in the nonlinear range. They also found that passive tanks are very effective in reducing the roll motion for ships having a pitch frequency that is nearly twice the roll frequency in sea states 5 and 6.

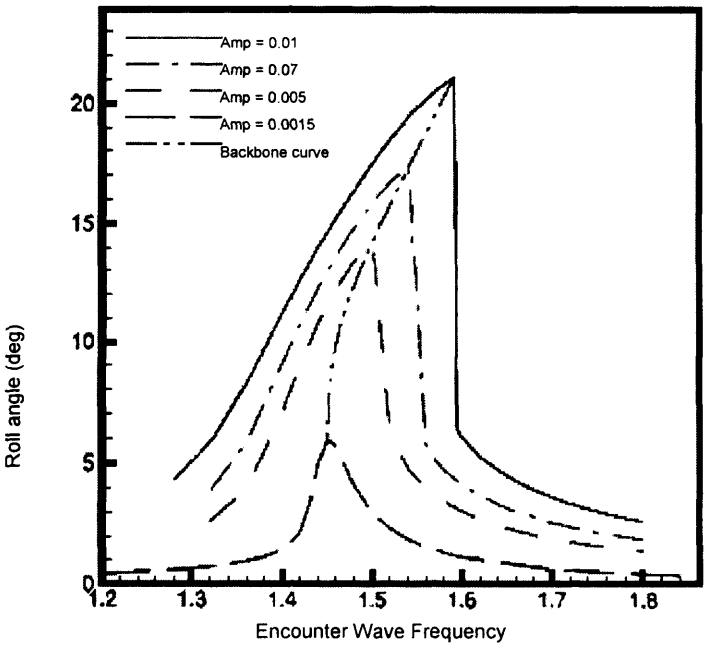

Fig. 2-14 Roll response in the non-linear range (From Youssef and co-workers[75])

2.4 Automatic Control

Much of the early work done on roll stabilization concentrated on the stabilization devices rather than their control, and many of the early devices while attractive in theory where not effective in practice due to the lack of suitable control systems. Minorsky [42], developed a theory for activated tanks in about 1928 by using Froude's rolling theory as (2-2):

$$I_{44}\ddot{x}_4 + k_1\dot{x}_4 + k_2\dot{x}_4^2 + W\overline{GM}x_4 + S = W\overline{GM}\alpha_0 \sin \omega t$$

He suggested that the stabilizing moment should be in phase with roll velocity, $\dot{x}_4$. He concluded that, in all cases, regular as well as erratic rolling, control of the water mass must be such as to fulfil the condition:

$$S = -k_s\dot{x}_4 \qquad \textbf{(2-23)}$$

where k_s is a constant relating the roll velocity to the stabilizing moment.

For regular synchronous rolling (Fig. 2-15), the active system merely increases the rate of transfer of the water of the equivalent passive system but does not change appreciably the phase of the water (Fig. 2-15 and Fig. 2-16 are reproduced from the original paper because of their historical value). For irregular rolling the active system should force the phase of the water so as to approximate the condition (2-23) even in this case. This can readily be seen in Fig. 2-16.

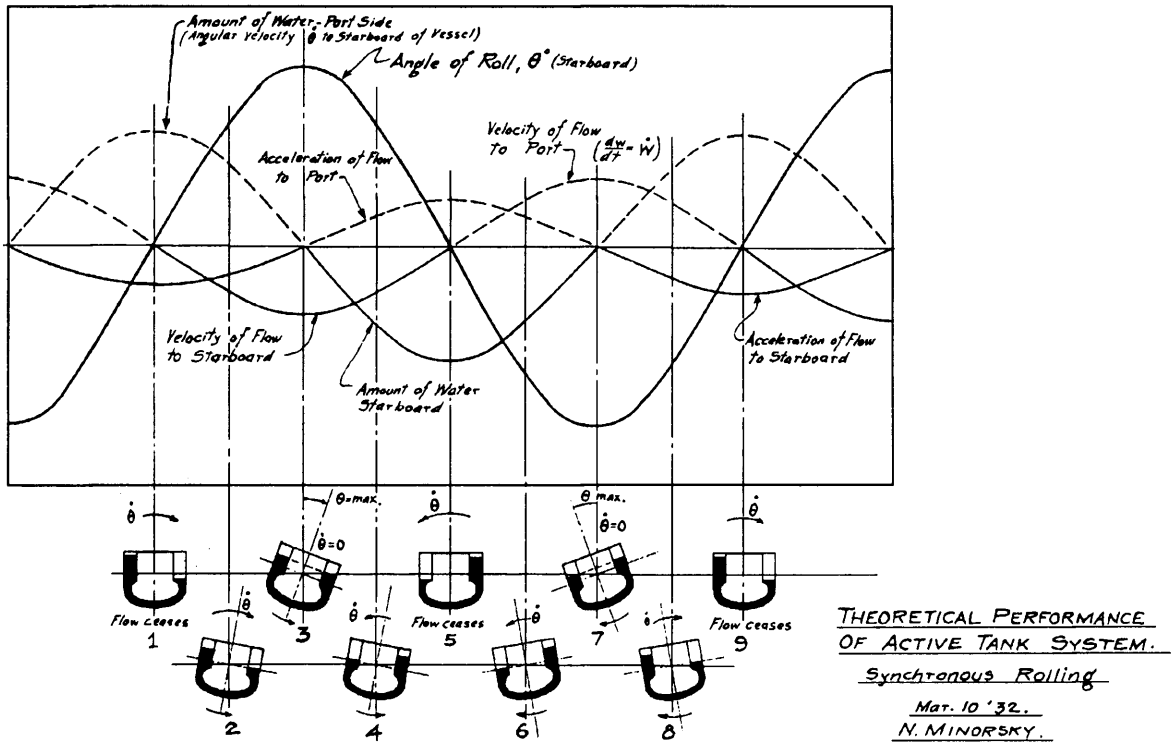

Fig. 2-15 Theoretical performance of active tank system (regular waves) (From Minorsky [42])

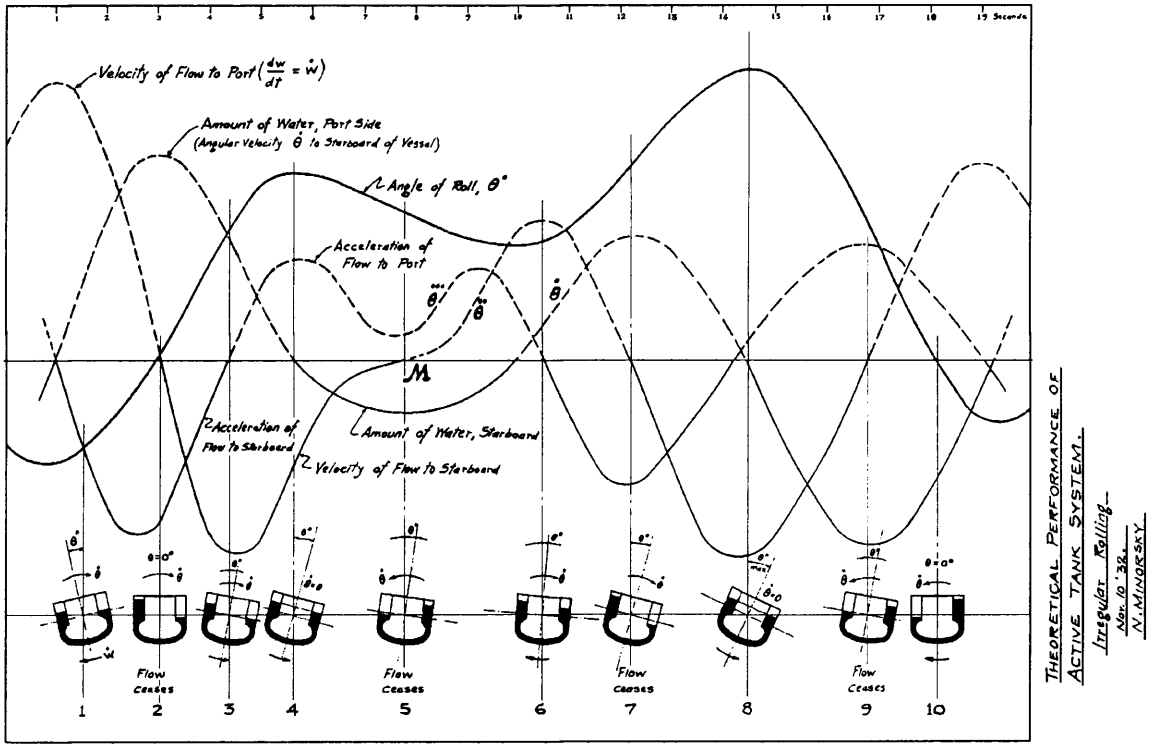

Fig. 2-16 Theoretical performance of active tank system (irregular waves) (From Minorsky [42])

Different methods of control can be introduced to satisfy the above condition (2-23). Consider the active tank system, where the lever arm, L, is fixed and the weight W is varied. In the moving weight system, the weight is fixed and the lever arm is changed by the controller. The righting moment can therefore be expressed as

$$S = -k_s \dot{x}_4 = -WL \tag{2-24}$$

Therefore an obvious control law follows;

$$W = a\dot{x}_4 \tag{2-25}$$

Where $a = k_s / L$

Differentiating with respect to time

$$\dot{W} = a\ddot{x}_4 \tag{2-26}$$

In which the control is performed on water rate according to the signal received from the roll accelerometer. Each of these equations could be used as the control law, as far as they satisfy the condition (2-23). Thus, the most important conclusion obtained by Minorsky was that:

If the stabilizing control is 'continuous' and the torque produced in this manner is in phase with angular velocity, the stabilizing action thus obtained is effective both for regular and erratic rolling.

On the basis of the small-scale laboratory test results, full-scale installation of this system was made on the USN destroyer *Hamilton.* The system used a pump with controllable pitch impeller blades [9]. In still water trials, it was found that by activating the stabilizer, *USS Hamilton* could be made to roll as much as 18° from the vertical. Minorsky's theory and test indicated, however, that the stabilization had sufficient capacity to stabilize the destroyer in a seaway, which would produce a roll of 30°. In actual operation, some very serious difficulties were experienced. Violent water hammer occurred in the blade shifting mechanism and the vibrations produced were picked up by the accelerometer. This had the effect of destroying the phase relationship of the water transfer, thus preventing adequate stabilization. In the 1920's and 30's control theory was not sufficiently advanced to compensate for this instability problem.

No doubt Minorsky's condition (2-23) is true for a ship in calm seas with no wave disturbances at all, but, considering a ship encountering different sea states, is this necessarily always true for all wave frequencies? Or is this only a coincidence and correct for a certain frequency such as the natural frequency? A simple model of a 2500t ship with a 20m beam is used to investigate the validity of this theory. Fig. 2-17 shows the block diagram of the ship, it has a natural frequency of 0.5rad/s and damping ratio of 0.1. Since the aim is to investigate the effect of the phase of the stabilizing moment on the roll reduction, the stabilizing moment is considered to have been produced by any arbitrary source of moment, for example a mass (m = 27t) moving athwartships causing a sine wave with an amplitude of 2700kNm. The ship is excited by waves of different frequencies from 0.1 to 1.0rad/s and the righting moment is assumed to be either in phase with roll velocity, or in phase with roll angle. The results of roll reductions are summarized in Fig. 2-18 where negative numbers present roll increase.

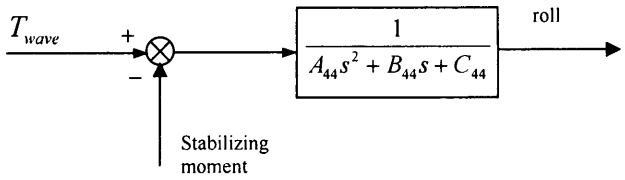

Fig. 2-17 Simple block diagram of a ship

It is evident that the roll has been reduced at some frequencies if the stabilizing moment is in phase with 'roll velocity' and reduced at other frequencies if the stabilizing moment is in phase with 'roll angle'. At some frequencies the tank increases the roll if the stabilizing moment is in phase with roll velocity.

Considering Fig. 2-18 it becomes apparent that the phase of the righting moment is independent of roll or roll velocity. This means that the stabilizing moment should not be necessarily in phase or out phase with one particular movement of the ship. Therefore the key factor for achieving the best stabilizing action becomes evident:

"The righting moment should be always in phase with the wave excitation."

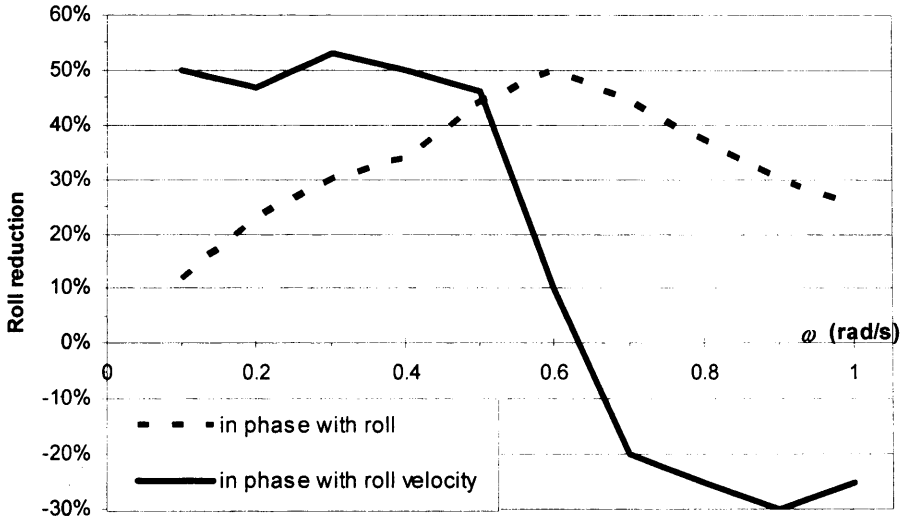

Fig. 2-18 Roll reductions at different excitation frequencies

This ensures that the resulting moment always acts in the opposite direction of the wave excitation, which naturally leads to roll reduction. The reason that ship roll is reduced if it is excited at its natural frequency and the stabilizing moment is in phase with roll velocity can be explained by taking into account the frequency response of the ship. At natural frequency, the phase difference between the excitation and the roll velocity is 90°; obviously the phase difference between the roll and roll velocity for a sine wave is also 90°; therefore if the righting moment is in phase with the roll velocity, it coincidently becomes in phase with the wave excitation. This definitely does not happen at other frequencies, which is evident from the above results. Therefore if a control strategy is to be selected to control the movement of the heavy weight or the motion of the water in a tank, it cannot simply follow the roll angle or one of its derivatives,

Chadwick [19], was the first to raise the issue of modern automatic control in ship stabilization, using transfer functions and block diagrams, Fig. 2-19. With 'feedback' control the stabilizer is positioned in accordance with the ship-motion signal only. That signal is chosen for primary control, which most perfectly complements the dynamic behaviour of the ship and stabilizer. His idea was that in the case of active U-tanks, the pump-blade angle should be controlled by roll acceleration. In the case of active fins, the fin angle should be controlled by roll velocity. The

diagrams are intended to emphasize the fact that even in the absence of a control signal the dynamics of ship and stabilizer may not be completely independent. Thus, block A contains something of the stabilizer, and block C contain something of the ship.

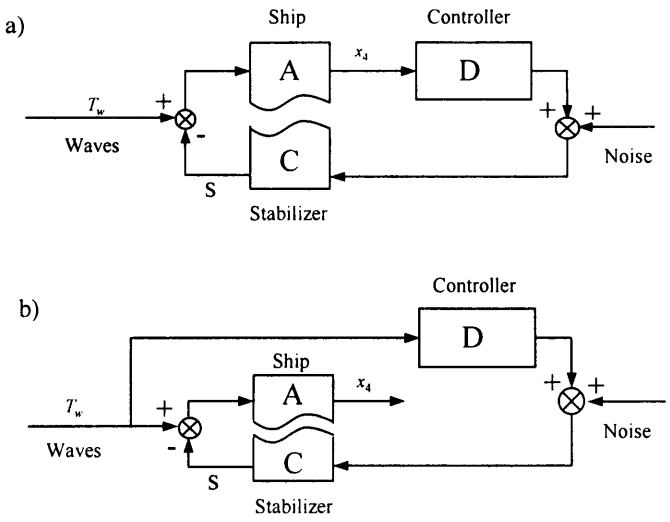

Fig. 2-19 Block diagrams for stabilized ship with a) feedback control; b) feedforward control, (Based on Chadwick [19]).

With the 'feedforward' method of control, the stabilizer is positioned in accordance with the forcing function only, i.e. the incident wave. In 1955 the measurement of the effective wave slope or other inputs presented a problem and therefore limited the use of feedforward control. Nowadays wave-height sensors are capable of measuring the input with great accuracy. The principal advantage of feedforward over feedback is that it avoids the closed loop and hence the problem of self-excitation. But feedback control has the advantage of being relatively independent of variations in system parameters such as ship displacement, GM, speed, etc.

Feedback control strategy is suitable only when the time constant of the actuator is considerably less than the time constant of the system to be controlled. Where this is not the case it is necessary to predict the state of the system so that the actuator motion can be initiated sufficiently far in advance to allow it to respond to the predicted (and hopefully actual) situation. This strategy is generally known as "active control" and is effectively feedforward.

The transfer functions of the control systems, with reference to Fig. 2-19, and neglecting the noise, are:

No control (Passive stabilization): $\frac{x_4}{T_w} = A$ **(2-27)**

Feedback control: $\frac{x_4}{T_w} = A\left[\frac{1}{1+ACD}\right]$ **(2-28)**

Feedforward control: $\frac{x_4}{T_w} = A[1-DC]$ **(2-29)**

Although the ship is usually described as a dynamic system with six degrees-of-freedom, for simplicity, Chadwick reasonably assumed the roll motion as a second order equation coupled only with sway and yaw. As an example he then applied the theory to the control of active fins. Webster [70] was probably the first who discussed the control systems of active anti-roll tanks with modern control theory. For the purpose of analysis of the overall system he used the non-dimensional equations of motion as follows;

Sway : $a_1\ddot{x}_2 + a_2\dot{x}_2 + a_3\ddot{x}_4 + a_4\dot{x}_4 + a_5\ddot{x}_6 + a_6\dot{x}_6 + a_7\ddot{\tau} = Y(t)$ **(2-30)**

Yaw: $b_1\ddot{x}_2 + b_2\dot{x}_2 + b_3\ddot{x}_4 + b_4\dot{x}_4 + b_5\ddot{x}_6 + b_6\dot{x}_6 + b_7\dot{\tau} = N(t)$

Roll: $c_1\dot{x}_2 + c_2\ddot{x}_4 + c_3\dot{x}_4 + c_4x_4 + c_5x_4^{\ 3} + c_6\ddot{x}_6 + c_7\ddot{\tau} + c_8\tau = K(t)$

Tank: $d_1\ddot{x}_2 + d_2\ddot{x}_4 + d_3x_4 + d_4\ddot{x}_6 + d_5\dot{x}_6 + d_6\ddot{\tau} + d_7\dot{\tau}|\dot{\tau}| + d_8\tau = P(t)$

Where *Y(t)*, *N(t)* and *K(t)* are wave excitations and *P(t)* is the required moment that has to be induced by the pump.

The equations are similar to Lloyd's equations (2-6) with some slight differences. Contrary to Lloyd's equations for sway and yaw, Webster does not have terms proportional to x_6. In the case of roll, Webster lacks terms proportional to $\ddot{x}_2, \dot{x}_6$ and x_6, and has an extra term proportional to x_4^3. The equation of the tank is also different and Webster has two extra terms proportional to $\dot{x}_6$ and $\dot{\tau}|\dot{\tau}|$. Lloyd's equations are the more widely used as they have no non-linear terms.

It is presumed that the impeller blade will be continually controlled by some servomechanism. Because of the inertia of the large blades, the linkage, etc. there will be a time lag between α the actual position of the pump blade, and α_c, the required position of the pump blade (Control signal). In addition there will be some maximum value of α limited by physical dimensions and cavitation onset. Therefore the servomechanism will be described as:

$$T_p\dot{\alpha} + \alpha = \alpha_c \tag{2-31}$$

The exciting waves are assumed to be unidirectional and result from the linear superposition of elementary sinusoidal waves of amplitude given by Neumann height spectrum and of random phases with a uniform probability distribution. On a ship stabilized by means of anti-rolling tanks, the stabilizing moment is give

$$S(t) = k_{st}(\eta_{st}{}^2\tau'' + \tau) \tag{2-32}$$

Where k_{st} and η_{st} are constant coefficients. Because $\eta_{st}{}^2$ is usually less than 0.10 for most typical cases, the effect of the tank water inertia is usually very small. The torque is produced mainly by the instantaneous lateral location of the centre of gravity of the tank water, reflected in the term τ of equation (2-32). Hence, the correcting force is not available immediately after the actuation of the pump. In addition to the phase lag in the servo for the pump blades, the signal has to proceed through the tank dynamics before this torque is available. Thus, at frequencies near the roll resonance one can anticipate a phase lag of approximately 180° between the pressure developed across the pump and the resulting roll angle. It is necessary to use a signal, which anticipates the roll motion in order to cancel the inherent phase lag of the ship and tank dynamics. Roll acceleration feedback provides a phase lead of 180° at all frequencies and provides sufficient anticipation to overcome the phase lag at roll resonance but this phase lead is not sufficient to prevent poor high frequency performance. Fortunately, as frequencies increase well past resonance, the ship's response decays quickly. The control system will require, in addition to the roll acceleration, roll velocity and roll angle terms in order to improve the roll response below roll resonance. The overall configuration of Webster's control system is shown in Fig. 2-20. Additional closed loops including the measurable quantities $\beta, \dot{\beta}, r, \dot{r}, \dot{\tau}$ and $\ddot{\tau}$ are also shown in this configuration. These loops are used in an attempt to improve the performance of the roll information feedback loop.

The signal actuating the impellor blade pitch is taken as:

$$\alpha_c(t) = \alpha_{fb}(t) + \alpha_{ff}(t) \tag{2-33}$$

Where

$$\alpha_{fb}(t) = (g_3\ddot{x}_4 + g_2\dot{x}_4 + g_1x_4) + (e_2\ddot{r} + e_1\dot{r})$$

$$\alpha_{ff}(t) = c_2\ddot{x}_2 + c_1\dot{x}_2 + d_2\ddot{x}_6 + d_1\dot{x}_6$$

The basic technique for choosing the 9 control gains was a trial an error method, since the author believed that using the Routh stability criterion or root-locus method would be extremely complicated for such a system. The gains were selected to minimise the motions resulting from an impulsive velocity step. With the limited computer power available in 1967 this was true but now a variety of self-tuning adaptive techniques are available.

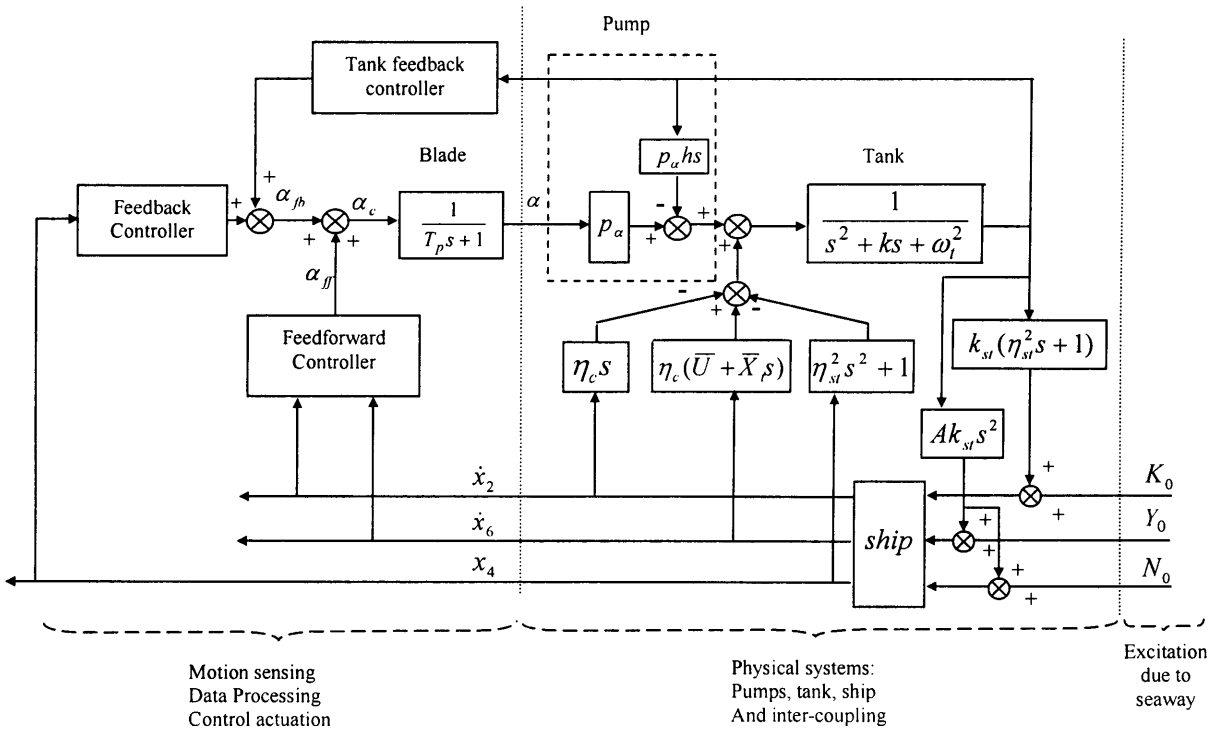

Fig. 2-20 Block diagram of control system (Based on Webster [70])

Roberts and Barboza [52], proposed that a "bang-bang" control strategy would provide the fastest transfer of water between the tanks. They used the following set of equations:

$$\text{Tank: } \ddot{\tau} + k\dot{\tau} + \omega_t^2 \tau - a_{4\tau}\ddot{x}_4 - c_{4\tau}x_4 = f_{sway} + \delta p \qquad \textbf{(2-34)}$$

$$\text{Ship: } \ddot{x}_4 + K\dot{x}_4 + \omega_s{}^2 x_4 - a_{\tau 4}\ddot{\tau} - c_{\tau 4}\tau = f_{roll}$$

where δp is the pressure differential function used as the control input and f_{roll}, f_{sway} are roll and sway wave disturbance respectively. The detailed mathematical model and derivation of coefficients is available in the paper by Roberts and Barboza [52]. It is possible to represent the dynamic of the tank ship system with space state equations as:

$$\dot{\mathbf{X}} = \mathbf{A}\mathbf{X} + \mathbf{B}\delta p(t) + \mathbf{C}\mathbf{F}(t) \qquad \textbf{(2-35)}$$

Where $\mathbf{X}$ is the state matrix defined as $[x_4, \tau, \dot{x}_4, \dot{\tau}]^T$ and $\mathbf{F}(t)$ is the disturbance matrix. Using the approach of Webster and Dagon [71], the optimal bang-bang controller and the control signal can be computed in accordance with Lyapunov stability theorem. This process results in:

$$\delta p = \delta p_{\max} sign(\mathbf{B}^T\mathbf{P}\mathbf{X})$$

and $\mathbf{P}$ is determined from:

$$\mathbf{A}^T\mathbf{P} + \mathbf{P}\mathbf{A} = -\mathbf{Q}$$

where $\mathbf{Q}$ is positive definite and is selected so that $\mathbf{X}^T\mathbf{Q}\mathbf{X}$ accounts for the kinetic and potential energy of the ship's roll system. These results in a control action which strives to reduce the scalar quantity $0.5x_4^2 + 0.5\dot{x}_4^2$. This strategy was simulated for a 76,000t and a 14,500t warship using U-tanks and showed much better performance compared with a passive tank.

In another control strategy Chen and co-workers [21] (and [20]) proposed a robust nonlinear state feedback controller for the pumps which could handle model uncertainties which arise mostly from unknown hydrodynamic effects in the ship model that was a nonlinear, three degree-of-freedom model of the ship. In brief, the design of the controller was a Lyapunov-based approach using a combination of sliding mode control and composite control for singularly

perturbed systems, with the help of the back stepping technique. It was shown that this design can effectively control roll motions of large amplitude, including capsize prevention.

Hsuesh and Lee [30], investigated an activated anti-roll tank system design for ship roll reduction and derived a control law based on optimal control. The goal of the control system was to optimise a cost function including terms for roll reduction and power consumption of the pumps. Different weights for each term ware tried and optimal weights were selected. A 1,174t ship was simulated under different sea loads to determine the efficiency of the design. The performance of the system was examined in different sea states and compared with the performance of a similar ship equipped with a passive tank. The activated system was reasonably robust and showed low sensitivity to the modelling error of the ship and the tank dynamics. An advantage of this approach is that the pump power is limited, hence preventing unrealistic power consumption and pumping rates.

Treakle and co-workers [63;64] approximated the motion of the water in a U-tank by the motion of a point mass that moves athwart ships. The complete 6-DOF nonlinear coupled mathematical model of the ship is available in the reference and the control of the moving mass is performed by a Proportional-Derivative (PD) controller where there are limitations on the maximum position, speed and acceleration that the moving mass can posses. They developed a single degree-of-freedom non-linear simulator (MOTSIM) to investigate the effect of different coefficients in both passive and active tanks and compared their results with the simulations using LAMP code. In all cases, application of anti-roll tanks showed improvement in roll reduction of the ship.

2.5 Concluding remarks

Roll is the least damped and has largest amplitude of all the unwanted motions of a ship. Maintaining motions within acceptable limits is crucial for the efficient operation of crew and equipment. Roll can be actively controlled by applying a restoring force either directly, by use of fins for example, or indirectly by altering the position of the centre of gravity. For truly effective roll damping the machinery must be combined with an effective control system. This

has been clearly demonstrated through the history of roll damping devices where a number of good solutions have failed because the control system and theory was not sufficiently developed.

The earliest devices used moving masses or more commonly tanks of water. Tanks have developed from simple passive free surface tanks mounted on the centre line to more sophisticated U-tanks and free-flooding tanks with active control. A major disadvantage of early passive tanks was that the free surface reduced the metacentric height so that roll stability was reduced and the tanks amplified roll motion at low wave encounter frequencies. In an attempt to overcome this and the slow response time of tank systems, various ingenious systems were developed but they were usually let down by the practical implementation of the control system. During the last 50 years fin stabilizers have gained prominence. Fins require minimal internal volume compared to tanks, require only modest power and also have a fast response. But they are external to the vessel which imposes limits on their size, they are also vulnerable. The forward engine room of HMS Nottingham was flooded due to the starboard stabilizer fin being ripped off when she struck Wolf Rock in 2002 [29]. Compared to fins, and especially bilge keels, tanks require more of the ship's internal volume, but this need not be in prime locations and they have the added benefit of providing protection to the vessel in the event of collision or enemy action.

Fins rely on forward motion to produce the restoring force and hence are ineffective below about 6 knots they also impose a drag penalty which increases with speed. By comparison tanks have been relatively ignored during the last half century because fin stabilisers have been able to provide a good alternative for most applications and tank systems have a reputation for poor performance. Recently there have been a growing number of requirements for stabilisation of vessels at slow speeds, while the advances in control theory and computational power provides tools to combat the poor response times of tank systems making them more attractive at higher speeds too.

Where a vessel's operating profile includes slow and medium speed operation a combination of fins and tanks might be considered. High speed vessels are usually inherently stable in roll at design speed, but at low speeds they can have poor roll characteristics as the hull form has been optimised for speed. A tank system could be a solution for such vessels which also have to operate at low speeds, for example the new USN Littoral Combat Ship (LCS). At high speed the tanks are emptied to reduce displacement, while at low speed they can be filled, free-flooding

tanks are particularly suited for this. By comparison a fin system which is large enough to provide roll stabilisation at slow speed could produce unacceptable drag at high speed.

Multi hulls, such as catamarans, trimaran and surface effect ships (SES) are also candidates for free-flooding tanks where they need to be stabilized at low operating speeds, or in the case of trimarans to combat parametric roll. Free surface tanks are not practical and U- tanks are difficult to fit. In addition the hulls are optimised for speed not seakeeping at slow speed. This is a particular issue for warships such as the LCS trimaran variant whose operating profile includes time at low speed (e.g. policing duties and mine hunting) as well as high speed sprints. Low speed roll reduction was identified as one of the key risks to be mitigated for the trimaran if it were to be used as the UK's Future Surface Combatant [57]. Free-flooding tanks offer a solution as they only have a small cross connection at the top and this can easily be run from one side hull to the other. Moreover the side hulls of catamarans, and especially trimarans, are well separated providing a large lever arm, so less water is required to achieve a given moment. The narrow beam of multihull side hulls means that they are often not utilised (indeed many are just voids) so that ample space for locating tanks is available. For trimarans and pentamarans the shallow draught of their side hulls may be an issue. For an SES the tanks can be drained and the flooding ports lifted clear of the water when on cushion resulting in an almost zero impact on drag.

Chapter 3

3 An overview on Adaptation Theory

3.1 Introduction

Adaptive systems are generally referred to systems whose structures change over time and adapt themselves to the changes in the environment around them in order to obtain their design purpose. This chapter discusses the general theory of adaptation and explains some models used in adaptation, the common methods used for adapting these models and some applications of adaptive systems. Limited time and space do not allow an explanation of every aspect of adaptive theory, and that is not the goal here. The aim is to familiarise someone who already has knowledge of automatic control with the theoretical concepts that are required to understand fully the applications presented in the following chapters.

3.2 The big picture

When an engineer designs a system he or she must also consider different conditions and environments the system is due to work in. If the exact condition of the system is known to some good extent or if the condition changes but the nature of the changes is known, it is possible to design a system to achieve a desired aim over range of conditions and environmental changes. However, sometimes the nature of the changes in the condition in which the system is to work is unknown. In this situation an adaptive design means that

the system has the ability to adapt constantly itself and its parameters to the new situation in order to maintain the desired design purpose. Adaptive systems are in their nature time-varying and nonlinear. Nonlinear means that adaptive systems do not follow the principle of superposition.

Adaptive systems are usually classified as being "open-loop" or "closed-loop". In an open-loop adaptive system, changes in the conditions, environment, and generally the "input" are monitored and the system is adapted according to some pre-known information consisting of a given case, which are the best parameters of the system that provide the best results. In a closed-loop adaptive system, the outcome or the "output" of the system is monitored to measure how well the system is performing. The adaptation is usually done based on the error or the difference between the desired output and the actual output of the system.

Choosing the right adaptive system whether open loop or closed loop depends on many factors. In an open loop system information about the input signal, the environment, and pre-acquisition about the performance of the system in a given condition is necessary. The availability of such information is therefore a crucial factor in designing an open loop adaptive system. Closed loop adaptation is the most widely used and has several advantages and a few disadvantages that need to be considered before making a final choice. A closed loop system can be applied to systems were little information about their dynamics are known or their dynamics changes with time. Even in the case of hardware failure the adaptive system will attempt to adapt the system in such a way to maintain the desired performance at a reasonable level. A closed loop system can account for nonlinearities in the system and nonstationary input signals. However just like normal closed loop control systems, closed loop adaptive systems also may become unstable and the adaptive parameters may diverge. Yet when properly designed closed loop adaptive systems are powerful control tools and widely used in practice (applications range from autopilot systems of airplanes to blood pressure stabilization systems).

3.3 Some applications of adaptive systems

Adaptive systems are usually presented with a structure as shown in Fig. 3-1. The input signal to the adaptive processor is shown by x, and the output by y. The output is then compared with a desired signal, d. That is the signal that the output should become equal to. The difference between the desired signal and the actual output is called the error signal shown by ε.

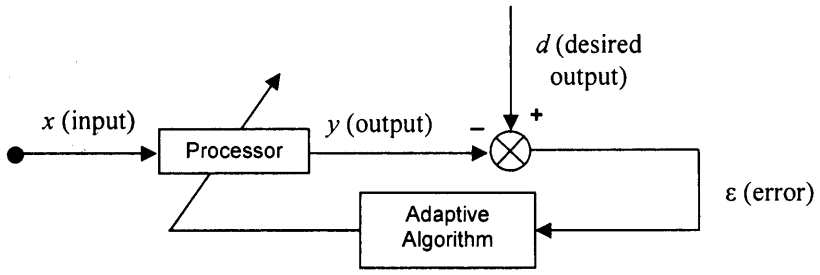

Fig. 3-1 General block diagram of an adaptive system

The error signal is the driving force that is used in adaptive algorithms to change the adaptive processors parameters in such a way that the output of the adaptive system becomes closer and closer to the desired signal. Some of the most important adaptation algorithms are discussed later on in this chapter.

Different applications of adaptation are generally related to the nature of the desired signal, d. For example in Fig. 3-2 the input signal to the adaptive processor is delayed version of the desired signal. In other words the desired signal is k-step ahead of the input

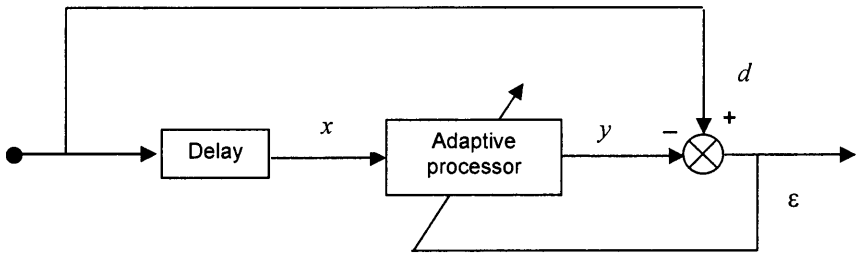

Fig. 3-2 Configuration of adaptive system used for prediction

signal meaning that the output of the adaptive processor should become the same as the future k-step ahead of the input. Therefore the aim of the adaptation system is to "predict" the future value of a given signal, in this case x.

The block diagram shown in Fig. 3-3, although very similar to the one in Fig. 3-2, is used for a totally different application. The input of the adaptive processor is the same input applied to an unknown plant which is to be modelled. It is intended that the output of the adaptive processor becomes the same as the output of the plant. If the error signal gets reasonably small, it means that given the same input, the adaptive processor generates the same output as the plant. In this case the adaptive processor can be used as a mathematical model of the unknown plant where only the input and output of the plant are known. This application of adaptive systems is known as "system identification" or "direct modelling". The adaptive system constantly tries to reduce the error signal; if the plant is time varying, the variation of the plant parameters causes a difference between the output of the plant and the output of the model and therefore an increase in the error signal is observed. The adaptive system then attempts to reduce the error signal by changing the model and building a more accurate model of the plant.

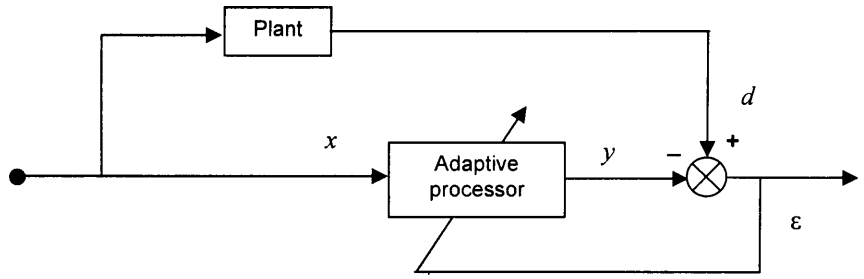

Fig. 3-3 Configuration of adaptive system used for system identification

Another very similar application of adaptive systems would be "inverse modelling" in which the output of the plant is given to the adaptive processor and the desired signal is the input of the plant (Fig. 3-4). In other words the adaptive processor is intended to be an "inverse model" of the unknown plant, meaning that if the processor is fed with the output of the plant it would generate the signal reasonably close to the input of the

unknown plant. Inverse modelling is used in applications such as digital filtering and adaptive control problems where the characteristics of the system to be controlled changes over time and therefore the parameters of the controller need to be adapted accordingly.

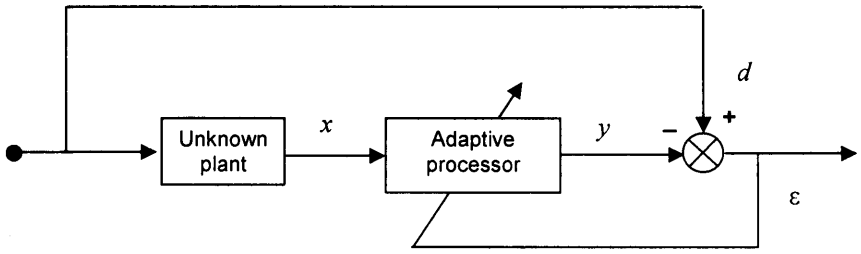

Fig. 3-4 Configuration of adaptive system used for inverse modeling

3.4 Adaptive linear combiner

The adaptive linear combiner is perhaps the most important model used in adaptive systems. A diagram of the general form of an adaptive linear combiner is shown in Fig. 3-5. The output of the linear combiner is essentially the summation of the previous values of the input signal multiplied by some coefficients called "gains" or "weights". This means that an input signal is fed into the linear combiner and then multiplied by a gain, w_0. Then this input signal is one step delayed and the result multiplied by another gain, w_1. This goes on until the L^{th} delayed input signal is multiplied by the gain w_L. L is known as the length of the linear combiner.

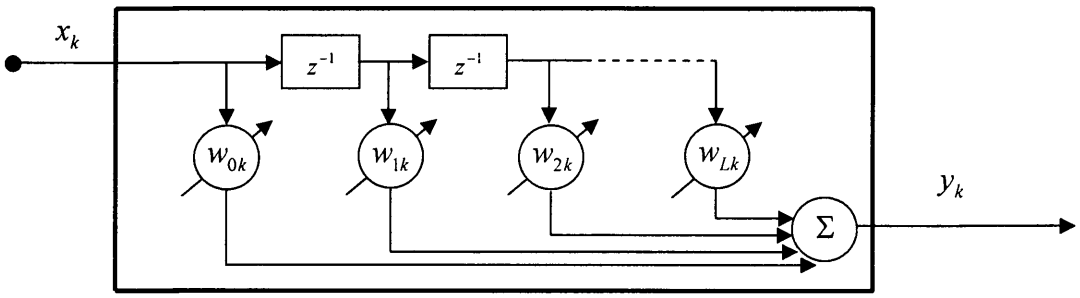

Fig. 3-5 General form of adaptive linear combiner

The output would therefore be the addition of all the above terms:

$$y_k = x_k w_{0k} + x_{k-1} w_{1k} + x_{k-2} w_{2k} + ... + x_{k-L} w_{Lk} \quad \textbf{(3-1)}$$

Where the index k denotes the value of that specific parameter at time k.

The values of the gains $w_0, w_1, ..., w_L$ are constantly updated in a way that the error signal becomes minimum and the desired aim is achieved. What is known as "adaptation" is simply the procedure of updating these weights and is done by algorithms called adaptation algorithms, some of which are explained briefly in this chapter.

The reason that the combiner is called "linear" is that the output is the addition of some values multiplied by some inputs. However, as the weights are adapted according to the input signal and the error signal, the output is no longer a strict linear combination of the inputs and therefore a combiner is mathematically nonlinear. Consider the two vectors $\mathbf{x}_k$ the input vector and $\mathbf{w}_k$ the weight vector where:

$$\mathbf{x}_k = [x_k \quad x_{k-1} \quad .... \quad x_{k-L}]^T$$

$$\mathbf{w}_k = [w_{0k} \quad w_{1k} \quad .... \quad w_{Lk}]^T$$

Where T denotes transpose of a vector, implying that both the input vector and the weight vector are column vectors. In this case where the input vector is present and past values of the same signal, the linear combiner is sometimes referred to as "transverse filter".
According to equation (3-1) the output of the filter is:

$$y_k = x_k w_{0k} + x_{k-1} w_{1k} + x_{k-2} w_{2k} + ... + x_{k-L} w_{Lk}$$

Using the vector notation the output can be expressed as:

$$y_k = \mathbf{w}_k^T \mathbf{x}_k \quad \textbf{(3-2)}$$

As explained earlier this output is compared with a desired signal and the difference forms the error signal:

$$\varepsilon_k = d_k - y_k = d_k - \mathbf{w}_k^T \mathbf{x}_k \quad \textbf{(3-3)}$$

Where ε_k shows the error signal at time *k*. It is the aim of the adaptive processor to reduce this error as much as possible by appropriately changing the weight vector.
A well-known criteria to realize whether the error signal has reached its minimum level or not, is to check the mean square of the error signal. Using equation (3-3) the square of the error signal is:

$$\varepsilon_k^2 = d_k^2 + \mathbf{w}_k^{\mathrm{T}}\mathbf{x}_k\mathbf{x}_k^{\mathrm{T}}\mathbf{w}_k - 2d_k\mathbf{x}_k^{\mathrm{T}}\mathbf{w}_k \tag{3-4}$$

Assume that the error signal, the desired signal and the input signal are statistically stationary, and that it is not just a case of adjusting the weight vector. Therefore the weight vector is constant at different times.
The expected value of the squared error signal is therefore:

$$E\left[\varepsilon_k^2\right] = E\left[d_k^2\right] + \mathbf{w}^{\mathrm{T}}E\left[\mathbf{x}_k\mathbf{x}_k^{\mathrm{T}}\right]\mathbf{w} - 2E\left[d_k\mathbf{x}_k^{\mathrm{T}}\right]\mathbf{w} \tag{3-5}$$

Now introduce two matrixes:
The first matrix **R** is known as the "input correlation matrix" and is defined as:

$$\mathbf{R} = E\left[\mathbf{x}_k\mathbf{x}_k^{\mathrm{T}}\right] = E\begin{bmatrix} x_{0k}^2 & x_{0k}x_{1k} & x_{0k}x_{2k} & \cdots & x_{0k}x_{Lk} \\ x_{1k}x_{0k} & x_{1k}^2 & x_{1k}x_{2k} & \cdots & x_{1k}x_{Lk} \\ \cdots & \cdots & \cdots & \cdots & \cdots \\ x_{Lk}x_{0k} & x_{Lk}x_{1k} & x_{Lk}x_{2k} & \cdots & x_{Lk}^2 \end{bmatrix} \tag{3-6}$$

The second matrix **P** is known as the "cross-correlation matrix" between the input signal and the desired response is defined as:

$$\mathbf{P} = E\left[d_k\mathbf{x}_k\right] = E\left[d_kx_{0k} \quad d_kx_{1k} \quad \cdots \quad d_kx_{Lk}\right]^{\mathrm{T}} \tag{3-7}$$

Using the above introduced matrixes it is possible to present the mean square error from equation (3-5) in a more convenient way:

$$\mathrm{MSE} = \xi = E\left[\varepsilon_k^2\right] = E\left[d_k^2\right] + \mathbf{w}^{\mathrm{T}}\mathbf{R}\mathbf{w} - 2\mathbf{P}^{\mathrm{T}}\mathbf{w} \tag{3-8}$$

Where ξ presents the mean square of the error signal.

By looking closely at equation (3-8) it can be realized that the mean square error is a quadratic function of the weight vector. In other words if equation (3-8) is expanded and all its components are shown, then all w terms will appear with either power one or two. Consequently if the mean square error is plotted as a function of the weight vector, the error function will, as all other quadratic functions, have a bowl shape or more technically speaking, a hyper-parabolic shape. This bowl-shape surface is known as the "performance surface". Fig. 3-6 shows a performance surface where the vertical axis is the mean square error of a filter formed of two weights.

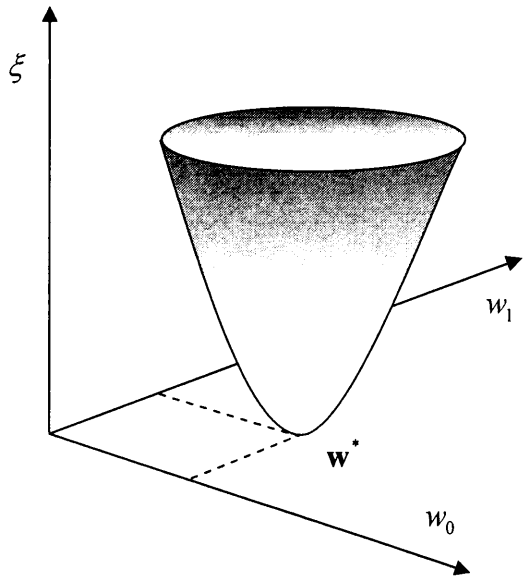

Fig. 3-6 Part of the performance surface of a transverse filter with two weights (L=1)

The point at the bottom of the bowl, denoted by $\mathbf{w}^*$, is the combination of different weight vectors that result in the least mean square error in equation (3-8) and it is the aim of the adaptation algorithms to find this point.

Many adaptive algorithms use the gradient of the performance surface. In other words they usually start with some initial value of weight vector and using the gradient of the performance surface at that point then decide how much to change the weight vector to get closer to the bottom of the bowl. It is worth mentioning that for an adaptive linear

combiner, the performance surface is always quadratic even for filters having more than two gains. This is clear by examining the equation of the performance surface, equation (3-4). Therefore there is no concern relating to existence of local minima, as there is only one global minimum in a quadratic surface.

The gradient of the performance surface is itself a column vector and can be derived by differentiating equation (3-8) with respect to the weight vector. If the gradient of the performance surface is presented by $\nabla(\xi)$ or simply ∇, it can be said that:

$$\nabla = \frac{\partial \xi}{\partial \mathbf{w}} = 2\mathbf{R}\mathbf{w} - 2\mathbf{P} \tag{3-9}$$

To obtain the weight vector that minimises the MSE, $\mathbf{w}^*$, the gradient of the MSE function should be zero:

$$\nabla = 2\mathbf{R}\mathbf{w}^* - 2\mathbf{P} = 0 \tag{3-10}$$

Which means that the optimum weight vector, sometimes called the Wiener weight vector is:

$$\mathbf{w}^* = \mathbf{R}^{-1}\mathbf{P} \tag{3-11}$$

The minimum least square error is therefore derived by substituting equation (3-11) in equation (3-8):

$$\begin{aligned} \xi_{\min} &= E\left[d_k^2\right] + \mathbf{w}^{*\mathrm{T}}\mathbf{R}\mathbf{w}^* - 2\mathbf{P}^{\mathrm{T}}\mathbf{w}^* \\ &= E\left[d_k^2\right] + [\mathbf{R}^{-1}\mathbf{P}]^{\mathrm{T}}\mathbf{R}\mathbf{R}^{-1}\mathbf{P} - 2\mathbf{P}^{\mathrm{T}}\mathbf{R}^{-1}\mathbf{P} \end{aligned} \tag{3-12}$$

This expression can be simplified using the basic matrix rules as:

1- Since the input correlation matrix is symmetric, $\mathbf{R}^{\mathrm{T}} = \mathbf{R}$ and $\left[\mathbf{R}^{-1}\right]^{\mathrm{T}} = \mathbf{R}^{-1}$.

2- $[\mathbf{AB}]^{\mathrm{T}} = \mathbf{B}^{\mathrm{T}}\mathbf{A}^{\mathrm{T}}$

3- $\mathbf{A}\mathbf{A}^{-1} = \mathbf{I}$

Therefore equation (3-12) simplifies to:

$$\xi_{\min} = E\left[d_k^2\right] - \mathbf{P}^{\mathrm{T}}\mathbf{w}^{*} \tag{3-13}$$

It It is also possible to express the above equation in another form:

$$\xi\ \xi = \xi_{\min} + (\mathbf{w} - \mathbf{w}^{*})^{\mathrm{T}}\mathbf{R}(\mathbf{w} - \mathbf{w}^{*}) \tag{3-14}$$

The optimum value of weights and the minimum MSE can therefore be found if sufficient statistical information if available about the input vector and desired signal. While statistical information of the desired signal is not difficult to obtain, similar information about the input signal might be limited because of practical reasons and difficulties of measuring this signal. Even if the input signal in measurable, for finding the correlation matrixes and the expected values of each element, the mathematical average of the elements should be calculated over a relatively large time frame. This inevitably leads to a very slow adaptation. As a result, most adaptation algorithms use estimations on how to approach the "bottom of the bowl".

3.5 Idea behind the gradient search methods

Many adaptive algorithms use the gradient of the performance surface in the way that they start with some initial value of weight vector and using the gradient of the performance surface at that point then decide how much to change the weight vector to get closer to the bottom of the bowl.

In a simple case where the transverse filter has only one weight to optimise, the least mean square function becomes a parabola (Fig. 3-7). At any given time, k, it is possible to find a better estimation of the optimum weight, w^{*}, by:

$$w_{k+1} = w_k - \mu\nabla_k \tag{3-15}$$

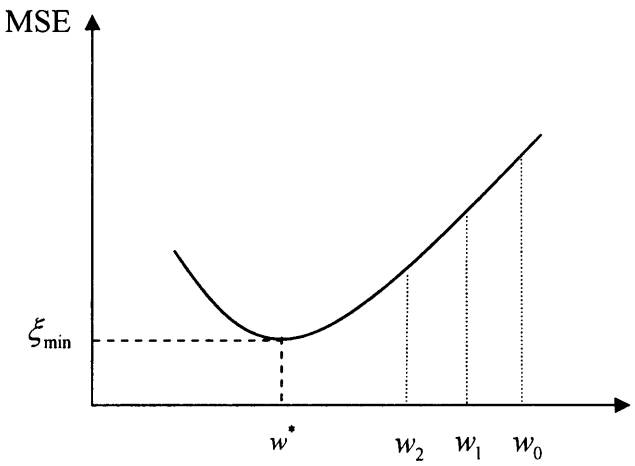

Fig. 3-7 Idea used in gradient search methods

Where ∇_k defines the gradient of the performance surface at step k. μ is a coefficient governing the amount of changes. If μ is a smaller number the corrections made are more gradual and the adaptation is slower. If μ is a larger number the corrections in the weight vector are also larger and the adaptation is faster but might not even converge. The value of μ is therefore a critical factor in convergence speed and stability of the adaptive system.

In order to investigate the effect of μ on the stability of the adaptation consider the simple case where the filter is formed of only one weight as in Fig. 3-7. It is possible to expand equation (3-15) in such a way so that the weight vector at any given time can be calculated by knowing the initial and final values of the weight vector:

$$w_k = w^* + (1-2\mu\lambda)^k (w_0 - w^*) \qquad \textbf{(3-16)}$$

Where λ is the eigenvalue of the matrix **R**. In this case since **R** is a one by one matrix λ becomes the same as the only element of **R** being R_{11}.Equation (3-16) is clearly a difference equation in which the geometric ratio is $(1-2\mu\lambda)$. The stability condition for equation (3-16) is that the absolute geometric ratio is less that one.

$$|1-2\mu\lambda| < 1 \text{ or } 0 < \mu < \frac{1}{\lambda} \qquad \textbf{(3-17)}$$

When the above condition is satisfied the gradient algorithm is stable and the weight vector will eventually converge to its optimum value, w^*. The rate of convergence is obviously determined by the value of μ.

If $(1-2\mu\lambda)$ is a positive number less than one, in other words if $0 < \mu < \frac{1}{2\lambda}$, then there is no oscillation in the transient weight vector and the system is regarded as "over-damped". If $(1-2\mu\lambda)$ is a negative number greater than -1, in other words if $\frac{1}{2\lambda} < \mu < \frac{1}{\lambda}$, then the weight vector overshoots its optimum value but converges in a decaying oscillation. This adaptive system is known as "under-damped". In the critical case, when $(1-2\mu\lambda)$ equals zero, the rate of convergence is the fastest and theoretically the weight vector should reach its optimum value in one step. In this case the process is called "critically-damped". These different conditions are graphically shown in Fig. 3-8:

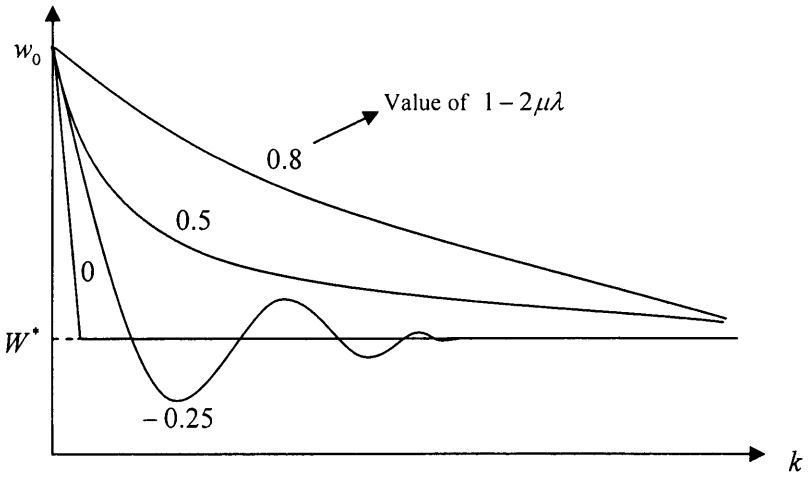

Fig. 3-8 Weight adjustment for different values of the geometric ratios

The mean square error at each step can also be presented [73] as a difference equation in the form of:

$$\xi_k = \xi_{\min} + \lambda(1-2\mu\lambda)^{2k}(w_0 - w^*)^2 \qquad \textbf{(3-18)}$$

The geometric ratio of the mean square error progression is therefore:

$$r_{mse} = (1-2\mu\lambda)^2$$

The stability criteria is that $0 < |r_{mse}| < 1$. However since r_{mse} is a positive number, the mean square error curve, known as the "learning curve", will always be over-damped and will never oscillate. For a single weight filter, the learning curve would look like:

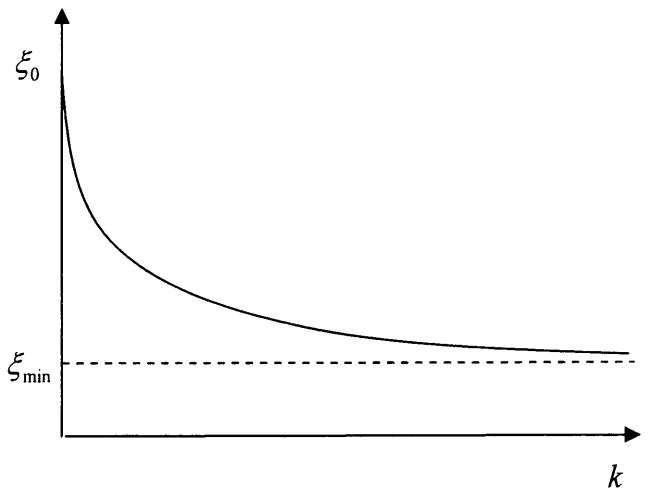

Fig. 3-9 The learning curve of a single weight vector when $r_{mse} = 0.5$

3.5.1 The steepest descent method for gradient search

The steepest descent method is a more generalized form of the gradient method explained earlier for a single weight vector. It works on the same principle that it starts with some initial value of weight vector and using the gradient of the performance surface at that point then decides how much to change the weight vector to get closer to the bottom of the bowl:

$$\mathbf{w}_{k+1} = \mathbf{w}_k - \mu\nabla_k \qquad \textbf{(3-19)}$$

Where ∇_k defines the gradient of the performance surface at step k. $\mathbf{w}_k$ is the weight vector at step k. In order to investigate the stability of this method when the filter is made of several weight equation (3-19) can be restructured [73] in the following form:

$$\mathbf{w}_{k+1} = (\mathbf{I} - 2\mu\mathbf{R})\mathbf{w}_k + 2\mu\mathbf{R}\mathbf{w}^* \tag{3-20}$$

Or

$$\mathbf{w}_k - \mathbf{w}_k^* = (\mathbf{I} - 2\mu\mathbf{R})^k (\mathbf{w}_k - \mathbf{w}_k^*) \tag{3-21}$$

Where **I** is an identity matrix with the dimensions equal to the number of the weights and **R** is the input correlation matrix. Equation (3-21) is also a difference equation with the following geometry ratio matrix:

$$\begin{bmatrix} 1-2\mu\lambda_0 & 0 & \dots & 0 \\ 0 & 1-2\mu\lambda_1 & \dots & 0 \\ 0 & 0 & \dots & \dots \\ \dots & \dots & \dots & 1-2\mu\lambda_L \end{bmatrix} \tag{3-22}$$

Where λ_0, λ_1, ... λ_L are the eigenvalues of the matrix **R** and it can be shown that its stability condition is that:

$$0 < \mu < \frac{1}{\lambda_{\max}} \tag{3-23}$$

Where $\lambda_{\max}$ is the largest eigenvalue of **R**. The convergence of the weight vector to its optimum value also depends on the values of λ_i.

A major property of the steepest descent method is that the changes of the weight vector are in the direction of the gradient. This can be better understood by considering a simple case when the filter has two gains. The performance surface is shown in Fig. 3-10 where the contours of constant mean square error are elliptical.

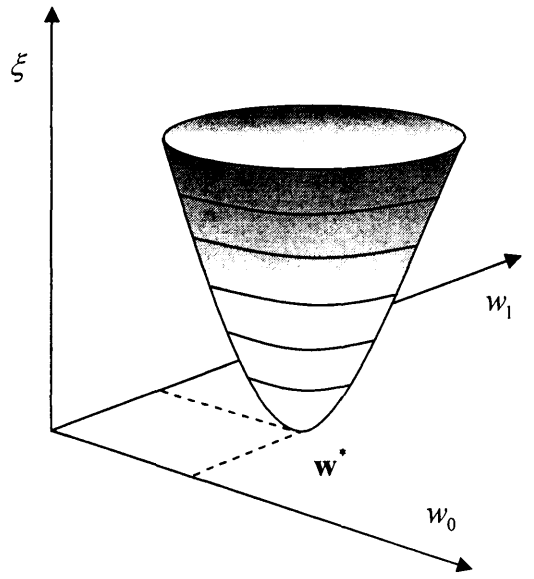

Fig. 3-10 Contours of constant mean square error shown on the performance surface of a transverse filter with two weights

If the paraboloid is cut by planes parallel to the $w_0 w_1$- plane, the result would be concentric ellipses of constant mean square error as illustrated in Fig. 3-11.

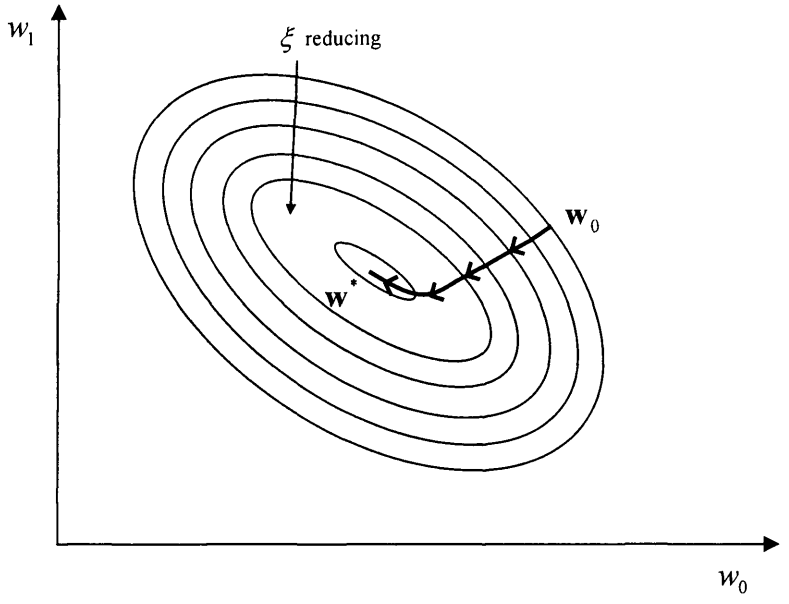

Fig. 3-11 Changes in the weight vector in steepest descent method

Starting with an arbitrary initial value of weight vector and applying equation (3-19) the next weight vector is derived which is on a smaller contour with a smaller mean square error. This continues until the centre of the ellipse is reached with the least value of least mean square error and the weight vector reaches its minimum. The property of the steepest descent method is that if the concessive weight vectors are connected, the resulting curve will always be normal to the least mean square error counters.

This clearly shows how sensitive the steepest descent method is to the initial weight vector. If the initial value is closer to the small diagonal the weight vector will travel a shorter path and therefore converges faster, while if the initial value is closer to the large diagonal, the convergence takes more steps.

3.5.2 Newton's method for gradient search

Newton's method for gradient search is a specific case of steepest descent method in which μ has its critical value. Theoretically Newton's method converges in one single step provided that the performance surface and its characteristics are well known. For this reason the Newton's method does not follow the path normal to the mean square error counters, but follows the path directly to the centre of the ellipse as shown in Fig. 3-12.

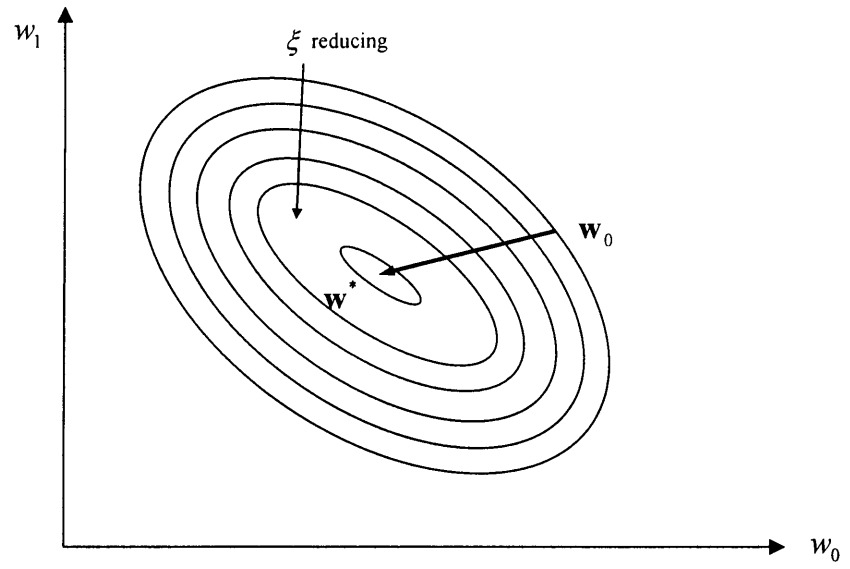

Fig. 3-12 Changes in the weight vector in Newton's method

Convergence in one step is valuable from an analytical point of view where cost and amount of calculation is crucial. Newton's method depends on the complete knowledge of the performance surface which is rarely the case in practice. Too fast an adaptation is not really always desirable. In many practical adaptive applications the function of the performance is unknown and has to be measured or estimated which itself takes some steps. Slow adaptation provides the opportunity of filtering process that eliminates the effect of noises generated in the gradient measurement process. Therefore in practical applications Newton's method is not as useful and exciting as it first appears to be.

3.6 Least Mean Square

The adaptation algorithms described earlier, the steepest descent and Newton's method are both based on the gradient of the performance surface. If there is not enough information available about the performance surface, the gradient should be estimated itself. Estimation of the gradient involves some approximation and adaptation itself which can be found in detail in any signal processing reference [73].

As alternatives other algorithms are available for descending on the performance surface, one of the simplest and most widely used of them is the least mean square algorithm usually abbreviated as LMS-algorithm. The basic idea behind this algorithm is described below.

Recalling from earlier, the aim of the adaptation process is to make the output of an adaptive controller become as close as possible to a desired signal. In other words it is intended to minimise the error signal defines as:

$$\varepsilon_k = d_k - y_k = d_k - \mathbf{w}_k^{\mathrm{T}}\mathbf{x}_k \qquad \textbf{(3-24)}$$

Where $\mathbf{x}_k$ is the input vector and $\mathbf{w}_k$ the weight vector as defined earlier. In order to reduce the error signal it is endeavoured to reduce the mean square of error as below:

$$\xi = E\left[\varepsilon_k^2\right] = E\left[d_k^2\right] + \mathbf{w}^{\mathrm{T}}\mathbf{R}\mathbf{w} - 2\mathbf{P}^{\mathrm{T}}\mathbf{w} \tag{3-25}$$

In the previous adaptation methods explained before, adaptation starts with some initial value of weight vector and using the gradient of the performance surface at that point then decide how much to change the weight vector to get closer to the bottom of the bowl:

$$\mathbf{w}_{k+1} = \mathbf{w}_k - \mu\nabla_k \tag{3-26}$$

Where ∇_k defines the gradient of the performance surface at step *k*. In the absence of information enough to calculate the gradient, some other techniques are used to approximate it. The idea of LMS-algorithm is simple; ε_k^2 itself is taken as an estimate of ξ_k. Subsequently the gradient of this estimated function is itself an estimate:

$$\hat{\nabla}_k = \begin{bmatrix} \dfrac{\partial \varepsilon_k^2}{\partial w_0} \\ \cdots \\ \dfrac{\partial \varepsilon_k^2}{\partial w_L} \end{bmatrix} = 2\varepsilon_k \begin{bmatrix} \dfrac{\partial \varepsilon_k}{\partial w_0} \\ \cdots \\ \dfrac{\partial \varepsilon_k}{\partial w_L} \end{bmatrix} \tag{3-27}$$

Where $\hat{\nabla}_k$ is the estimated gradient of the performance surface at step *k*. Using equation (3-24) this can be simplified to:

$$\hat{\nabla}_k = -2\varepsilon_k\mathbf{x}_k \tag{3-28}$$

The validity of this assumption can be verified if it is proved that the expected value of this estimated gradient is equal to the real gradient:

$$E[\hat{\nabla}_k] = \nabla_k \tag{3-29}$$

Starting from the left side of the above equation and knowing from (3-28) that:

$$E[\hat{\nabla}_k] = E[-2\varepsilon_k\mathbf{x}_k] = -2E[\varepsilon_k\mathbf{x}_k] \tag{3-30}$$

Substituting from equation (3-24):

$$-2E[\varepsilon_k \mathbf{x}_k] = -2E[d_k \mathbf{x}_k - \mathbf{x}_k \mathbf{x}_k^T \mathbf{W}] = 2E[\mathbf{x}_k \mathbf{x}_k^T \mathbf{W}] - 2E[d_k \mathbf{x}_k] \quad \textbf{(3-31)}$$

Remembering the definition of matrixes **R** and **P**, it can be concluded that:

$$2E[\mathbf{x}_k \mathbf{x}_k^T \mathbf{w}] - 2E[d_k \mathbf{x}_k] = 2(\mathbf{R}_k \mathbf{w}_k - \mathbf{P}_k) = \nabla_k \quad \textbf{(3-32)}$$

Reviewing equations (3-29) to (3-32) it is shown that:

$$E[\hat{\nabla}_k] = \nabla_k$$

Which means the simplification made in the estimation of the gradient vector is justifiable. Having such a simple formula for estimating the gradient, the weight vectors can also be updated using this estimation in equation (3-26) and deriving a new relationship which is the base of LMS-algorithm:

$$\mathbf{w}_{k+1} = \mathbf{w}_k + 2\mu\varepsilon_k \mathbf{x}_k \quad \textbf{(3-33)}$$

Similar to the case of steepest descent and Newton's method, μ is the governing factor of speed and stability of the adaptation. As before if μ is a smaller number the corrections made are more gradual and the adaptation is slower. If μ is a larger number the corrections in the weight vector are also larger and the adaptation is faster but might not even converge. It can be shown that the stability condition for convergence of the filter weights is that [73]:

$$0 < \mu < \frac{1}{tr[\mathbf{R}]} \quad \textbf{(3-34)}$$

Where $tr[\mathbf{R}]$ is the "trace of matrix **R**", defined as the sum of the diagonal elements of **R**. If the LMS-algorithm is not used, in order to have a reasonable estimate of the gradient surface each element of equation (3-25) should be known. Although each component of this equation is known, for finding the expected value of each term a relatively large sample of that data should be available and averaged over time. The result is then squared and differentiated to find the gradient of the performance surface. In LMS-algorithm

however, no squaring, averaging, or differentiation is done and is particularly useful for practical applications.

Taking the instantaneous value of ε_k^2 as an estimate of ξ_k without any averaging, inserts some noise in the gradient components. Fig. 3-13 shows a typical behaviour of weight vector being optimised using LMS-algorithm for a filter consisting of two weights. The noise observed is similar even for filters with higher weights. The path of the weight vector is by principle normal to the error counters, however because of the noise involved this is not followed all the time. Higher values of μ also adds to the noise. However the noise is attenuated with time by the adaptive process as the error signal reduces itself.

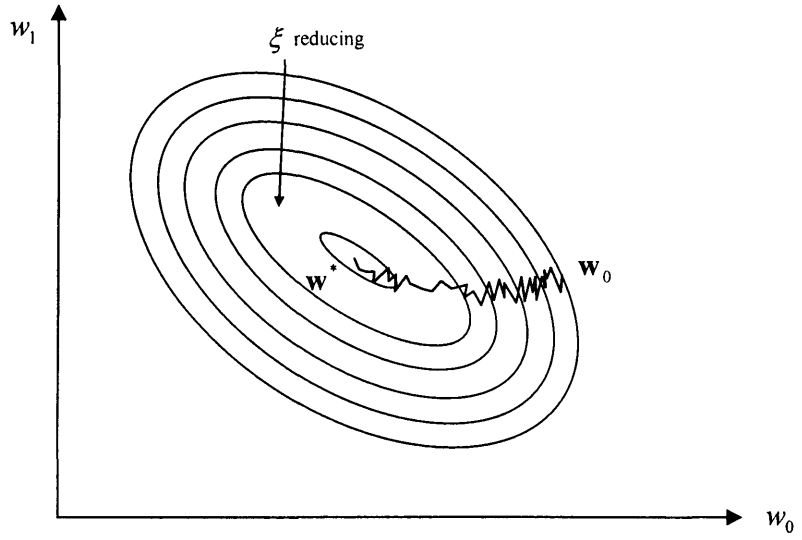

Fig. 3-13 Changes in the weight vector in LMS method

3.7 Concluding remarks

What was explained in this chapter was the principle core of adaptation. It was by no means even a complete basic reference; however, it has covered what is necessary for the reader in order to understand the following chapters and mainly the adaptive control strategy used in Chapter 6 and Chapter 7.

The particular application for which adaptive theory is being used is for a ship-tank system. A more advanced controller is required when limited information about the plant is available, or the plant properties changes over time. In this particular application, the exact dynamics of the ship-tank system is not known. The mathematical models developed in Chapter 5 give a good insight, but in practice there always exist characteristics that are not modelled. The dynamic transfer function of the ship also varies in different weathers and under different loading conditions. This implies that if the ship-tank system is modelled with an adaptive linear filter its performance surface is not always available. In the light of the concepts explained in this chapter it is not easy to use steepest descent or Newton's methods as both of them require knowledge of the performance surface. It will be seen in Chapter 7 that the LMS algorithm of adaptation has been used for this particular application where adaptation is performed by estimation of the least mean square error.

Chapter 4

4 Prediction of Waves

4.1 Introduction

This chapter introduces one of nature's forces that is responsible for rolling a ship: sea waves. As explained before in the introduction, this thesis presents a new original strategy in controlling the actuating pumps of an active U-tank based on predicting the waves reaching the ship in the near future according to the history of the waves in the past few minutes. The pumps therefore move the water in a manner to counteract the wave moments by the time they arrive. It is therefore necessary to have knowledge of the wave anatomy and how to predict it.

This chapter explains the physics of waves and the statistical modelling usually applied. Different sources and textbooks have been consulted for this reason [10;40]. It then investigates the predictability of waves over a short period of time and describes different models for predicting them using the concepts of adaptive control explained in Chapter 3. The results from this chapter are used in the following chapters. Chapter 6 describes a control algorithm in which the prediction of incoming waves is used for roll stabilization. Sea waves are usually considered to be sinusoid for initial modelling and investigation of a marine vehicle. However any solution for a particular problem in marine engineering solved for sine waves only might be valuable from a pure academic point of view, but would certainly lack credit in practice. In reality the sea does not have a regular surface but rather an irregular and complex one.

4.2 Basic wave theory

Although in reality, ocean waves seem to be very irregular, it has been possible to assign some statistical data to them by observing the height of the waves over a certain period of time. The sea surface varies from time to time and from place to place. The main factor that changes the pattern of the sea is the wind. Depending on the wind speed or the "Beaufort number" the surface of the sea varies. The "sea state" is the condition of the sea at any given time and place and presented by number between 0 to 9 (0 being a mirror surface sea and 9 a sea at storm). There are many statistical parameters describing the state of the sea, but there are ones of particular interest to this application. Fig. 4-1 shows a schematic of an irregular sea wave. The parameters shown on the picture are described in more details below:

ζ Wave elevation being the instantaneous displacement of the surface of the sea at rest.

ζ_a Apparent wave amplitude being the vertical distance from the mean water level to a peak or a trough.

h_w Apparent wave height being the distance between a successive peak and trough.

T_z Apparent zero crossing period being the time difference between two successive upwards crossing of zero in a record.

T_c Apparent period being the time difference between two successive crests.

L_w Apparent wave length being the horizontal distance between two adjacent crests in the direction of advance.

The average wave height is defined as the mathematical mean of many measurements of wave heights (ζ_a) and is shown by $\overline{\zeta}_a$.

Apart from wave height there is also another wave parameter known as wave slope which is obtained by differentiating the equations of wave height with respect to time. This parameter is used especially in investigating ship motions. One of the most important properties of an irregular sea wave is "characteristic wave height" or "significant wave

height" which is the mean of the heights of the one-third highest waves for a given record shown by $(h_w)_{1/3}$.

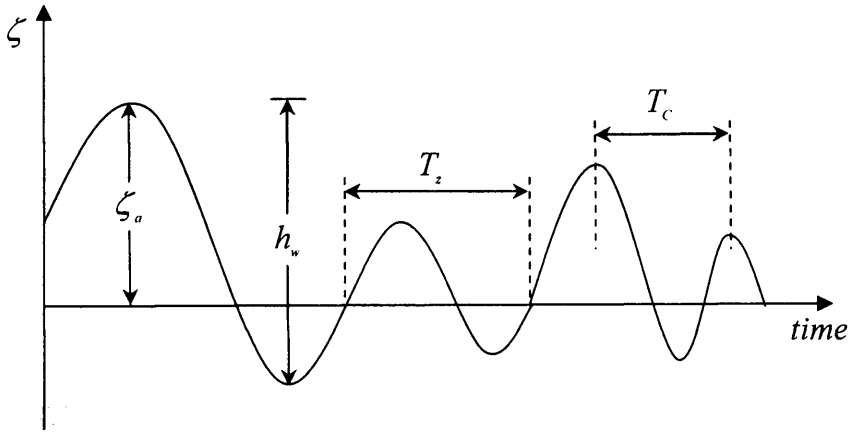

Fig. 4-1 Schematic of an irregular sea wave elevation at a fixed point

In order to have a better insight into the sea conditions in different weathers, the statistical properties of sea waves are presented in Table 4-1 which was agreed by the World Meteorological Organisation (WMO) in 1970. Each sea state number corresponds to a range of significant wave heights and there is no indication of period.

Sea State	Description	Significant Wave Height	
		Range (m)	Mean (m)
0	Calm (glassy)	0	0
1	Calm (ripped)	0 – 0.1	0.05
2	Smooth (wavelets)	0.1 – 0.5	0.3
3	Slight	0.5 – 1.25	0.875
4	Moderate	1.25 – 2.5	1.875
5	Rough	2.5 – 4.0	3.25
6	Very rough	4.0 – 6.0	5.0
7	High	6.0 – 9.0	7.5
8	Very high	9.0 – 14.0	11.5
9	Phenomenal	Over 14.0	Over 14

Table 4-1 World Meteorological Organisation sea state code [10]

A more detailed table of sea state statistical characteristics was developed in 1964 and is generally referred to as L. Moskowitz and W. Pierson sea state [10] table (see Table 4-2). However this table is not in SI units.

Sea State	Description	Wind Speed (Kts)	Significant Wave Height (Ft)	Significant Range of Periods (Sec)	Average Period (Sec)	Average Length of Waves (Ft)
0	The sea is like a mirror. Ripples formed with the appearance of scales, but without foam crests.	3	<.5	<.5 - 1	0.5	1.5
		4	<.5	.5 - 1	1	2
1	Small wavelets, still short but more pronounced, form; crests have a glassy appearance but do not break	5	0.5	1 - 2.5	1.5	9.5
		7	1	1 - 3.5	2	13
		8	1	1 - 4	2	16
2	Large wavelets form; crests begin to break. Foam of a glassy appearance forms; there may be scattered whitecaps.	9	1.5	1.5 - 4	2.5	20
		10	2	1.5 - 5	3	26
		11	2.5	1.5 - 5.5	3	33
		13	3	2 - 6	3.5	39.5
3	Small waves form, becoming longer; whitecaps are fairly frequent	14	3.5	2 - 6.5	3.5	46
		15	4	2 - 7	4	52.5
		16	4.5	2.5 - 7	4	59
		17	5	2.5 - 7.5	4.5	65.5
4	Moderate waves appear, taking a more pronounced form; there are many whitecaps and a chance of some spray	18	6	2.5 - 8.5	5	79
		19	7	3 - 9	5	92
		20	7.5	3 - 9.5	5.5	99
5	Large waves begin to form; white foam crests are more extensive everywhere. There is some spray.	21	8	3 - 10	5.5	105
		22	9	3.5 - 10.5	6	118
		23	10	3.5 - 11	6	131.5
		25	12	4 - 12	7	157.5
6	The sea heaps up and white foam from breaking waves begins to be blown in streaks along the direction of the wind. Spindrift begins	27	14	4 - 13	7.5	184
		29	16	4.5 - 13.5	8	210
		31	18	4.5 - 14.5	8.5	236.5
		33	20	5 - 15.5	9	262.5
7	Moderately high waves of greater length form; edges of crests break into spindrift. The foam is blown in well-marked streaks along the direction of the wind. Spray affects visibility	37	25	5.5 - 17	10	328.5
		40	30	6 - 19	11	394
		43	35	6.5 - 21	12	460
		46	40	7 - 22	12.5	525.5
8	High waves form. Dense streaks of foam appear along the direction of the wind. The sea begins to roll. Visibility is affected	49	45	7.5 - 23	13	591
		52	50	7.5 - 24	14	655
		54	55	8 - 25.5	14.5	722.5
		57	60	8.5 - 26.5	15	788
9	Exceptionally high waves. Sea completely covered with long white patches of foam. Everywhere edges of wave crests are blown into froth. Visibility seriously affected.	61	70	9 - 28.5	16.5	920
		65	80	10 - 30.5	17.5	1099
		69	90	10.5 - 32.5	18.5	1182
		73	100	11 - 34.5	19.5	1313.5

Table 4-2 definition of different sea states by Moskowitz and Pierson (revised December 1964) [10]

4.3 Wave Spectrum

As mentioned earlier in reality ocean waves seem to be very irregular. The pattern of the sea is also never repeated from one time to another. However this irregular wave pattern can be generated by addition of a large number of sinusoidal waves. Each sinusoid wave carries a portion of the total energy of the wave being equal to $\frac{1}{2}\rho g\zeta_a^2$ per unit square of sea surface. The final irregular sea is shaped by adding all sinusoidal waves and therefore the total energy of the sea wave per unit square is defined by:

$$E_T = \frac{1}{2}\rho g(\zeta_{a1}^2 + \zeta_{a2}^2 + ... + \zeta_{an}^2) \quad \textbf{(4-1)}$$

For any sea wave it is thus possible to plot the energy portion of each sinusoidal component versus the frequency (or sometimes the period or wavelength) of that component. This plot is called "energy spectrum" of that sea wave.

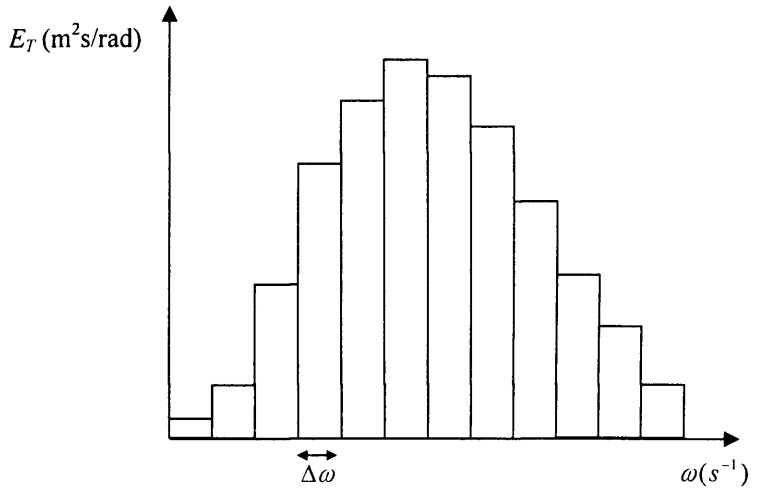

Fig. 4-2 A discrete energy spectrum of an irregular sea wave

As a final step it should be noted that sea waves are actually generated with sinusoidal waves of all frequencies from 0 to ∞ and $\Delta\omega$ becomes very small and tends to $d\omega$. Therefore the energy of a particular range of frequencies can be found by integrating the energy spectrum between those frequencies.

A brief note is now required on how sea waves are generated. As mentioned earlier waves are generated as a result of wind blowing over the sea. At first the wavelengths are shorter and more like ripples. The energy of the waves is mostly carried by high frequency waves. Gradually as the wind continues to blow longer waves are created until finally the sea becomes "fully developed" in which the wind has no more effect on the pattern. In other words the sea becomes stable. During this procedure the maximum value of the energy spectrum shifts towards the lower frequencies. For a fully developed sea the energy of the waves is concentrated on waves having lower frequencies (Fig. 4-3). Unlike a wave histogram that has a Gaussian form, energy spectrum can have any shape.

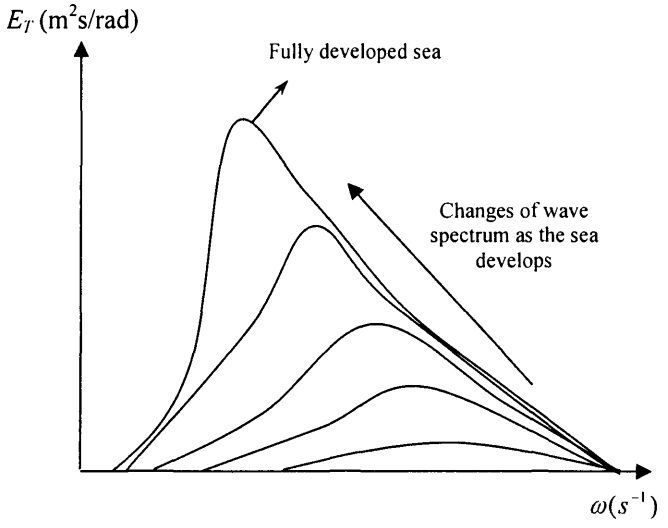

Fig. 4-3 Energy spectrum of an irregular sea wave developing

A more widely used spectrum is obtained by dividing equation (4-1) by ρg:

$$E_T = \frac{1}{2}(\zeta_{a1}^2 + \zeta_{a2}^2 + ... + \zeta_{an}^2) \qquad \textbf{(4-2)}$$

and plotting it versus frequency. The area under this curve is generally noted as m_0, and if multiplied by ρg gives the total energy per unit squared of sea wave. This new spectrum is called "wave spectrum" and its ordinate is called "spectral density of wave energy", denoted by $S_\zeta(\omega_w)$.

It is very important to note that like all other spectral density functions the numerical value of $S_\zeta(\omega_w)$ at a particular frequency, say 0.8 rad/s, has no physical meaning. It is only the area under the function between two frequencies that bears a physical meaning and that is half the sum of squared amplitude of sine waves that have frequencies in that range:

$$\int_{\omega_1}^{\omega_2} S(\omega)d\omega = \frac{1}{2}\sum_{i=\omega_1}^{\omega_2}\zeta_{a(i)}^2 \qquad \textbf{(4-3)}$$

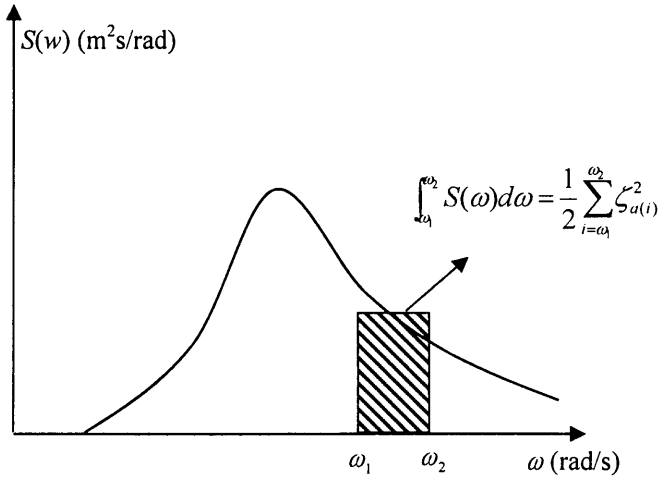

Fig. 4-4 Wave spectrum of an irregular sea wave

The significant wave height is obtained by

$$(h_w)_{1/3} = 4.0\sqrt{area} \qquad \textbf{(4-4)}$$

Which as stated earlier the area under the curve is:

$$m_0 = \int_0^\infty S(\omega)d\omega \qquad \textbf{(4-5)}$$

Other statistical values that can be derived from a wave spectrum are average zero crossing period, $\tilde{T}_z$, average crest to crest crossing period, $\tilde{T}_c$, and average apparent wavelength, $\tilde{L}_w$:

$$\widetilde{T}_z = 2\pi\sqrt{\frac{m_0}{m_2}} \tag{4-6}$$

$$\widetilde{T}_c = 2\pi\sqrt{\frac{m_2}{m_4}}$$

$$\widetilde{L}_w = 2\pi g\sqrt{\frac{m_0}{m_4}}$$

Where m_2 and m_4 are defined as the second and forth moment of the area under the spectrum respectively:

$$m_2 = \int_0^\infty \omega^2 S(\omega)d\omega \tag{4-7}$$

$$m_4 = \int_0^\infty \omega^4 S(\omega)d\omega$$

Other useful information that can be obtained from a wave spectrum is:

1- The range of frequencies that is important for further analysis in a particular weather.
2- The frequency bearing the maximum energy and hence the maximum height.
3- The existence of swell at low frequencies.

In order to analyse the behaviour of a ship in sea waves, it is later on required to generate sea waves using the parameters already explained especially m_1, m_2, and $(h_w)_{1/3}$ as it will be explained in the following section.

4.4 Standard Wave Spectrum

It is suggested that if the wave spectrum of a particular sea wave is not available, International Towing Tank Conference (ITTC) spectral formulation be used which is as follows:

$$S(\omega) = \frac{A}{\omega^5}e^{-B/\omega^4} \tag{4-8}$$

Where A and B are defined for two cases:

a) If the significant wave height, $(h_w)_{1/3}$, is known:

$A = 8.10 \times 10^{-3} g^2$ where g is the gravity in appropriate unit.

$B = 3.11 \times 10^4 / h_{1/3}^2$ if the significant wave height is in centimetres, or

$B = 33.56 / h_{1/3}^2$ if the significant wave height is in feet

b) If both significant wave height, $(h_w)_{1/3}$, and significant wave period, T_1 are known:

$A = 173 h_{1/3}^2 / T_1^4$

$B = 691 / T_1^4$

Where significant wave period, T_1 is given by:

$$T_1 = 2\pi \sqrt{\frac{m_0}{m_1}}$$

$$m_1 = \int_0^\infty \omega S(\omega) d\omega$$

Experience has shown that this period can be taken as the observed period.

4.5 Wave generation software

The sea waves used for simulations throughout this thesis are created using a wave generation code developed by the author which works based on the above theories. It asks the user the sea state required, the length of the wave (in seconds), and the frequency bandwidth. Then using ITTC formulation using statistical information available (Table 4-2) for that particular sea state it builds the standard wave spectrum. Next step is finding the area under the spectrum for the length of the bandwidth and using it to calculate the amplitude of sinusoidal wave corresponding to that frequency. This is done for frequencies starting from 0 rad/s up to a final frequency depending on the sea state (varying from 1 rad/s to 8 rad/s) using intervals equal to the frequency bandwidth the user has requested. For less advanced users a default value of 0.02 rad/s is assigned to the frequency bandwidth. Having a sinusoidal wave for each frequency, a random phase is

given to each wave and finally they are superimposed to produce an irregular sea wave. The interface of the software is shown in Fig. 4-5 followed by how the output wave and wave spectrum produced look like in Fig. 4-6:

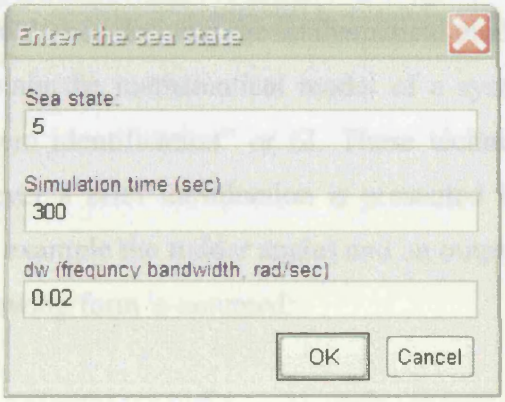

Fig. 4-5 Snap shot of the sea wave generator software

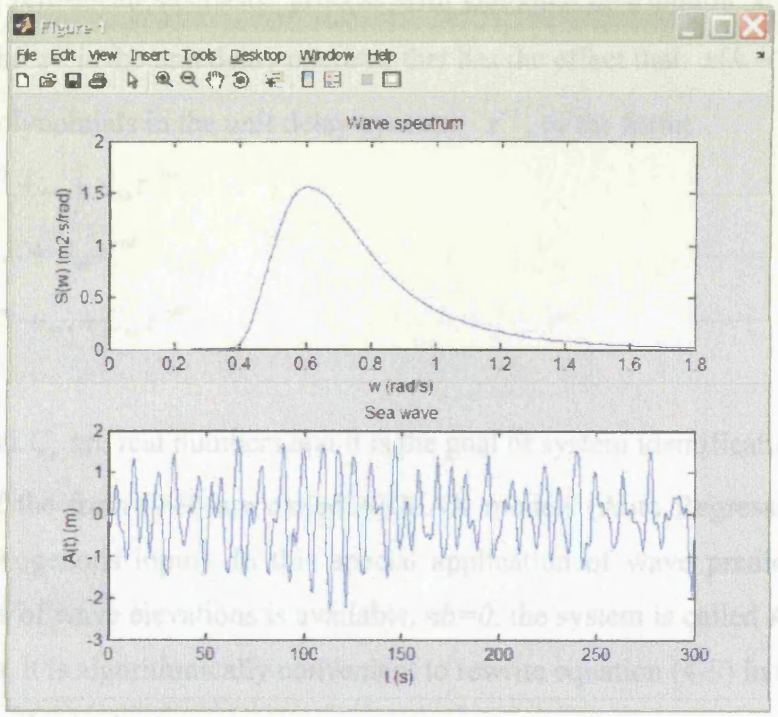

Fig. 4-6 Sea wave and wave spectrum generated by the software

4.6 Wave Prediction

As mentioned in the introduction of this chapter the control strategy of the active U-tank pumps is based on predicting the waves reaching the ship in the near future according to the history of the waves in the past few minutes. Given the mathematical model of a system, it is straightforward to transform it into predictor form in the way explained later in this section. The main problem is deriving the mathematical model in the first instance. The techniques used to obtain the mathematical model of a system from given input-output data is called "system identification" or SI. These techniques are explained in detail in Ljung [39], however a brief introduction is presented here as follows. For a system with an input u (for example the rudder angle) and an output y (say ship heading), a discrete model of the following form is assumed:

$$A(z^{-1})y(k) = B(z^{-1})u(k) + C(z^{-1})e(k) \tag{4-9}$$

Where

$y(k), u(k)$ are system's output and input respectively. $e(k)$ is a noise term and is assumed to be a zero-mean stochastic process with Gaussian distribution. k is a discrete time index and the z^{-1} is the unit delay operator that has the effect that: $x(k-1) = z^{-1}x(k)$

A, B and C are polynomials in the unit delay operator z^{-1}, of the form:

$$A(z^{-1}) = 1 + A_1 z^{-1} + \ldots + A_{na} z^{-na}$$

$$B(z^{-1}) = B_1 z^{-1} + \ldots + B_{nb} z^{-nb}$$

$$C(z^{-1}) = 1 + C_1 z^{-1} + \ldots + C_{nc} z^{-nc}$$

Where A_i, B_i and C_i are real numbers and it is the goal of system identification to derive them. Models of the form (4-9) are called ARMAX models (Auto Regressive Moving Average with eXogenous input). In this special application of wave prediction where only a time series of wave elevations is available, $nb=0$, the system is called ARX. When using SI methods, it is algorithmically convenient to rewrite equation (4-9) in the form:

$$y(k) = \theta^T(k-1)\phi(k-1) + e(k) \tag{4-10}$$

where

$$\theta^T(k-1) = [A_1 \ldots A_{na}\ B_1 \ldots B_{nb}\ C_1 \ldots C_{nc}]$$
$$\phi^T(k-1) = [-y(k-1) \ldots -y(k-na)\ \ u(k-1) \ldots u(k-nb)\ \ e(k-1) \ldots e(k-nc)]$$

If the best one-step-ahead prediction is defined for (4-10) using the information (the estimation of $\theta^T(k-1)$ and $\phi(k-1)$) up to and including step k-1 as

$$\hat{y}(k \mid k-1) = E[y(k)] \tag{4-11}$$

where E is the estimation operator.

Assuming that $e(k)$ is a zero-mean process then:

$$\hat{y}(k \mid k-1) = E[y(k)] \tag{4-12}$$
$$= E[\theta^T(k-1)\phi(k-1)] + E[e(k)] = \theta^T(k-1)\phi(k-1)$$

If one-step-ahead prediction error is denoted by $\varepsilon(k)$ then

$$\varepsilon(k) = y(k) - \hat{y}(k \mid k-1) \tag{4-13}$$

It is the task of the adaptation algorithm to minimize this error. Generally a criterion of how well the model $\theta(k)$ is performing is the sum of the squares of the prediction errors:

$$V_N(\theta) = \frac{1}{N}\sum_{k=1}^{N}\varepsilon^2(k) \tag{4-14}$$

where N is the number of samples collected. There are different algorithms to minimize $V_N(\theta)$ (see Ljung[39] for details). The general form of the basic algorithm is

$$\theta(k) = \theta(k-1) + \gamma(k)P(k)n(k)[y(k) - \hat{y}(k)] \tag{4-15}$$

where

$\gamma(k)$ is a time varying gain known as the forgetting factor

$P(t)$ is related to the covariance of the estimation

$n(t)$ is related to the gradient of $y(t)$ with respect to $\theta(t)$

Once the ARMAX model is derived and the values of the parameters estimated, $\theta(k)$, are proved to minimize $V_N(\theta)$ the model can be used to predict not only one-step-ahead but also *k*-steps-ahead using the information gathered so far.

In the case of predicting the incoming waves the number of prediction steps required is derived from the delay between the control signal and the moment created by the tank. So if the required stabilizing moment is created 5 second after the control signal the wave prediction is performed for the next 5 seconds to compensate the inevitable lag. The order of the ARX model, *na,* is set as twice the prediction steps required. This has been derived from trial and error analysis and it has been shown that it gives the best prediction [14-16]. After this point increasing the order of the model does not have any significant effect on the prediction. The effect of variations of *na* on the prediction has been investigated in more depth by Broome and Pittaras [14-16].

Better prediction can be achieved if there is stronger correlation between the past values of a signal. A signal having weak correlation becomes less predictable. In the case of predicting waves, there is a good correlation between past values and the energy of the wave is concentrated around a dominant frequency (Fig. 4-4).

Fig. 4-7 shows the result of 10 steps-ahead (5 seconds) wave slope prediction for sea state 5 using an ARX20 model where the sample time is 0.5 second (wave slope or wave angle was earlier defined in section 4.2). The similarity of the predicted and actual wave remains during the whole period of simulation, apart from the first 50 seconds required for the algorithm to establish a set of coefficients and for initial transients to decay. Fig. 4-8 shows the expected 10-step-ahead prediction error, $E[\varepsilon(k)]$ where Fig. 4-8a shows the expected prediction error during the transient state and Fig. 4-8b shows the expected prediction after the transient has decayed. It is clear that after the transient period has passed, the prediction error gets to a reasonably low level.

The prediction accuracy is inversely proportional with the length of prediction ahead required (see Broome and Pittaras [14-16]) . So prediction for 4 seconds ahead is

performed much better than prediction for 10 seconds ahead. Fig. 4-9 and Fig. 4-10 show the effect of increasing prediction horizon on accuracy of the prediction for the same input wave. The results are shown for after 130s where the initial perturbations have decayed and expected error reaches its minimum value. Fig. 4-11 shows how the minimum expected error increases with the number of steps ahead the prediction is performed.

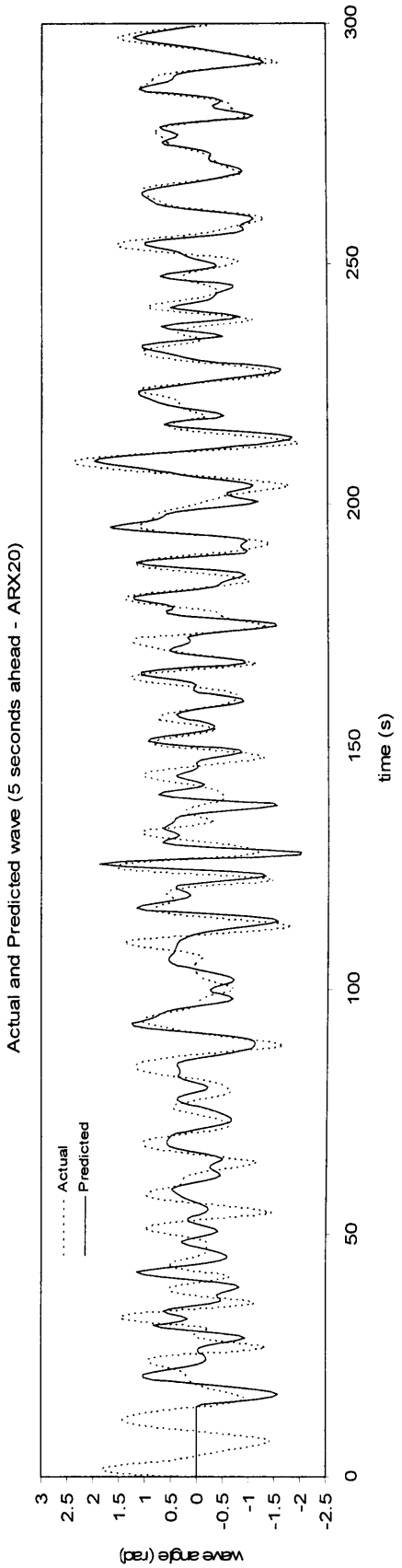

Fig. 4-7 Comparison between measured and predicted wave.

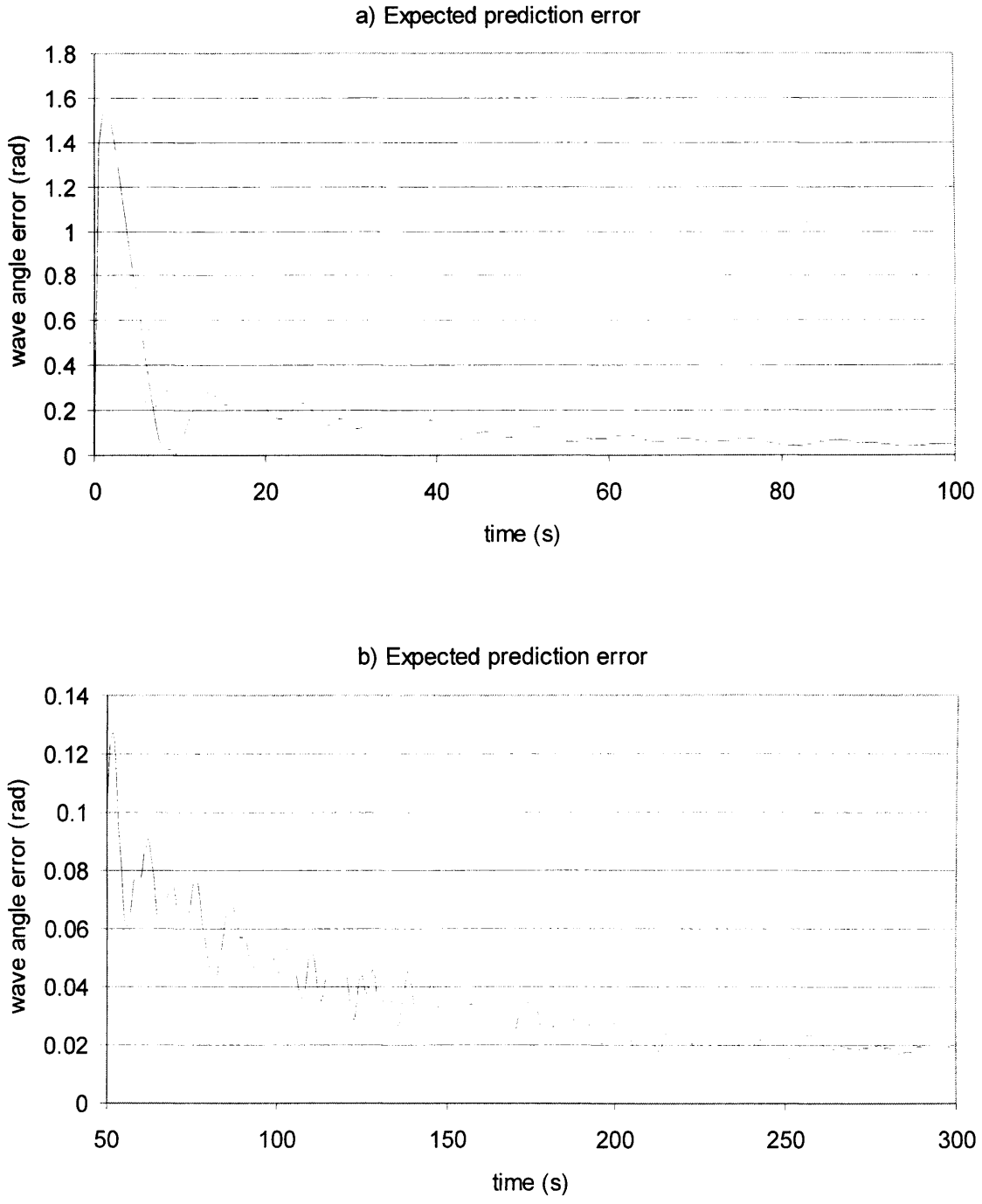

Fig. 4-8 Expected prediction error $E[e(t)]$ a) during the transient state b) after the transient has decayed

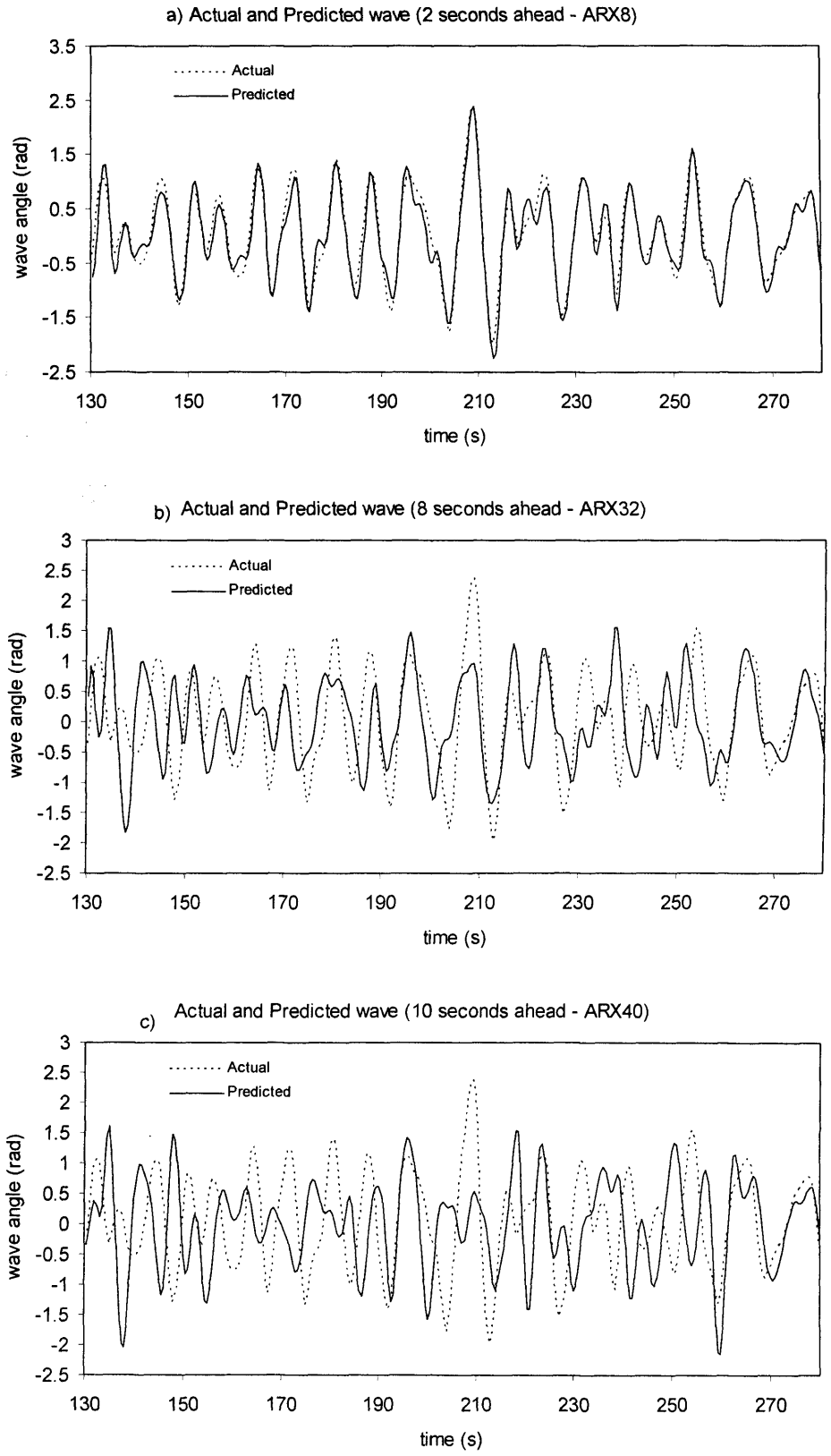

Fig. 4-9 Comparison between measured and predicted wave: a) 2s ahead b) 8s ahead c) 10s ahead

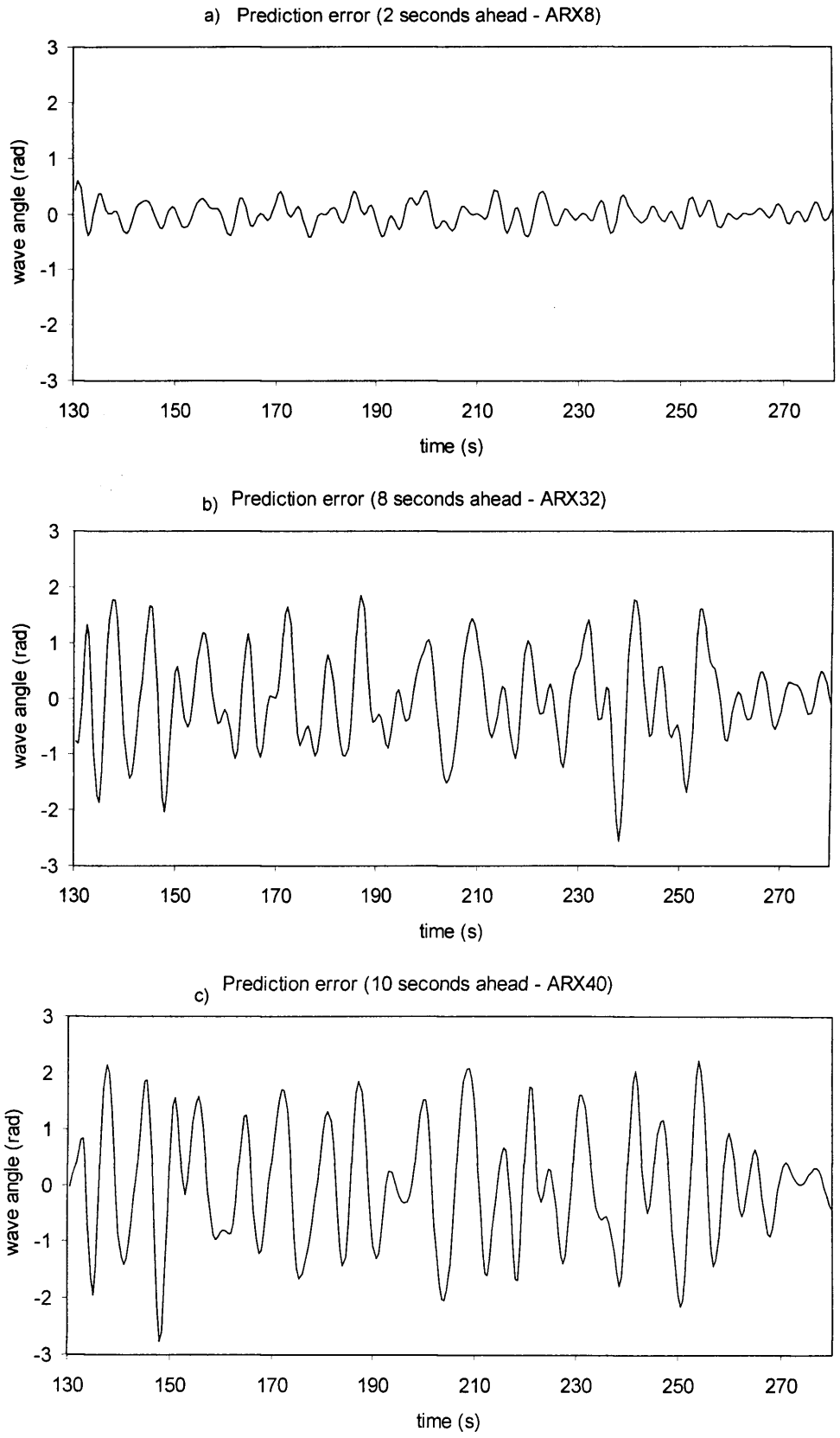

Fig. 4-10 Prediction error signal, $e(t)$, for: a) 2s ahead b) 8s ahead c) 10s ahead

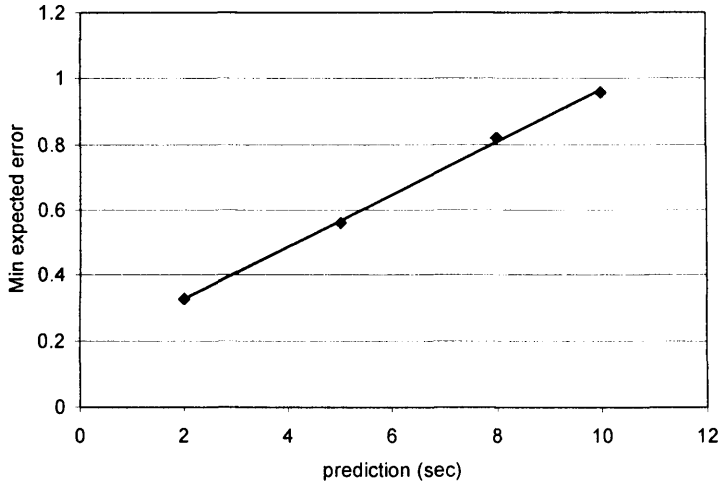

Fig. 4-11 Minimum expected prediction error v. seconds of prediction ahead

4.7 Concluding remarks

In this chapter the physics of waves and the statistical modelling usually applied for them was explained. Later the predictability of waves over a short period of time was investigated and different models for predicting them using the concepts of adaptive control explained in Chapter 3 were explained. The results from this chapter are used in the following chapters where a control algorithm in which the prediction of incoming waves is used for roll stabilization.

Chapter 5

5 Dynamic Modelling of U-shape Anti-roll tanks

5.1 Introduction

In this chapter U-shape anti-roll tanks are mathematically modelled by two different approaches: one method uses the Euler equation and is based on fluid mechanics principles; the other uses the Lagrange energy method and is based on dynamics of solid materials. Modelling is first done for the motion of water inside a fixed tank where the tank has no motion itself and then further developed for a tank experiencing sway and roll motion.

Models derived from both methods have been successfully used in marine engineering applications for years. It is the intention of this chapter to compare the two approaches and investigate whether two methods so different in their fundamentals provide the same solution using the same assumptions and tank.

5.2 Modelling of a fixed tank

5.2.1 Modelling of a fixed tank by Euler equation

The modelling procedure of a U-tank requires using many mathematical equations and therefore in order to have a better understanding of the dynamics of a U-tank on a ship at first instance mathematical modelling of a simple U-tank is investigated as if the tank is fixed on the ground. The following procedure is based on Stigter's modelling of U-tanks [61] which is also modified by Lloyd [40]. Fig. 5-1 shows a simple U-tank.

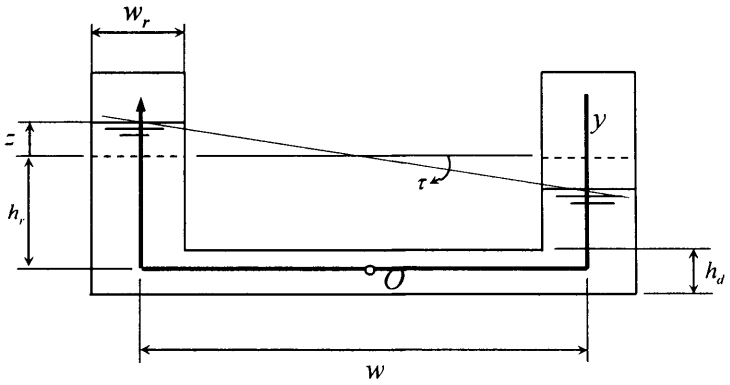

Fig. 5-1 Axis system and tank dimensions

The connecting duct has a constant rectangular cross-section and the length of the tank in the fore/aft direction is x_t and constant for all y. The walls are parallel and the air pressure above the water is ignored. The origin O is at the midpoint of the connecting duct and an axis y runs down one reservoir, along the duct and up the other reservoir of the U-tube. Therefore the indexes r and d represent the reservoir and the duct respectively. n is the width of the tank perpendicular to the y axis in the plane of the page. Note that n is a variable, which has different values h_d on the duct and w_r on the two reservoirs. It is assumed that there is no flow in the n direction. This assumption might not be always true, especially if $h_d \neq w_r$, also there will be multidimensional flow particularly at the bends. However, this assumption greatly helps in simplifying the dynamics of the tank.

It is assumed that the motion of a unit mass of fluid in the tank is governed by a simplified version of Euler's equation:

$$\frac{\partial v}{\partial t} + v\frac{\partial v}{\partial y} = Y - \frac{1}{\rho}\frac{\partial P}{\partial y} \qquad \textbf{(5-1)}$$

Where

Y is the external force per unit mass

ρ is the density of the fluid inside the tank and is assumed constant

v is the fluid velocity along the positive y direction

As the reservoirs and the duct were assumed to be of constant cross section one may write everywhere except at the junctions between the duct and the reservoirs:

$$\frac{\partial v}{\partial y} = 0 \tag{5-2}$$

Neglecting these corner effects equation (5-1) reduces to

$$\frac{\partial v}{\partial t} = Y - \frac{1}{\rho}\frac{\partial P}{\partial y} \tag{5-3}$$

or, since there are now only two variables,

$$\frac{dv}{dt} = Y - \frac{1}{\rho}\frac{dP}{dy} \tag{5-4}$$

The velocity of the fluid in the two reservoirs is

$$v_r = \dot{z} = \frac{w}{2}\dot{\tau} \tag{5-5}$$

where τ is the "tank angle" defined in Fig. 5-1 and is assumed to be small (The validity of this assumption is investigated in section 5.2.1.1). From the continuity equation the velocity at any point in the tank is

$$v = \frac{w_r v_r}{n} = \frac{w_r w}{2n}\dot{\tau} \tag{5-6}$$

The external force per unit mass Y is made up of contributions due to the accelerations applied to the tank and the friction forces arising from the losses in any throttled valve, wall friction, bends etc.

For the fixed tank these contributions are mainly:

a) The acceleration due to gravity along the y direction: a_g

a_g is equivalent to -g in the starboard reservoir, +g in the port reservoir, and zero in the duct.

b) The frictional or damping forces. Although these are expected to be proportional to the square of the local velocity it is convenient to assume that the damping can be linearised and it is proportional to the velocity. Therefore it can be shown that the frictional force per unit mass is approximately

$$\frac{-qv}{n}$$

where q is a coefficient of resistance to be estimated or determined by experiment. Equation (5-4) then becomes

$$\frac{w_r w}{2n}\ddot{\tau} = -a_g - q\left(\frac{w_r w}{2n^2}\right)\dot{\tau} - \frac{1}{\rho}\frac{dP}{dy}$$

or

$$\frac{w_r w}{2n}\ddot{\tau} + q\left(\frac{w_r w}{2n^2}\right)\dot{\tau} + a_g = -\frac{1}{\rho}\frac{dP}{dy} \quad (m/s^2) \tag{5-7}$$

or

$$\frac{\rho w_r w dy}{2n}\ddot{\tau} + q\left(\frac{\rho w_r w dy}{2n^2}\right)\dot{\tau} + \rho a_g dy = -dP \quad (Pa) \tag{5-8}$$

This equation is now integrated with respect to y to obtain an equation giving the motion of the fluid in the tank (in terms of the tank angle τ) as a function of the pressure difference at the surface in the two reservoirs. Strictly, the integration should proceed from the surface level in the starboard reservoir (negative y) to the surface level in the port reservoir (positive y). It is obtained

$$\frac{\rho w_r w I_1}{2}\ddot{\tau} + \frac{\rho q w_r w I_2}{2}\dot{\tau} + \rho I_3 = P_{starboard} - P_{port} \quad (Pa) \tag{5-9}$$

where

$$I_1 = \int \frac{dy}{n} = \int_{-h_r}^{0} \frac{dy}{w_r} + \int_{w/2}^{w/2} \frac{dy}{h_d} + \int_{0}^{h_r} \frac{dy}{w_r} = \frac{w}{h_d} + \frac{2h_r}{w_r}$$

$$I_2 = \int \frac{dy}{n^2} = \int_{-h_r}^{0} \frac{dy}{w_r^2} + \int_{w/2}^{w/2} \frac{dy}{h_d^2} + \int_{0}^{h_r} \frac{dy}{w_r^2} = \frac{w}{h_d^2} + \frac{2h_r}{w_r^2}$$

$$I_3 = \int a_g dy = \int_{-h_r}^{0} g dy + \int_{w/2}^{w/2} (0) dy + \int_{0}^{h_r} (-g) dy = 0$$

It is also evident that the pressure difference between port and starboard is

$$P_s - P_p = -\rho g \Delta h = -\rho g (2z) = -\rho g w \tau \qquad \textbf{(5-10)}$$

Therefore

$$\left(\frac{\rho w_r w}{2} \left[\frac{w}{h_d} + \frac{2h_r}{w_r} \right] \right) \ddot{\tau} + \left(\frac{\rho q w w_r}{2} \left[\frac{w}{h_d^2} + \frac{2h_r}{w_r^2} \right] \right) \dot{\tau} + (\rho g w) \tau = 0 \quad \textbf{(Pa)} \qquad \textbf{(5-11)}$$

It is also possible to express this equation as a function of moment applied to the tank fluid by multiplying it by the surface of the reservoir and the moment arm $w w_r x_l / 2$; this leads to

$$a_{\tau\tau} \ddot{\tau} + b_{\tau\tau} \dot{\tau} + c_{\tau\tau} \tau = 0 \quad \textbf{(Nm)} \qquad \textbf{(5-12)}$$

where

$$a_{\tau\tau} = Q_l w_r \left[\frac{w}{2h_d} + \frac{h_r}{w_r} \right]$$

$$b_{\tau\tau} = Q_l q w_r \left[\frac{w}{2h_d^2} + \frac{h_r}{w_r^2} \right]$$

$$c_{\tau\tau} = Q_l g$$

$$Q_l = \frac{\rho w_r w^2 x_l}{2}$$

Therefore the natural frequency and the damping ratio of the tank are

$$\omega_n = \sqrt{\frac{c_{\tau\tau}}{a_{\tau\tau}}} = \sqrt{\frac{2gh_d}{ww_r + 2h_r h_d}} \tag{5-13}$$

$$\varsigma = \frac{b_{\tau\tau}}{2\omega_n a_{\tau\tau}} = \frac{q(ww_r^2 + 2h_r h_d^2)}{\sqrt{8w_r^2 h_d^3 g(ww_r + 2h_r h_d)}} \tag{5-14}$$

An important point observed from (5-13) and (5-14) is that the natural frequency and the damping ratio are independent from the density of the fluid inside the tank and tank width x_t.

5.2.1.1 Validity of assuming small tank angle

For small values of θ it is generally considered that $\theta \approx \tan\theta$ and $\cos\theta \approx 1$. It is desirable to know for what values of θ the above assumptions are true. Table 5-1 compares θ and $\tan\theta$ for several angles and demonstrating the percentage of error caused in the response of the tank.

Rad	Degree	Tan	% error
0.0000	0.00	0.0000	0.00
...	...	...	...
0.1700	9.74	0.1717	0.97
0.1800	10.31	0.1820	1.08
...	...	...	...
0.2600	14.90	0.2660	2.26
0.2700	15.47	0.2768	2.44
...	...	...	...
0.3400	19.48	0.3537	3.88
0.3500	20.05	0.3650	4.12
...	...	...	...
0.4300	24.64	0.4586	6.24
0.4400	25.21	0.4708	6.54

Table 5-1Comparison between θ and $\tan\theta$

It is evident that for angles less than about 10° degrees the difference between the angle and the tangent of the angle is negligible (less than 1%). Even for angles of 25° the small angle approximation for the tangent function introduces an error of less than 7%. The corresponding errors for the sine function approximation are roughly half those of the tangent approximation. For a ship in calm weather the roll angle is usually less than 10 degrees and in rough weather the roll angle rarely gets more than 25 degrees. Therefore the assumption of small angles is a fairly reasonable one in the derivation of equation (5-12). Even so it is of interest to find out how the equation of motion looks like for larger values of τ. In this case

$$z = \frac{w}{2}\tan\tau \tag{5-15}$$

therefore

$$\dot{z} = \frac{w}{2}\frac{\dot{\tau}}{\cos^2\tau} \tag{5-16}$$

The velocity at any point of the tank is therefore

$$v = \frac{ww_r}{2n}\frac{\dot{\tau}}{\cos^2\tau} \tag{5-17}$$

As obtained from (5-4):

$$\frac{dv}{dt} = Y - \frac{1}{\rho}\frac{dP}{dy}$$

substituting (5-16) into this equation leads to

$$\frac{ww_r}{2n}\left[\frac{\ddot{\tau}\cos^2\tau + (2\sin\tau\cos\tau)\dot{\tau}^2}{\cos^4\tau}\right] = -g - \left[\frac{qww_r}{2n^2}\right]\frac{\dot{\tau}}{\cos^2\tau} - \frac{1}{\rho}\frac{dP}{dy}$$

or using the same notations used above:

$$a_{\tau\tau}\left[\frac{1}{\cos^2\tau}\ddot{\tau} + \frac{2\sin\tau}{\cos^3\tau}\dot{\tau}^2\right] + \frac{b_{\tau\tau}}{\cos^2\tau}\dot{\tau} + c_{\tau\tau}\tau = 0$$

or

$$a_{\tau\tau}\left[\ddot{\tau}+2\dot{\tau}^2\tan\tau\right]+b_{\tau\tau}\dot{\tau}+c_{\tau\tau}(\cos^2\tau)\tau=0 \qquad \textbf{(5-18)}$$

where

$$a_{\tau\tau}=Q_t w_r\left[\frac{w}{2h_d}+\frac{h_r}{w_r}\right]$$

$$b_{\tau\tau}=Q_t q w_r\left[\frac{w}{2h_d^2}+\frac{h_r}{w_r^2}\right]$$

$$c_{\tau\tau}=Q_t g$$

$$Q_t=\frac{\rho w_r w x_t}{2}$$

Fig. 5-2 compares the response of the tank (free oscillations of the water level inside the tanks given an initial displacement) based on two different equations obtained: (5-12) using small angle approximation values of tank angle and (5-18) without using the small angel approximations for the tank angle [See AppendixI, small_angles_effect.m for the programming code]. An important conclusion derived above and further proved by the figures is that for the values of tank angle that usually happen in practice (usually less than 15 degrees) the assumption that τ = tanτ is reasonable and compared to other assumptions (e.g. ignoring head loss at bends) the error introduced by this assumption is small.

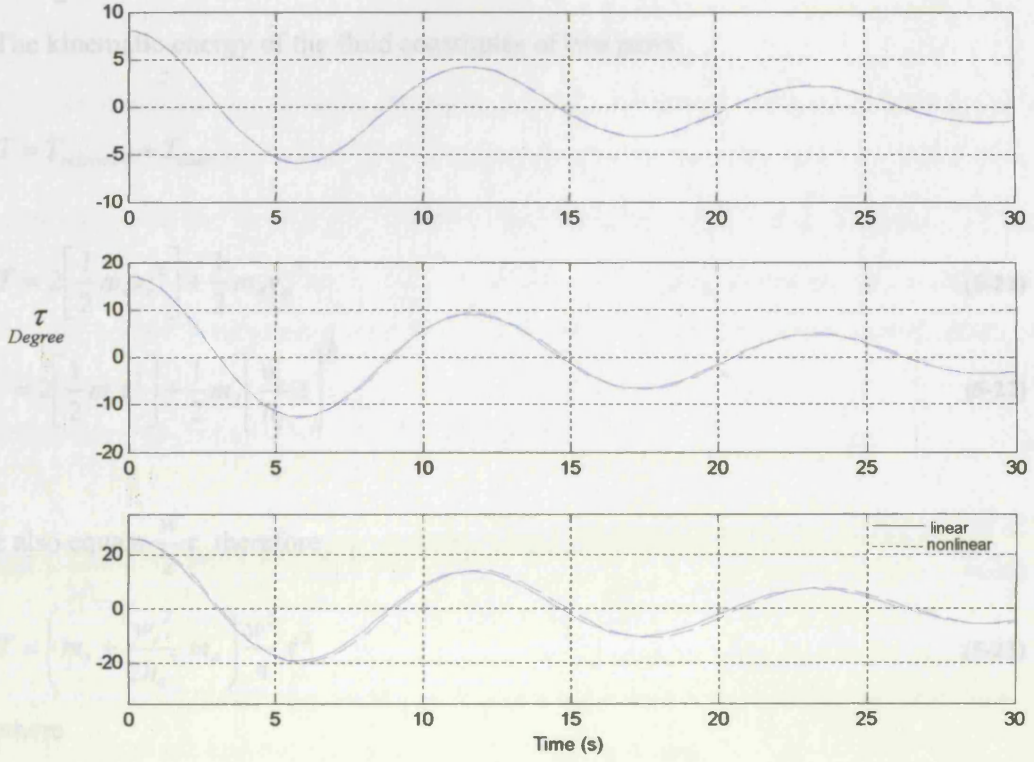

Fig. 5-2 The response of the tank with (5-12) and without (5-18) small angle approximations

5.2.2 Modelling a fixed tank by the energy method

In the previous section dynamics of a fixed tank was derived using the Euler method. In this part the equation of motion of fluid in the tank is obtained by the energy method.

From Fig. 5-1 the potential energy of the fluid is

$$U = mg\Delta h = 2(\rho w_r x_t z)g\frac{z}{2} = \rho w_r x_t g z^2 \qquad \textbf{(5-19)}$$

knowing that $z = \frac{w}{2}\tau$ and substituting in (5-19) follows

$$U = \frac{1}{4}\rho w_r x_t w^2 g\tau^2 = \frac{1}{2}Qg\tau^2 \qquad \textbf{(5-20)}$$

where

$Q = \frac{1}{2}\rho w^2 w_r x_t$ as Stigter [61] has defined.

The kinematic energy of the fluid constitutes of two parts

$$T = T_{reservoirs} + T_{duct}$$

$$T = 2\left[\frac{1}{2} m_r v_r^{\ 2}\right] + \frac{1}{2} m_d v_d^{\ 2} \tag{5-21}$$

$$= 2\left[\frac{1}{2} m_r \dot{z}^2\right] + \frac{1}{2} m_d \left[\frac{w_r}{h_d}\dot{z}\right]^2 \tag{5-22}$$

z also equals $\frac{w}{2}\tau$ therefore

$$T = \left(m_r + \frac{w_r^{\ 2}}{2h_d^{\ 2}} m_d\right)\frac{w^2}{4}\dot{\tau}^2 \tag{5-23}$$

where

$$m_r = \rho w_r h_r x_t$$

$$m_d = \rho w h_d x_t$$

substituting in (5-23) and using (5-20) yields

$$T = \frac{Q w_r}{2}\left(\frac{w}{2h_d} + \frac{h_r}{w_r}\right)\dot{\tau}^2 \tag{5-24}$$

The general from of Lagrange equation is as

$$\frac{d}{dt}\left(\frac{\partial T}{\partial \dot{\tau}}\right) - \frac{\partial T}{\partial \tau} + \frac{\partial U}{\partial \tau} = \overline{Q_i} \tag{5-25}$$

From (5-20), (5-24) and (5-25) it can be derived that

$$\frac{\partial T}{\partial \dot{\tau}} = Q w_r \left(\frac{w}{2h_d} + \frac{h_r}{\omega_r}\right)\dot{\tau} \tag{5-26}$$

$$\frac{\partial U}{\partial \tau} = Qg\tau \tag{5-27}$$

In order to be able to compare the equations from the energy method and the Euler's method, the damping force $\overline{Q_i}$ it is considered to be (as Stigter's suggested [40]) proportional to the velocity of the fluid and equal to $-b_{\tau\tau}\dot{\tau}$. The advantage of the energy method is that if later a better modelling of damping forces would be obtained, it could be easily substituted with the existing one without any further modification of other terms.

Substituting (5-26) and (5-27) in (5-25) leads to

$$Qw_r\left(\frac{w}{2h_d}+\frac{h_r}{w_r}\right)\ddot{\tau}+b_{\tau\tau}\dot{\tau}+Qg\tau=0 \quad (Nm) \tag{5-28}$$

which is exactly the same equation as Stigter's equation for the tank. It is evident that the damping ratio and the natural frequency of the tank are:

$$\varsigma=\frac{b_{\tau\tau}}{2\omega_n a_{\tau\tau}}=\frac{q(ww_r^2+2h_rh_d^2)}{\sqrt{8w_r^2h_d^3g(ww_r+2h_rh_d)}} \tag{5-29}$$

$$\omega_n=\sqrt{\frac{c_{\tau\tau}}{a_{\tau\tau}}}=\sqrt{\frac{2gh_d}{ww_r+2h_rh_d}} \tag{5-30}$$

It is of interest to consider the effect of variation of different tank dimensions on the natural frequency and damping ratio. This is done and the results are presented in Fig. 5-3.

A tank has been considered with the following reference dimensions:

w = 20m

h_r = 5m

h_d = 1m

w_r = 3m

x_t = 1m

q = 0.11 (coefficient explained in section 5.2.1)

The values ω_n and ς for the reference values are 0.55 and 0.08 respectively.

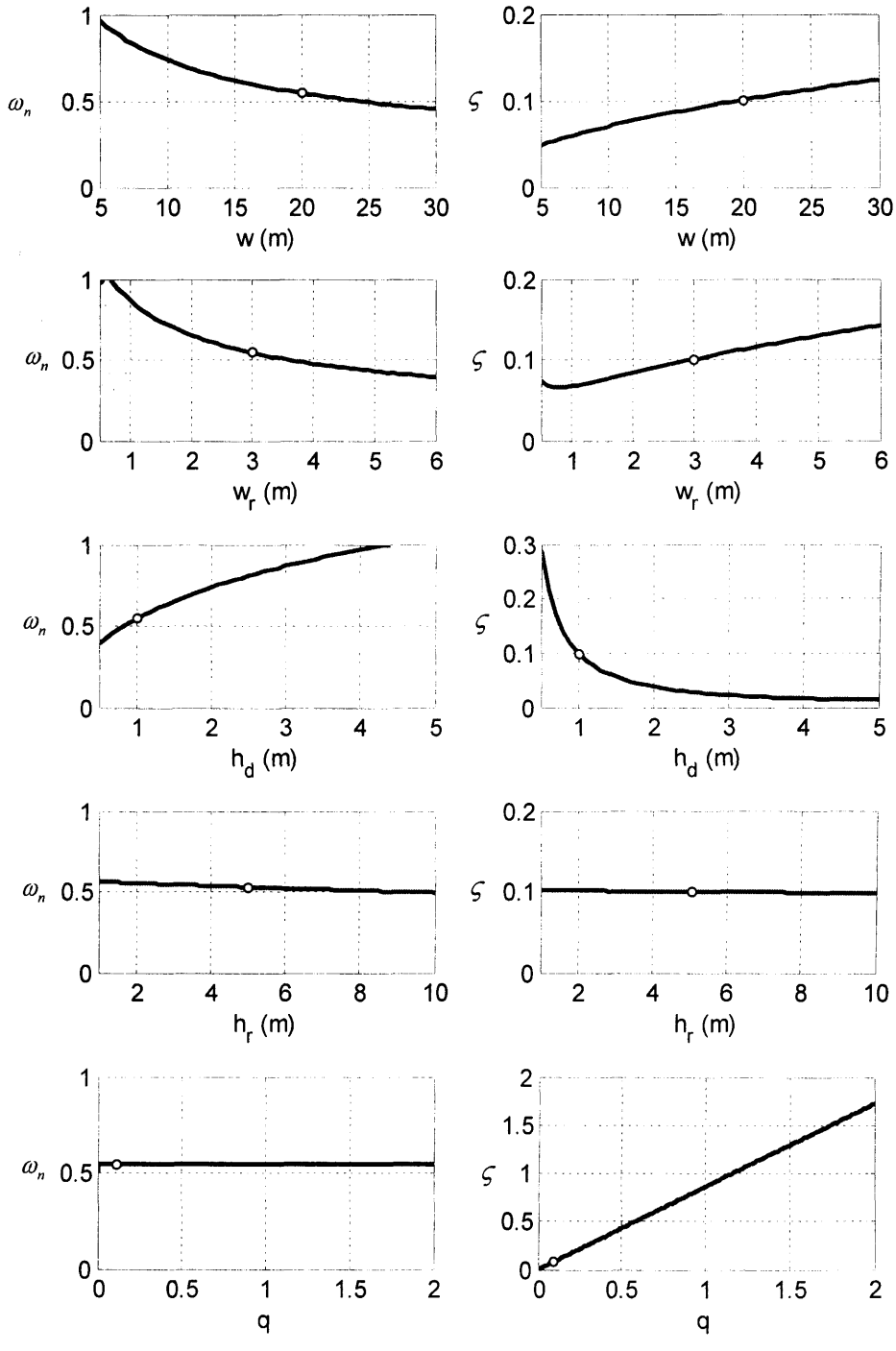

Fig. 5-3 The effect of dimensional variations on ω_n and ς

It is evident that the natural frequency decreases with the widths w and w_r, and increases with the duct depth h_d. The reverse is true for the damping ratio. The tank width, x_t, does not appear in the equations of the damping ratio (5-29) and natural frequency (5-30) and therefore has no effect on them. However, the natural frequency and damping ratio are quite insensitive to the depth of the fluid in the tank, h_r. It follows that there is little scope for adjusting either the natural frequency or the damping ratio after the tank has been designed and fitted to the ship, by simply altering the water depth in the reservoirs. A more practical method for altering the characteristics of a U-tank is by application of flow obstructions (see Lee and Vassalos [37]).

5.3 Modelling of a tank having roll and sway motion

5.3.1 Modelling by Euler equation

In this part the motion of the water inside a U-tank is modelled assuming the tank itself is subjected to roll and sway motion. The procedure is basically the same as earlier and equation (5-4) is derived as before

$$\frac{dv}{dt} = Y - \frac{1}{\rho}\frac{dP}{dy}$$

However this time Y is made up of other contributions due to the accelerations applied to the tank, as shown in Fig. 5-4. They are:

1) The damping forces are estimated using the same assumptions made before:
   $$\frac{-qv}{n}$$
2) The component of acceleration due to the gravity along y direction is $-g\cos\phi_1$
3) The acceleration due to the roll motion of the tank is
   $$-r\ddot{x}_4\cos(\phi_2 - \pi/2) = -r\ddot{x}_4\sin\phi_2$$
   where r is the distance between the centre of rotation of the tank and the element of water volume in the tank.
4) The component of sway acceleration in the y

a) in the duct $Y_L = \ddot{x}_2 \cos x_4 \approx \ddot{x}_2$

b) in the reservoirs $Y = \ddot{x}_2 \sin x_4 \approx 0$

since $\ddot{x}_2$ is not large and x_4 are assumed to be small.

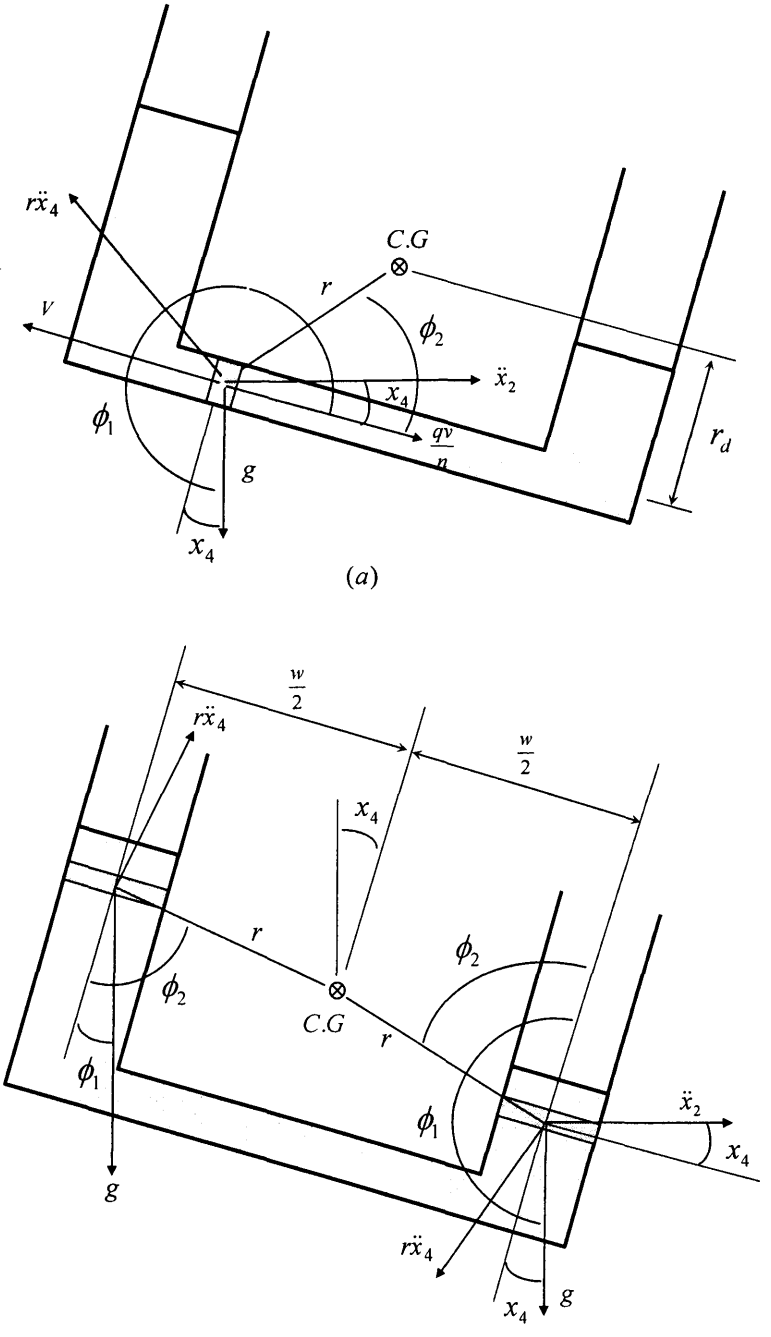

Fig. 5-4 External forces applied to unit mass in a) duct and b) reservoirs

Equation (5-4) then becomes

$$\frac{w_r w}{2n}\ddot{\tau} = -g\cos\phi_1 - r\ddot{x}_4 \sin\phi_2 + Y_L - q\left(\frac{w_r w}{2n^2}\right)\dot{\tau} - \frac{1}{\rho}\frac{dP}{dy}$$

or

$$\frac{w_r w}{2n}\ddot{\tau} + q\left(\frac{w_r w}{2n^2}\right)\dot{\tau} + g\cos\phi_1 + r\ddot{x}_4 \sin\phi_2 - Y_L = -\frac{1}{\rho}\frac{dP}{dy} \quad (m/s^2) \qquad \textbf{(5-31)}$$

or

$$\frac{\rho w_r w dy}{2n}\ddot{\tau} + q\left(\frac{\rho w_r w dy}{2n^2}\right)\dot{\tau} + \rho g\cos\phi_1 dy + \rho r\ddot{x}_4 \sin\phi_2 dy - \rho Y_L dy = -dP \ (Pa) \qquad \textbf{(5-32)}$$

As before this equation is integrated with respect to y to obtain an equation giving the motion of the fluid in the tank (in terms of the tank angle τ) as a function of the pressure difference at the surface in the two reservoirs. Strictly, the integration should proceed from the surface level in the starboard reservoir (negative y) to the surface level in the port reservoir (positive y). It is obtained

$$\frac{\rho w_r w I_1}{2}\ddot{\tau} + \frac{\rho q w_r w I_2}{2}\dot{\tau} + \rho g I_3 + \rho I_4 \ddot{x}_4 + \rho\ddot{x}_2 I_5 = P_{starboard} - P_{port} \quad (Pa) \qquad \textbf{(5-33)}$$

where

$$I_1 = \int\frac{dy}{n} = \int_{-h_r}^{0}\frac{dy}{w_r} + \int_{-w/2}^{w/2}\frac{dy}{h_d} + \int_{0}^{h_r}\frac{dy}{w_r} = \frac{w}{h_d} + \frac{2h_r}{w_r}$$

$$I_2 = \int\frac{dy}{n^2} = \int_{-h_r}^{0}\frac{dy}{w_r^2} + \int_{-w/2}^{w/2}\frac{dy}{h_d^2} + \int_{0}^{h_r}\frac{dy}{w_r^2} = \frac{w}{h_d^2} + \frac{2h_r}{w_r^2}$$

$$I_3 = \int\cos\phi_1 dy = \int_{-h_r}^{0} -dy + \int_{-w/2}^{w/2} x_4 dy + \int_{0}^{h_r} dy = wx_4$$

(Assuming small roll angles and from Fig. 5-4 it can be concluded that $\cos\phi_1 = 1$ in the port reservoir, -1 in the starboard reservoir, and $\cos\left(\frac{3\pi}{2} + x_4\right) = \sin x_4$ in the duct.)

$$I_4 = \int r\sin\phi_2 dy = \int_{-h_r}^{0} \frac{w}{2} dy + \int_{w/2}^{w/2} r_d dy + \int_0^{h_r} \frac{w}{2} dy = w(r_d + h_r)$$

(Note that From Fig. 5-4 it can be seen that $r\sin\phi_2 = w/2$ anywhere in the reservoirs and $r\sin\phi_2 = r_d$ anywhere in the duct)

$$I_5 = -\int dy = -\int_{-h_r}^{0} (0) dy - \int_{w/2}^{w/2} dy - \int_0^{h_r} (0) dy = -w$$

and from (5-10) it is known that $P_s - P_p = -\rho g w \tau$. It is again possible to express this equation as a function of moment applied to the tank fluid by multiplying it by the surface of the reservoir and the moment arm $ww_r x_t/2$; this leads to

$$a_{\tau 2}\ddot{x}_2 + a_{\tau 4}\ddot{x}_4 + c_{\tau 4}x_4 + a_{\tau 6}\ddot{x}_6 + a_{\tau\tau}\ddot{\tau} + b_{\tau\tau}\dot{\tau} + c_{\tau\tau}\tau = 0 \qquad (Nm) \qquad \textbf{(5-34)}$$

where the coefficients are

$$a_{\tau 2} = -Q_t$$

$$a_{\tau 4} = Q_t(r_d + h_r)$$

$$c_{\tau 4} = Q_t g$$

$$a_{\tau 6} = -Q_t x_{B1}$$

$$a_{\tau\tau} = Q_t w_r \left[\frac{w}{2h_d} + \frac{h_r}{w_r}\right]$$

$$b_{\tau\tau} = Q_t q w_r \left[\frac{w}{2h_d^2} + \frac{h_r}{w_r^2}\right]$$

$$c_{\tau\tau} = Q_t g$$

and

$$Q_t = \frac{\rho w_r w^2 x_t}{2}$$

x_{B1} is the distance between the centre of gravity of the tank and the centre of gravity of the ship in the fore/aft direction.

5.3.2 Modelling by Energy method

Using the same notations and assumptions as in 5.2.1 and referring to Fig. 5-5 the potential energy of the fluid is

$$U = mg\Delta h \cong \left[\rho w_r x_t \left((\tau + x_4)\frac{w}{2}\right)\right] g\left[(\tau + x_4)\frac{w}{2}\right] \qquad \textbf{(5-35)}$$

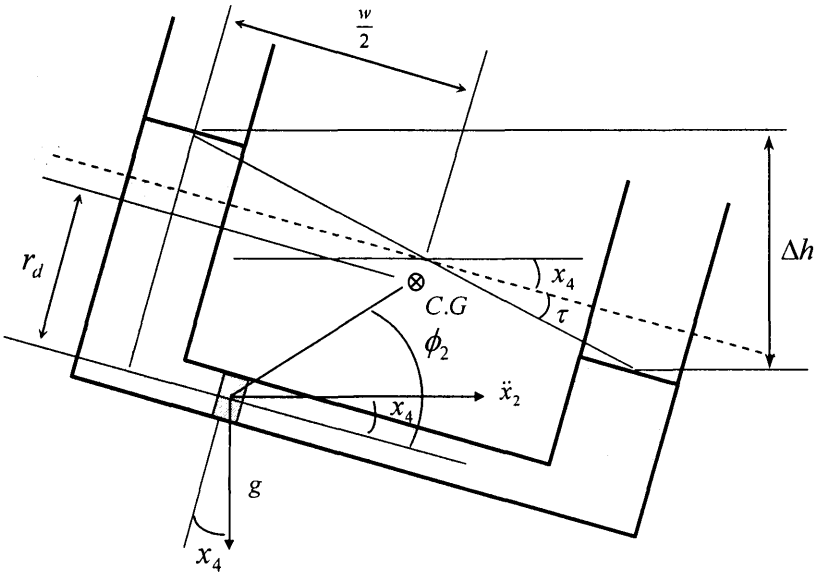

Fig. 5-5 parameters of a tank used in energy method

Simplifying (5-35) leads to:

$$U = \frac{1}{4}\rho w_r x_t g w^2 (\tau + x_4)^2 = \frac{1}{2} Q g (\tau + x_4)^2 \qquad \textbf{(5-36)}$$

where

$Q = \frac{1}{2}\rho w^2 w_r x_t$ as Stigter [61] has defined.

The kinematic energy of the fluid constitutes of two parts

$T = +T_{reservoirs} + T_{duct}$

Using the same simplifications as Stigter, it is considered that yaw and sway have negligible effect on the motion of the fluid inside the reservoirs. However the mass velocity of a water element inside the duct is composed of the apparent velocity of the element plus the velocity caused by roll and sway. Therefore:

$$T = 2\left(\frac{1}{2}mv^2\right)_{reservior} + \left(\frac{1}{2}mv^2\right)_{duct} \tag{5-37}$$

$$T = 2\left(\frac{1}{2}m(\dot{z} + \dot{x}_4 r\sin\phi_2)^2\right)_{reservior} + \left(\frac{1}{2}m\left\{\frac{w_r}{h_d}\dot{z} + \dot{x}_4 r\sin\phi_2 - \dot{x}_2\cos x_4\right\}^2\right)_{duct} \tag{5-38}$$

From Fig. 5-4 it is clear that $r\sin\phi_2 = w/2$ anywhere in the reservoirs and $r\sin\phi_2 = r_d$ anywhere in the duct. z also equals $\frac{w}{2}\tau$ and for small roll angles $\cos x_4 \approx 1$. Therefore:

$$\begin{aligned} T = &\left(m_r + \frac{w_r^{\,2}}{2h_d^{\,2}}m_d\right)\frac{w^2}{4}\dot{\tau}^2 + \left(2m_r\frac{w^2}{4} + m_d r_d\frac{ww_r}{2h_d}\right)\dot{x}_4\dot{\tau} - m_d\frac{ww_r}{2h_d}\dot{x}_2\dot{\tau} \\ &+ \frac{1}{2}m_r w^2\dot{x}_4^{\,2} + \frac{1}{2}m_d\dot{x}_2^{\,2} - m_d r_d\dot{x}_2\dot{x}_4 \end{aligned} \tag{5-39}$$

where

$$m_r = \rho w_r h_r x_t$$

$$m_d = \rho w h_d x_t$$

substituting in (5-39) and further simplifying yields

$$T = \frac{Qw_r}{2}\left(\frac{w}{2h_d} + \frac{h_r}{w_r}\right)\dot{\tau}^2 + Q(r_d + h_r)\dot{x}_4\dot{\tau} - Q\dot{x}_2\dot{\tau} + Qh_r\dot{x}_4^{\,2} + \frac{1}{2}\rho w h_d x_t\dot{x}_2^{\,2} + \rho w h_d x_t\dot{x}_4\dot{x}_2 \tag{5-40}$$

The general from of Lagrange equation is as

$$\frac{d}{dt}\left(\frac{\partial T}{\partial \dot{\tau}}\right)-\frac{\partial T}{\partial \tau}+\frac{\partial U}{\partial \tau}=\overline{Q}_i \tag{5-41}$$

From (5-20) and (5-24) it can be derived that

$$\frac{\partial T}{\partial \dot{\tau}}=Qw_r\left(\frac{w}{2h_d}+\frac{h_r}{\omega_r}\right)\dot{\tau}-Q\dot{x}_2+Q(r_d+h_r)\dot{x}_4 \tag{5-42}$$

$$\frac{\partial U}{\partial \dot{\tau}}=Qg(\tau+x_4) \tag{5-43}$$

substituting (5-42) and (5-43) into (5-41) yields that

$$Qw_r\left(\frac{w}{2h_d}+\frac{h_r}{\omega_r}\right)\ddot{\tau}+b_{\tau\tau}\dot{\tau}+Qg\tau-Q\ddot{x}_2+Q(r_d+h_r)\ddot{x}_4+Qgx_4=0 \tag{5-44}$$

which is exactly the same equation as Stigter's equation of tank (5-34).

It is amazing to observe that two different approaches with different fundamentals provide identical results. One method is based on principles of fluid mechanics while the other considers the fluid in the tank as a moving object and investigates the variation in its kinematic and potential energy. This can be justified by considering the original derivation of the Euler equation for the fluid itself. The Euler equation is developed by considering a small element of fluid and applying Newton's second Law of motion which is also the base of deriving the energy of a moving object in the Lagrange equation. This is an interesting example to show that different disciplines of science are simply branches of the same tree, share the same fundamental principles and on occasions they converge to the same point.

5.4 Concluding remarks

In this chapter U-shape anti-roll tanks was mathematically modelled by two different approaches: one method uses the Euler equation and is based on fluid mechanics principles; the other uses the Lagrange energy method and is based on dynamics of solid materials.

The choice of which method depends on ones level of understanding from principles of a science. Overall Euler's method is easier to follow but requires more calculations, while the energy method is shorter and requires less knowledge of fluid mechanics, although especial attention should be paid to the derivation of potential and kinematic energies. The overall mass velocity of the fluid in the reservoirs and the duct consists of the fluid motion in the tank in addition to motion caused by the ship's roll and sway. It is important to choose the correct components of roll and sway motion, which have effect in the direction of y (the coordinate used to derive the equations). The roll and sway motion of the ship each impose a force on each mass element of the water inside the tank. This force has two components: one in the direction of y, and one perpendicular to it. Only the component in the direction of y, is the one having effect on water level of the tanks.

If it is intended to perform modification on tank shape and perhaps consider more realistic behaviour of fluid it is easier to use Euler's method which would not require major changes in the calculations. For example, assume it is intended to investigate the effect of sloping walls on the side tanks. If the energy method is applied almost all the modelling should be performed from the very early stages. This is while if the Euler method is used, the structure of all the equations in the model will remain the same. The difference will only be applied to the cross section equations and change some parts of the integration procedure.

Chapter 6

6 Application of wave prediction in Active Anti-roll Tanks

6.1 Anti-roll passive tanks

As mentioned in the previous chapter U-shaped passive tanks consist of two reservoirs connected with a water duct along the bottom (Fig. 6-1). As the water moves from one leg of the U-tank to the other leg, the position of the centre of gravity of the water inside the tank changes, causing a moment equal to the weight of the water times the distance between the centre of gravity of the water inside the tank and the centre of gravity of the ship (close to the centre line plane). If correctly done, this moment opposes the moment induced by the waves and tends to stabilize the ship. It is clear that if the reservoirs could be placed further apart, there could be more significant motion of the centre of gravity and larger moment arm, therefore creating larger stabilization moments. The overall function of the system is independent of the ship forward speed, therefore suitable for low speed or even stationary operations.

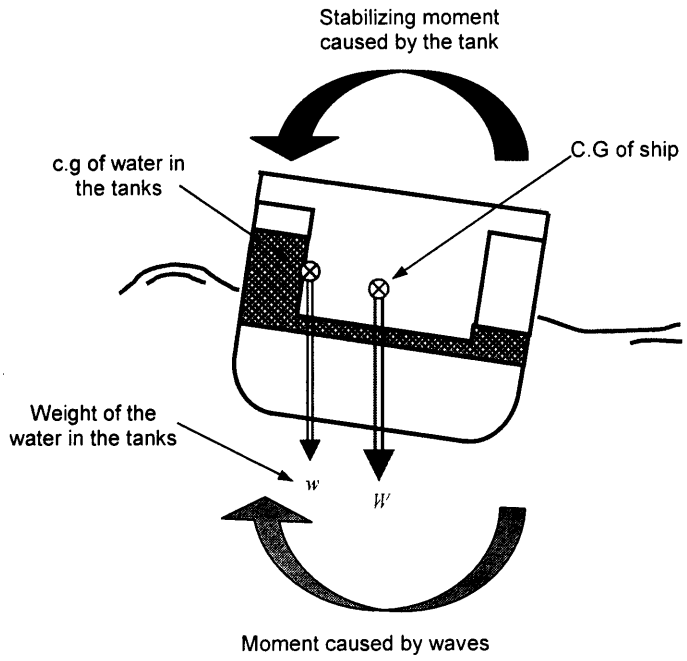

Fig. 6-1 Arrangement of passive tank

The main disadvantage of passive tanks is that although there is considerable roll reduction when the encountered waves have the same frequency as the ship's roll resonance frequency, the roll is increased in other excitation frequencies due to the extra degree of freedom the tanks induce [5;27], and in reality a ship is mostly excited by waves having frequencies other than the roll natural frequency (Fig.6-2).

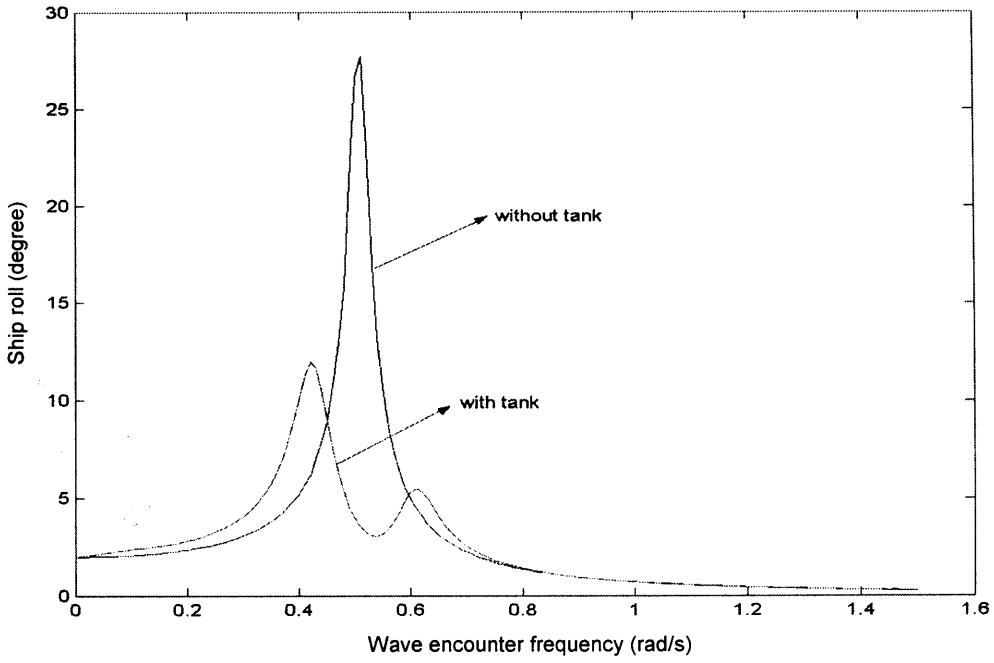

Fig.6-2 The effect of passive tanks on roll reduction

The water in the tank does not get athwart ship quickly enough as the ship rolls. This means that the system has a time delay when responding to a signal demanding a stabilizing moment. The efficiency of the tank would be improved generally if changes were made to enable the water to flow athwart ships more quickly. It is also difficult to control the water, sloshing from one leg of the U-tank to the other, threatening the safety of the ship in rough weather [69]. Reducing the width of the U-tank is also not a reasonable option as this reduces the stabilizing moment arm and consequently reduces the righting effect.

The rapid transfer of water from one leg of the tank to the other could be accomplished by pumps placed in the water duct or pressured air provided to the tank tops. Active tanks do exist in textbooks and articles; however they are not widely practiced in commercial applications. The reason is simple: there is a general fear that excessive power is required to operate the pumps or air blower.

6.2 Control strategy

Results of the current study so far suggest that for best stabilization "the righting moment should be always in phase with the wave excitation". This ensures that the stabilizing moment always acts in the opposite direction of the wave excitation, which naturally leads to roll reduction. This task has to be fulfilled by a suitable control strategy.

The difficulty for the control system is that tank stabilizers depend for their action on the displacement of water with relation to the centre line of the vessel and therefore cannot be made to respond simultaneously to a signal demanding a stabilizing moment, since time is required to move the water from one position to another. This means that if the sensor detects that the ship has rolled to starboard, the control system commands the pump to force the water to the port. However as it takes a few seconds to do so, by the time the water is pumped to the port the ship might herself be rolling to the port too which means that not only has the tank not stabilized the roll but also has increased the roll. As a solution one may suggest that a predictive system is required to predict the motion of the ship for a few seconds ahead and then pump the water accordingly. There have been other interesting applications in prediction of ship motion in the past. Broome and Pittaras have used the time prediction of ship motion to improve the safety of helicopter and aircraft landing on carriers and naval other naval ships [14-16]. In the particular application of roll stabilization there is a requirement to predict the force causing the ship motion, i.e. the waves, in the near future. The accuracy of the prediction can be greatly improved with better systems of monitoring the sea waves around the ship using radars or other vision methods (There are some research being undertaken in some leading centres in this area including using Stereo Vision-Based Measurements at US Naval Academy [50]).

The control strategy proposed in this study is as follows:
The moment created by the waves is essentially proportional to the wave height. Therefore using a wave height meter the moment created by the waves is monitored and recorded over a period of time and an Auto regressive (AR) model of the waves is created

which has the ability to predict the incoming waves for a few seconds ahead. Details of the prediction method were explained in Chapter 4. The prediction time is based on the time required for the pump to move the water inside the tank to the desired position and may vary in different working condition. This predicted wave is in fact the cause of the ship's roll motion and therefore it is the goal of the control system to counteract this moment. In other words the predicted wave is used as the set point of the controller and the water in the tank is pumped in such a manner to create an opposite moment equal to the predicted wave therefore by the end of the predicted time that the wave reaches the ship the stabilizing moment is already created and counteracts the wave (This is schematically presented in Fig. 6-3 while Fig. 6-4 shows the control diagram). The controller before the pump has the task of ensuring that the water level in the tank is following the set point, which is the output of the wave predictor and by using the Ziegler Nichols method is a gain set to be half the gain that brings the system to the verge of instability.

This "feedforward control" strategy has been used in numerous applications in electrical engineering; noise cancellation inside cars, vibration cancellation in helicopter cabin and sound filtering are a few examples of this highly effective control strategy [73].

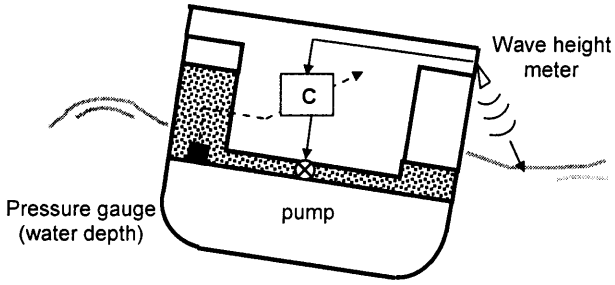

Fig. 6-3 Control scheme for active roll stabilization

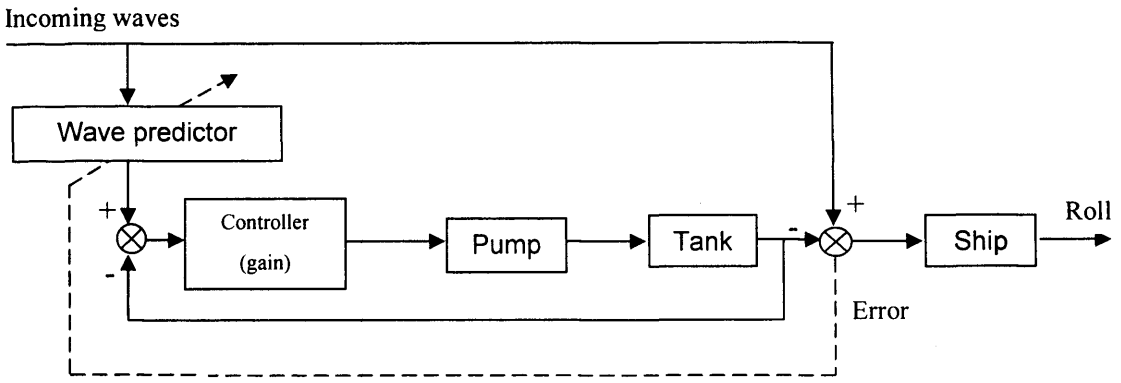

Fig. 6-4 Suggested active control strategy

The wave predictor block was explained in detail in Chapter 4. The idea was generating a predictive ARX model in the form of:

$$y(k) = \boldsymbol{\theta}^T(k-1)\boldsymbol{\varphi}(k-1) + e(k) \qquad \textbf{(6-1)}$$

Where $\boldsymbol{\varphi}(k-1)$ is a vector containing the input/output information and $\boldsymbol{\theta}^T(k-1)$ is a vector containing the coefficients that need to be adapted in order to reach optimum prediction using minimization of sum of the squares of the prediction errors:

$$V_N(\boldsymbol{\theta}) = \frac{1}{N}\sum_{k=1}^{N}\varepsilon^2(k) \qquad \textbf{(6-2)}$$

Once the ARMAX model is derived and the values of the parameters estimated, $\boldsymbol{\theta}(k)$, are proved to minimize $V_N(\boldsymbol{\theta})$ the model can be used to predict k-steps ahead using the information gathered so far.

In the case of predicting the incoming waves the number of prediction steps required is derived from the delay between the control signal and the moment created by the tank. So if the required stabilizing moment is created 5 seconds after the control signal the wave prediction is performed for the next 5 seconds to compensate the inevitable lag. The order of the ARX model, *na,* is set as twice the prediction steps required. This has been derived from trial and error analysis [14;15] and it has been shown that it gives the best prediction. After this point increasing the order of the model does not have any

significant effect on the prediction. Better prediction can be achieved if there is stronger correlation between the past values of a signal. A signal having weak correlation becomes less predictable. In the case of predicting waves, there is a good correlation between past values and the energy of the wave is concentrated around a dominant frequency (see wave spectrum in Chapter 4). Results of wave prediction for different sea states are presented in Chapter 4.

6.3 Simulations and results

In this section the proposed control strategy is simulated for two ship models a monohull and a trimaran. The mathematical model of the ship tank system used in this study is derived using the Euler method extracted from Lloyd[40]:

Tank

$$a_{\tau 2}\ddot{x}_2 + a_{\tau 4}\ddot{x}_4 + c_{\tau 4}x_4 + a_{\tau 6}\ddot{x}_6 + a_{\tau\tau}\ddot{\tau} + b_{\tau\tau}\dot{\tau} + c_{\tau\tau}\tau = \alpha P \qquad \textbf{(6-3)}$$

Roll

$$a_{42}\ddot{x}_2 + b_{42}\dot{x}_2 + (I_{44} + a_{44})\ddot{x}_4 + b_{44}\dot{x}_4 + c_{44}x_4 + a_{46}\ddot{x}_6 + b_{46}\dot{x}_6 + c_{46}x_6 - [a_{4\tau}\ddot{\tau} + c_{4\tau}\tau] = F_4$$

where

F_4	Wave moment
τ	Tank angle defined as in Fig. 7-14
P	Pressure of the air provided at the top of the tank
α	Coefficient relating the pressure applied with the tank dynamics
$x_2, \dot{x}_2, \ddot{x}_2$	Sway, sway velocity and sway acceleration
$x_4, \dot{x}_4, \ddot{x}_4$	Roll, roll velocity and roll acceleration
$x_6, \dot{x}_6, \ddot{x}_6$	Yaw, yaw velocity and yaw acceleration
a_{ij}, b_{ij} and c_{ij}	Ship hydrodynamic coefficients

In this study a simplified version of the above equations is used in order to restrict the motion of the ship to roll only. Therefore:

Tank

$$a_{\tau 4}\ddot{x}_4 + c_{\tau 4}x_4 + a_{\tau\tau}\ddot{\tau} + b_{\tau\tau}\dot{\tau} + c_{\tau\tau}\tau = \alpha P \quad \text{(6-4)}$$

Roll

$$(I_{44} + a_{44})\ddot{x}_4 + b_{44}\dot{x}_4 + c_{44}x_4 - [a_{4\tau}\ddot{\tau} + c_{4\tau}\tau] = F_4$$

Where P is the pressure applied to the water inside the tank by the pump or blower and α is a constant.

The simulations are performed on two ships with the specifications in

Table 6-1. The ships have been chosen firstly by availability of roll characteristic data, and secondly it is intended to show the suitability of the method for two ships with different sizes and shapes. Ship 1 is a model of *La Salle* class US Command ship and is a monohull. Ship 2 is a model based on a trimaran the *RV Triton.*

	Ship 1	Ship 2
Type	Monohull	Trimaran
Displacement	9600 tonne	5300 tonne
Overall Beam	32 m	25 m
Length	156 m	150 m
GM	2 m	1.9 m
Water mass to ship	1.8%	1.2%

Table 6-1 Major parameters of the ships used in the simulation

The ship-tank coefficients in equation (6-4) are derived from Chapter 5 equation (5-34). The ship hydrodynamic coefficients for ship 1 are derived from geometrical parameters of the ship (full calculations presented in Appendix II as a MATLAB code) while the hydrodynamic coefficients for ship 2 have been extracted from a PhD thesis at the department of mechanical engineering of University College London, specifically dedicated to the roll motion of trimaran ships [28].

As it is clear from equation (6-4), the model of the ship used is linear, however in order to make the model more realistic some restrictions have been added to the model. The restrictions are that the flow rate inside the tank cannot exceed the pump capacity, and that the level of the water inside the tank cannot exceed the tank height. This has been implemented by adding saturation blocks to the MATLAB Simulink model of the system. It is worth mentioning that the control systems developed in this thesis are not dependant on the ship model. In other words, unlike classical feedback controllers where the parameters of the controller are designed based on the plant's transfer function, the control systems in this study are unaffected by the ship-tank transfer function. The plant model plays the part of generating most probable response to the external forces and what is of particular interest is not the dynamics of the model but rather its output. The only data used are the wave height information which is performed by a wave height meter and the roll motion of the ship. The same controller can be applied to a real ship with the difference that this time data is extracted from actual readings rather than from a simulation. Therefore using a more detailed model (and it does not matter if it is or is not non-linear) does not necessarily improve the accuracy of the controller. It might lead to a more realistic output, but again it must be emphasized that the controller has not been designed based on the plant's model.

The U-tank dimensions used in this simulation are presented in Table 6-2 where the geometric parameters are introduced in Fig. 6-5 and x_t is the length of the tank in the fore/aft direction. Both tanks are situated 1.5m above the centre of roll of the ship.

	Ship1	Ship2
w	32m	20m
w_r	3m	3m
h_r	3m	3m
h_d	1m	1m
x_t	3.5m	2m

Table 6-2 Dimension of the U-tanks

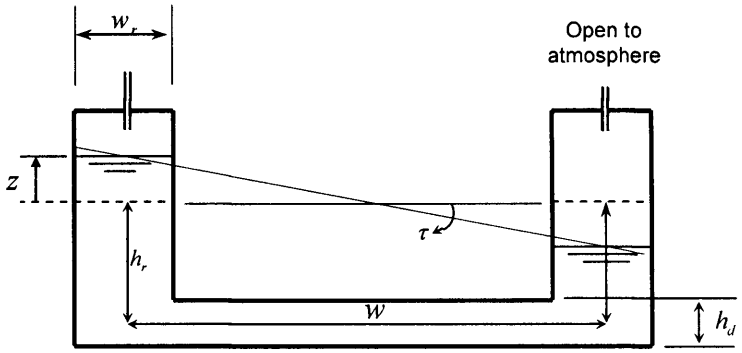

Fig. 6-5 U-tank and its geometric parameters

The pump model is assumed to be a first order lag system with a limitation on the maximum volume flow rate it can provide Q. The power consumption of the pump has been calculated using the generally agreed equation [35]:

$$P = QH\frac{\gamma}{368\eta} \tag{6-5}$$

Where

P Power consumption of the pump (kW)

Q Pump capacity (m^3/h)

γ Specific gravity of the fluid (1 for water)

η Efficiency of the pump

H Total head (m)

Obviously as z changes at each moment, the power consumption of the pump changes accordingly and exhibits an oscillatory behaviour having an average value. The connecting duct is divided into two channels and a separate pump is placed in each channel which pumps the water in one direction and blocks the way when the other pump is moving the water in the opposite direction. This means that the duct cross section is halved (as x_t is divided by two), this is probably the worst case and a bi-directional pump might be an alternative. The dynamic model of the pump is assumed to be a first

order differential equation with a time constant of 1 second, meaning the pump is able to achieve its full capacity in 4 seconds. The full capacity of the pump is assumed to be $3m^3/s$. The transient response of a pump with this characteristics is shown in Fig. 6-6.

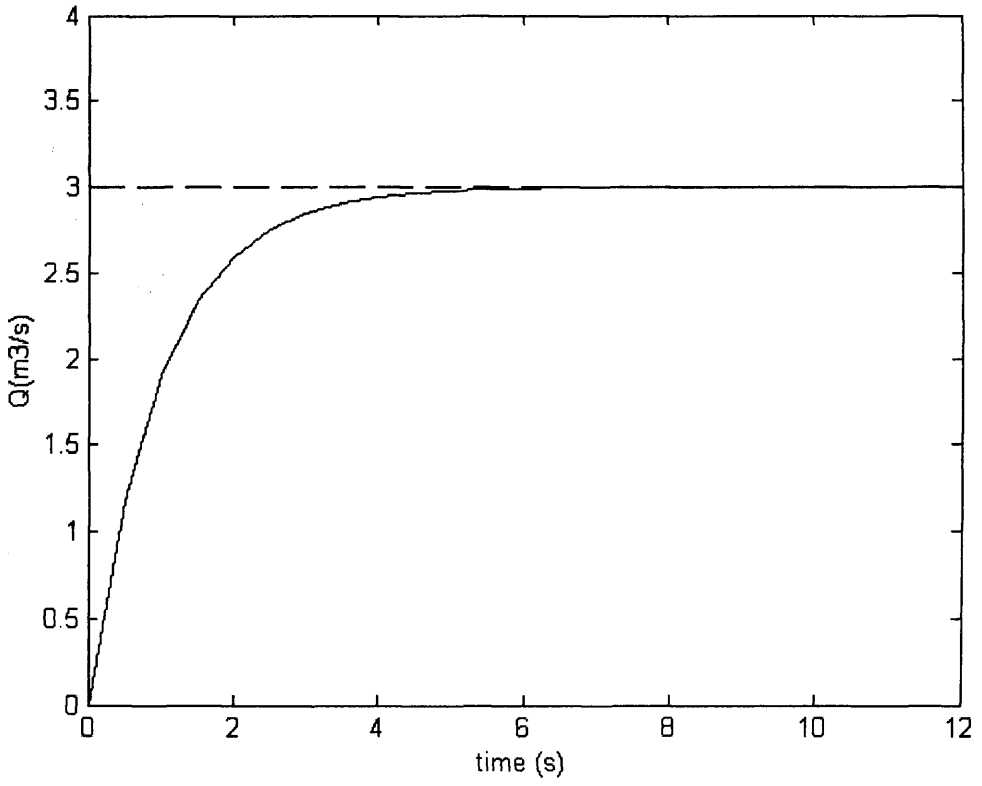

Fig. 6-6 Transient response of the pump used in the simulations

The following figures present the results of the simulation. The parameters investigated and shown in the figures are the frequency response of the ship for different wave slopes (wave slope is defined as the derivative of wave elevation and is generally used in application relating to roll motion of the ship) with and without the active tank; the maximum water level in the tanks and the average values of power consumption at each frequency. The waves applied in this part are assumed to be sinusoid while irregular waves are discussed in the next sub-section. Fig. 6-7 shows the simulation results for ship 1 (the monohull) using the pump. Fig. 6-8 shows the simulation results for ship 2 (the trimaran) using the pump.

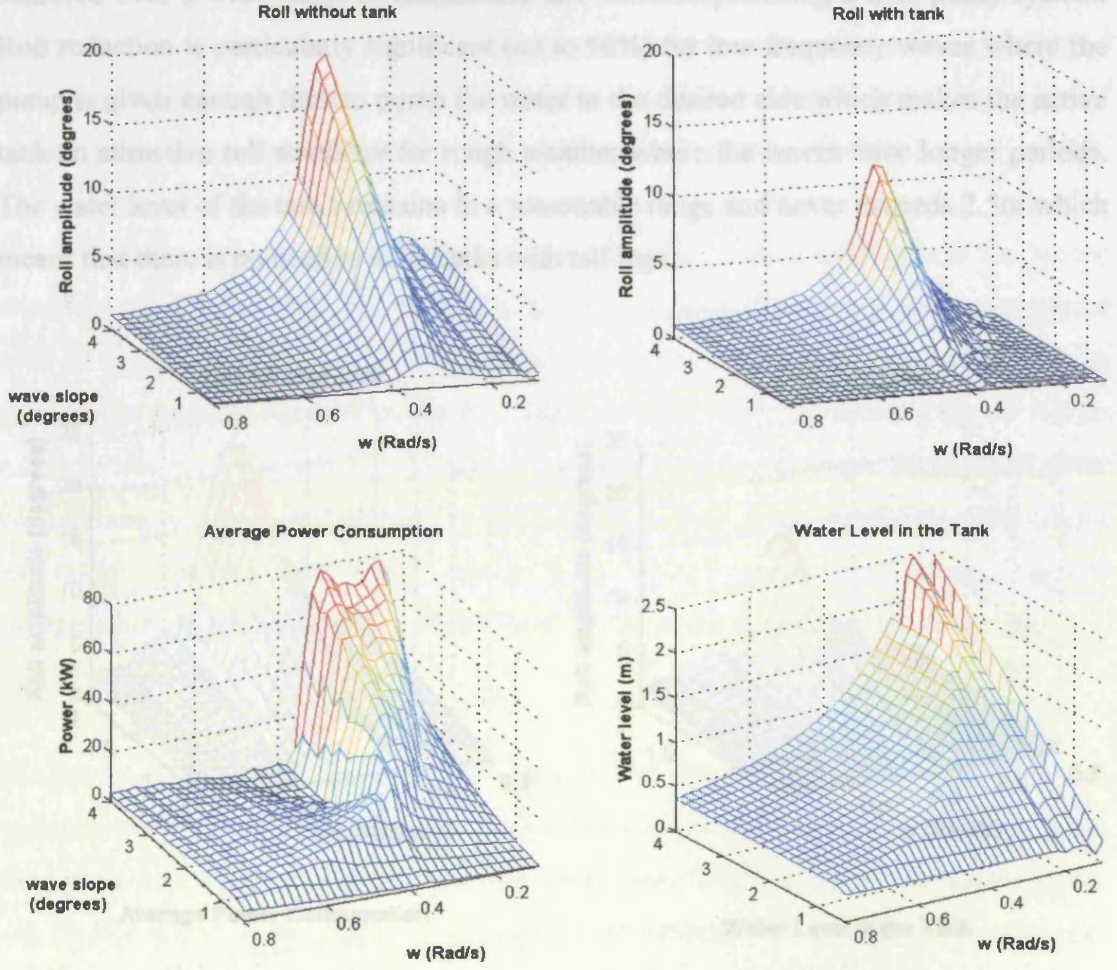

Fig. 6-7 Simulation results for ship 1 (monohull) using the pumps with sinusoidal waves

Fig. 6-7 shows the simulation results for ship 1 (monohull) using the pumps and considerable roll reduction can be observed for waves having different frequencies and wave slopes. The roll reduction achieved is satisfactory, reaching about 40% (defined as the reduction in roll amplitude caused by employing anti-roll tanks divided by the roll amplitude when no tank is used) on average. This method seems to provide reasonable roll reduction particularly when the ship is excited with low frequency waves. The reason is that there is enough time available to pump the water athwart ships and provide the maximum amount of stabilizing moment at the right time it is required. The maximum height of water level inside the tanks (z) is also shown which suggests that the water level never gets too high. It is clear from the figures that reasonable roll reduction can be

achieved over a wide range of frequencies and wave slopes using a tank-pump system. Roll reduction is particularly significant (up to 90%) for low frequency waves where the pump is given enough time to pump the water to the desired side which makes the active tank an attractive roll stabilizer for rough weather where the waves have longer periods. The water level of the tanks remains in a reasonable range and never exceeds 2.5m which means that there is no need to have tanks with tall legs.

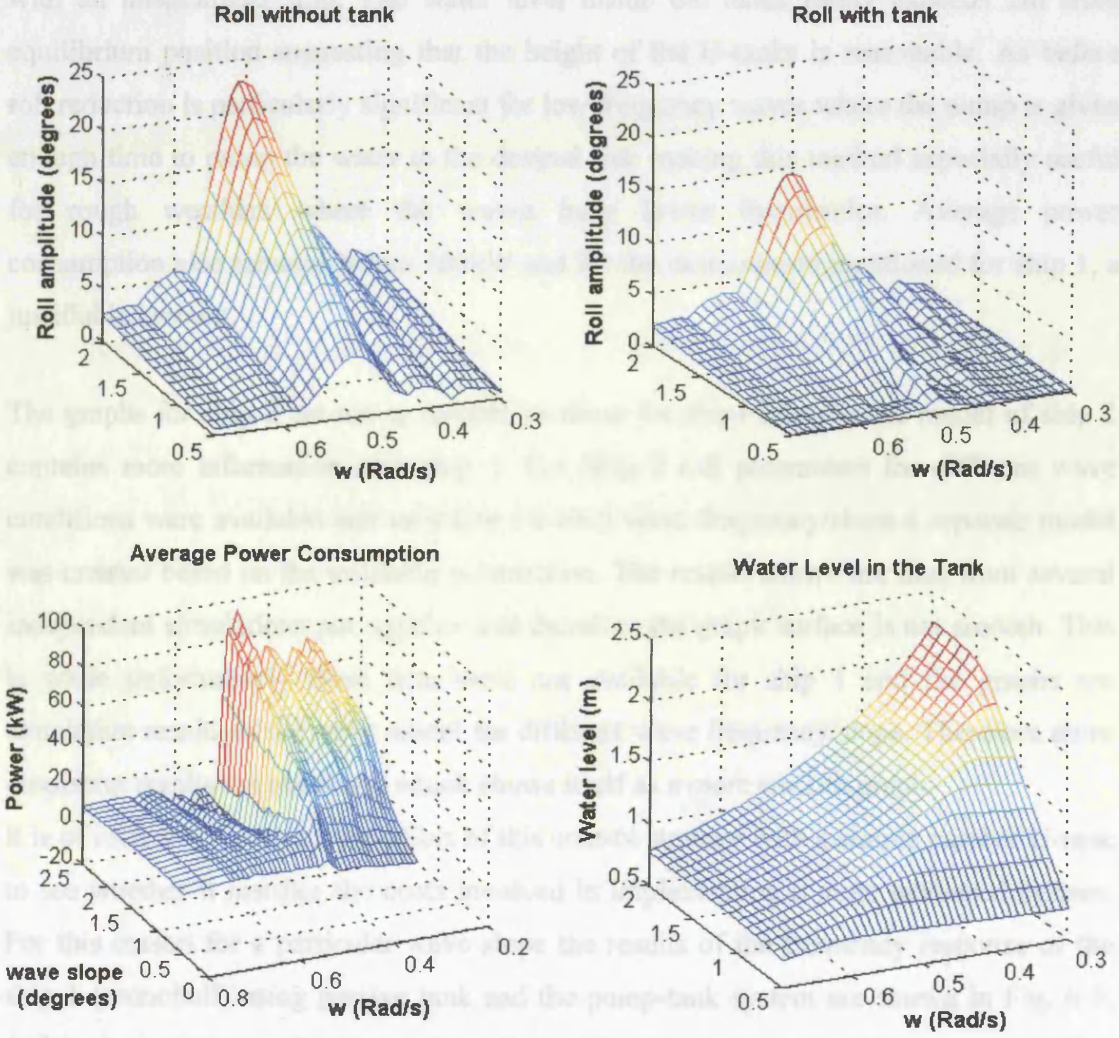

Fig. 6-8 Simulation results for ship 2 (trimaran) using the pumps with sinusoidal waves

A valuable conclusion is that the average power consumption of the pump remains well below 80 kW for most of the cases. Knowing that the average power consumption of active fin stabilizers is in the range of 50kW, the use of active tanks which are capable of reducing the roll motion in all forward speeds proves to be fairly sensible.

Fig. 6-8 shows the results of the simulation for ship 2 (trimaran) where the above argument stays valid. Roll motion is halved for most wave frequencies/slopes compared with an unstabilized ship. The water level inside the tanks rarely exceeds 2m from equilibrium position suggesting that the height of the U-tanks is reasonable. As before roll reduction is particularly significant for low frequency waves where the pump is given enough time to pump the water to the desired side making this method especially useful for rough weathers where the waves have lower frequencies. Average power consumption also remains below 100kW and for the same reason mentioned for ship 1, a justifiable amount.

The graphs for ship 2 are not as smooth as those for ship1 because the model of ship 2 contains more information than ship 1. For Ship 2 roll parameters for different wave conditions were available and therefore for each wave frequency/slope a separate model was created based on the available information. The results shown are thus from several independent simulations put together and therefore the graph surface is not smooth. This is while unfortunately these data were not available for ship 1 and the graphs are simulation results of the same model for different wave frequency/slope. Therefore more consistent results are generated which shows itself as a more smooth graph.
It is of interest to compare the effect of this control strategy with a simple passive U-tank to see whether it justifies the costs involved in implementing a more advanced system. For this reason for a particular wave slope the results of the frequency response of the ship 1 (monohull) using passive tank and the pump-tank system are shown in Fig. 6-9. Although a passive tank reduces the roll significantly at the natural frequency, at other frequencies such as 0.25 rad/s the roll is doubled as a result of the free surface effect. By using the active tank it has been possible to maintain 40-50% roll reduction at all frequencies.

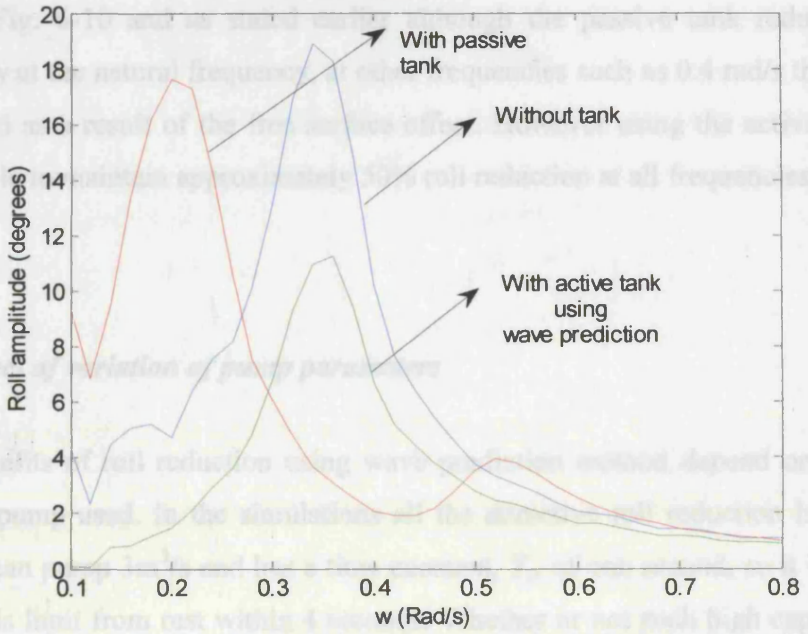

Fig. 6-9 Frequency response of ship 1 with pumps-active and passive (wave slope=4°)

The same analysis has been performed for ship 2 (trimaran) the result of which is shown in Fig. 6-10.

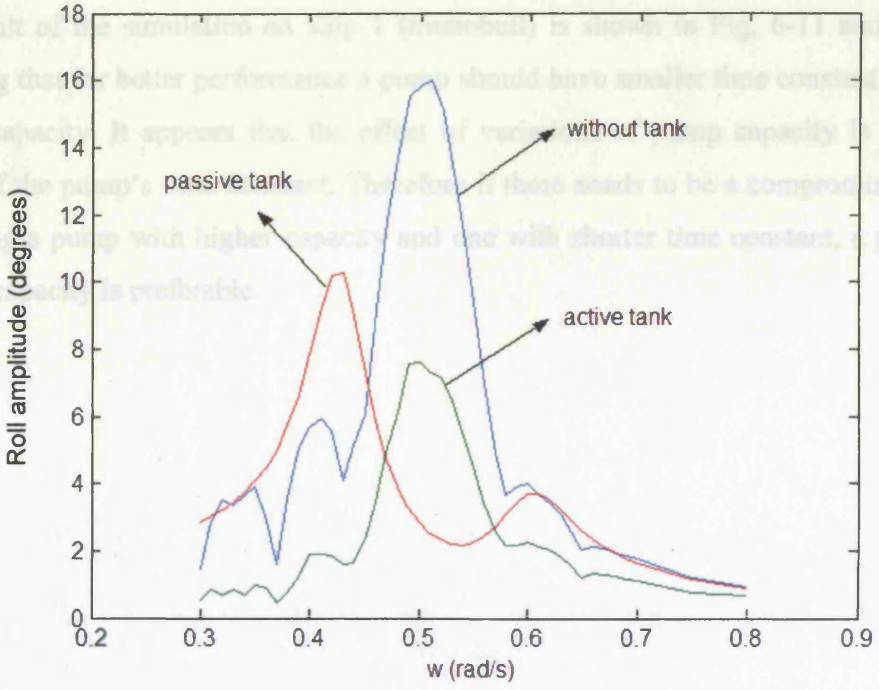

Fig. 6-10 Frequency response of ship 2 with pumps-active and passive (wave slope=4°)

Based on Fig. 6-10 and as stated earlier although the passive tank reduces the roll significantly at the natural frequency, at other frequencies such as 0.4 rad/s the roll has in fact doubled as a result of the free surface effect. However using the active tank it has been possible to maintain approximately 50% roll reduction at all frequencies.

6.3.1 Effect of variation of pump parameters

All the benefits of roll reduction using wave prediction method depend on one crucial factor: the pump used. In the simulations all the attractive roll reduction is based on a pump that can pump $3m^3/s$ and has a time constant, T_s, of one second, so it is capable of reaching this limit from rest within 4 seconds. Whether or not such high capacity pumps could be used on a ship remains a vital point. As stated earlier the pump is assumed to be a first order transfer function with a time constant equal to T_s with limitation on the maximum flow it can provide, Q. It is of interest to investigate the effect of varying the time constant T_s of the pump, and the pump capacity, Q. For a particular wave slope (4°) the result of the simulation on ship 1 (monohull) is shown in Fig. 6-11 and Fig. 6-12 showing that for better performance a pump should have smaller time constant and larger pump capacity. It appears that the effect of variations of pump capacity is more than those of the pump's time constant. Therefore if there needs to be a compromise between choosing a pump with higher capacity and one with shorter time constant, a pump with higher capacity is preferable.

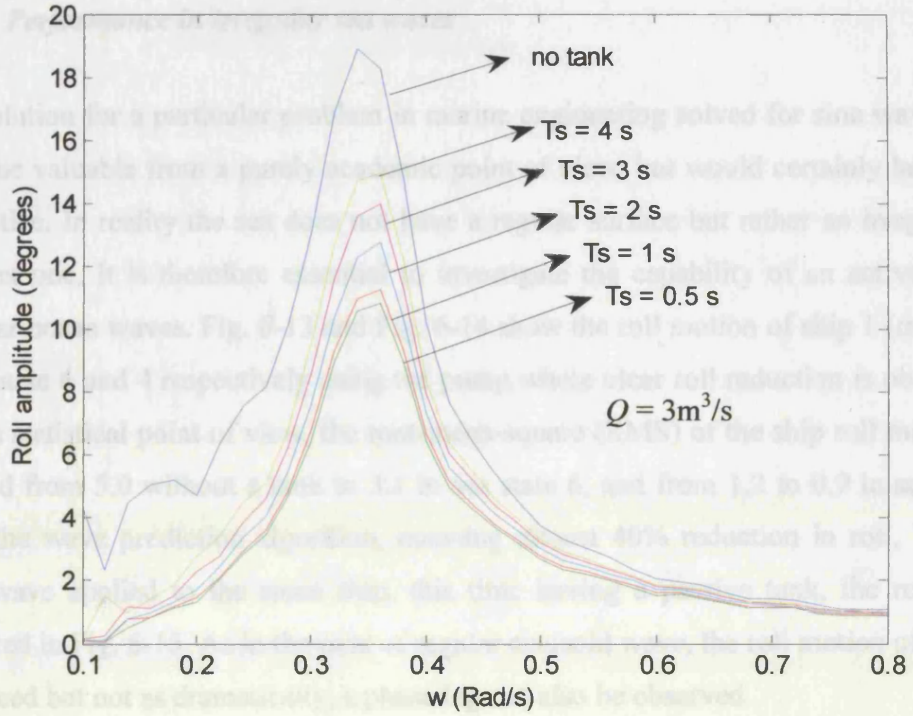

Fig. 6-11 The effect of variations of time constant of the pump on roll reduction of ship 1

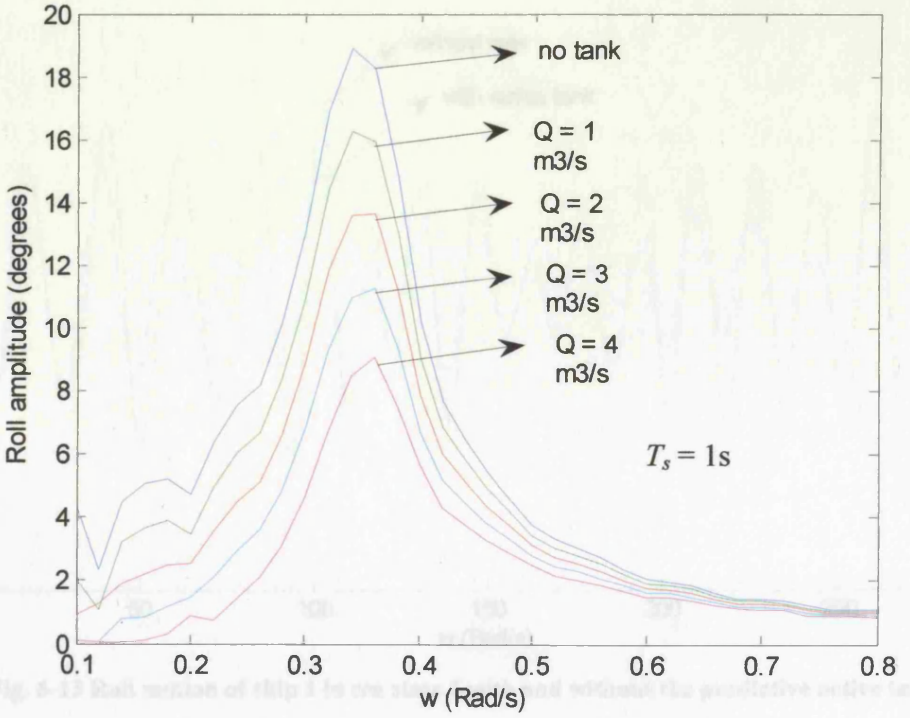

Fig. 6-12 The effect of variations of pump capacity on roll reduction of ship 1

6.3.2 Performance in irregular sea waves

Any solution for a particular problem in marine engineering solved for sine waves only, might be valuable from a purely academic point of view, but would certainly lack credit in practice. In reality the sea does not have a regular surface but rather an irregular and complex one. It is therefore essential to investigate the capability of an active tank in irregular ocean waves. Fig. 6-13 and Fig. 6-14 show the roll motion of ship 1 (monohull) in sea state 6 and 4 respectively using the pump where clear roll reduction is observable. From a statistical point of view, the root-mean-square (RMS) of the ship roll motion has dropped from 5.0 without a tank to 3.1 in sea state 6, and from 1.2 to 0.9 in sea state 4 using the wave prediction algorithm, meaning almost 40% reduction in roll. With the same wave applied to the same ship, this time having a passive tank, the results are presented in Fig. 6-15. As in the case of regular sinusoid wave, the roll motion of the ship is reduced but not as dramatically, a phase lag can also be observed.

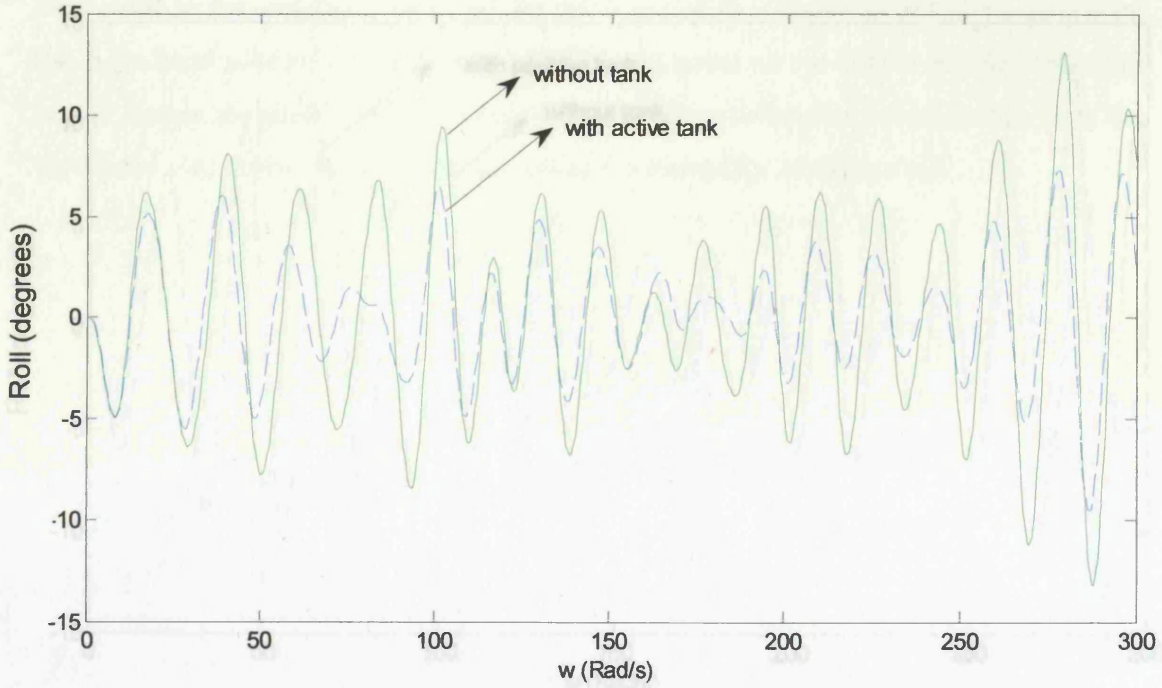

Fig. 6-13 Roll motion of ship 1 in sea state 6 with and without the predictive active tank

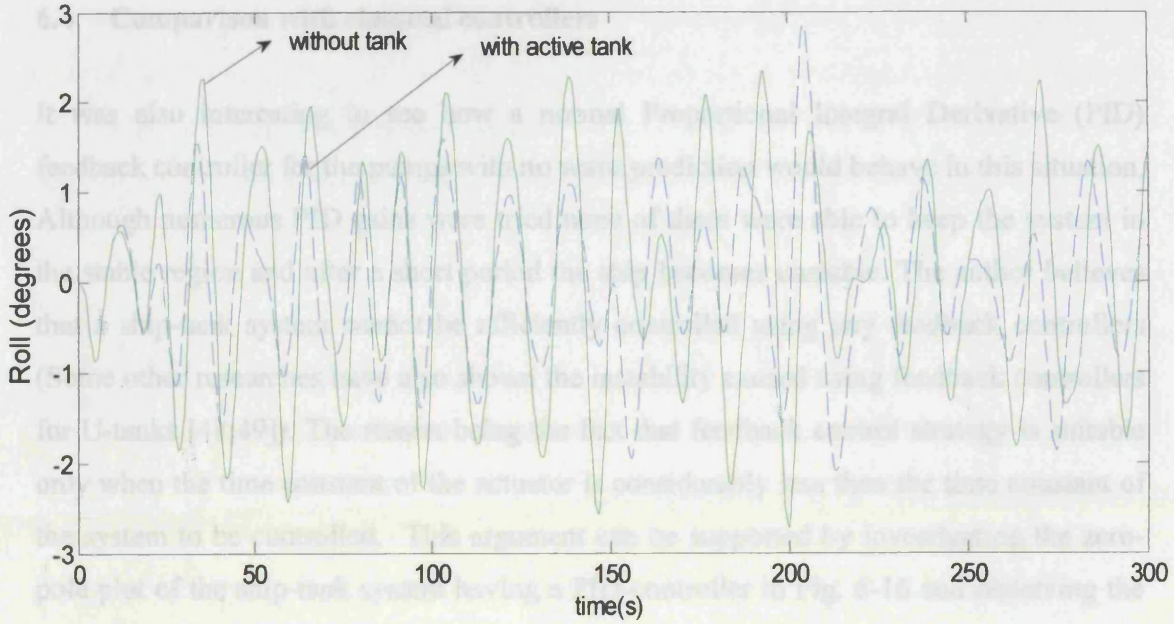

Fig. 6-14 Roll motion of ship 1 in sea state 4 with and without the predictive active tank, (note vertical scale).

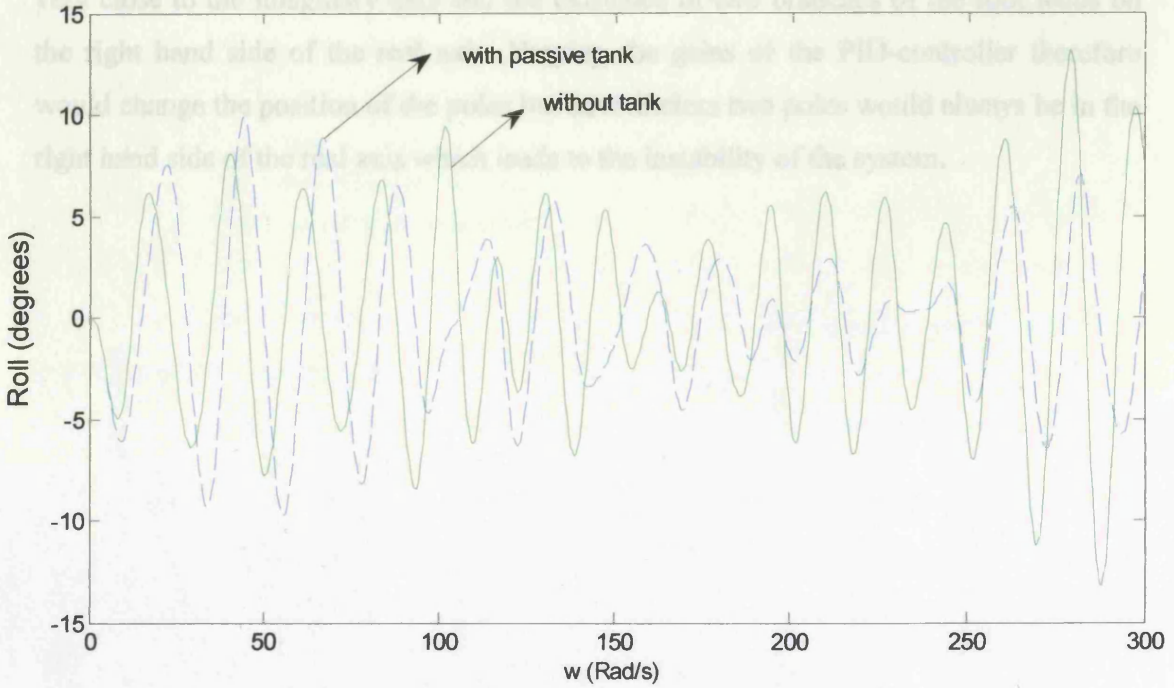

Fig. 6-15 Roll motion of ship 1 in sea state 6 with and without the passive tank

6.4 Comparison with classical controllers

It was also interesting to see how a normal Proportional Integral Derivative (PID) feedback controller for the pumps with no wave prediction would behave in this situation. Although numerous PID gains were tried none of them were able to keep the system in the stable region and after a short period the ship becomes unstable. The author believes that a ship-tank system cannot be efficiently controlled using any feedback controllers (Some other researches have also shown the instability caused using feedback controllers for U-tanks [48;49]). The reason being the fact that feedback control strategy is suitable only when the time constant of the actuator is considerably less than the time constant of the system to be controlled. This argument can be supported by investigating the zero-pole plot of the ship-tank system having a PID-controller in Fig. 6-16 and observing the sensitive region close to the origin which is shown in detail in Fig. 6-17.

The zero-pole plot of this system reveals the existence of two dominant complex poles very close to the imaginary axis and the existence of two branches of the root locus on the right hand side of the real axis. Varying the gains of the PID-controller therefore would change the position of the poles but nevertheless two poles would always be in the right hand side of the real axis which leads to the instability of the system.

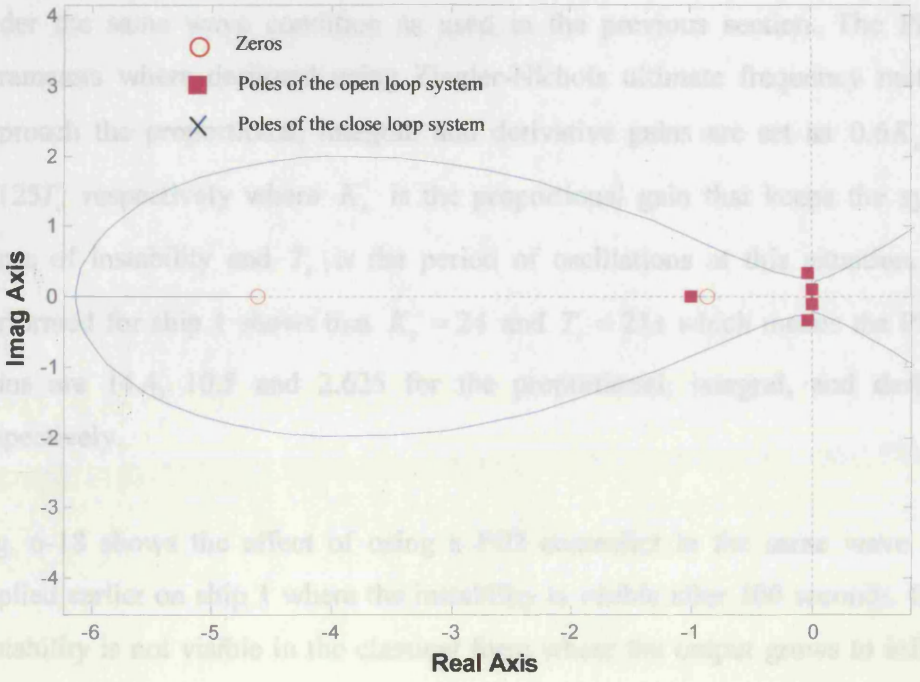

Fig. 6-16 Zero-pole plot of ship-tank using a PID-controller

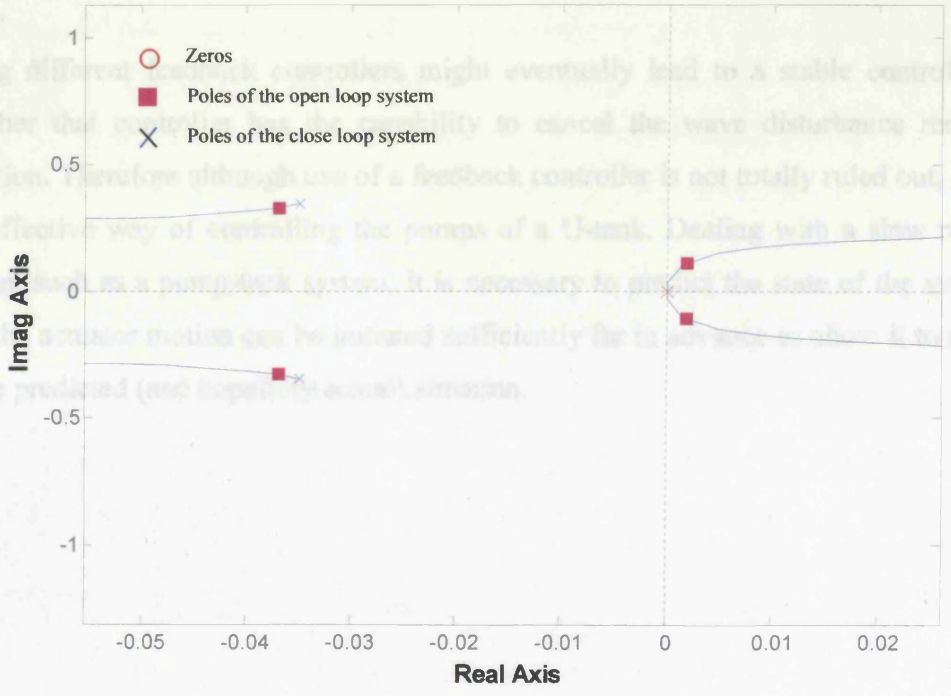

Fig. 6-17 detail of Fig. 6-16

A PID-controller has been designed to control the pumps of the U-tank used in ship 1 under the same wave condition as used in the previous section. The PID-controller parameters where designed using Ziegler-Nichols ultimate frequency method. In this approach the proportional, integral, and derivative gains are set as $0.6K_c$, $0.5T_c$ and $0.125T_c$ respectively where K_c is the proportional gain that keeps the system on the verge of instability and T_c is the period of oscillations at this situation. Simulations performed for ship 1 shows that $K_c = 24$ and $T_c = 21\text{s}$ which means the PID-controller gains are 14.4, 10.5 and 2.625 for the proportional, integral, and derivative gains respectively.

Fig. 6-18 shows the effect of using a PID controller in the same wave condition as applied earlier on ship 1 where the instability is visible after 100 seconds. Of course the instability is not visible in the classical form where the output grows to infinity. This is because of the limited volume of the tanks that prevents the actuating signal from growing beyond than a certain amount. The instability shows itself as accumulation of water in one of the tanks only (Fig. 6-19).

Using different feedback controllers might eventually lead to a stable controller, but whether that controller has the capability to cancel the wave disturbance remains a question. Therefore although use of a feedback controller is not totally ruled out, it is not the effective way of controlling the pumps of a U-tank. Dealing with a slow response system such as a pump-tank system, it is necessary to predict the state of the system so that the actuator motion can be initiated sufficiently far in advance to allow it to respond to the predicted (and hopefully actual) situation.

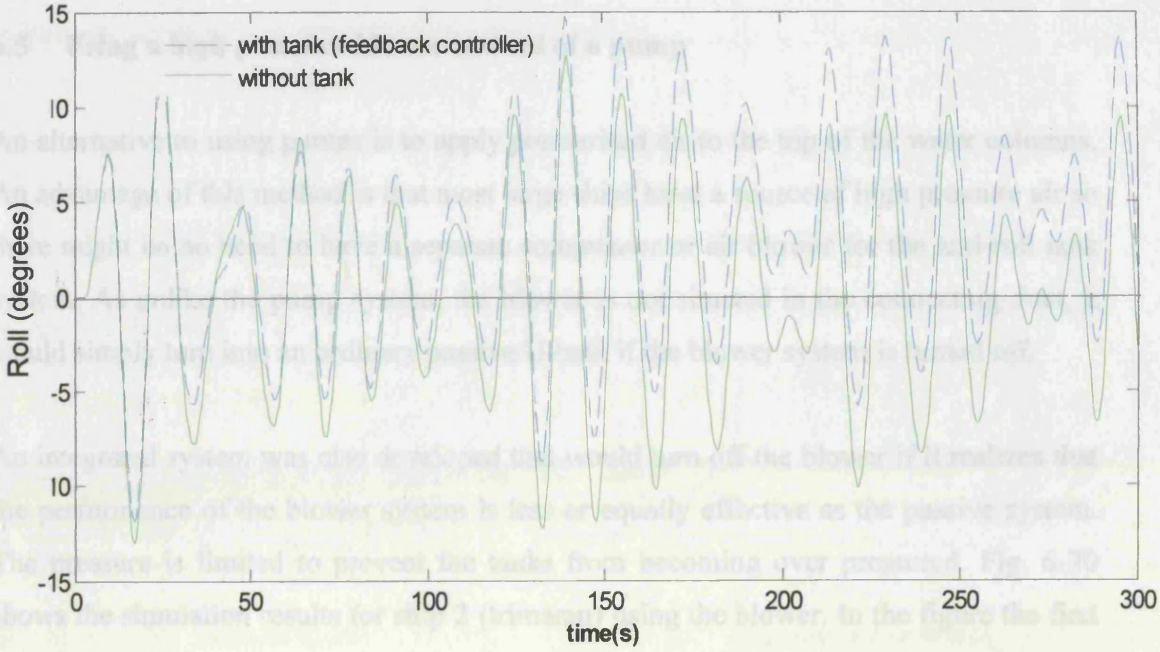

Fig. 6-18 Roll motion of ship 1 in sea state 6 with and without active tank using feedback controller

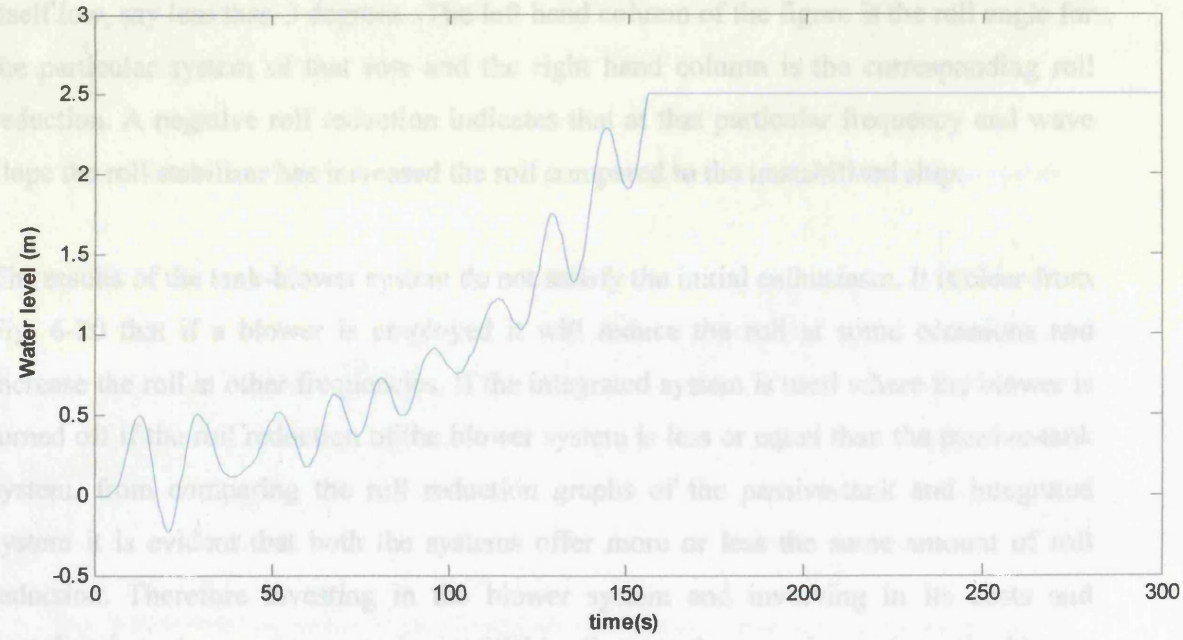

Fig. 6-19 Level of water inside a tank of ship 1 in sea state 6 using feedback controller

6.5 Using a high pressure blower instead of a pump

An alternative to using pumps is to apply pressurised air to the top of the water columns. An advantage of this method is that most large ships have a source of high pressure air so there might be no need to have a separate compressor or air blower for the anti-roll tank system. As unlike the pump system, the blower is not situated in the connecting duct, it would simply turn into an ordinary passive U-tank if the blower system is turned off.

An integrated system was also developed that would turn off the blower if it realizes that the performance of the blower system is less or equally effective as the passive system. The pressure is limited to prevent the tanks from becoming over pressured. Fig. 6-20 shows the simulation results for ship 2 (trimaran) using the blower. In the figure the first row shows the result for a passive tank only, the second row shows the results for a blower system only (which produces pressures about 5 bar), and the third row presents the results for an integrated system in which the blower is turned off if the roll reduction of the blower system is less or equal than the passive system or when the roll angle is itself low, say less than 3 degrees.. The left hand column of the figure is the roll angle for the particular system of that row and the right hand column is the corresponding roll reduction. A negative roll reduction indicates that at that particular frequency and wave slope the roll stabilizer has increased the roll compared to the unstabilized ship.

The results of the tank-blower system do not satisfy the initial enthusiasm. It is clear from Fig. 6-20 that if a blower is employed it will reduce the roll at some occasions and increase the roll at other frequencies. If the integrated system is used where the blower is turned off if the roll reduction of the blower system is less or equal than the passive-tank system, from comparing the roll reduction graphs of the passive-tank and integrated system it is evident that both the systems offer more or less the same amount of roll reduction. Therefore investing in the blower system and involving in its costs and complications does not seem to be justifiable. Even at the occasions where the blower

system provided more roll reduction than the passive-tank system, it required a large air volume of about $10m^3/s$, which is fairly unreasonable.

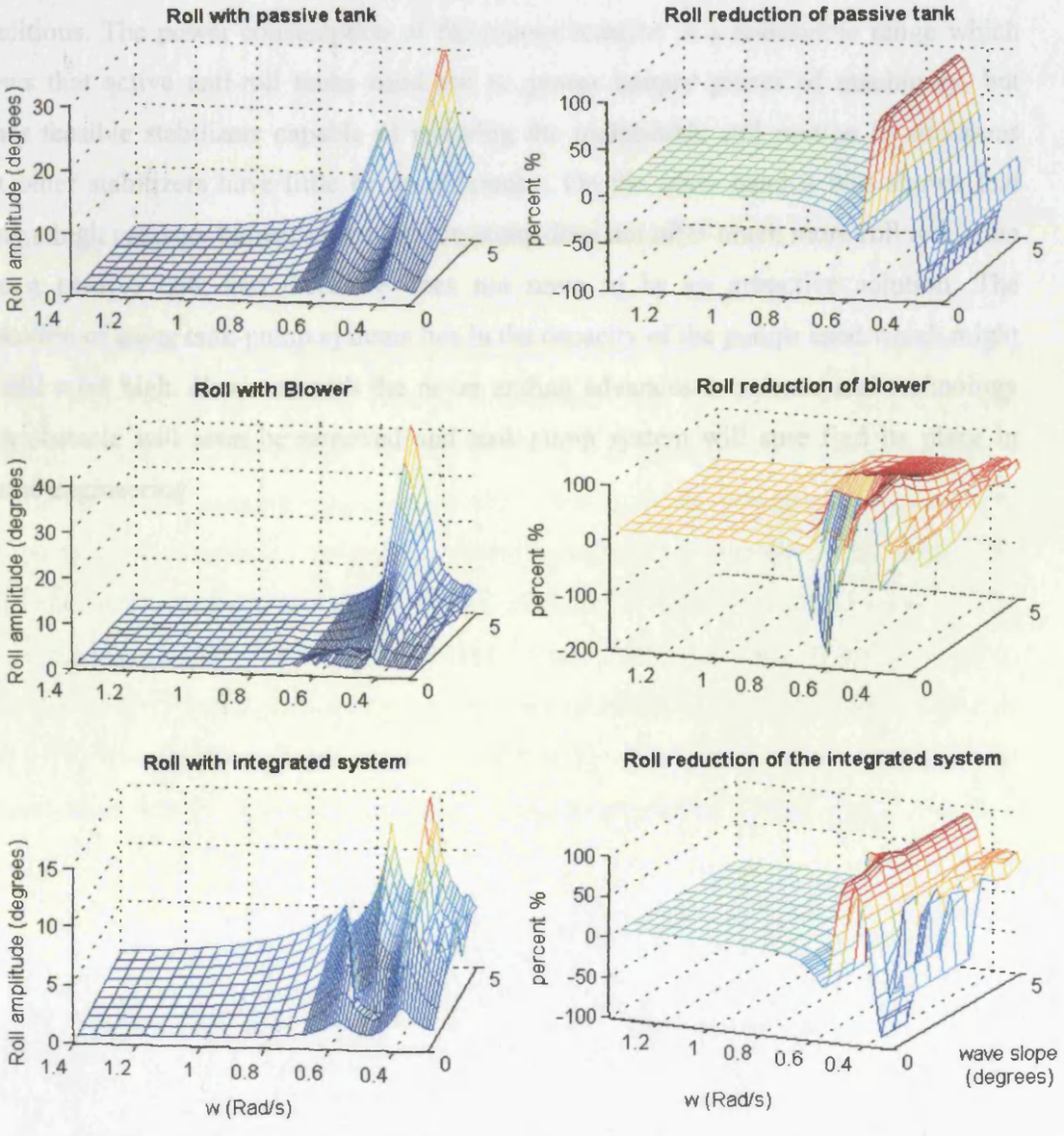

Fig. 6-20 Simulation results for ship 2 (trimaran) using the blower with sinusoidal waves

6.6 Concluding remarks

This chapter has described a new strategy for controlling active anti-roll tanks based on predicting the incoming waves using an ARX model and pumping the water between the legs of the tank before the waves reach the ship. Significant roll reduction has been experienced using the new methodology especially when the period of the incoming waves is relatively large which makes this stabilizer much attractive for severe weather conditions. The power consumption of the pumps remains in a reasonable range which shows that active anti-roll tanks need not be power hungry pieces of machinery, but rather feasible stabilizers capable of reducing the undesirable roll motion in situations that other stabilizers have little or no efficiency. On the other hand it was shown that using a high pressure blower instead of the pump does not offer much more roll reduction than a passive tank and therefore does not seem to be an attractive solution. The limitation of using tank-pump systems lies in the capacity of the pumps used which might be still a bit high. However with the never ending advances in science and technology such obstacle will soon be removed and tank-pump system will sure find its place in marine engineering.

Chapter 7

7 Adaptive inverse controller

7.1 Introduction

The goal of any control system is to make the output of a plant follow a desired value. This value might be constant and the controller acts as a regulator, or it might be a varying signal as in the case of a servo mechanism. Fig. 7-1 shows a standard unity feedback control diagram where $y(t)$ is the output of the plant and the controller's task is to make sure that this output remains reasonably close to the desired reference signal, $r(t)$. In other words it is aimed to design a controller in such a way to minimize the error, $e(t)$, or the difference between $r(t)$ and $y(t)$. The controller is usually designed having some knowledge about the plant and the control requirements. In some cases it is more important to have better stability (in terms of less oscillations in the response) while in some other cases a fast response might be the priority. In another case an optimal usage of the actuator and the economic cost of the controller might be the main design criteria.

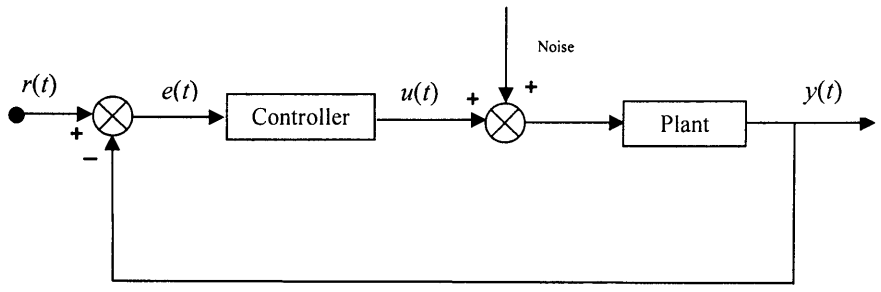

Fig. 7-1 Unity feedback control system

No matter what the design criteria are, knowledge of the plant and its transfer function is essential. However, when limited information about the plant is available, or the plant properties change over time, a more advanced controller is required. In the particular application of roll stabilization, the dynamic transfer function of the ship also varies in different weathers and under different loading conditions. Moreover the waves acting as the noise disturbing the plant are irregular in nature and add to the complexity of the control system.

As a solution adaptive controllers are utilized that are designed in a way to compensate for the above mentioned changes in the plant. An adaptive controller is usually in the form of a transverse filter discussed in Chapter 3. The goal of the controller is to minimize the error, $e(t)$, in the mean-square sense by altering the filter gains to some optimum values. The methods discussed in Chapter 3 for optimising the gains of a transverse filter are of particular interest in this chapter.

7.2 Adaptive inverse control

As it is clear from the name, an unknown plant is controlled by an input command signal applied through a controller whose transfer function approximates the inverse of the plant's transfer function. Therefore it can be concluded that ideally if a reference signal is applied to such a system the output of the plant would be the same as the required reference signal (Fig. 7-2).

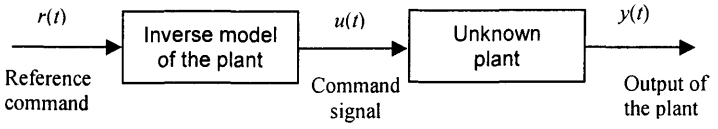

Fig. 7-2 Inverse model control system

The inverse model is itself a linear filter and using any least square algorithms discussed in Chapter 3 it is possible to optimize the gains in a way that if the output of the plant is applied to it, the filter generates a signal similar to the input of the plant (Fig. 7-3). In

other words the adaptation algorithm tries to minimize the difference between the plant output and the filter's input. A close fit implies that the overall transfer function of the cascade of the plant and the filter is unity, at least within the frequency band of the plant input. In general, close fits can be achieved when the length of the filter, k, is adequately long, even when the unknown plant has many poles and zeros.

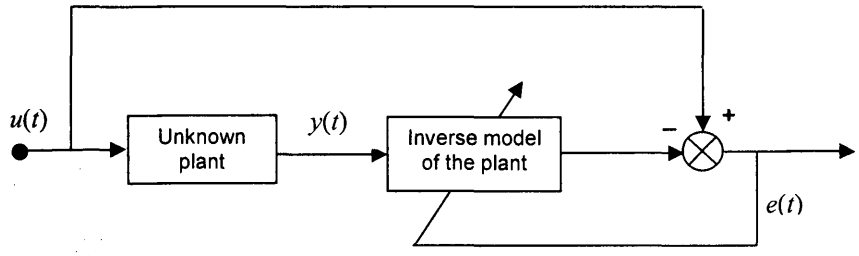

Fig. 7-3 Principle of inverse plant modelling

It should be taken into account that the output of the inverse model appears with some delay as it takes some time for the signal $u(t)$ to pass through the plant and the filter. This is while the reference signal $u(t)$ is available immediately for comparison, meaning that the output of the inverse model tries to get close to a reference signal at the wrong time which might lead to instability of the system. As a solution it is beneficial to have some idea about the plant and an estimate of the delay involved in the formation of the output, and therefore applying the same delay to the reference input before comparing them (Fig. 7-4).

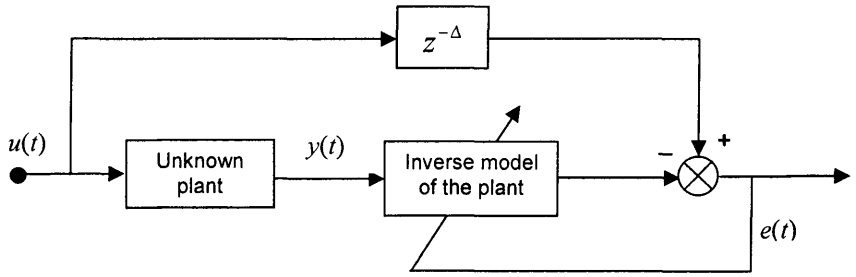

Fig. 7-4 Principle of inverse plant modelling with delay

By understanding the above context, an essential block to be used in the inverse controller strategy is formed. The overall control strategy is demonstrated in Fig. 7-5. The controller is simply the delayed inverse model of the plant exactly copied before the plant block. The cascade of the plant and the controller approaches unity as the error signal, $e(t)$, reduces. Therefore if the filter adaptation is performed correctly, in the absence of any noise, the output of the plant, $y(t)$, would eventually follow the desired reference signal, $r(t)$ but with some delay, Δ :

$$y(t) = r(t - \Delta) \tag{7-1}$$

The result is that if a step reference is applied to the system there will be a step change in the plant output but only after Δ steps delay.

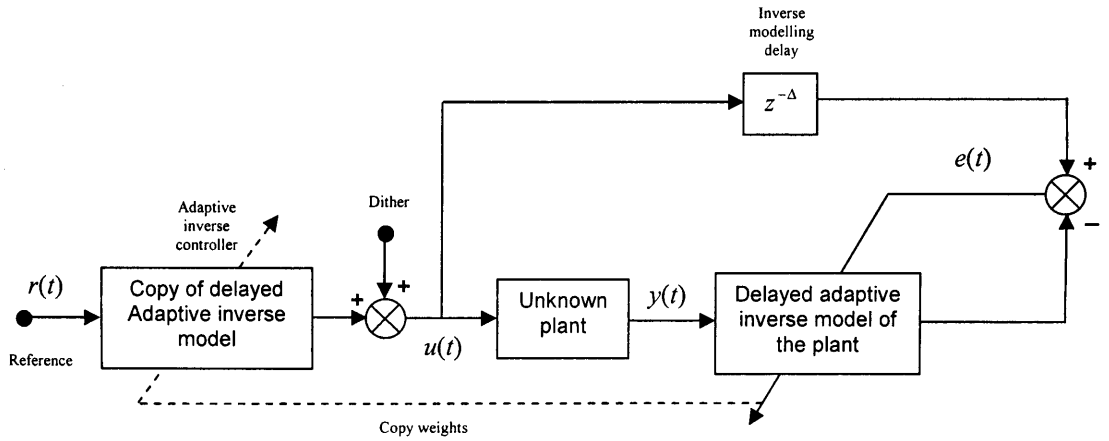

Fig. 7-5 Adaptive inverse model control system block diagram

Proper adaptation of the filter gains can only be performed when the adaptive inverse model of the plant is well excited by varying inputs and considering the effect of them on the output. When there is not much excitation from the reference signal, a dither signal must also be applied to the system to excite the adaptive process. The dither must not be too strong to cause unnecessary noise in the plant output and yet strong enough to provide the minimum excitation required for the process of adaptation.

7.3 Filtered-x LMS Algorithm

Addition of noise to the plant, for example sea waves in the case of a ship, considerably complicates the control problem. The noise, usually added to the plant output, is fed directly as the input of the adaptive filter (Fig. 7-6). This added input is not correlated with the desired output, the delayed $u(t)$ signal. Therefore the nature of the signal applied to the input of the filter is changed and the input covariance matrix $\mathbf{R}$ changes as well. Remembering from Chapter 3 that the adaptive gains finally converge to the Wiener solution in the form of $\mathbf{R}^{-1}\mathbf{P}$, one can easily see the undesirable effect of the added noise on the final gains of the inverse model. In the overall control picture this leads to an incorrect inverse controller and subsequent poor performance.

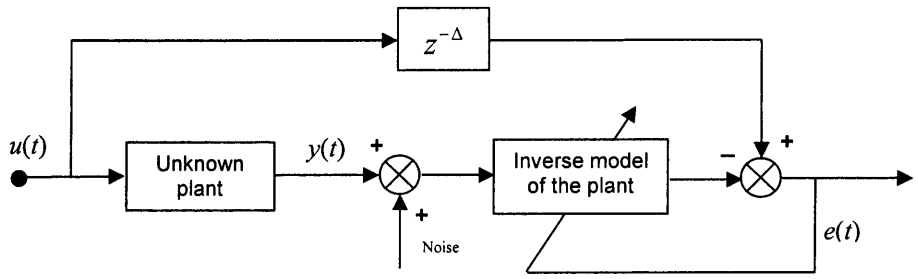

Fig. 7-6 Inverse modelling of a plant with Noise

A method to overcome the problem is placing the adaptive inverse model not after the plant, but before it (Fig. 7-7). This way the noise does not appear in the adaptive filter input. Therefore if the adapting input (the desired signal) in derived correctly the noise appearing in the error signal has no effect on the converged solution. The challenge is that the error $e(t)$ in this case is the plant output added with some noise and not the adaptation error. If this error is fed directly into the adaptation block the adaptive process will find a totally irrelevant solution or even be driven unstable. Therefore fundamental changes are required for the error signal before using it in the LMS block. The method is known as "filtered-x LMS algorithm" and will be discussed in more detail.

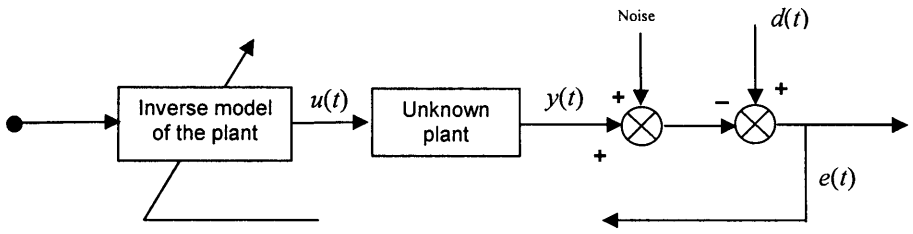

Fig. 7-7 Initial idea of filtered-x algorithm (the missing bits are completed in the following figures)

In order to have a better idea of how a filtered-x algorithm works it is essential to have a good understanding of the LMS adaptation block. The block diagram of LMS adaptive filter is shown in Fig. 7-9 in both overall form (a), and in detail in (b).

In order to complete the block diagram of Fig. 7-7, the first step is to neglect the noise and connect the adaptive filter to the plant in a way to derive a desired signal (Fig. 7-8). This adaptive filter, when optimized possesses the same gains as the adaptive filter of Fig. 7-7 in the absence of noise.

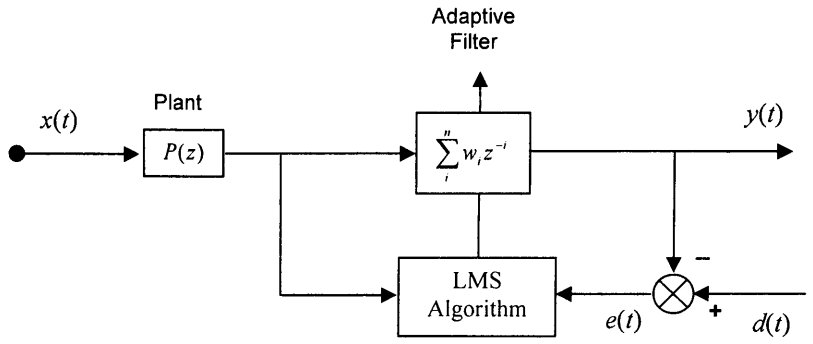

Fig. 7-8 Adaptation of a filtered-x algorithm

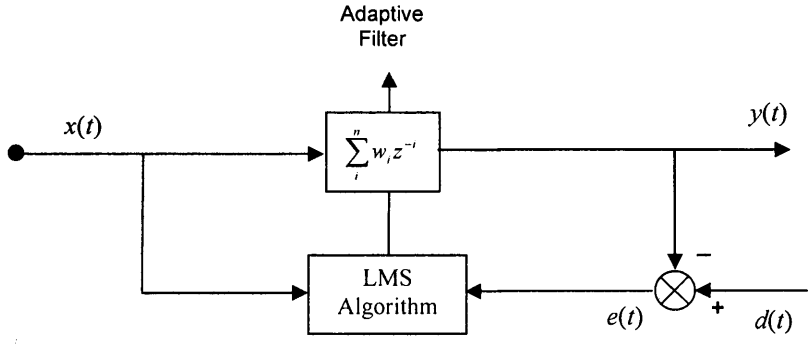

(a)

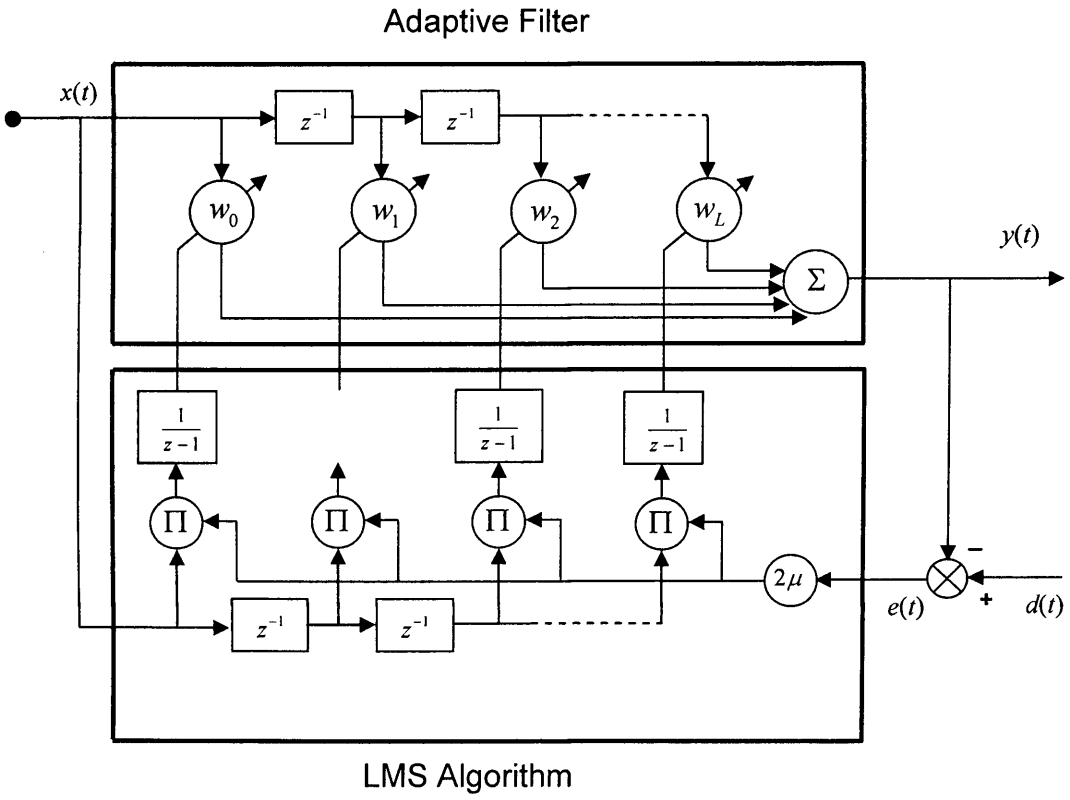

(b)

Fig. 7-9 Block diagram of LMS adaptive filter: (a) in overall form (b) in detail

It is possible to rearrange the block diagram of Fig. 7-8 in a way to become similar to the block diagram of a filtered-x algorithm (Fig. 7-7) by moving the plant block after the adaptive filter and applying the plant output as the input of the LMS block (Fig. 7-10).

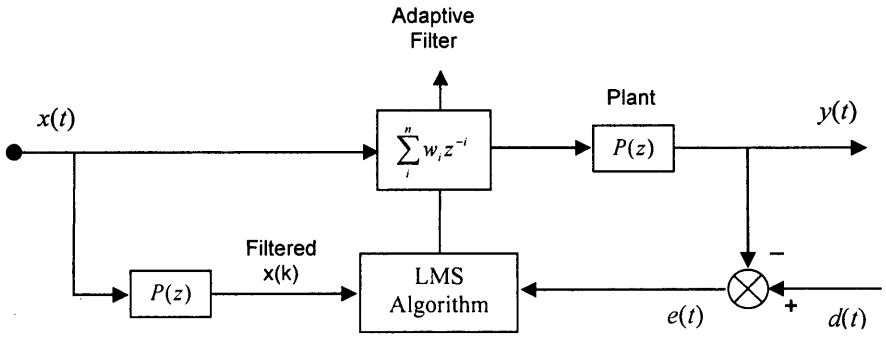

Fig. 7-10 Rearranged form of block diagram Fig. 7-8

Comparing Fig. 7-8 and Fig. 7-10 it is clear that the input to the LMS algorithm is exactly the same at all times. The error signal is also the same if the gains of the adaptive filters are identical and that the plant and the adaptive filter were commutable. This could be true if the adaptive filters were linear and time invariant, which is clearly not the case (Fig. 7-9). However, if the plant is linear (in the range of operation) and the adaptation is slow, the adaptive filters can, with good approximation, be considered linear and commutable with the plant. Therefore if the adaptation of the gains is started from the same initial values they will vary similarly and converge to same values. At this point the addition of plant noise has no effect on the expected value of the gain vectors of the adaptive filter, but just causes maladjustment in the final values (Fig. 7-11). The algorithm created this way has been used in many applications and has shown to be stable [73] and a suitable way to complete the missing parts of the block diagram of Fig. 7-7.

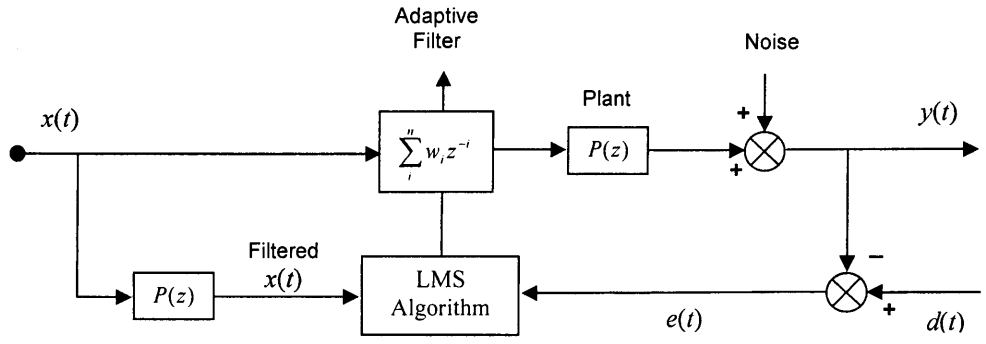

Fig. 7-11 Development of filtered-x algorithm in presence of noise

7.4 Inverse Control Using Filtered-x LMS Algorithm

It is now possible to use the filtered-x algorithm which was adapted above to build an inverse controller. The only problem is that the plant also appears in the block diagram, so either complete knowledge of the transfer function of the plant is required or it has to be estimated by another adaptive filter. The former is clearly not the case as the reason for applying the inverse controller in the first place is that the plant is not completely known or its variations with time is not clear. Therefore the plant model needs to be derived using another adaptive filter.

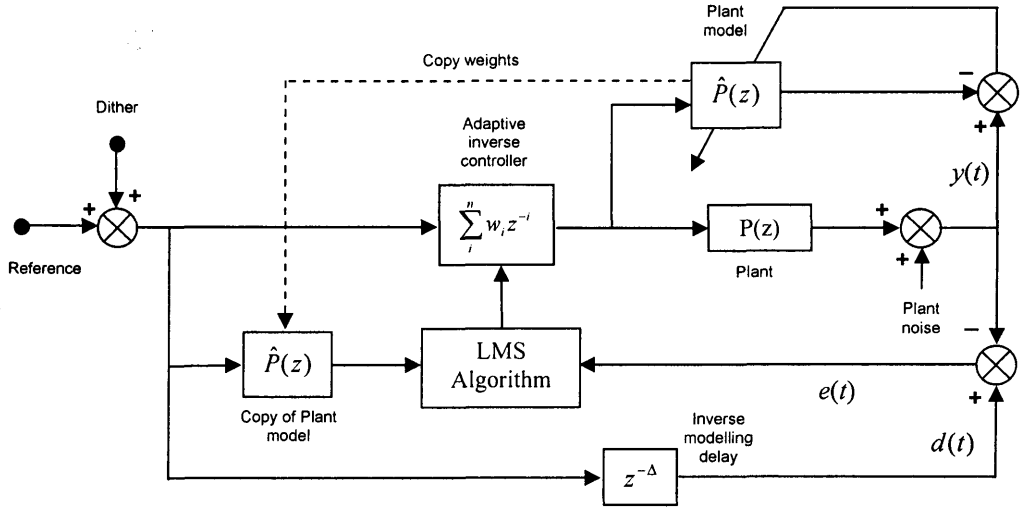

Fig. 7-12 Adaptive inverse control diagram using filtered-x LMS algorithm

A possible scheme of such configuration is demonstrated in Fig. 7-12. There are two separate adaptive filters in the block; one for direct modelling of the plant, the other for filtered-x inverse modelling of the plant to form an inverse controller. The gains from the direct model of the plant are exactly copied to the block before the LMS algorithm where a filtered reference signal is required as the input of the LMS algorithm.

When both the filters converge a step change in the reference signal will cause a step change in the plant output after Δ steps. If a feedback is applied to the plant for reducing the correlated output noise, the combination of the plant and its feedback should be considered as an "equivalent" plant and used for both adaptive filters.

7.5 Filtered-x LMS Algorithm applied to active anti-roll tanks

The nature of the problem of roll stabilization seems to be in good harmony with the philosophy of inverse control using filtered-x LMS; the tank-pump system is very difficult to model and requires in-depth research in the field of fluid mechanics. The dynamic transfer function of the ship also varies in different weathers and under different loading conditions. Moreover the sea waves acting as the noise disturbing the plant are irregular in nature and add to the complexity of the control system. All these factors are however dealt with effectively in the control strategy using filtered-x LMS algorithm discussed so far. The block diagram shown in Fig. 7-12 can be effectively adapted for the particular application of roll reduction as shown in Fig. 7-13.

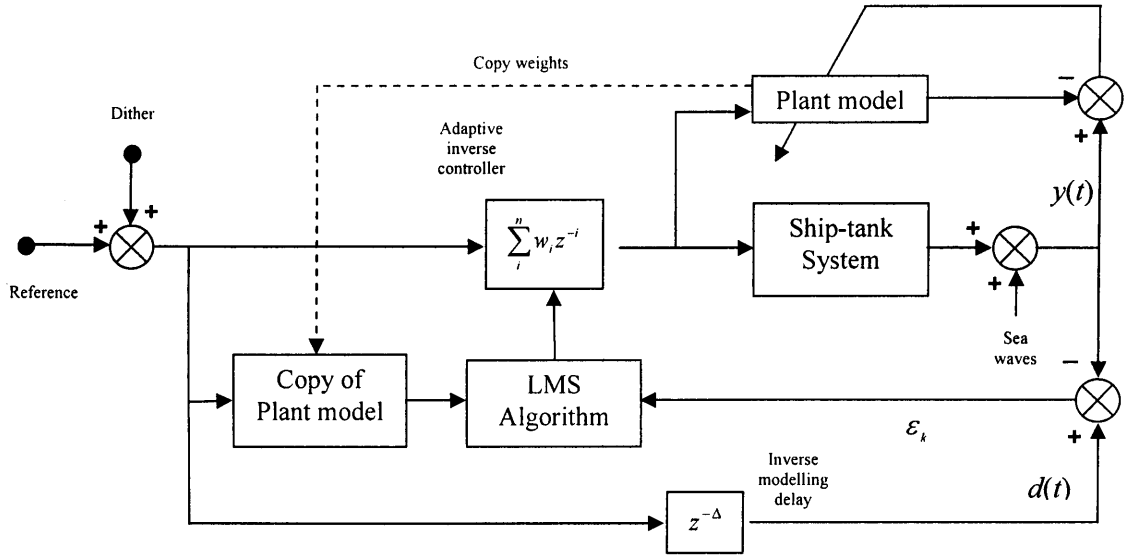

Fig. 7-13 Adaptive inverse model control diagram using filtered-x LMS algorithm

The proposed control strategy is simulated for a particular ship model. The mathematical model of the ship tank system used in this study is derived using the Euler method extracted from Lloyd [40]:

Tank

$$a_{\tau 2}\ddot{x}_2 + a_{\tau 4}\ddot{x}_4 + c_{\tau 4}x_4 + a_{\tau 6}\ddot{x}_6 + a_{\tau\tau}\ddot{\tau} + b_{\tau\tau}\dot{\tau} + c_{\tau\tau}\tau = \alpha P \quad \textbf{(7-2)}$$

Roll

$$a_{42}\ddot{x}_2 + b_{42}\dot{x}_2 + (I_{44} + a_{44})\ddot{x}_4 + b_{44}\dot{x}_4 + c_{44}x_4 + a_{46}\ddot{x}_6 + b_{46}\dot{x}_6 + c_{46}x_6 - [a_{4\tau}\ddot{\tau} + c_{4\tau}\tau] = F_4$$

where

F_4	Wave moment
τ	Tank angle defined as in Fig. 7-14
P	Pressure of the air provided at the top of the tank
α	Coefficient relating the pressure applied with the tank dynamics
$x_2, \dot{x}_2, \ddot{x}_2$	Sway, sway velocity and sway acceleration
$x_4, \dot{x}_4, \ddot{x}_4$	Roll, roll velocity and roll acceleration
$x_6, \dot{x}_6, \ddot{x}_6$	Yaw, yaw velocity and yaw acceleration
a_{ij}, b_{ij} and c_{ij}	Ship hydrodynamic coefficients

In this study a simplified version of the above equations is used in order to restrict the motion of the ship to roll only. Therefore:

Tank

$$a_{\tau 4}\ddot{x}_4 + c_{\tau 4}x_4 + a_{\tau\tau}\ddot{\tau} + b_{\tau\tau}\dot{\tau} + c_{\tau\tau}\tau = \alpha P \quad \textbf{(7-3)}$$

Roll

$$(I_{44} + a_{44})\ddot{x}_4 + b_{44}\dot{x}_4 + c_{44}x_4 - [a_{4\tau}\ddot{\tau} + c_{4\tau}\tau] = F_4$$

Where P is the pressure applied to the water inside the tank by the pump or blower and α is a constant.

The simulations are performed for a *La Salle* class US Command ship (ship 1 in Chapter 6) where the specifications of the ship required for this simulation was available:

Maximum Speed	21 knots
Displacement	9600 tonne
Overall Beam	32 m
Length	156 m
Waterline length	150 m
Water mass to ship	1.8%

Table 7-1 Major parameters of the ship used in the simulation

The U-tank dimensions used in this simulation are presented in Table 7-2 where the geometric parameters are introduced in Fig. 7-14 and x_t is the length of the tank in the fore/after direction. The tank is situated 1.5m above the centre of rotation of the ship.

w	32 m
w_r	3 m
h_r	3 m
h_d	1 m
x_t	3.5 m

Table 7-2 Dimension of the U-tank

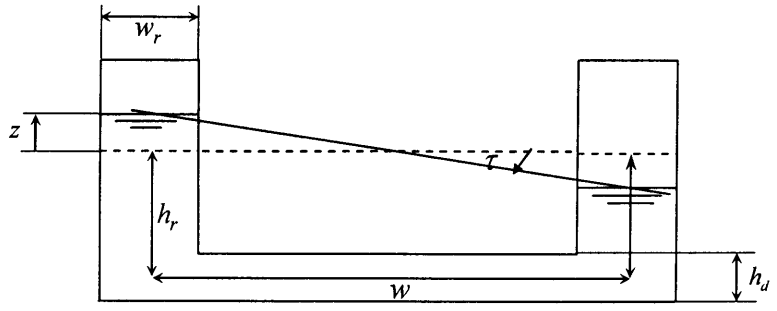

Fig. 7-14 U-tank and its geometric parameters

The ship-tank system is excited by sea waves generated using the wave generating software developed by the author. The waves simulate the conditions of sea state 6. The roll motion of the ship with and without the inverse controller are presented in Fig. 7-15. Considerable roll reduction is observed once the inverse controller and ship-tank model's gains have converged and settled to their final values. The gains of the inverse controller settle to their final values (Fig. 7-16) after about 400 seconds after the start of the simulation (Fig. 7-17) and the root mean square of the error (the difference between the actual roll of the ship and the desired roll being zero) gradually reduces (Fig. 7-18). Root mean square is usually defined by:

$$e_{rms} = \frac{\sqrt{e_1^2 + e_2^2 + e_3^2 + ... + e_N^2}}{N} \tag{7-4}$$

However here, the root mean square of the error has been calculated using 50 seconds windows so that the initial high errors before the adaptation would not affect the root mean square of the error for too long.

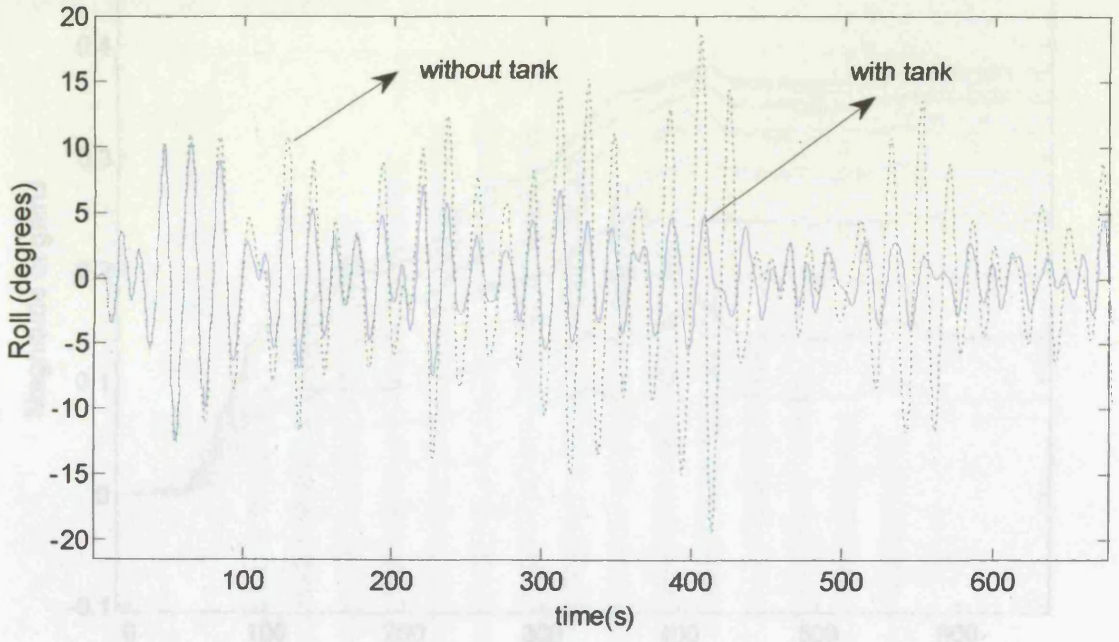

Fig. 7-15 Roll reduction of the anti-roll tank with active U-tank using filtered-x LSM algorithm

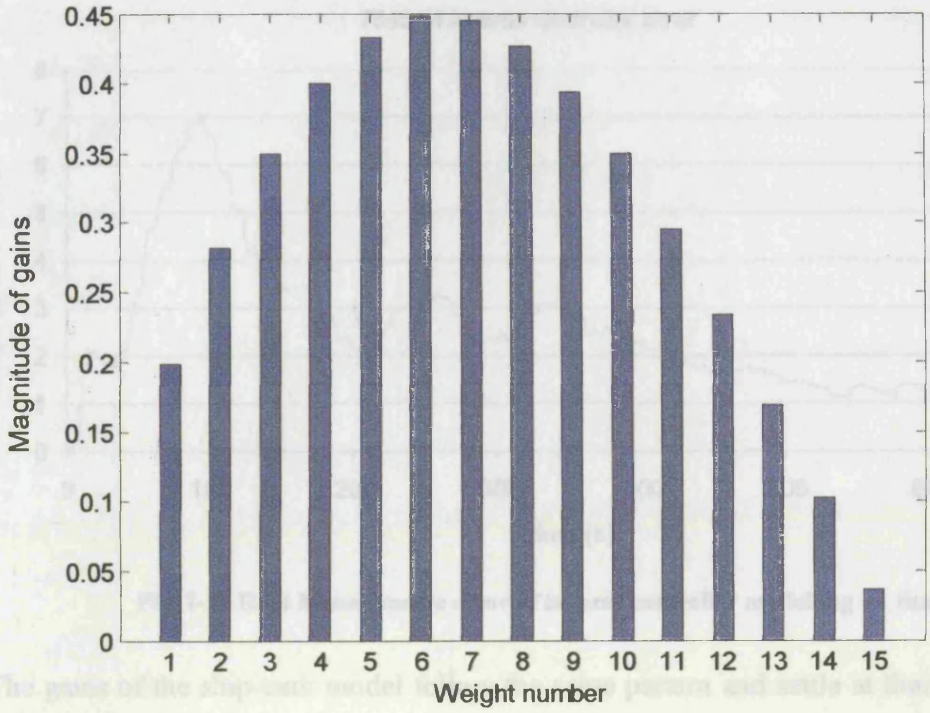

Fig. 7-16 Gains of inverse controller after adaptation (L=15 and Δ=8)

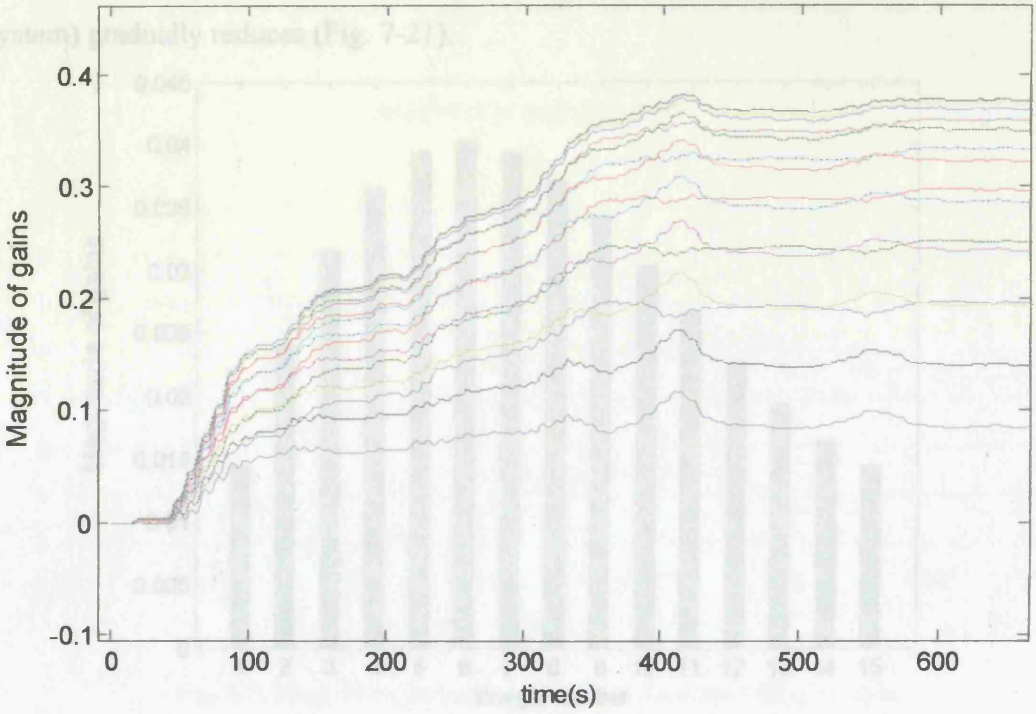

Fig. 7-17 Adaptation of inverse controller's gains with time (L=15 and Δ=8)

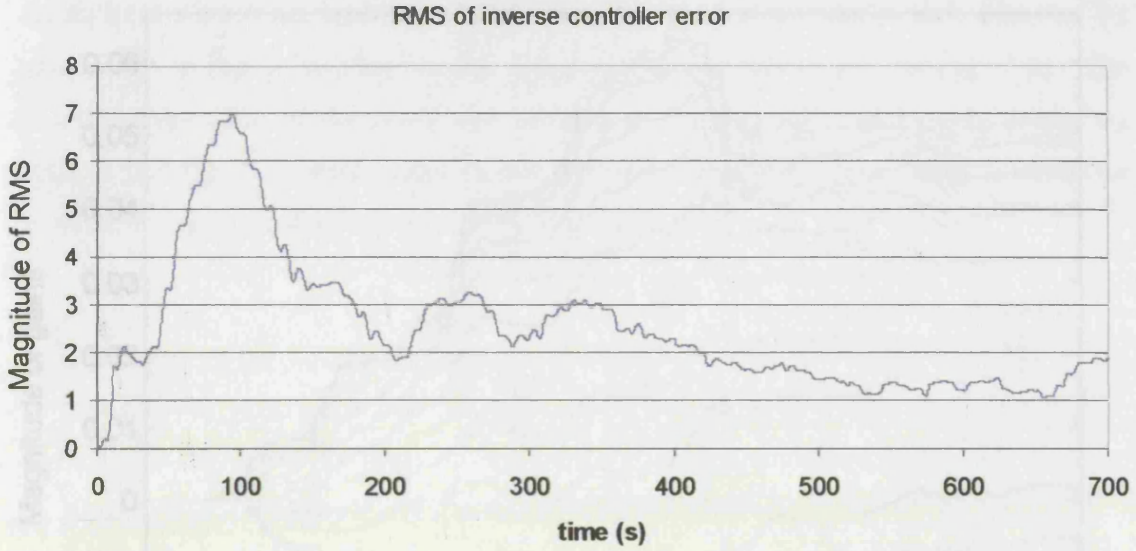

Fig. 7-18 Root Mean Square error of inverse controller modelling vs. time

The gains of the ship-tank model follow the same pattern and settle at their final values (Fig. 7-19) after about 450 seconds after the start of the simulation (Fig. 7-20) and the root mean square of the error (the difference between the actual roll of the ship and roll motion generated at the output of the ship-tank model given the same input as the actual system) gradually reduces (Fig. 7-21).

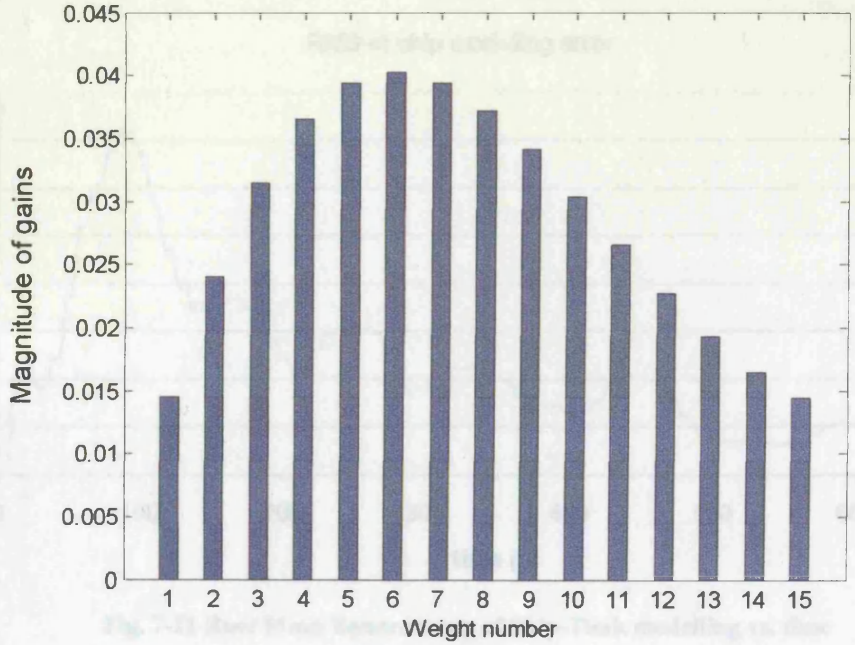

Fig. 7-19 Gains of Ship-Tank model after adaptation (L=15)

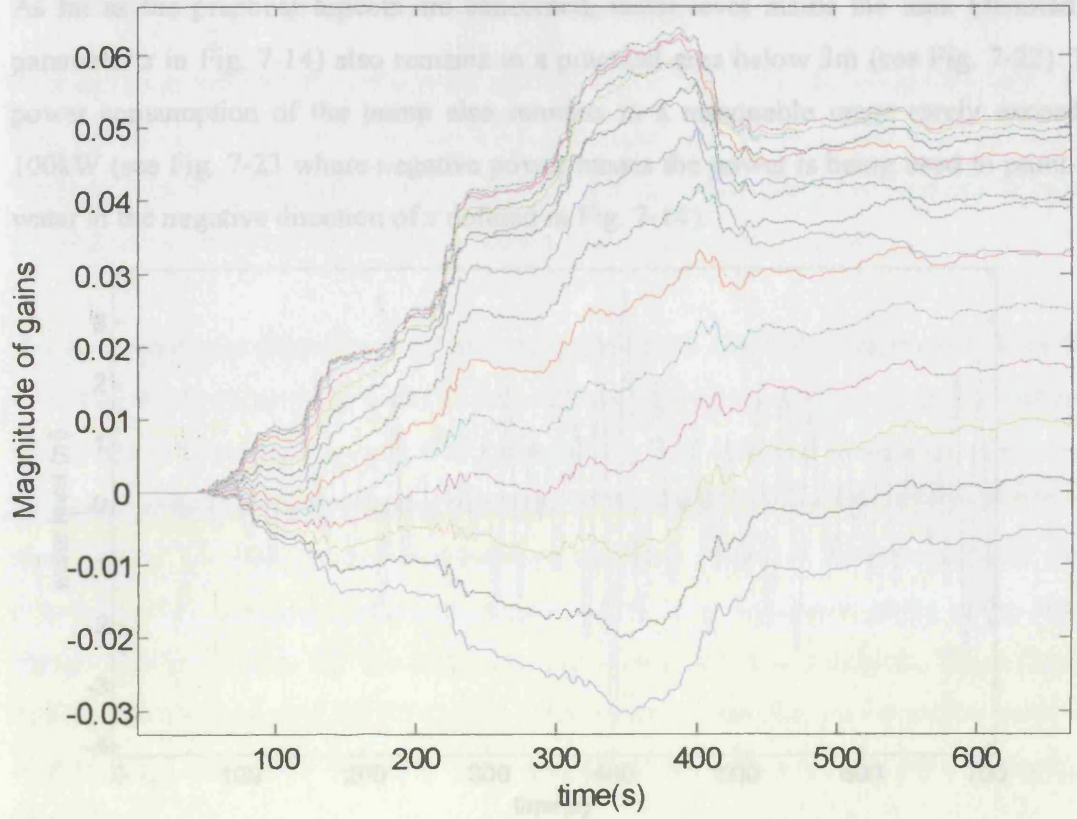

Fig. 7-20 Adaptation of Ship-Tank model's gains with time (L=15)

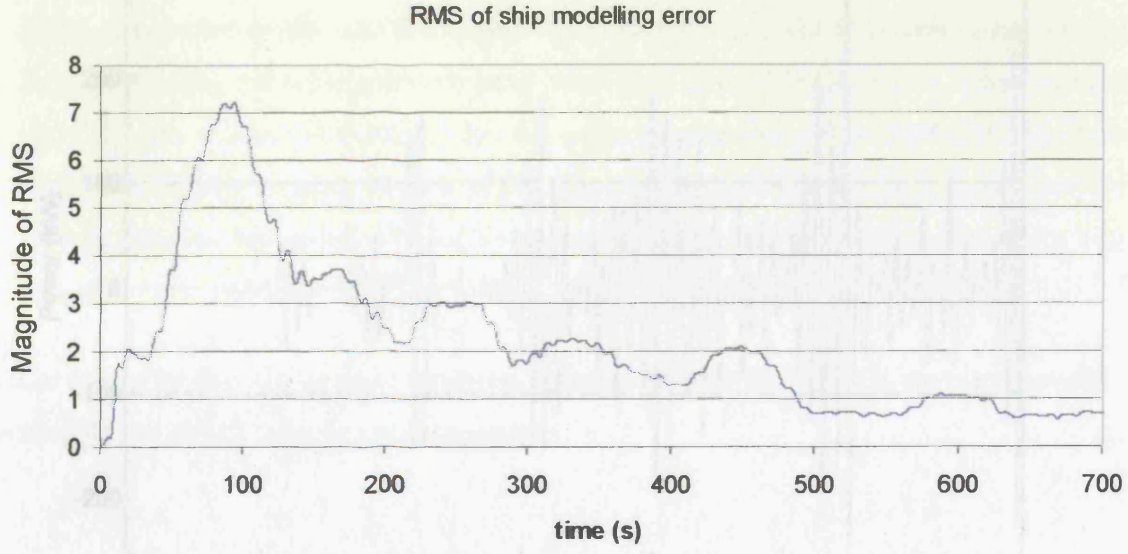

Fig. 7-21 Root Mean Square error of Ship-Tank modelling vs. time

As far as the practical aspects are concerned, water level inside the tank (denoted by parameter z in Fig. 7-14) also remains in a practical area below 3m (see Fig. 7-22). The power consumption of the pump also remains in a reasonable range rarely exceeding 100kW (see Fig. 7-23 where negative power means the power is being used to pump the water in the negative direction of z defined in Fig. 7-14).

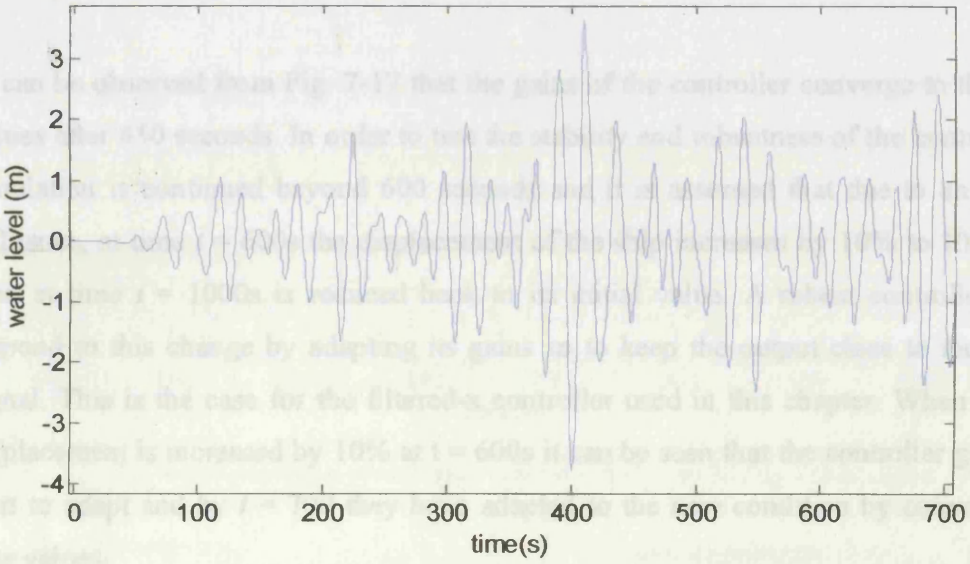

Fig. 7-22 level of water inside the U-tanks from equilibrium

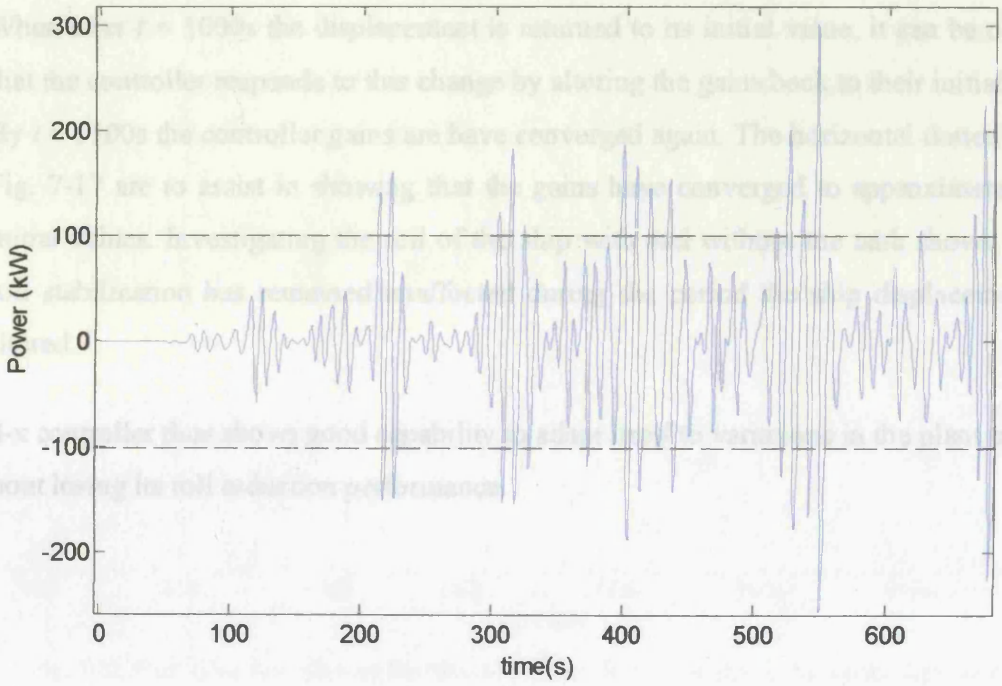

Fig. 7-23 Power consumption of the pump

7.6 Robustness and stability of filtered-x controller

As a test to investigate the robustness and stability of the filtered-x controller, one of the ship's parameters that has effect on the roll motion (say displacement due to change of loading) is assumed to change during normal ship operation due to an external influence, it is then observed how the controller would adapt to the new situation.

It can be observed from Fig. 7-17 that the gains of the controller converge to their final values after 450 seconds. In order to test the stability and robustness of the controller the simulation is continued beyond 600 seconds and it is assumed that due to an external influence, at time t = 600s the displacement of the ship increases by 10% to 10500t and then at time t = 1000s is reduced beck to its initial value. A robust controller would respond to this change by adapting its gains so to keep the output close to the desired signal. This is the case for the filtered-x controller used in this chapter. When the ship displacement is increased by 10% at t = 600s it can be seen that the controller gains also start to adapt and by t = 700 they have adapted to the new condition by converging to new values.

When after t = 1000s the displacement is returned to its initial value, it can be observed that the controller responds to this change by altering the gains back to their initial values. By t = 1100s the controller gains are have converged again. The horizontal dotted lines in Fig. 7-17 are to assist in showing that the gains have converged to approximately their initial values. Investigating the roll of the ship with and without the tank shows that the roll stabilization has remained unaffected during the period the ship displacement was altered.

The filtered-x controller thus shows good capability to adapt itself to variations in the plant transfer function without losing its roll reduction performance.

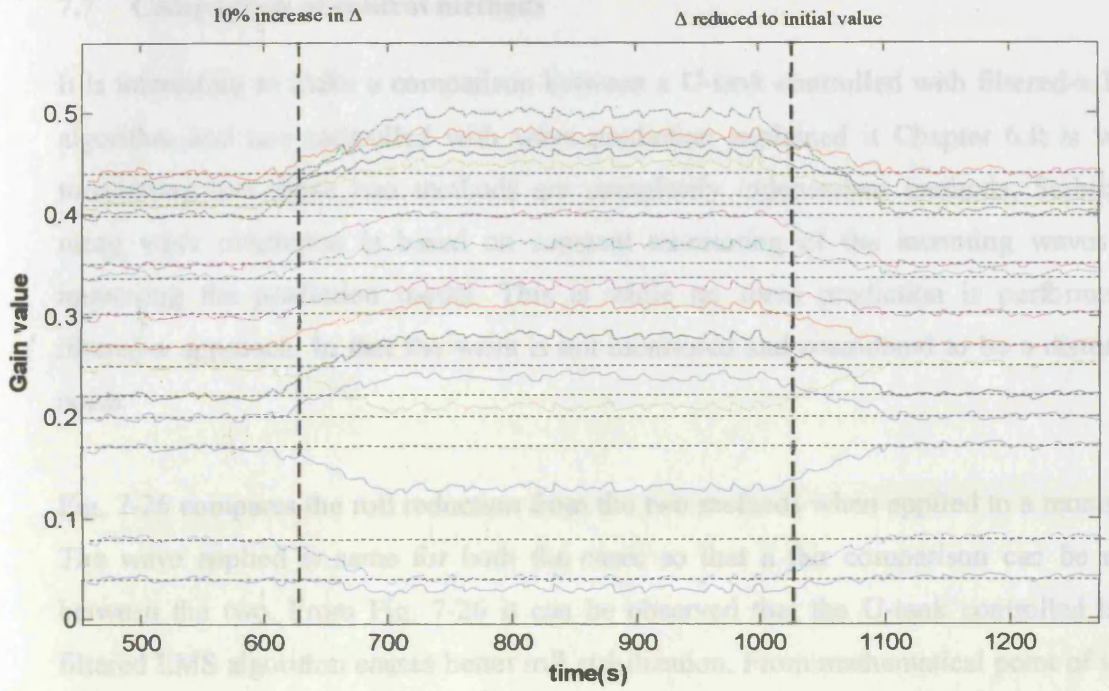

Fig. 7-24 Adaptation of controller gains due to change in ship displacement

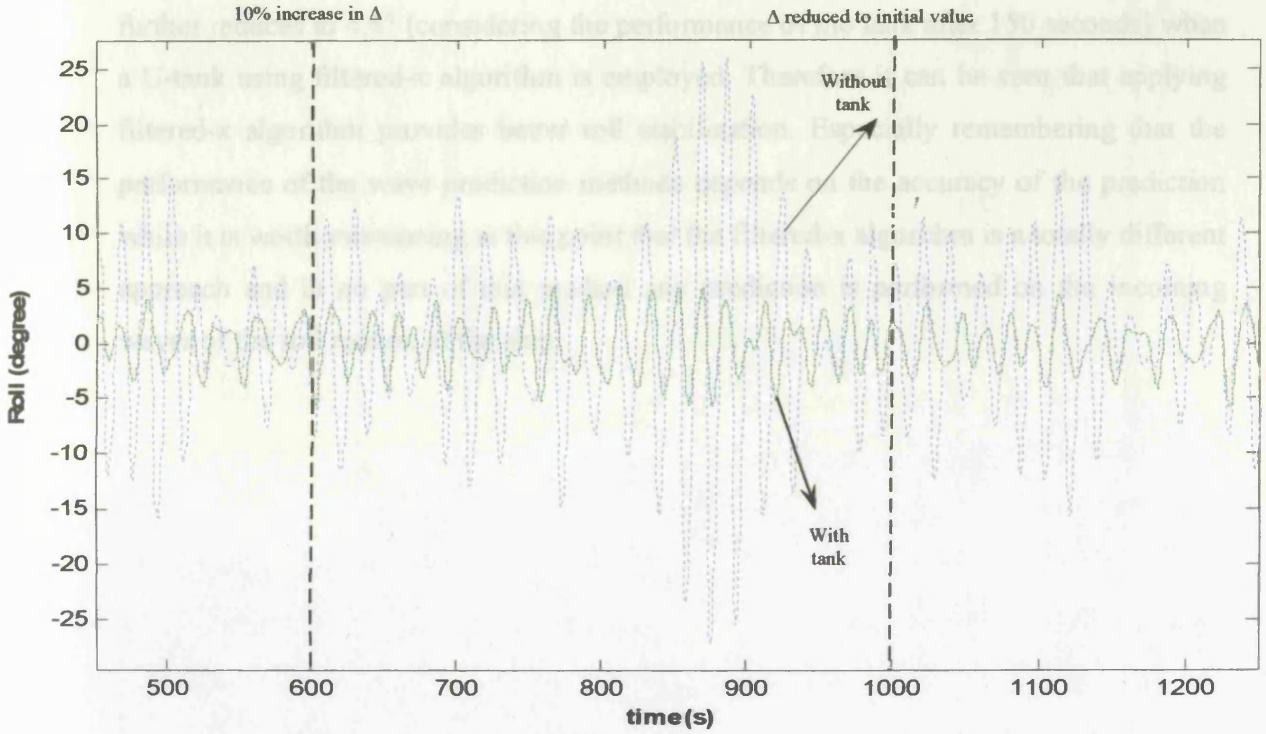

Fig. 7-25 Roll reduction effect of the filtered-x controller when ship's displacement is changed

7.7 Comparison of control methods

It is interesting to make a comparison between a U-tank controlled with filtered-x LMS algorithm and one controlled with wave prediction explained it Chapter 6.It is worth mentioning that these two methods are completely independent methods; Stabilizing using wave prediction is based on constant monitoring of the incoming waves and improving the prediction model. This is while no wave prediction is performed in filtered-x approach. In fact the wave is not monitored and considered to be a disturbing noise.

Fig. 7-26 compares the roll reduction from the two methods when applied to a monohull. The wave applied is same for both the cases so that a fair comparison can be made between the two. From Fig. 7-26 it can be observed that the U-tank controlled by x-filtered LMS algorithm causes better roll stabilization. From mathematical point of view, the ship that has no tanks fitted rolls with root mean square value equal to 12.8°, while the rms for the roll motion of the ship with wave prediction controller drops to 5.3° and further reduces to 4.6° (considering the performance of the tank after 150 seconds) when a U-tank using filtered-x algorithm is employed. Therefore it can be seen that applying filtered-x algorithm provides better roll stabilization. Especially remembering that the performance of the wave prediction methods depends on the accuracy of the prediction while it is worth mentioning at this point that the filtered-x algorithm is a totally different approach and in no part of this method any prediction is performed on the incoming waves or the roll motion of the ship.

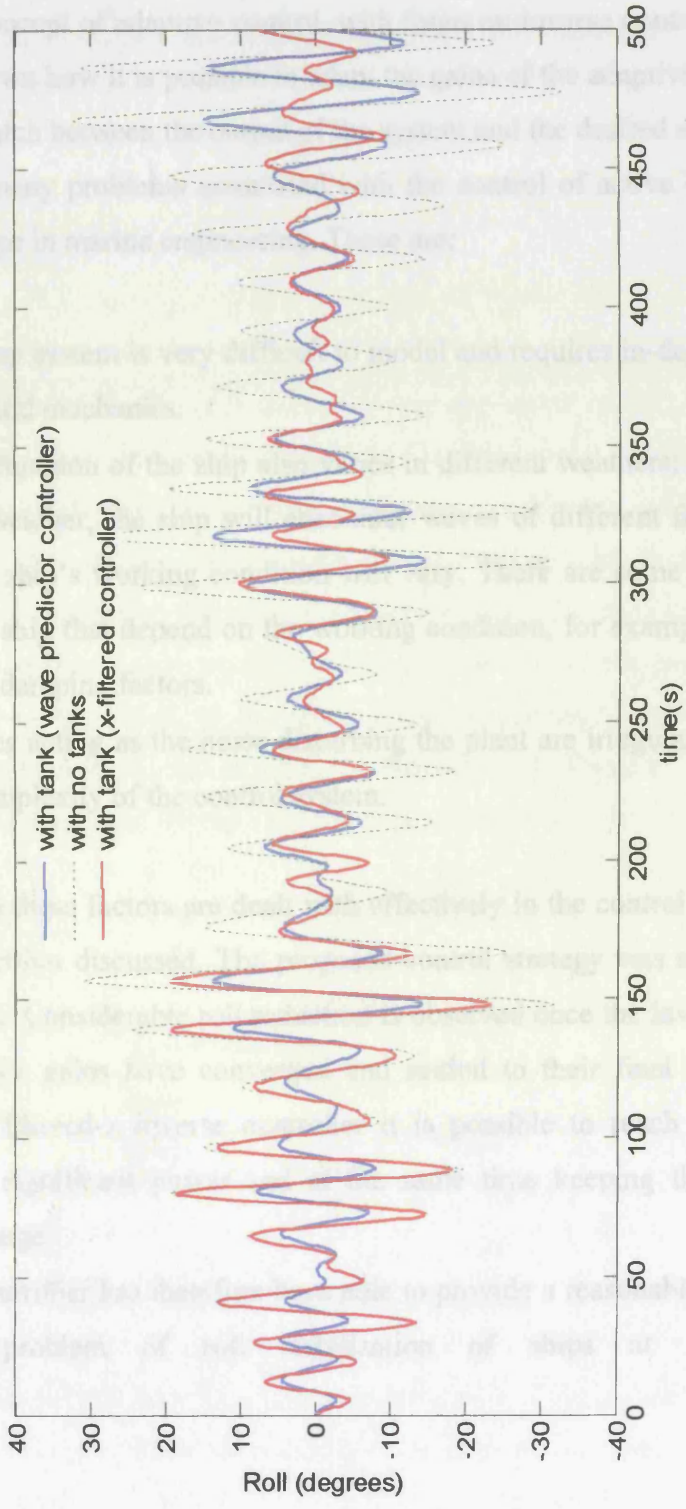

Fig. 7-26 comparison of roll reduction using U-tank applying wave prediction and x-filtered LMS algorithm to control the pumps

7.8 Concluding remarks

In this chapter the concept of adaptive control, with focus on inverse control, was briefly discussed. It was shown how it is possible to adapt the gains of the adaptive filter in order to provide a close match between the output of the system and the desired reference.
However there are many problems associated with the control of active U-tanks which make them a challenge in marine engineering. These are:

- The tank-pump system is very difficult to model and requires in-depth research in the field of fluid mechanics.
- The transfer function of the ship also varies in different weathers; this is because in different weather, the ship will encounter waves of different frequencies and therefore the ship's working condition will vary. There are some hydrodynamic properties of ship that depend on the working condition, for example added mass and different damping factors.
- The sea waves acting as the noise disturbing the plant are irregular in nature and add to the complexity of the control system.

It was shown that all these factors are dealt with effectively in the control strategy using filtered-x LMS algorithm discussed. The proposed control strategy was simulated for a particular ship model. Considerable roll reduction is observed once the inverse controller and ship-tank model's gains have converged and settled to their final values. It was proved that with a filtered-x inverse controller it is possible to reach roll reduction without consuming significant power and at the same time keeping the water level variations at a low range.
Filtered-x inverse controller has therefore been able to provide a reasonable and practical solution to the problem of roll stabilization of ships at slow speeds.

Chapter 8

8 Roll reduction of ships using anti-roll n-tanks

8.1 Introduction

In another configuration of anti-roll tanks, known as "external tanks" or in some cases "free-flooding tanks", a pair of tanks are provided on either side of the vessel and these are open to the sea (Fig. 8-1). The term "external" is in fact a misnomer, as the tanks are an integral part of the ship. The name "free-flooding" is also not suitable for this application because in many occasions the flooding of the water is controlled and forced in one direction rather than being free. Therefore in order to have a more appropriate name, based on their general shape, the name "n-shape" tanks has been used, this is consistent with the previously mentioned U-shape tanks. (The connecting duct of a U-tank is situated at the bottom and forms a U shape while in an n-tank the connecting duct is at the top, resembling the letter "n").

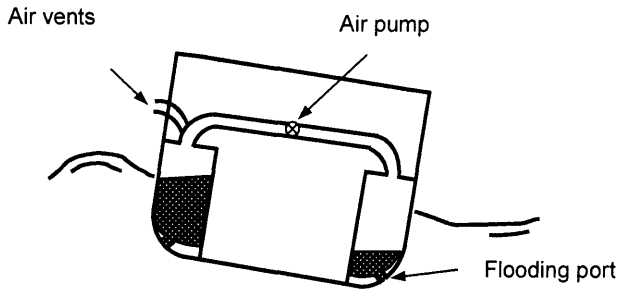

Fig. 8-1 Configuration of passive n-shape tanks

The advantage of n-tanks is that there is no need to move a mass of water athwart ships and so a faster reaction to roll is possible which naturally leads to better roll reduction. A second

advantage of n-tanks is that the removal of the water crossover duct reduces ship impact and so they are a more practical proposition for multi hull craft. The hulls of catamarans or the side hulls of trimarans are ideal spaces for n-tanks. They contain low value space, and are often void. In addition multi hulls usually have greater beams, for trimarans the overall beam is typically 25% to 50% greater than an equivalent monohull of the same displacement. As the beam increases the size of tank decreases to obtain the same restoring moment. Also as the tanks are internal to the hull not only are they less susceptible to hull emergence as external devices such as bilge keels and fins, but also they will still provide a restoring moment when the hull is clear of the water. Moreover, at high speeds where fins have superior performance, the tanks can be emptied and roll stabilization can be achieved by fins alone. This opens up the potential for stabilisation of weight sensitive vessels such as SES at low speeds by n-tanks. For monohulls the tanks also provide additional hull protection, and as the side tanks are controlled independently they can be used to assist with damage control stability. This work is timely as a number of high speed multi hull vessels are now being developed that have a requirement for good sea keeping at slow speeds, for example the US Navy Littoral Combat Ship (LCS). For the LCS tasks where good roll stabilisation is required at low or zero speed include; recovery and launch of boats and unmanned vehicles, MCM operations and cargo transfer in open waters as part of the sea basing concept.

There are some disadvantages of using n-tanks; use of seawater as a working fluid has a considerable impact on the design in terms of corrosion, fouling and maintenance. Modelling of the system is more difficult due to the complex 3D flow systems at the entry port. They also require large flooding ports in the side of the ship to allow the seawater to enter and leave the tanks. As a result of water flowing into and out of the tanks when the ship is underway, momentum drag can ensue, this can be reduced by locking off the system at higher speeds when the tanks become less effective. It is even possible to drain the tanks (especially if they were fitted to an SES when the entrance grills could be lifted clear of the water when on cushion). The commercially available Slo-Rol system uses a similar principle but it relies on compressed air for control of the water levels, and there are no valves at the base of the tank. Slo-Rol systems are in fact a type of free-flooding tanks where air pressure is used to assist in emptying the tanks. It was designed for, and has been installed on, various stationary drilling rigs and vessels used in the oil industry. The tank tops are below the water line so that by venting the tanks they flood completely effectively switching off the system. A disadvantage

of this system is that the tanks must be built and regularly tested to withstand high air pressures.

One of the few cases of installation of free-flooding tanks was in 1931 when tanks were retrofitted to 6 USN cruisers of the *Pensacola* and *Northampton* classes. The tanks had no air cross connection, despite initial misgivings the tanks were successful reducing the roll motion by 30-40% and increasing the roll period by 20%. The active n-tank concept was developed in the early 1960's by Bell and Walker [8], (Fig. 8-2). It is seen that two tanks are provided, one on either side of the vessel and open to the sea. Air at a low pressure is supplied to a pipe connecting the tops of the tanks.

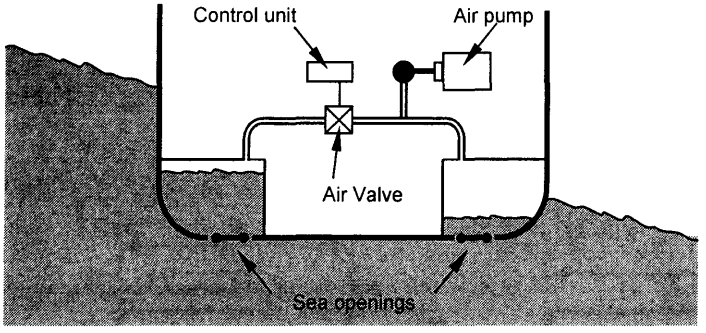

Fig. 8-2 Active n-tank system based on Bell and Walker [8]

If the ship rolls and the valve in the interconnecting air channel is left open, the tank on the lower side will fill with water. At the end of the roll, the valve is closed. This traps the water in the tank and it is then lifted during the next half roll, at the end of which the valve is opened briefly. During this interval water is discharged from one tank and enters the other. The full tank is now in the lower position, and damping of the motion of the vessel occurs as each tank is in turn raised full of water. Results showed that the roll could be reduced by approximately 60% with such a stabilizing system [65].

Some difficulty arises when the vessel is given forward speed; the water tends to enter the tanks and partially fill them, so reducing the efficiency. This can be prevented by fitting guide fins at the entrance to the tanks, which may also be operated by the control in addition

to the valve in the air channel. Potential exists to improve the performance of an n-tank system and three ideas will be briefly developed in the remainder of this chapter.

8.2 Mathematical Modelling of the n-tank

A detailed mathematical model of n-tanks has been developed by Webster [72] in 1988 for the free-flooding tanks which were considered for retrofitting to the aircraft carrier *USS Midway*. A similar method is used here but with some modifications in order to make the mathematical structure of the model suitable for simulations using MATLAB Simulink. Fig. 8-3 shows the side hull of a typical trimaran when the tank is being filled. The flooding port is assumed to be a rectangle at the bottom left hand side of the tank with dimensions $d \times b$. The length of the tank in the fore/after direction is x_t and the width at its top is w_r. In this case the vents on the top of the tank are open to air therefore the pressure of the air inside the tank is assumed to remain at atmospheric.

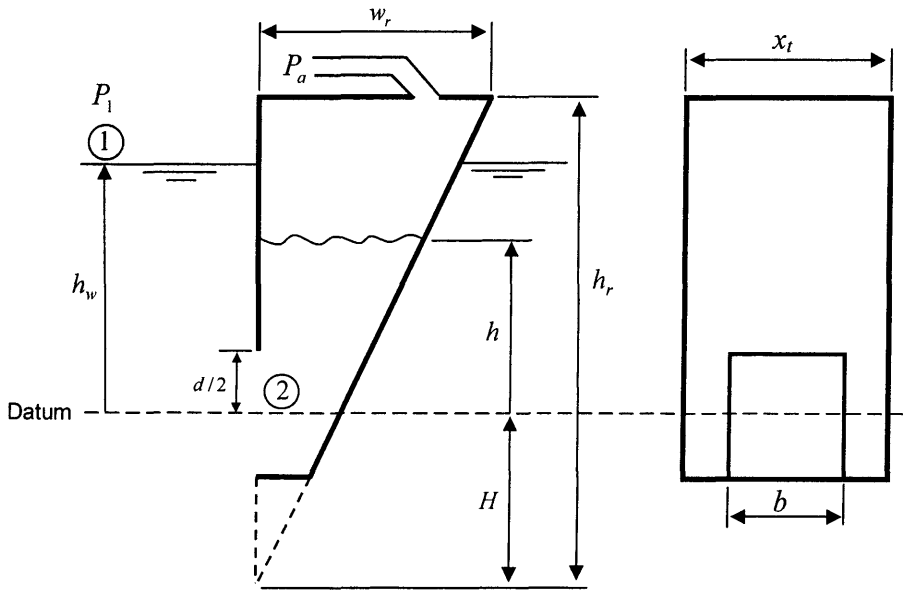

Fig. 8-3 Schematic of the n-tank being filled

At each instant the Bernoulli equation between points 1 and 2 can be expressed as:

$$\frac{P_1}{\rho_1} + \frac{v_1^2}{2} + gh_1 = \frac{P_2}{\rho_2} + \frac{v_2^2}{2} + gh_2 \qquad \textbf{(8-1)}$$

Where P is the hydrostatic pressure of each point v is the mass velocity of the fluid and h the height above some reference height. By setting the datum level so that h_2 is zero and setting point 1 at the external water surface ($P_1 = 0$), assuming constant density and taking the instantaneous value of v_1 as small compared to other significant terms equation (8-1) can be reduced to:

$$gh_w = \frac{P_2}{\rho} + \frac{v_2^2}{2} \tag{8-2}$$

Since the density of water is much greater than air a good approximation of v_2 is given by

$$v_2 = \sqrt{2g(h_w - h)} \tag{8-3}$$

However in the above analysis assumes inviscid flow and the real velocity is considerably smaller than that given by equation 8-3. A better approximation to the actual velocity is obtained by introducing a discharge coefficient, C_d. For a sharp-edged orifice this is usually in the range 0.60 to 0.65

$$v_2 = C_d\sqrt{2g(h_w - h)} \tag{8-4}$$

For a given external water level the volume flow rate into the tank Q_{in} can be considered as a function of the area of the flooding port $d \times b$ and the water velocity v_2 if the orifice is regarded as "small" [41]. In this case the orifice is small when, $|h_w - h| > d$ even outside this condition the absolute errors in flow rate are small as the velocity is low.

$$Q_{in} = C_d bd\sqrt{2g(h_w - h)} \tag{8-5}$$

In order to find an expression for the height of the water inside the tank, it is known that

$$Q_{in} = A\dot{h} \tag{8-6}$$

Where A is the area of the free surface of the water inside the tank at any given time

$$A = (h + H)\left(\frac{w_r}{h_r}\right)x_t \tag{8-7}$$

Therefore;

$$C_d b d\sqrt{2g(h_w - h)} = (h + H)\left(\frac{w_r x_t}{h_r}\right)\frac{dh}{dt} \tag{8-8}$$

Integrating over a time step Δt

$$\int_t^{t+\Delta t} dt = \frac{w_r x_t}{C_d b d h_r \sqrt{2g}} \int_{h_1}^{h_2} \frac{h + H}{\sqrt{(h_w - h)}} dh \tag{8-9}$$

Yields;

$$\Delta t = \left[\frac{-2w_r x_t}{3C_d b d h_r \sqrt{2g}}\left\{(h + 2h_w + 3H)\sqrt{h_w - h}\right\}\right]_{h_1}^{h_2} \tag{8-10}$$

A similar method is applied to derive a model of the tank when it is being emptied. The differences are that the flow direction is reversed and the pressure of the air inside the tank may be increased using a high pressure blower which will decrease the emptying time. This can be easily performed by adding a water pressure head term h' to 8-3 which corresponds to the over pressure in the tank.

$$v_2 = \sqrt{2g(h' + h - h_w)} \tag{8-11}$$

Hence the

$$\Delta t = \left[\frac{2w_r x_t}{3C_d b d h_r \sqrt{2g}}\left\{(h + 2(h_w - h') + 3H)\sqrt{h' + h - h_w}\right\}\right]_{h_1}^{h_2} \tag{8-12}$$

The results are calculated using MATLAB Simulink. h_w is calculated at each time step from knowledge of the incident wave and the roll and heave of the ship and h from knowledge of the tank conditions.

8.3 Simulation and results

Five different situations were considered starting with the base line of a ship with no tanks and then passive n-tanks with fixed inlet ports. This is followed by investigation of adaptive control of the inlet port area, optimising its size for a particular sea condition, but not varying it during a particular roll cycle. Then use of a valve to control the inlet port during a roll cycle. Finally the use of compressed air to assist emptying the tanks is investigated. A 2D (roll and heave) ship dynamic model based on specifications from the trimaran RV Triton, was used, see Table 8-1. This is also "ship 2" from Chapter 6. Note that for a roll angle of greater than 15° side hull emergence is likely. Eight pairs of n-tanks located in the side hulls are considered, each being 1m long. The ship is assumed to have an ahead speed of 2 knots and a heading angle equal to 70°, so chosen as to cause large roll motion.

Centre hull		*Side Hulls*	
Length WL	150m	Length WL	60m
Beam WL	10.80m	Beam WL	1.80m
Draught	6.18m	Draught	3.00m
Overall ship			
Beam	25m		
Displacement	5281t		
GM	1.50m		

Table 8-1 Details of the Trimaran Ship used for the simulations

8.3.1 A fix flooding port (Passive tank)

In this simple configuration the flooding port is assumed to be 70cm square. The simulation was performed on a range of regular sinusoidal incoming sea waves varying in frequency and wave slope. Fig. 8-4 shows the results for the case with wave slope 4°. For other waves slopes the result has approximately the same general shape with a different maximum roll angle. It can be seen that without tanks the ship has a peak response at a frequency just under 0.5rad/s. With the tanks significant roll reduction has been achieved at 0.5rad/s, with moderate reduction at higher frequencies, but below about 0.45rad/s the n-tanks have an adverse effect and increase the roll motion of the ship.

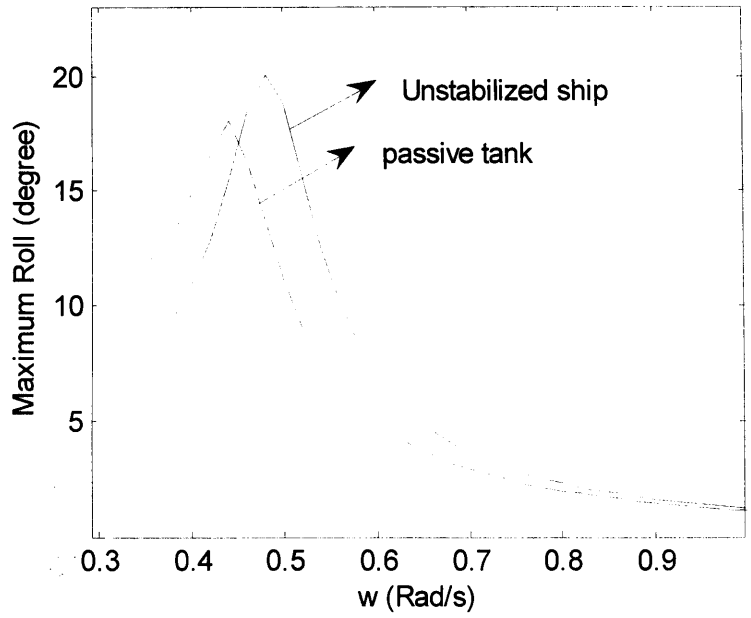

Fig. 8-4 Roll reduction effect of a passive n-tank, wave slope 4°.

8.3.2 Adapting flooding port

The above simulation shows that a fixed area flooding port is not suitable for wave frequencies much less than the ship's natural frequency. In this configuration an adaptive algorithm is used to adjust the width of the flooding port in order to achieve the maximum roll reduction possible. The height of the port, d, is kept constant at 70cm and the width, b, can be varied from 0 to 80cm. Note that the port is tuned to a certain wave encounter frequency and does not continuously vary within a cycle. The block diagram of the control system is shown in Fig. 8-5 and the adaptive algorithm is based on a simple gradient search method.

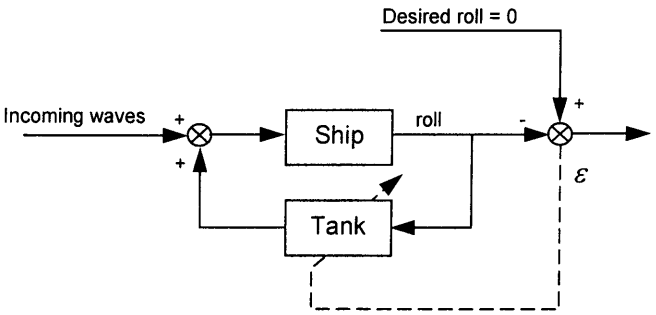

Fig. 8-5 Block diagram of the adaptive control system of the n-tank

If the difference between the desired roll motion (ideally zero) and the ship's actual roll motion is defined by ε, the Mean Square Error (MSE) of ε, is defined as the average of the values of ε^2 over a period of time which can be regarded as the Expectation of ε.

$$\xi = E\left[\varepsilon_k^2\right] \tag{8-13}$$

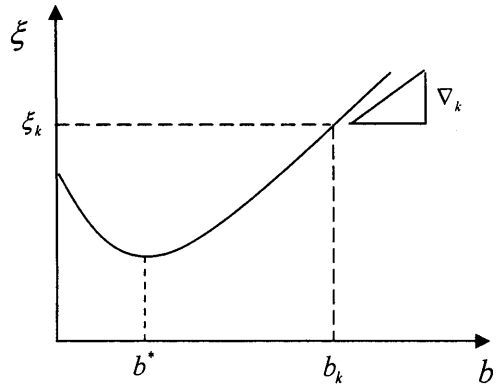

Fig. 8-6 Diagram of MSE vs. the width of the tank port.

Where E is the symbol for Expectation and ξ is the MSE of ε. If ξ is plotted as a function of width of the tank inlet port, b, regardless of the shape of the function, it has a minimum in the range of 0 to 80cm which is the goal of the adaptive algorithm to set the width of the port to this value where the roll motion of the ship becomes minimum, see Fig. 8-7.

The width of the tank at any time, b_k, is derived from:

$$b_{k+1} = b_k - \mu\nabla_k \tag{8-14}$$

Where μ is the adaptation gain and it is the factor that determines the speed of adaptation and ∇_k is the gradient of ξ at each point. As rapid convergence is not an issue in this specific application, it is possible to find an approximation of the gradient of the function from:

$$\nabla_k = \frac{\xi_k - \xi_{k-1}}{b_k - b_{k-1}} \tag{8-15}$$

In summary the adaptive algorithm works as follows. Each time the port of the tank is opened by b_k, the MSE, ξ_k, is calculated by observing the roll motion of the ship over a period of time (say 10 roll cycles). Using (8-15) the gradient of ξ is obtained and inserted into (8-14) to derive the next value of b_k.

The results of the roll reduction are presented in Fig. 8-7. (Different colours do not correspond to particular contours and are automatically generated by the software for better visibility and clarity). Note frequency decreases from left to right. The percentage of roll reduction is defined as the amplitude of roll without the tanks minus the roll amplitude with the tanks divided by the former. The results show that the controller closes the ports when the tanks might worsen the roll response and adapts the port to an optimum width when they can improve it. In this case the optimum width is fully open. Therefore at no instance the roll would be increased.

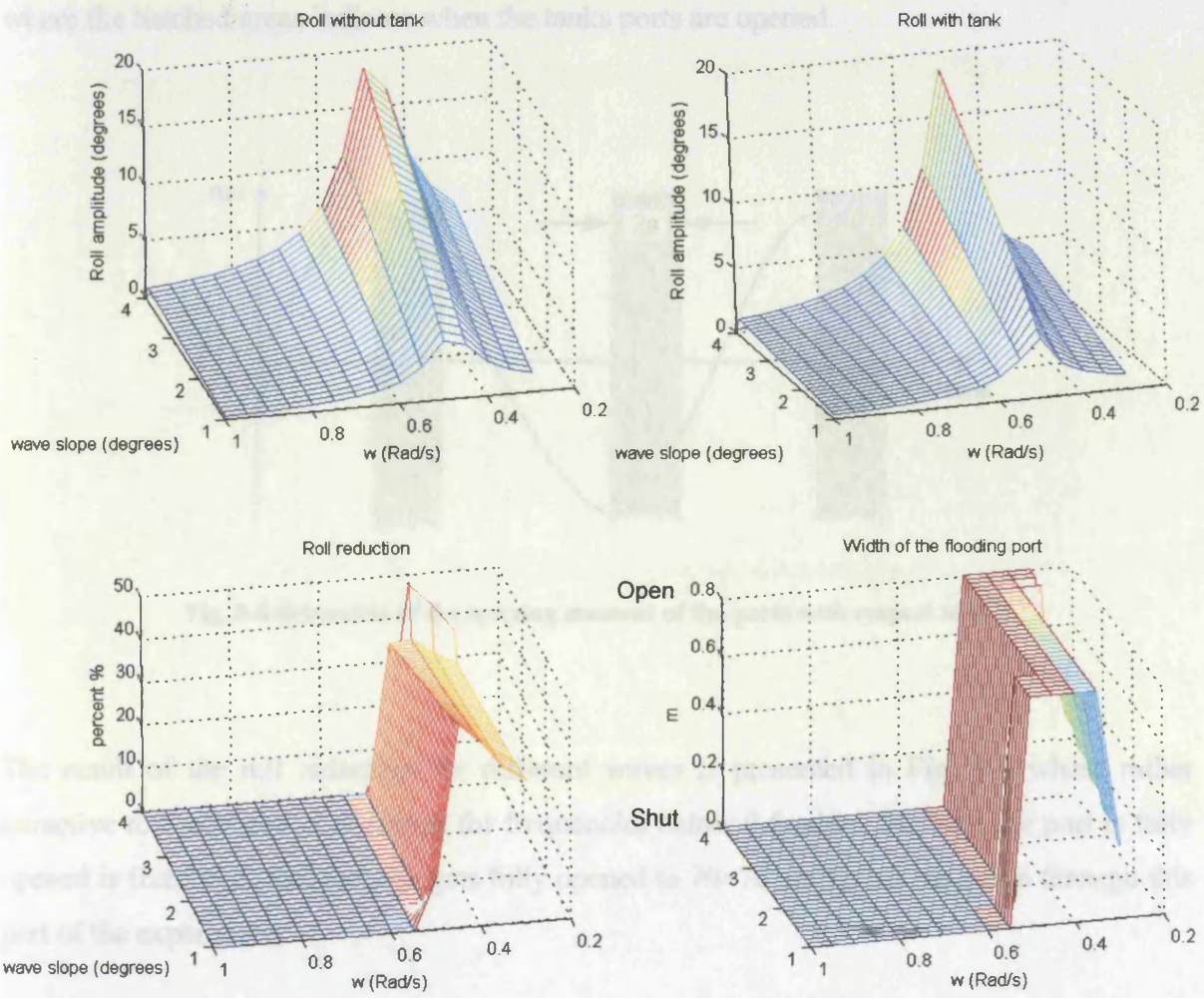

Fig. 8-7 Roll reduction effect of an n-tank with adaptive port

8.3.3 Opening and closing flooding port

The next step is to replace the variable area inlet port with a simpler valve. The flooding port opens and closes according to the roll motion of the ship. Initially the port valve is considered to be closed and the ship level. The ship rolls to starboard and at the moment that the roll reaches its maximum, and the ship starts to roll towards the port, the inlet port is opened and water fills the tank, after 2s the port closes and the water is trapped in the tank. The weight of the water creates a force opposing the roll motion. Half a cycle later, at the moment that the ship reaches its maximum roll to the port side the port opens again for 2s and allows the water to drain, the port closes, and the cycle repeats. The operation of the ports is shown in Fig. 8-8 where the hatched areas indicate when the tanks ports are opened.

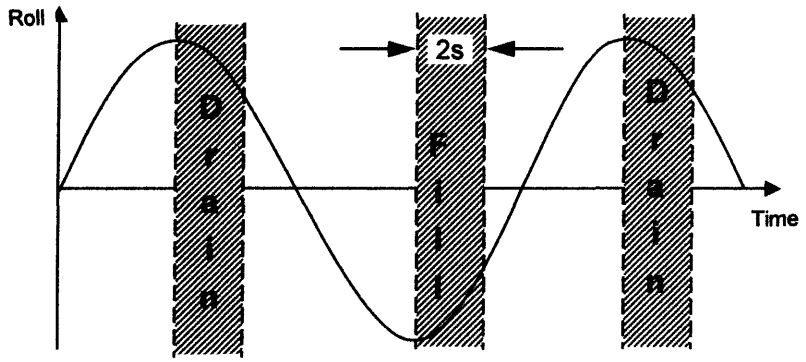

Fig. 8-8 Schematic of the opening moment of the ports with respect to roll

The result of the roll reduction for different waves is presented in Fig. 8-9 where rather attractive roll reduction is observed for frequencies below 0.6rad/s. The time the port is fully opened is fixed at 2s and the port gets fully opened to 70×70 cm for all sea states through this part of the experiment.

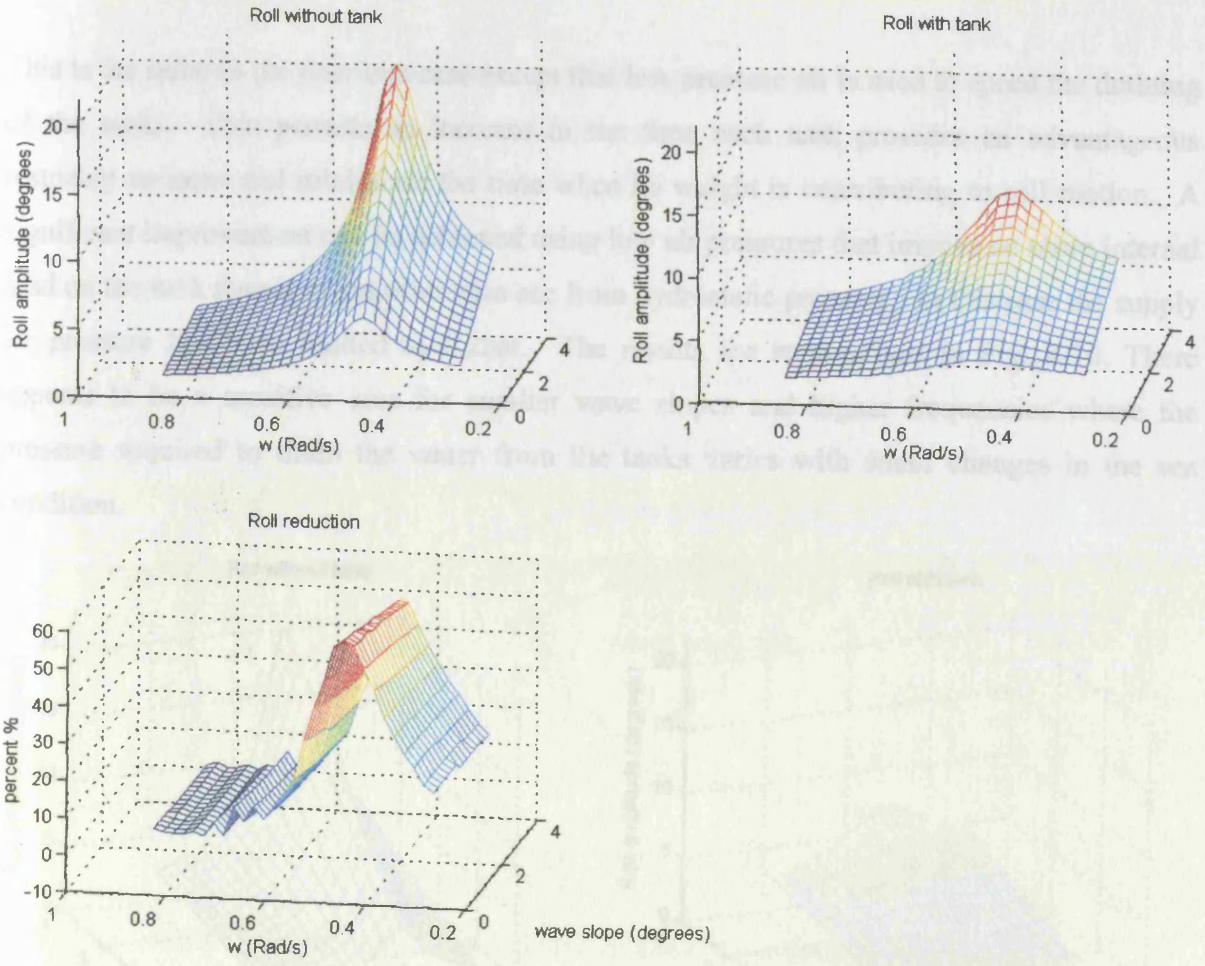

Fig. 8-9 Roll reduction effect of an n-tank with closing port

8.3.4 Closing flooding port with a blower

This is the same as the previous case except that low pressure air is used to speed the draining of the tanks. This permits an increase in the time each tank provides an advantageous restoring moment and minimises the time when its weight is contributing to roll motion. A significant improvement can be achieved using low air pressures that impose no more internal load on the tank than it might otherwise see from hydrostatic pressure. In this case the supply air pressure has been limited to 0.2bar. The results are summarised in Fig. 8-10. There appears to be a sensitive area for smaller wave slopes and higher frequencies where the pressure required to drain the water from the tanks varies with small changes in the sea condition.

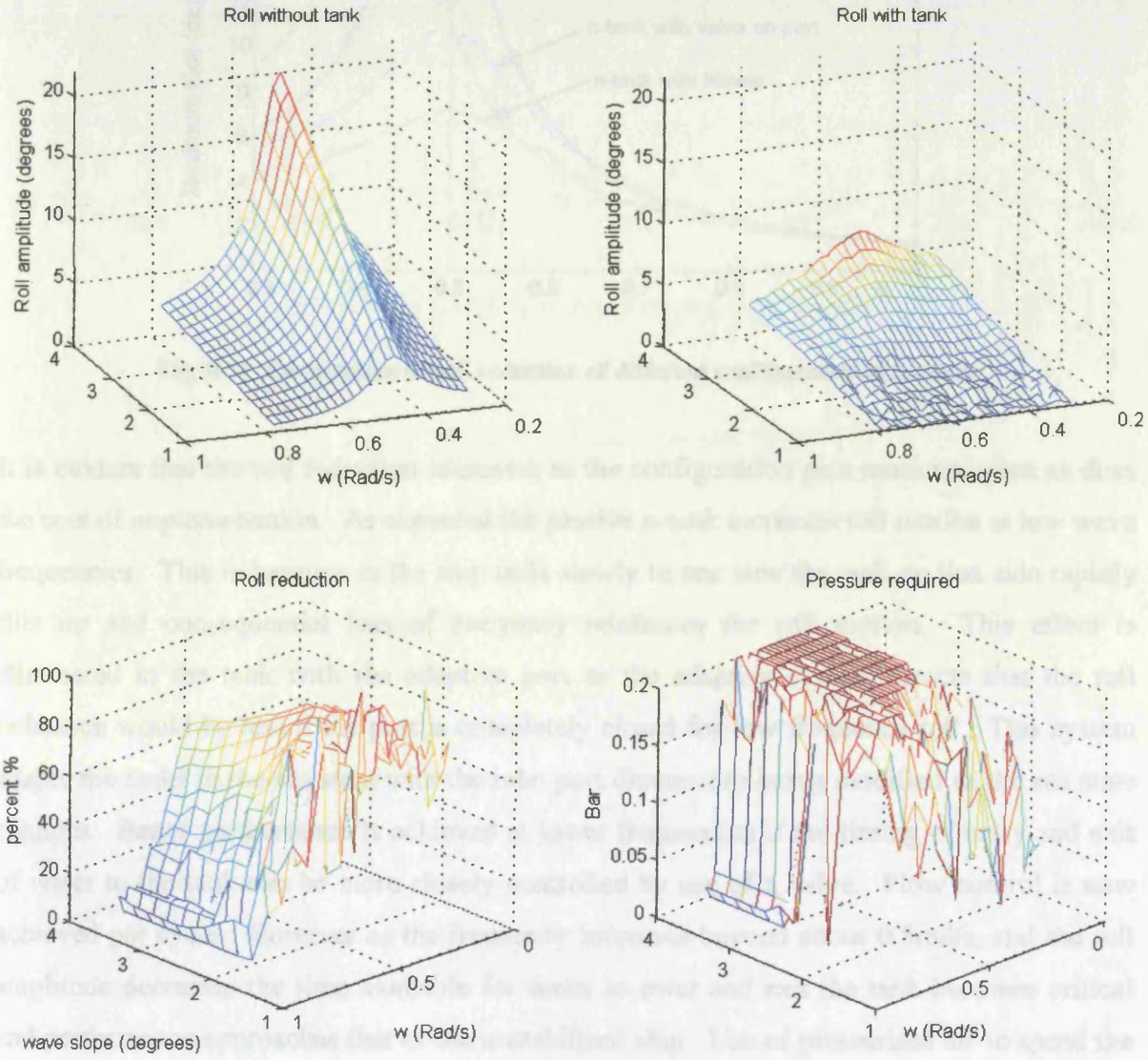

Fig. 8-10 Roll reduction effect of an n-tank with assistance of a blower and the pressure required

8.4 Summary

In order to compare the effect of different tank configurations in a similar wave condition the simulated ship is excited by a regular sinusoidal wave with wave slope of 4°, the results are presented in Fig. 8-11.

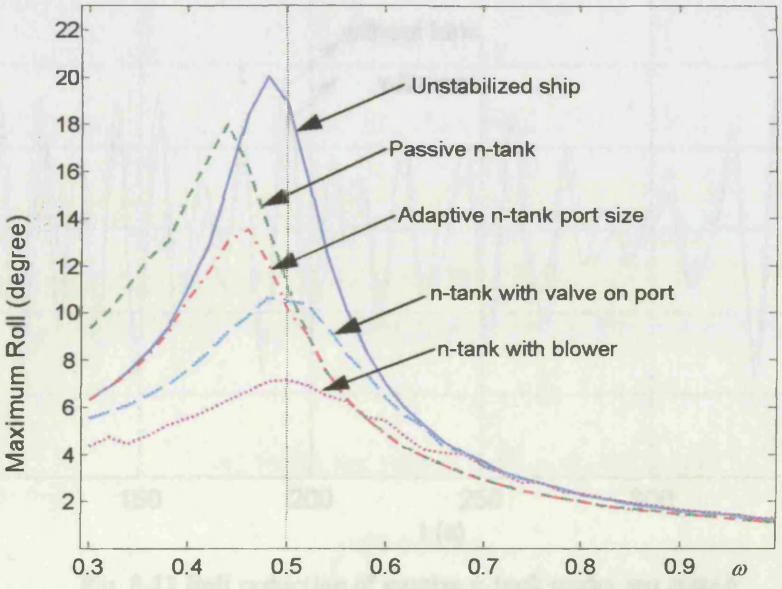

Fig. 8-11 Comparison of roll reduction of different configuration of n-tanks

It is evident that the roll reduction increases as the configuration gets more complex as does the cost of implementation. As expected the passive n-tank increases roll motion at low wave frequencies. This is because as the ship rolls slowly to one side the tank on that side rapidly fills up and consequential loss of buoyancy reinforces the roll motion. This effect is eliminated in the tank with the adaptive port as the adaptive system detects that the roll reduction would be less if the port is completely closed for low frequency roll. This system adapts the tanks to the sea state with the inlet port dimensions being modified as the sea state changes. Better performance is achieved at lower frequencies if the timing of entry and exit of water to the tank can be more closely controlled by use of a valve. Flow control is now achieved per cycle. However as the frequency increases beyond about 0.5rad/s, and the roll amplitude decreases the time available for water to enter and exit the tank becomes critical and performance approaches that of the unstabilized ship. Use of pressurised air to speed the draining of the tanks clearly improves the performance but at a cost of increased complexity and power.

It was also desirable to investigate whether the relative performance of the tanks is the same when the waves are not regular sine waves but irregular sea waves. The results of the simulation are presented in Fig. 8-12 to Fig. 8-15 for the above mentioned ship experiencing sea state 6.

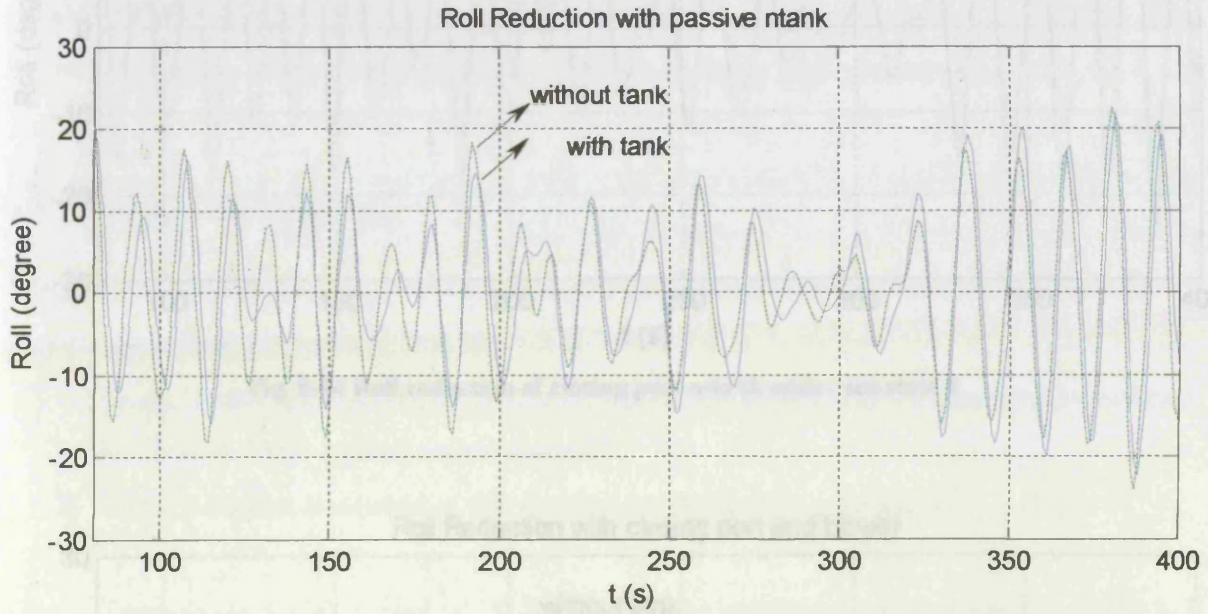

Fig. 8-12 Roll reduction of passive n-tank under sea state 6

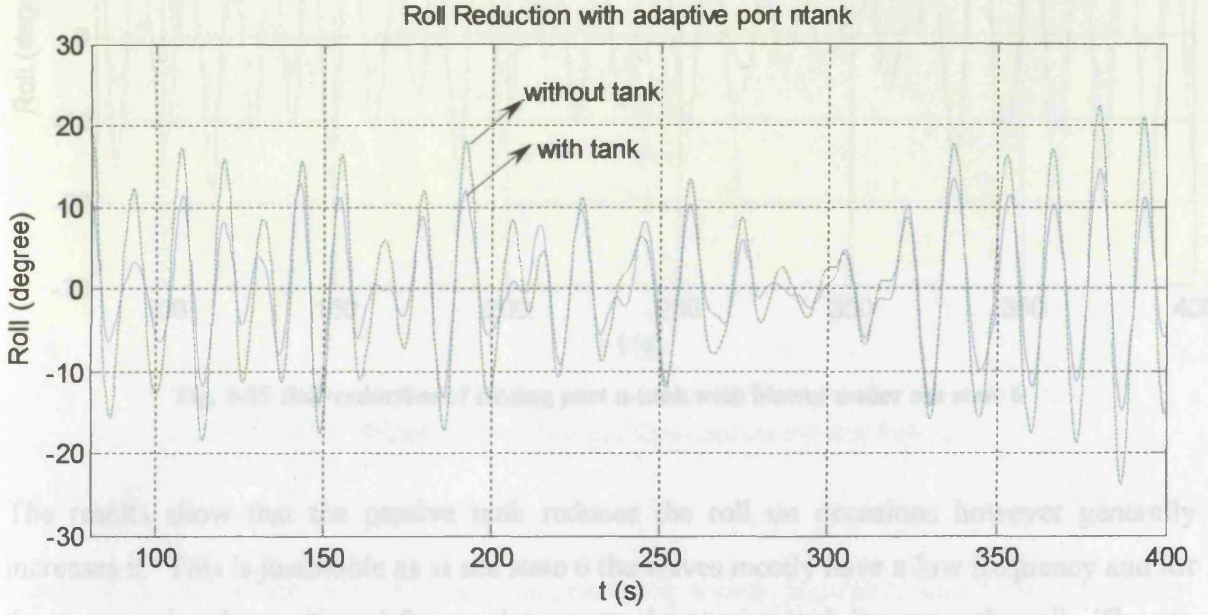

Fig. 8-13 Roll reduction of adaptive port n-tank under sea state 6

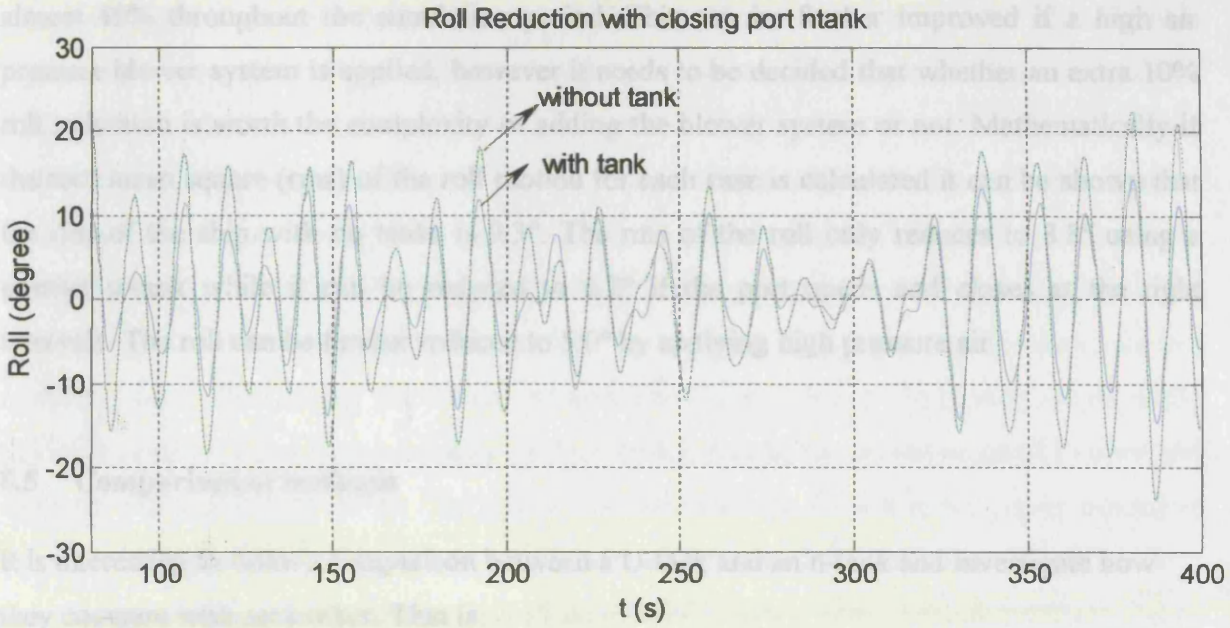

Fig. 8-14 Roll reduction of closing port n-tank under sea state 6

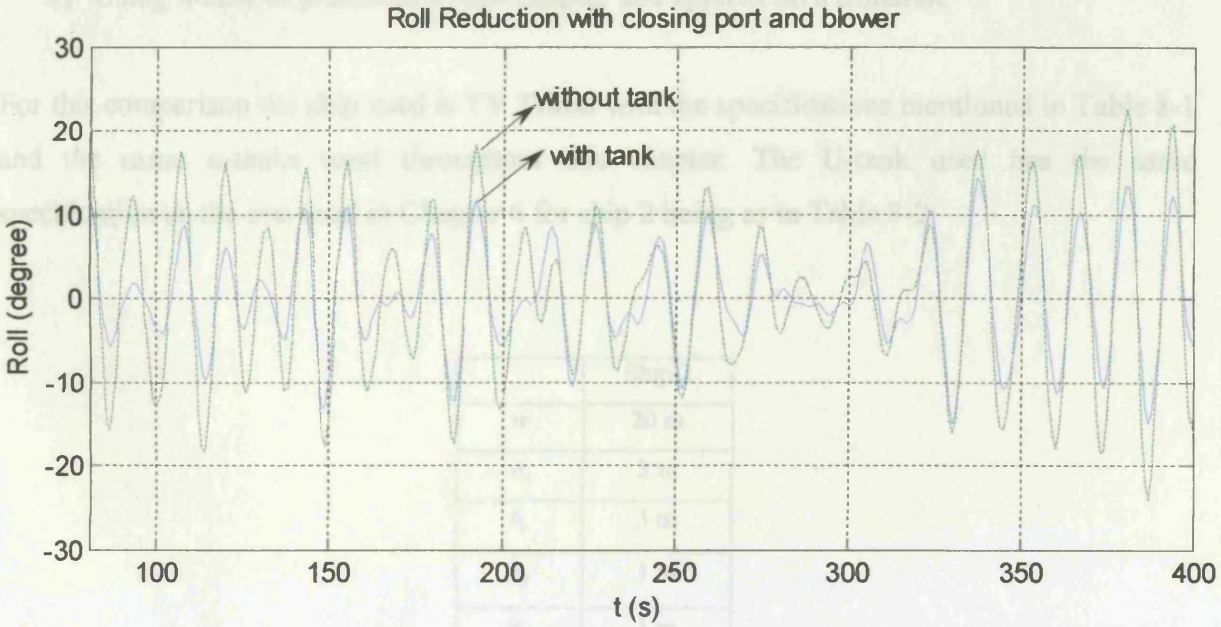

Fig. 8-15 Roll reduction of closing port n-tank with blower under sea state 6

The results show that the passive tank reduces the roll on occasions however generally increases it. This is justifiable as at sea state 6 the waves mostly have a low frequency and for the reasons already mentioned for regular waves, the passive tank increases the roll. The use of the adaptive system to identify the best dimensions for the port shows no further improvement. The results of the tank with closing port show an attractive roll reduction of

almost 40% throughout the simulation period. This can be further improved if a high air pressure blower system is applied, however it needs to be decided that whether an extra 10% roll reduction is worth the complexity of adding the blower system or not. Mathematically if the root mean square (rms) of the roll motion for each case is calculated it can be shown that the rms of the ship with no tanks is 9.3°. The rms of the roll only reduces to 8.8° using a passive n-tank while it can be reduced to 6.2° if the port opens and closes at the right intervals. The roll can be further reduced to 5.0° by applying high pressure air.

8.5 Comparison of methods

It is interesting to make a comparison between a U-tank and an n-tank and investigate how they compare with each other. That is:

1) Using U-tank and applying x-filtered LMS algorithm to control the pumps (introduced in Chapter 7 and applied on a monohull).
2) Using n-tank as presented in this chapter and applied on a trimaran.

For this comparison the ship used is TV Triton with the specifications mentioned in Table 8-1 and the same n-tanks used throughout this chapter. The U-tank used has the same specification as the one used in Chapter 6 for ship 2 being as in Table 8-2:

	Ship 2
w	20 m
w_r	3 m
h_r	3 m
h_d	1 m
x_t	2 m

Table 8-2 Details of the Trimaran Ship used for the simulations

Fig. 8-16 compares the roll reduction caused using n-tank approach, and U-tank applying x-filtered algorithm to control the pumps. The ship used here is the same trimaran used in this chapter. The wave applied to it is also the same for both the n-tank and U-tank so that a fair comparison can be made between the two. From Fig. 8-16 it can be observed that the U-tank

controlled by x-filtered LMS algorithm causes better roll stabilization. From a mathematical point of view, the ship that has no tanks fitted rolls with root mean square value equal to 5.4° degrees, while the rms for the roll motion of the ship with n-tanks drops to 3.6° and further reduces to 3.0° when a U-tank using filtered-x algorithm is employed. On the other hand n-tank has the advantage that usually on a trimaran the geometry of the hull precludes the use of U-tanks. In the very early design stages there needs to be space provided for the tanks and the connecting duct. However n-tanks can be added to a ship at later stages and use the space that is usually empty. Moreover, the power consumed by the n-tank and the U-tank are of totally different order; the power consumption of the n-tank is mostly the power required to open and close the incoming water ports. The power consumption of a U-tank is the power needed to pump few meters of water in a second and obviously of a much higher value. Therefore there is a choice to be made between a better roll stabilization, power consumption and convenience of implementation.

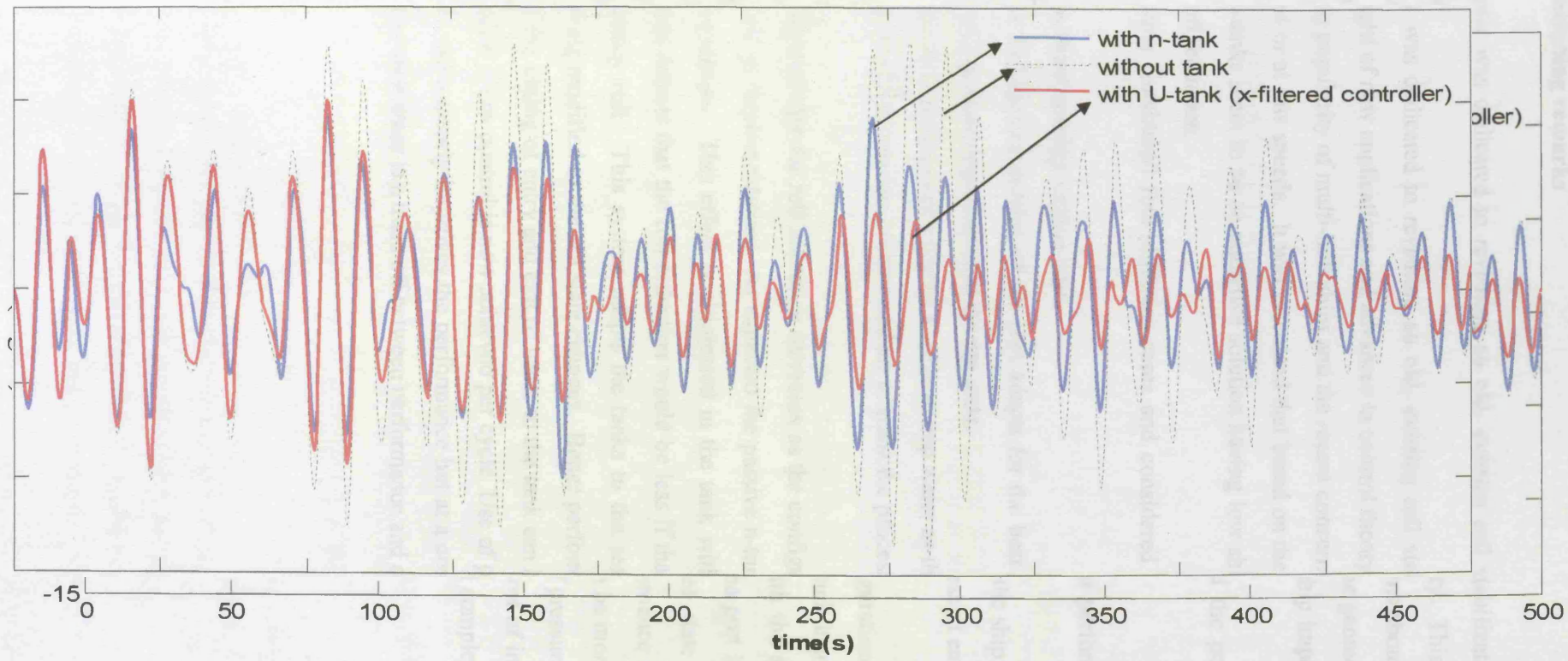

Fig. 8-16 comparison of roll reduction using n-tank and U-tank applying wave prediction for pump control

8.6 Concluding remarks

This chapter was dedicated to revisiting an old, existing roll stabilization system, namely n-tanks, in light of new applications and advances in control theory. This was encouraged by the increasing popularity of multi-hull ships and the recent concerns about their roll reduction when stopped or at low speeds. It was discussed that based on the geometric shape of multi-hull ships, n-tanks seem to be an attractive solution having low ship impact and potential for significant roll reduction.

The simulations considered four different cases and considered the powering and control issues:

a) n-tank with fixed opening section port.

b) n-tank that the opening section of the port adapts for the best performance based on the frequency of the incoming waves and the sea state.

c) n-tank where the opening port includes a valve to trap water as the ship rolls.

d) n-tank that uses high pressure compressed air to assist the process of emptying the tanks.

Simulations showed that the roll reduction increases as the configuration gets more complex as does the cost of implementation. As expected the passive n-tank increases roll motion at low wave frequencies. This effect is eliminated in the tank with the adaptive port as the adaptive system detects that the roll reduction would be less if the port is completely closed for low frequency roll. This system adapts the tanks to the sea state with the inlet port dimensions being modified as the sea state changes. Better performance is achieved at lower frequencies if the timing of entry and exit of water to the tank can be more closely controlled by use of a valve. Flow control is now achieved per cycle. Use of pressurised air to speed the draining of the tanks clearly improves the performance but at a cost of increased complexity and power. However there is a trade off between performance and complexity.

Chapter 9

9 Discussion and further work

The undeniable benefits of a stable ship platform would raise interest in any research performed in the area of roll stabilization. There is also particular interest in roll stabilization of ships at slow or zero speed (such as MCMs, FPSO vessels, ships during launching or recovering boats or loads, cable layers, and survey ships) where fin stabilizers that work well at higher speeds lose their efficiency.

This project was dedicated to the idea of improving the performance of anti-roll tanks as a substitute for fins at slow or zero speed. In the literature review in Chapter 2 it was shown that during the development of tank stabilizing systems the weak link in most systems was the control system. While the ideas of the 19th and early to mid 20th Centuries were sound the technology to implement them was not available, only now with advanced control theory and high speed computing power can the potential of some of these systems be exploited. The idea of using a pump to push the water in the right direction is not new and goes well back to 1920s. However, because of the limitations in the automatic control theory at that time the pumps were controlled by a simple feedback controller that was shown to be inappropriate for this application.

It seemed that there was a need for a thorough investigation in the domain of anti-roll tanks to apply the current advanced technological and computational techniques to some older ideas that could not be explored in the past because of those limitations. This PhD project was dedicated to developing older ideas that could not be practically realized before by applying

modern control methods. It also developed some new techniques which can solve the problem of roll stabilization at slow speeds.

The original approaches conducted in this PhD project can be categorized in three major parts:

9.1 Active U-tank using wave prediction algorithm

It was discussed in Chapter 6 that the difficulty for the control system of active U-tanks is that tank stabilizers depend for their action on the displacement of water with relation to the centre line of the vessel and therefore cannot be made to respond simultaneously to a signal demanding a stabilizing moment, since time is required to move the water from one position to another. This means that if the sensor detects that the ship has rolled to starboard, the control system commands the pump to force the water to the port. However as it takes a few seconds to do so, by the time the water is pumped to the port the ship might herself be rolling to the port too which means that not only has the tank not stabilized the roll but also has increased the roll.

As a solution a new control method was introduced in Chapter 6 which was based on predicting the incoming waves. Using a wave height meter the moment created by the waves is monitored and recorded over a period of time and an auto regressive (AR) model of the waves is created which has the ability to predict the incoming waves for a few seconds ahead. Details of the prediction method were explained in Chapter 4. The prediction time is based on the time required for the pump to move the water inside the tank to the desired position. This predicted wave is in fact the cause of the ship's roll motion and therefore it is the goal of the control system to counteract this moment. In other words the predicted wave is used as the set point of the controller and the water in the tank is pumped in such a manner to create an opposite moment equal to the predicted wave therefore by the end of the predicted time that the wave reaches the ship the stabilizing moment is already created and counteracts the wave. Simulation results for both a trimaran model and a monohull model show that reasonable roll reduction can be achieved over a wide range of frequencies, wave slopes, and sea states using a tank-pump system. Roll reduction is particularly significant for low frequency waves where the pump is given enough time to pump the water to the desired side which makes the active

tank an attractive roll stabilizer for rough weather and higher sea states where the waves have longer periods.

The power consumption of the pumps remains in a reasonable range which shows that active anti-roll tanks need not be power hungry pieces of machinery, but rather feasible stabilizers capable of reducing the undesirable roll motion in situations that other stabilizers have little or no efficiency. On the other hand it was shown that using a high pressure blower instead of the pump does not offer much more roll reduction than a passive tank and therefore does not seem to be an attractive solution.

The accuracy of this method depends on the accuracy of the wave prediction. Any future work regarding methods to gather reliable information about the incoming waves can greatly improve the efficiency of this method. This can be done with better systems of monitoring the sea waves around the ship using radars or other vision methods.

9.2 Active U-tank using Least Mean Square algorithm

There are many problems associated with the control of active U-tanks which make them a challenge in marine engineering. These are difficulties involved in the modelling of ship-tank system in addition to the irregular nature of the sea waves acting as the noise disturbing the plant adding to the complexity of the control system.

As a solution adaptive controllers are utilized that are designed in a way to compensate for the above mentioned changes in the system. An adaptive controller is usually in the form of a transverse filter discussed in Chapter 3. The goal of the controller is to minimize the roll in the mean-square sense by altering the filter gains to some optimum values. The methods discussed in Chapter 3 for optimizing the gains of a transverse filter are applied in Chapter 7. In particular, the nature of the problems discussed above seems to be in good harmony with the philosophy of inverse control using filtered-x least mean square.

The proposed control strategy was simulated for a particular ship model. Considerable roll reduction was observed once the inverse controller and ship-tank model's gains have converged and settled to their final values. It was proved that with a filtered-x inverse

controller it is possible to reach roll reduction without consuming significant power and at the same time keeping the water level variations within the tank at a low range. Filtered-x inverse controller has therefore been able to provide a reasonable, affordable and practical solution to the problem of roll stabilization of ships at slow speeds.

9.3 Using n-tank for roll stabilization of multihulls

Recent developments of multihulls, including trimarans, on a commercial scale has raised the issue of their roll stabilization. This becomes further challenging noting that the hull geometry of some multihulls may preclude the application of conventional U-tanks. It is therefore not surprising that at the 1999 RINA Trimaran conference, slow speed roll stabilization was identified as a key issue in the design and assessment of Trimaran FSCs [57].

As an original approach a new configuration of tanks called n-tank by the author was suggested in Chapter 8 where parts of the side hulls is used as a means of roll stabilization using the sea water. The port and starboard legs are open to the sea and there is no internal water connection between the two tanks but there may be an air connection at the top of the tanks. These tanks are named "n-shape" tanks in this thesis, this is consistent with the previously mentioned U-shape tanks. (The connecting duct of a U-tank is situated at the bottom and forms a U shape while in an n-tank the connecting duct is at the top, resembling the letter "n"). The simulations considered four different cases and considered the powering and control issues:

a) n-tank with fixed opening section port.
b) n-tank that the opening section of the port adapts for the best performance based on the frequency of the incoming waves and the sea state.
c) n-tank where the opening port includes a valve to trap water as the ship rolls.
d) n-tank that uses compressed air to assist the process of emptying the tanks.

The conclusion drawn was that the roll reduction increases as the configuration gets more complex as does the cost of implementation. As expected the passive n-tank increases roll motion at low wave frequencies. This is because as the ship rolls slowly to one side the tank on that side rapidly fills up and consequential loss of buoyancy reinforces the roll motion. This effect is eliminated in the tank with the adaptive port as the adaptive system detects that

the roll reduction would be less if the port is completely closed for low frequency roll. This system adapts the tanks to the sea state with the inlet port dimensions being modified as the sea state changes. Better performance is achieved at lower frequencies if the timing of entry and exit of water to the tank can be more closely controlled by use of a valve. Flow control is now achieved per cycle. However as the frequency increases beyond about 0.5rad/s, and the roll amplitude decreases the time available for water to enter and exit the tank becomes critical and performance approaches that of the unstabilized ship. Use of pressurized air to speed the draining of the tanks clearly improves the performance but at a cost of increased complexity and power.

Although the modelling and equations derived in this thesis considered the coupling effect of roll with other degrees of freedom, based on the data available to the author, the above mentioned methods were simulated for a ship having roll motion only using both regular and irregular sea waves for a range of sea states. Limited data was available to the author to perform the simulations. Most of the hydrodynamic coefficients of the ships used in this study were derived from the available parameters and could therefore lack accuracy. Further more no data was available about the ships which had had an anti-roll tank installed on them, meaning a comparison between the techniques presented in this study could not be possible. If further data (especially more hydrodynamic parameters) about the ship can be accessed it would be possible to test the control algorithms when considering the coupling motion of roll with heave and yaw. It can then be investigated whether applying more than one tank on the ship can further decrease the roll. It can also be interesting to see whether the techniques can be applied to damp other ship motions such as heave and pitch.

The fluid modelling of the tanks was also performed with some assumptions and simplifications. Some of these simplifications included the small angle approximations, neglecting the head loss in the corner of the U-tank, the effect of probable vortexes created, etc. Probably a more detailed modelling of the tanks would assist in further understanding of the behaviour of tanks and their effect in roll stabilization.

The performance of all these methods must inevitably be investigated experimentally using a small model which would finally lead to full scale experiment. There are other problems associated with the small scale modelling as well; the viscous forces dominate the inertia forces as the model gets smaller. In a full scale system however, considering the motion of

high amount of water inside the tank, the situation could be the opposite. Therefore the modelling process needs to be done considering this point.

9.4 Conclusions

The major aim of this thesis was to apply new control theories to the existing idea of anti-roll tanks which had been shown historically to suffer from the lack of an effective control system. It was shown during the literature review that the weak link in the development of anti-roll tanks is in fact their pump controllers. The controllers applied through the years have all been feedback controllers. It was shown during this study that although it might be possible to control the pumps of anti-roll tanks with a feedback controller, this is not the most efficient way of doing so. The nature of the particular application of roll stabilization using anti-roll tanks is more in harmony with feedforward control: the controller must lead the excitation. It was shown that the weakness of the controllers used for roll stabilization of anti-roll tanks lied in the philosophy and the point of view towards this challenging control problem. Once the problem is looked at from a different angle, it could be controlled much more effectively. Both the control strategies introduced and developed in this thesis (1- using wave prediction and 2- using filtered-x least mean square algorithm) were feedforward and they were both shown to have reached satisfying roll reduction and reasonable power consumption.

The wave prediction method uses the information obtained from monitoring wave heights over a period of time to build a recursive model of the wave and therefore predict the incoming waves in the near future. Using the predicted wave pattern it is then possible to pump the water in the correct direction before the wave reaches the ship. Therefore the righting moment is available at the time it is most effective. The accuracy of the prediction is thus very important for the controller to work efficiently. Any errors in the prediction have effect on the roll stabilization; on the other hand any device capable of increasing the available information about the incoming waves would consequently improve the effect of the control strategy. The filtered-x least mean square algorithm does not depend on any wave reading or prediction for its optimum performance. It forms an adaptive inverse controller which tries to minimise the error signal being the difference between the roll motion and a

desired signal. It has the potential to adapt itself to changes in the ship parameters and provides significant roll reduction.

Another objective of this thesis was to develop a solution for roll stabilization of multi-hull vehicles at slow speed. The method developed in this study was the introduction of "n-tanks". In this strategy the anti-roll tanks are located in the side hulls of a multi-hull vessel and was shown to reach significant roll reduction. The use of n-tanks will provide a solution to the problem of stabilising catamarans, trimarans, or even surface effect ships (SES) at slow speeds by making use of the low value volume in the side hulls with minimum impact on the box structure volume. An added advantage, especially for SES, is that when not in use the tanks can be easily emptied.

If the roll reduction of n-tanks on multi-hull ships, and wave prediction or filtered-x LMS algorithms on U-tanks is proved in practice, the maritime community will benefit from a new generation of roll stabilizers which are capable of reducing the roll motion at slow speeds, in a wide range of sea states without any need to tune the hardware.

References

[1] "Stabilisation: Faster response for passive stabilisation tanks," *Marine Engineers Review*, no. May, p. 40, 1999.

[2] "Stabilization: Swinging pendulum," *Marine Engineers Review*, no. May, p. 42, 1999.

[3] "Stabilization: The advantages of multiple passive tanks located topsides," *Marine Engineers Review*, no. May, p. 41, 1999.

[4] "Stabilization/Roll control," *Marine Engineers Review*, no. May, p. 33, 2002.

[5] A. F. Abdel Gawad, S. A. Ragab, A. H. Nayfeh, and D. T. Mook, "Roll stabilization by anti-roll passive tanks," *Ocean Engineering*, vol. 28, p. 457, 2001.

[6] V. Armenio and M. La Rocca, "On the analysis of sloshing of water in rectangular containers: numerical and experimental investigation," *Ocean Engineering*, vol. 23, no. 8, pp. 705-739, 1996.

[7] D. W. Bass, "Roll stabilization for small fishing vessels using paravanes and anti-roll tanks," *Marine Technology*, vol. 35, no. 2, pp. 74-84, 1998.

[8] J. Bell and P. Walker, "Activated and passive controlled fluid tank system for ship stabilization," *Transactions of Society of Naval Architects and Marine Engineers*, vol. 74, p. 150, 1966.

[9] S. Bennett, "Ship stabilization: History," in *Concise encyclopedia of traffic and transportation systems*. M. Papageorgiou, Ed. New York: Pergamon, 1991, pp. 454-459.

[10] R. Bhattacharyya, *Dynamics of marine vehicles* Wiley-Interscience publication, 1978.

[11] H. J. R. Biles, "Model experiments with anti-rolling tanks," *Transactions of Institution of Naval Architects*, vol. 67, p. 179, 1925.

[12] R. Birmingham, B. Webster, T. Roskilly, and E. Jones, "The application of artificial intelligence to roll stabilization for a range of loading and operating conditions," *International Journal of Maritime Engineering, The Transactions of the Royal Institution of Naval Architects*, vol. Part A 2003.

[13] J. J. V. D. Bosch and J. H. Vugts, "On roll damping by free surface tanks," *Transactions of Royal Institution of Naval Architects*, vol. 108, p. 345, 1966.

[14] D. R. Broome, "Application of ship motion prediction II," *Transactions of Institute of Marine Engineering*, vol. 110, pp. 135-153, 1998.

[15] D. R. Broome, "Application of ship motion prediction I," *Transactions of Institute of Marine Engineering*, vol. 110, pp. 77-93, 1998.

[16] D. R. Broome and A. Pitttaras, "The Time Prediction of Ship Motion at Sea," 1990.

[17] A. Cariou and G. Casella, "Liquid sloshing in ship tanks: a comparative study of numerical simulation," *Marine Structures*, vol. 12, no. 3, pp. 183-198, 1999.

[18] M. S. Celebi and H. Akyildiz, "Nonlinear modeling of liquid sloshing in a moving rectangular tanks," *Ocean Engineering*, vol. 29, no. 12, pp. 1527-1553, 2002.

[19] J. H. Chadwick, "On the stabilization of roll," *Transactions of Society of Naval Architects and Marine Engineers*, vol. 63, p. 237, 1955.

[20] S. L. Chen, S. W. Shaw, H. K. Khalil, and A. W. Troesch, "Robust stabilization of large amplitude ship rolling in beam seas," *Journal of Dynamic Systems, Measurement and Control*, vol. 122, pp. 108-113, 2000.

[21] S. L. Chen, S. W. Shaw, H. K. Khalil, and A. W. Troesch, "Robust stabilization of large amplitude ship rolling in regular beam seas," *Nonlinear Dynamics and Control*, vol. 91, pp. 93-9, 1996.

[22] M. J. Chern, A. G. L. Borthwick, and R. Eatock Taylor, "A pseudospectral transformation of 2-D non-linear waves," *Journal of Fluids Structure*, vol. 13, no. 5, pp. 607-630, 1999.

[23] R. P. Dummett, "MVSearoad Tamar modifications to improve ship motions," *The Austrailan Naval Architect*, vol. 2, no. 3 1998.

[24] H. Frahm, "Results of trails of the anti-rolling tanks at sea," *Transactions of Institution of Naval Architects*, vol. 53, p. 183, 1911.

[25] A. Francescutto, V. Armenio, and M. La Rocca, "On the roll motion of a ship with partially filled unbaffled and baffled tanks: numerical and experimental investigation," *The Proceedings of the Sixth International Offshore and Polar Engineering Conference*, vol. 3, pp. 377-386, 1996.

[26] W. Froude, "On the rolling of ships," *Transactions of Institution of Naval Architects*, vol. 2, p. 180, 1861.

[27] G. J. Goodrich, "Development and design of passive roll stabilisers," *Transactions of Royal Institution of Naval Architects*, vol. 111, p. 81, 1969.

[28] T. Grafton, "The Roll Motion of Trimaran Ships." PhD thesis University College London, UK, 2007.

[29] I. S. Groom, "HMS Nottingham - The view from HQ1," *Journal Marine Design and Operations*, vol. 3, p. 33, 2003.

[30] W. J. Hsueh and Y. J. Lee, "A design for ship stabilization be activated anti-roll tanks," *Journal of Marine Science and Technology*, vol. 2, no. 2, p. 77, 1997.

[31] T. Ikeda and N. Nakagawa, "Non-linear vibrations of a structure caused by water sloshing in a rectangular tank," *Journal of Sound and Vibration*, vol. 201, no. 1, pp. 23-41, 1997.

[32] Y. Ikeda and T. Yoshiyama, "A study on flume-type anti-rolling tank," *Journal of the Kansai Society of Naval Architects*, vol. 216, p. 111, 1991.

[33] K. Kagawa, K. Fujita, M. Matsuo, H. Koukawa, and Y. Zensho, "Development of tuned liquid damper for ship vibration," *Transactions of the West Japan Society of Naval Architects*, vol. 81, p. 181, 1990.

[34] K. Kagawa, K. Fujita, M. Matsuo, H. Koukawa, and Y. Zensho, "Development of tuned liquid damper for ship vibration," *Transactions of the West Japan Society of Naval Architects*, vol. 78, p. 251, 1989.

[35] I. J. Karassik and T. McGuire, *Centrifugal pumps*, 2 ed. New York: Chapman & Hall : International Thomson, 1998.

[36] Y. Koike, K. Tanida, M. Mutaguchi, T. Murata, M. Imazeki, and E. Hiroshige, "Development of Hybrid antti-rolling device for ships and test at sea," *Recent Progress on Science and Technology, IHI*, vol. 6, pp. 20-26, 1997.

[37] B. S. Lee and D. Vassalos, "An investigation into the stabilization effects of anti-roll tanks with flow obstructions," *International Shipbuilding Progress*, vol. 43, no. 433, p. 70, 1996.

[38] Z. Liu and Y. Huang, "A new method for large amplitude sloshing problems," *Journal of Sound and Vibration*, vol. 175, no. 2, pp. 185-195, 1994.

[39] L. Ljung, *System Identification: Theory for the user*. New Jersey: P T R Prentice Hall, 1987.

[40] A. R. J. M. Lloyd, *Seakeeping: Ship behaviour in rough weather*. Chichester: Ellis Horwood Limited, 1989.

[41] B. S. Massey, *Mechanics of Fluids*. London: D. Van Nostrand Company Ltd, 1968.

[42] N. Minorsky, "Problems of anti-rolling stabilization of ships by the activated tank method," *American Society of Naval Engineers*, vol. 47, p. 87, 1935.

[43] R. Moaleji and A. R. Greig, "Inverse Control for Roll Stabilization of Ships Using Active Tanks," *7th IFAC Conference on Manoeuvring and Control of Marine Craft (MCMC) Lisbon*, 2006.

[44] R. Moaleji and A. R. Greig, "Roll Reduction of Ships Using Anti-roll n-tanks," *World Maritime Conference (WMC), London*, 2006.

[45] R. Moaleji and A. R. Greig, "On the Development of anti-roll tanks," *Ocean Engineering*, vol. 34, pp. 103-121, 2007.

[46] V. J. Modi and M. L. Seto, "Suppression of flow-induced oscillations using sloshing liquid dampers: analysis and experiments," *Journal of Wind Engineering*, vol. 67-68, no. 1-3, pp. 611-625, 1997.

[47] M. N. Parker, "Brief review of ship stabilization systems," *Naval Engineers Journal*, vol. 77, no. 4, p. 640, 1965.

[48] T. Phairoh and J. K. Hauang, "Modeling and Analysis of Ship Roll Tank Stimulator," *Ocean Engineering*, vol. 32, no. 8-9, pp. 1037-1053, 2005.

[49] T. Phairoh and W. J. Hsueh, "Adaptive Ship Roll Mitigation by Using a U-tube Tank," *Ocean Engineering*, vol. 34, no. 3-4, pp. 403-415, 2007.

[50] J. A. Piepmeier and J. Waters, "Analysis of stereo vision-based measurements of laboratory water waves," *IEEE International Geoscience and Remote Sensing Symposium (IGARSS 04)*, vol. 5, pp. 3588-3591, 2004.

[51] G. Popov, S. Sankar, and T. S. Sankar, "Dynamics of liquid sloshing in baffled and compartmented road containers," *Journal of Fluids Structure*, vol. 7, no. 7, pp. 803-821, 1993.

[52] G. N. Roberts and T. L. Barboza, "Analysis of warship roll stabilisation by controlled anti-roll tanks with the aid of digital simulation," *International Conference on CONTROL 88, 13-15 April 1988*, pp. 672-676, 1988.

[53] P. C. Sames, D. Marcouly, and T. E. Schellin, "Sloshing in rectangular and cylindrical tanks," *Journal of Ship Research*, vol. 46, no. 3, pp. 186-200, 2002.

[54] F. H. Sellers and J. P. Martin, "Selection and evaluation of ship roll stabilization systems," *Marine Technology*, vol. 29, no. 2, pp. 84-101, 1992.

[55] K. L. Shyu and H. C. Kuo, "Dynamic behaviour of a U-type tuned liquid damper," *International Shipbuilding Progress*, vol. 43, no. 436, p. 331, 1996.

[56] Sirehna, "Web page accessed," http://www.ec-nantes.fr/sirehna/gallery/pacdg/pacdg.htm Accessed 23rd May 2005.

[57] R. K. Skarda and M. Walker, "Merits of the monohull and trimaran against the requirement for the future surface combatant," *International Conference of Design and Operation of Trimaran Ships, RINA*, pp. 129-142, 2004.

[58] A. Souto Iglesias and V. Gonzalez, "Passive stabilizer tanks simulation using SPH models," *Proceeding of the Fluid Structure Interaction, Halkidiki, Greece*, vol. 1, pp. 35-44, 2001.

[59] A. Souto Iglesias, I. Laiz, S. Abril, and R. Adab, "Passive stabilizer tanks simulation using SPH models," *Proceedings of Fourth International Conference on Marine Technology, Sczcecin, Poland*, vol. 1, pp. 171-181, 2001.

[60] A. Souto Iglesias, L. Perez Rojas, and R. Zamora Rodriguez, "Simulation of anti-roll tanks and sloshing type problems with smoothed particle hydrodynamics," *Ocean Engineering*, vol. 31, pp. 1169-1192, 2004.

[61] C. Stigter, "The performance of U-tanks as a passive anti-rolling device," *Royal Institution of Naval Architects*, no. ISP-13 (144), p. 249, 1966.

[62] L. M. Sun and Y. Fujino, "A semi-analytical model for tuned liquid damper (TLD) with wave breaking," *Journal of Fluids Structure*, vol. 8, no. 5, pp. 471-488, 1994.

[63] T. W. Treakle, "A time domain numerical study of passive and active anti-roll tanks to reduce ship motion," *MSc Thesis. Virginia Polytechnic Institute*, 1998.

[64] T. W. Treakle, D. T. Mook, S. I. Liapis, and A. H. Nayfeh, "A time domain method to evaluate the use of moving weights to reduce the roll motion of a ship," *Ocean Engineering*, vol. 27, pp. 1321-1343, 2000.

[65] J. Vasta, A. J. Gidding, A. Taplin, and J. J. Stilwell, "Roll stabilization by means of passive tanks," *Transactions of Society of Naval Architects and Marine Engineers*, vol. 69, p. 411, 1961.

[66] J. H. G. Verhagen and L. Van Wijngaarden, "Non-linear oscillations of fluid in a container," *Journal of Fluid Mechanics*, vol. 22, no. 4, pp. 737-751, 1965.

[67] J. H. Vugts, "A comparative study on four different passive roll damping tanks, Part I," *Report 109S of the Netherlands Ship Research Centre TNO*, 1968.

[68] P. Watts, "On a method of reducing the rolling of ships at sea," *Transactions of Institution of Naval Architects*, vol. 24, p. 165, 1883.

[69] P. Watts, "The use of water chambers for reducing the rolling of ships at sea," *Transactions of Institution of Naval Architects*, vol. 26, p. 30, 1885.

[70] W. C. Webster, "Analysis of the control of activated anti-roll tanks," *Transactions of Society of Naval Architects and Marine Engineers*, vol. 75, p. 296, 1967.

[71] W. C. Webster and P. Dagon, "An analysis of the control of activated anti-roll tanks," *Hydronautics Inc*, 1966.

[72] W. C. Webster, J. F. Dalzell, and R. A. Barr, "Prediction and measurement of the performance of free-flooding ship anti-rolling tanks," *Transactions of Society of Naval Architects and Marine Engineers*, vol. 96, p. 333, 1988.

[73] B. Widrow and S. Stearns, *Adaptive Signal Processing* Prentice-Hall, 1985.

[74] S. K. Yalla, "Liquid dampers for mitigation of structural response:Theoretical developement and experimental validation," *PhD Thesis, University of Notre Dame, Department of Civil Engineeering*, USA, 2001.

[75] K. S. Youssef, S. A. Ragab, A. H. Nayfeh, and D. T. Mook, "Design of passive anti-roll tanks for roll stabilization in the nonlinear range," *Ocean Engineering*, vol. 29, p. 177, 2002.

[76] Z. Zhong, J. M. Falzarano, and R. M. Fithen, "A numerical study of U-tube passive anti-rolling tanks," *Proceedings of the Eight International Offshore and Polar Engineering Conference, Montreal, Canada*, vol. 3, pp. 504-513, 1998.

Appendix I: Selected codes used in simulations

Pri_utank_trimaran.m

```
% this code provides dimensions used in other U-tank simulations
% it is considered that there are two pannels in the duct.


w=20;% (m)
wr=2;% (m)
hr=3;% (m)
hd=1;% (m)
rd=-1.5;%(m)
q=0.117;
xt=2;% (m)
ro=1;% (Ton)
xB=0;
n=0.5; % The ratio of (xt reservoir/xt duct)

Q=(ro*wr*xt*w^2)/2;      % (Ton.m)

att=Q*wr*(n*w/(2*hd)+hr/wr);% (KN.m/Rad/s^2)
ctt=Q*9.81;              % (KN.m/Rad/s)
btt=Q*q*wr*(w/(2*hd^2)+hr/wr^2);% (KN.m/Rad)
wn=sqrt(ctt/att);        % (Rad/s)S
mu=btt/(2*att*wn);       % Damping ratio

at2=-n*Q;
at4=Q*(n*rd+hr);
ct4=Q*9.81;
at6=-Q*xB;
```

U_tank_passive_parameters_effect.m

```
% 30 June 2003
% This program investigates the effect of parameter deviation
% (w, wr, hd, hr, q) on natural frequency and damping ratio of the tank

w=20;% (m)
wr=3;% (m)
hr=3;%  (m)
hd=1;%  (m)
rd=-1.5;%(m)
q=0.117;
xt=2;%  (m)
ro=1;% (Ton)

%********** variation of w *****************

out=[5 0.95 0.05];
for w=5:0.5:30

   Q=(ro*wr*xt*w^2)/2;% (Ton.m)

   att=Q*wr*(w/(2*hd)+hr/wr);% (KN.m/Rad/s^2)
   ctt=Q*9.81;            % (KN.m/Rad/s)
   btt=Q*q*wr*(w/(2*hd^2)+hr/wr^2);% (KN.m/Rad)
   wn=sqrt(ctt/att);      % (Rad/s)
   mu=btt/(2*att*wn);     % Damping ratio

   out=[out;w wn mu];
end

subplot(5,2,1);
plot(out(:,1),out(:,2));axis([5 30 0 1]),grid
xlabel('w (m)');
% ylabel('w_n (Rad/s)');
subplot(5,2,2);
plot(out(:,1),out(:,3));axis([5 30 0 0.2]),grid
xlabel('w (m)');
% ylabel('zeta');

%***************** variation of wr ******************

w=20;
out=[0.5 1 0.07];
for wr=0.5:0.1:6

   Q=(ro*wr*xt*w^2)/2;% (Ton.m)

   att=Q*wr*(w/(2*hd)+hr/wr);% (KN.m/Rad/s^2)
   ctt=Q*9.81;            % (KN.m/Rad/s)
```

```
   btt=Q*q*wr*(w/(2*hd^2)+hr/wr^2);% (KN.m/Rad)
   wn=sqrt(ctt/att);        % (Rad/s)
   mu=btt/(2*att*wn);       % Damping ratio

   out=[out;wr wn mu];
end

subplot(5,2,3);
plot(out(:,1),out(:,2));axis([0.5 6 0 1]),grid
xlabel('w_r (m)');
% ylabel('w_n (Rad/s)');
subplot(5,2,4);
plot(out(:,1),out(:,3));axis([0.5 6 0 0.2]),grid
xlabel('w_r (m)');
% ylabel('zeta');

%***************** variation of hd ********************

wr=3;
out=[0.5 0.3885 0.2686];
for hd=0.5:0.1:5

   Q=(ro*wr*xt*w^2)/2;% (Ton.m)

   att=Q*wr*(w/(2*hd)+hr/wr);% (KN.m/Rad/s^2)
   ctt=Q*9.81;              % (KN.m/Rad/s)
   btt=Q*q*wr*(w/(2*hd^2)+hr/wr^2);% (KN.m/Rad)
   wn=sqrt(ctt/att);        % (Rad/s)
   mu=btt/(2*att*wn);       % Damping ratio

   out=[out;hd wn mu];
end

subplot(5,2,5);
plot(out(:,1),out(:,2));axis([0.5 5 0 1]),grid
xlabel('h_d (m)');
% ylabel('w_n (Rad/s)');
subplot(5,2,6);
plot(out(:,1),out(:,3));axis([0.5 5 0 0.3]),grid
xlabel('h_d (m)');
% ylabel('zeta');

%***************** variation of hr ********************

hd=1;
out=[1 0.5625 0.1];
for hr=1:0.1:10

   Q=(ro*wr*xt*w^2)/2;% (Ton.m)
```

```
   att=Q*wr*(w/(2*hd)+hr/wr);% (KN.m/Rad/s^2)
   ctt=Q*9.81;            % (KN.m/Rad/s)
   btt=Q*q*wr*(w/(2*hd^2)+hr/wr^2);% (KN.m/Rad)
   wn=sqrt(ctt/att);      % (Rad/s)
   mu=btt/(2*att*wn);     % Damping ratio

   out=[out;hr wn mu];
end
subplot(5,2,7);
plot(out(:,1),out(:,2));axis([1 10 0 1]),grid
xlabel('h_r (m)');
% ylabel('w_n (Rad/s)');
subplot(5,2,8);
plot(out(:,1),out(:,3));axis([1 10 0 0.2]),grid
xlabel('h_r (m)');
% ylabel('zeta');

%********** variation of q ****************

hr=3;
out=[0 0.5 0];
for q=0:0.01:2

   Q=(ro*wr*xt*w^2)/2;% (Ton.m)

   att=Q*wr*(w/(2*hd)+hr/wr);% (KN.m/Rad/s^2)
   ctt=Q*9.81;            % (KN.m/Rad/s)
   btt=Q*q*wr*(w/(2*hd^2)+hr/wr^2);% (KN.m/Rad)
   wn=sqrt(ctt/att);      % (Rad/s)
   mu=btt/(2*att*wn);     % Damping ratio

   out=[out;q wn mu];
end

subplot(5,2,9);
plot(out(:,1),out(:,2));axis([0 2 0 1]),grid
xlabel('q');
% ylabel('w_n (Rad/s)');
subplot(5,2,10);
plot(out(:,1),out(:,3));axis([0 2 0 2]),grid
xlabel('q');
% ylabel('zeta');
```

U_tank_passive_small_angles_effect.m

```
% 1 July 2003

% This program solves the ODE of linear and nonlinear
%  systems of the tank alone for different initial values
%  and plots them on the same graph


t0=0;
tf=30;
y0=0.14; % Rad, 8.02 degree

[t,y]=ode45('tank_alone_function',[t0 tf],[y0;0]);
[t2,y2]=ode45('tank_alone_func_nonlinear',[t0 tf],[y0;0]);

subplot(311);
plot(t,y(:,1)*180/pi);grid
hold on
subplot(311);
plot(t2,y2(:,1)*180/pi,'--');
hold off

%********* Y0=0.3 Rad **************

t0=0;
tf=30;
y0=0.3; % Rad, 17.8 degree

[t,y]=ode45('tank_alone_function',[t0 tf],[y0;0]);
[t2,y2]=ode45('tank_alone_func_nonlinear',[t0 tf],[y0;0]);

subplot(312);
plot(t,y(:,1)*180/pi);grid
hold on
subplot(312);
plot(t2,y2(:,1)*180/pi,'--');
hold off


%********* Y0=0.46 Rad **************

t0=0;
tf=30;
y0=0.46; % Rad, 26.5 degree

[t,y]=ode45('tank_alone_function',[t0 tf],[y0;0]);
[t2,y2]=ode45('tank_alone_func_nonlinear',[t0 tf],[y0;0]);

subplot(313);
```

```
plot(t,y(:,1)*180/pi);grid
hold on
subplot(313);
plot(t2,y2(:,1)*180/pi,'--');xlabel('Time (s)');
hold off
```

sea_state.m

```
% sea_state.m matlab file
% This code generates sea waves in time domain based on Bretschneider or
%  ITTC wave spectum
% Reza Moaleji, University College London
% 4 Augost 2004

prompt={'Sea state:','Simulation time (sec)', 'dw (frequncy bandwidth, rad/sec)'};
default={num2str(5),num2str(300),num2str(0.02)};
ans=inputdlg(prompt,'Enter the sea state',1,default);
seastate=str2num(ans{1});
t_final=str2num(ans{2});
dw=str2num(ans[69]);

%********* You can modify the following parameters **********
%  H= Significant wave height (meter)
%  T= Significant wave period (seconds)

switch seastate
   case 0; H=0;   T=0.75; w_final=8;  dt=0.1;
   case 1; H=0.05; T=2;   w_final=4;  dt=0.1;
   case 2; H=0.3;  T=4;   w_final=3;  dt=0.2;
   case 3; H=0.875;T=5.5; w_final=3;  dt=0.4;
   case 4; H=1.875;T=7;   w_final=2;  dt=0.4;
   case 5; H=3.25; T=8;   w_final=1.8;dt=0.5;
   case 6; H=5;   T=9.5;  w_final=1.6;dt=0.5;
   case 7; H=7.5;  T=12;  w_final=1.4;dt=0.5;
   case 8; H=11.5; T=15;  w_final=1.2;dt=0.5;
   case 9; H=15;  T=21;  w_final=1;  dt=0.5;
   otherwise
     error('This is not a valid sea state; sea state must be an integer between 0 and 9')
end

%********** This part generates the wave spectrum and derives the wave
%         amplitude for each frequency component

A=173*(H^2)/(T^4);
B=691/(T^4);

wave_amp=0;
SW=0;

for w=dw:dw:w_final

   S=A/w^5*exp(-B/w^4);
   A_w=sqrt(2*S*dw);

   SW=[SW;S];
```

```
  wave_amp=[wave_amp;A_w];
end


%***** This part generates single sin waves having frequencies between
%     0:dw:w_final having amplitude as derived from the wave spectrum and
%     random phase

w=[0:dw:w_final]';
nw=w_final/dw+1; % number of frequencies used

sea_wave=zeros(t_final/dt+1,1);
phase=2*pi*rand(1,nw);


for i=1:nw
  sinw=0;
  for t=0.1:dt:t_final
     sinw=[sinw;wave_amp(i)*sin(w(i)*t+phase(i))];% makes a sin wave component having
frequency w
  end
  sea_wave=[sea_wave sinw];
end
wave=sum(sea_wave')';% adds the sin components together

%************************************************************************

w=[0:dw:w_final]';
t=[0:dt:t_final];

subplot(211)
plot(w,SW)
title('Wave spectrum');
xlabel('w (rad/s)');
ylabel('S(w) (m2.s/rad)');

subplot(212)
plot(t,wave)
title('Sea wave');
xlabel('t (s)');
ylabel('A(t) (m)');

% clear A A_w B H S SW dw i nw phase sea_wave sinw w w_final wave_amp
```

U_tank_pump.m

```
% This code runs the simulink file "active_tank_pump2" for numerous wave conditions

pre_tank3

h=0.5; %sample time
k_final=200/h;
output=zeros(1,10);

for omega=0.1:0.02:0.9

  for alpha=0.4:0.2:4

    phase=0;
    sim active_tank_pump2

    start_point=20/h+1; % the 1 is to make the start point exactly 20 sec, otherwise it is
20/h=40=19.5sec
    one_cycle=round(2*pi/omega/h);
    [peak_T_wave,r]=max(T_wave(start_point:start_point+one_cycle));% finds where the
wave is max after 20 sec up to a period
    [peak_T_tank,s]=max(T_tank(start_point+r-1:start_point+r-1+one_cycle));% finds how
many steps after that point T_wave is max
    k_step_ahead=s-1;
    k_step_ahead_pre=s-1;
    omega,alpha

    while (k_step_ahead>0)&(k_step_ahead_pre>=k_step_ahead)
      phase=phase+5;
      sim active_tank_pump2
      start_point=20/h+1;
      one_cycle=round(2*pi/omega/h);
      [peak_T_wave,r]=max(T_wave(start_point:start_point+one_cycle));
      [peak_T_tank,s]=max(T_tank(start_point+r-1:start_point+r-1+one_cycle));
      k_step_ahead_pre=k_step_ahead;
      k_step_ahead=s-1;

    end

    x4max=max(without_tank(150:200));
    x4max_damped=max(with_tank(150:200));
    roll_reduction=(x4max-x4max_damped)/x4max*100;
    tank_angle=max(tank_a(150:200));
    capacity=max(Qt(150:200));
    pmax=max(power(150:200));
    period=2*pi/omega;
    p_av=(2*pmax/omega)/period;
```

```
    output=[output;omega period alpha x4max x4max_damped roll_reduction tank_angle
capacity pmax p_av ];

  end
end
```

ntank_blower.m

```
% This code runs the simulation for n-tank blower for numerous wave conditions

pre_ntank
dt=0.2;

h=dt; %sample time

% output=zeros(1,8); % This term is comment only if you are resuming the
% simulation after a failure

start_point=100;% recording start time for finding the max of a parameter
end_point=150;
ts=start_point/h+1; % the 1 is to make the start point exactly 20 sec, otherwise it is
20/h=40=19.5sec
tf=end_point/h+1;

for omega=0.8:0.02:1
%    for alpha=1:0.2:5
     alpha=4;

     omega,alpha
     temp=[0 1000];
     for pressure=0:1000:20000
        sim ship_ntank_closing_port_speed_blow2
        x4max_damped=max(with_tank(ts:tf));
        temp=[temp;pressure x4max_damped];
        pressure
     end
     [roll_min,s]=min(temp(:,2));
     pressure=temp(s,1)

     sim ship_ntank_closing_port_speed_blow2

     x4max=max(without_tank(ts:tf));
     x4max_damped=max(with_tank(ts:tf));
     roll_reduction=(x4max-x4max_damped)/x4max*100;
     water_height=max(h_starboard(ts:tf));
     period=2*pi/omega;
     output=[output;omega period alpha x4max x4max_damped roll_reduction water_height
pressure];

%    end
end
```

ntank_closing_port.m

```
% This code runs the n-tank when the port opens and closes in each period for numerous
wave conditions

pre_ntank
dt=0.5;

h=dt; %sample time

output=zeros(1,8); % This term is comment only if you are resuming the
% simulation after a failure

start_point=100;% recording start time for finding the max of a parameter
end_point=150;
ts=start_point/h+1; % the 1 is to make the start point exactly 20 sec, otherwise it is
20/h=40=19.5sec
tf=end_point/h+1;

for omega=0.3:0.02:1
  for alpha=1:0.2:5

    omega,alpha
    temp=[0 1000];
    for b=0:0.05:0.8
      sim ship_ntank_closing_port_speed2
      x4max_damped=max(with_tank(ts:tf));
      temp=[temp;b x4max_damped];
      b
    end
    [roll_min,s]=min(temp(:,2));
    b=temp(s,1)

    sim ship_ntank_closing_port_speed2

    x4max=max(without_tank(ts:tf));
    x4max_damped=max(with_tank(ts:tf));
    roll_reduction=(x4max-x4max_damped)/x4max*100;
    water_height=max(h_starboard(ts:tf));
    period=2*pi/omega;
    output=[output;omega period alpha x4max x4max_damped roll_reduction water_height
b];

  end
end
```

Appendix II: Hydrodynamic properties of ships

Ship1

```
% this code provides dimensions used in other U-tank simulations and calculates
% hydrodynamic coefficients.
% it is considered that there are two panels in the duct.

%************ Ship parameters ********************

GM=2;
displacement=9560;
beam=32;
k44=0.3*beam;
I44=displacement*k44^2;     % longitude moment of inertial

a44 = I44*1.05;             % added mass effect considered constant 5%
c44= GM*displacement*9.81;
Wn=sqrt(c44/a44);
b44=(2*0.1*Wn)*a44;         % b44 chosen in away to cause 0.1 damping ratio


%************ tank parameters **************

w=32;% (m)
wr=3;% (m)
hr=2;% (m)
hd=1;% (m)
rd=-1.5;%(m)
q=0.117;
xt=3.5;% (m)
ro=1;% (Ton)
xB=0;
n=0.5; % The ratio of (xt reservoir/xt duct)

ratio=(2*(wr*hr)+w*hd)*xt/displacement*100;

Q=(ro*wr*xt*w^2)/2;      % (Ton.m)
att=Q*wr*(n*w/(2*hd)+hr/wr);% (KN.m/Rad/s^2)
ctt=Q*9.81;              % (KN.m/Rad/s)
btt=Q*q*wr*(w/(2*hd^2)+hr/wr^2);% (KN.m/Rad)
wn=sqrt(ctt/att);        % (Rad/s)S
mu=btt/(2*att*wn);       % Damping ratio
at2=-n*Q;
at4=Q*(n*rd+hr);
ct4=Q*9.81;
at6=-Q*xB;
```

Appendix III: Outcome publications of this thesis

The following publications have so far resulted from this thesis. The full papers are not represented here as they are very similar to the relevant chapters, but full publication details are presented:

- **R. Moaleji, A.R. Greig. "On the development of anti-roll tanks" Ocean Engineering. 34 (2007) 103-121**

Abstract: This paper reviews the development of ship anti-roll tanks from the 1880s to the present day including their modelling and control strategies. Mention is also made of other ship roll stabilization systems and the application of the technology to stabilization of other structures. The potential for the use of roll stabilization tanks on modern, high speed multi-hull craft which also have a low speed operational requirement is also discussed.

- **R. Moaleji, A.R. Greig. "Roll reduction of ships using anti-roll n-tanks" World Maritime Conference, Institute of Marine Engineers Science and Technology (IMarEST), March 2006, London.**

Abstract: Roll reduction of ships above about 6kts can be effectively achieved using active fin stabilizers but at slow or zero speeds another method is required. This paper considers a tank configuration which we call "n-tank", also know as free flooding tanks. The port and starboard legs are open to the sea and there is no internal water connection between the two tanks but there may be an air connection at the top of the tanks. The configuration of "n-tanks" makes them particularly useful for application to multi-hull craft. A requirement is developing for high speed multihulls to have good sea keeping at low speeds. The paper commences with a brief history of the development of roll stabilization tanks, a mathematical model of triangular prismatic n-tanks is then derived and the results of simulations on a representative trimaran are presented. Five cases are considered starting with the base line of passive n-tanks with fixed inlet ports. Different controls of the opening port and use of compressed air to assist emptying the tanks is then investigated.

- **R. Moaleji, A.R. Greig. "Inverse control for roll stabilization of ships using active tanks", 7th IFAC Conference on Manoeuvring and Control of Marine Craft (MCMC'2006) September 2006, Lisbon.**

Abstract: Roll stabilization of ships at slow speeds or at rest has for long been a challenge in Marine engineering. One of the common methods of doing so is using anti-roll tanks which are available in passive form or an active form where a pump is used to move the water. This paper presents a new strategy in controlling the actuating pumps of an active U-tank with an adaptive inverse controller using filtered-x least mean square algorithm. The paper includes a brief introduction on the history of anti-roll tanks followed by the generation of a mathematical model of a U-tank and application to a sample ship.